1-1-2003

Seismic behavior and retrofitting of reinforced concrete moment resistant frames

Shahram Talebi
Ryerson University

Seismic Behavior and Retrofitting of Reinforced Concrete Moment Resistant Frames

By

Shahram Talebi (B.A.Sc)

Tabriz University, Iran, 1994

A thesis

Presented to Ryerson University

in Partial Fulfillment of the

Requirements for the Degree of

Master Applied Science

in the Program of

Civil Engineering

Ryerson University

Toronto, Ontario, Canada, 2003

Your file Votre référence
ISBN: 0-612-87171-1
Our file Notre référence
ISBN: 0-612-87171-1

DECLARATION

I hereby declare that I am the sole author of this thesis. I authorize Ryerson University to lend this thesis to other institutions or individuals for the purpose of scholarly research.

I further authorize Ryerson University to reproduce this thesis by photocopying or by other means, in total or in part, at the request of other institutions or individuals for the purpose of scholarly research.

MASTER APPLIED SCINCE (2003) **Ryerson University**

(Civil Engineering) **Toronto, Ontario**

TITLE: Retrofitting of Reinforced Concrete Moment Resistant Frames Designed for Different Levels of Ductility

SUPERVISOR: Dr. R. Kianoush

NUMBER OF PAGES: 208Pages

BORROWER'S PAGE

Ryerson University requires the signatures of all persons using or photocopying this thesis. Please sign below, and give address and date.

Name	Address	Date

Seismic Behavior and Retrofitting of Reinforced Concrete Moment Resistant Frames
Master Applied Science, September 2003
Shahram Talebi
Structural Engineering
Ryerson University

ABSTRACT

Many multistory reinforced concrete frame structures built prior to 1970's located in seismic zones have been designed only for gravity loads without any considerations for lateral loads. These structures are referred to as Gravity Load Designed (GLD) frames. The lack of seismic considerations in GLD structures results in non-ductile behavior that may cause the lateral load resistance of these buildings to be insufficient for even moderate earthquakes.

Based on the current Canadian practice as prescribed by CAN3-A23.3 –1994, reinforced concrete structures located in seismic zones should be designed as ductile or nominally ductile frames. In this study, a typical 5-story frame building is designed as a) ductile, b) nominally ductile and c) GLD frame. Analytical investigation is performed to evaluate and to compare the performance of each frame. The study includes "pushover" analysis and non-linear time-history analysis. The results in terms of story displacement, ductility, shear, drift, sequence of cracking and yielding and the damage potential are presented. As a result of the poor performance of the GLD frame, it is retrofitted with fiber-reinforced polymers (FRP). Different retrofitting schemes using FRP are used to compare the behavior in terms of ductility. In this study, the behavior of the retrofitted frame is compared with the that of the GLD frame.

Based on the results of this study, a guideline for improving the seismic performance of reinforced concrete frame structures is provided.

ACKNOWLEDGMENTS

I would like to express my sincere appreciation to Dr. R. Kianoush, supervisor of this project, for his advice, encouragement and time spent throughout the course of this study.

The excellent accompanying and assistance of the other professors and staffs of the Department of Civil Engineering are deeply appreciated.

Sincere gratitude is due to the members of Examining Board, for their time spent in reviewing this thesis and their valuable comments and suggestions. The Examining Board consisted of Dr. M. Lachemi, Dr. R. Kianoush, Dr. A. Hossain and Dr. L. Amleh

Much appreciation is extended to my mother, father, sisters, brother and all the best friends. Their prayers, love, encouragement and supplication always accompanied me to face the hardness and difficulty.

Finally, this undertaken could never have been achieved without the spiritual support from my merciful God. Thank God.

This work is dedicated to my wonderful mother

TABLE OF CONTENTS

LIST OF FIGURES

LIST OF TABLES

NOTATION

a	depth of equivalent rectangular concrete stress block. mm
A_{ftp}	cross-sectional area of FRP material, mm^2
A_s	area of tension steel reinforcement, mm^2
A'_s	area of compression steel reinforcement, mm^2
b	width of compression face of member, mm
b_e	effective width of compression face of member, mm
b_{ftp}	width of the external FRP reinforcement, mm
b_w	minimum effective web width within depth d, mm
C	distance from extreme compression face to neutral axis, mm
C_b	distance from extreme compression face to neutral axis for balanced conditions,
C_c	internal force due to compression in concrete, N
C_s	internal force due to compression steel reinforcement, N
d	distance from extreme compression face to centroid of tension steel reinforcement, mm
d'	distance from extreme compression face to the centroid of compression steel reinforcement, mm
d_{ftp}	effective depth of FRP stirrups, mm
E_c	modulus of elasticity of concrete, MPa
h	overall depth of member, mm
M_r	factored moment resistance, N.mm
A_c	area of concrete core of spirally reinforced compression member measured out-to out of spiral, mm^2
A_g	gross area of column section, mm^2
A_h	area of one leg of the horizontal reinforcement, mm^2
A_{st}	total area of longitudinal steel reinforcement, mm^2
b	width of rectangular section, mm
b_w	minimum effective web width within depth d, mm
d	distance from extreme compression face to centroid of tension steel reinforcement, mm
D_c	core column dimension in the loading direction from center-to-center of peripheral horizontal reinforcement, mm
D_g	external diameter of circular column, mm

E_{FRP} modulus of elasticity of FRP, MPa

E_s modulus of elasticity of steel, MPa

f'_c specified compressive strength of concrete, MPa

f'_{cc} compressive strength of confined concrete, MPa

f_{frp} tensile stress in FRP , MPa

f_{frpu} ultimate tensile strength of FRP , MPa

f_{lfrp} ultimate confinement pressure due to FRP strengthening, MPa

f_{hy} yield stress of horizontal steel reinforcement, MPa

f_s stress in steel reinforcement at specified loads, MPa

f_y specified yield stress of steel reinforcement, MPa

h overall thickness of member, mm

k_e strength reduction factor applied for unexpected eccentricities

l_u unsupported length of compression member, mm

n number of legs of horizontal column ties in the loading direction

N_b number of layers of FRP sheet

P_D axial dead load, N

P_f factored axial load, N

P_L axial live load, N

P_{rmax} factored axial load resistance, N

r radius of comer, mm

S spacing of steel shear reinforcement measured parallel to the longitudinal axis of the member or the spiral pitch, mm

t_{frp} thickness of one layer of FRP reinforcement, mm

α_1 ratio of average stress in rectangular compression block to the specified concrete compressive strength

α_{pc} performance coefficient for circular columns

α_{pr} performance coefficient for rectangular columns

ε_{frp} strain in FRP reinforcement

ε_{frpe} effective strain in FRP reinforcement

Φ member resistance factor

Φ_c resistance factor for concrete

Φ_{frp} resistance factor for FRP

Φ_s resistance factor for steel reinforcing bars

λ factor to account for low density concrete

ω_w volumetric ratio of FRP strength to concrete strength

LIST OF TERMS

Building Performance Level: A limiting damage state, considering structural and nonstructural building components, used in the definition of Performance

Brittle Fracture: The tearing or splitting of a member with little or no prior ductile deformation.

Capacity: The permissible strength or deformation for a component action.

Confined Region: That portion of a reinforced concrete component in which the concrete is confined by closely spaced special transverse reinforcement restraining the concrete in directions perpendicular to the applied stress.

Damping: For floor vibrations, it is the rate of decay of amplitude.

Dead Load: Loads due to the weight of the components making up the structure and that are intended to remain permanently in place.

Deflection: The displacement of a structural member or system under load.

Deformation: The act of distorting or changing the shape or dimensions of a structural element or body resulting from forces or stresses.

Demand: The amount of force or deformation imposed on an element or component.

Design Earthquake Ground Motion: The earthquake affects that buildings and structures are specifically proportioned to resist

Drift: The lateral movement or deflection of a structure.

Drift Index: The ratio of the lateral deflection to the height of the building.

Ductility: Is the ability of a material to withstand large inelastic deformations without fracture.

Ductility Factor: The ratio of the total deformation at maximum load to the elastic-limit deformation.

Ductile Element: An element capable of sustaining large cyclic deformations beyond the attainment of its nominal strength without any significant loss of strength.

Non-ductile Element: An element having a mode of failure that results in an abrupt loss of resistance when the element is deformed beyond the deformation corresponding to the development of its nominal strength. Non-ductile elements cannot reliably sustain significant deformation beyond that attained at their nominal strength.

Dynamic Load: A load that varies with time, which includes seismic loads, and other loads created by rapid movement.

Effective Length: The equivalent length, KL, used in compression formulas. This method estimates the interaction effects of the total frame on a compression member by using K factors to equate the strength of a framed compression member of length L to an equivalent pin-ended member of length KL subject to axial load only.

Effective Length Factor (K): The ratio between the effective length and the un-braced length of a member measured between center of gravities of the bracing members. K values are given for several idealized conditions in which joint rotation and translation are realized.

Effective Moment of Inertia: The moment of inertia of the cross section of a member that remains elastic when partial plastification takes place.

Elastic Analysis: The analysis of a member, which assumes that material deformation disappears on removal of the force, that produced it and the material returns to its original state.

Equations of Equilibrium: The equations relating a state of static equilibrium of a member or structure when the resultant of all forces and moments are equal to zero. Three equations must be fulfilled simultaneously: Sum of the forces in the X-direction must equal zero, sum of the forces in the Y-direction must equal zero, and the sum of the moments about any point must equal zero for a two dimensional structure.

Factor of Safety: Is the ratio of the ultimate load for a member divided by the allowable load for a member and must always be greater than unity.

Factored Load: The product of the nominal load and a load factor.

Frame: A structural framing system consisting of members joined together with moment or rigid connections, which maintain their original angular relationship under load without the need for bracing in its plane. See Rigid Frame.

Frequency: A measure of floor vibration. It is the speed of the oscillations of vibration and is expressed in cycles per second or Hz (Hertz).

Hysteretic: A term that describes the behavior of a structural member subjected to reverse, repeated load into the inelastic range whose plot of load verses displacement is characterized by loops. The enclosed area within these loops indicates the amount of energy dissipated during inelastic loading.

Inelastic Action: Deformation of a material, which does not disappear when the force that produced it is removed.

Inelastic deformation. Occurs when an element deforms as force is applied, but does not return to its original shape after the force is removed.

Internal Pressure: The pressure inside a building, which is a function of the wind velocity and the number and locations of openings.

Inter-Story Drift: The relative horizontal displacement of two adjacent floors in a building. Inter-story drift can also be expressed as a percentage of the story height separating the two adjacent floors.

Load: An external force or other action acting on a member or structure. It can be from permanent construction, environmental effects, differential settlement, occupants, and material objects.

Load Combination: The combination of loads, which produce the worse loading condition in a structural member.

Modulus of Elasticity (E): Is the slope of the straight-line portion of the stress-strain curve in the elastic range found by dividing the unit stress in ksi by the unit strain in in/in. For all structural steels, the value is usually taken as 29,000 ksi. This is also called Young's Modulus.

Neutral Axis: The surface in a member where the stresses change from compression to tension, i.e., represents zero strain and therefore zero stress. The neutral axis is perpendicular to the line of applied force.

P-Delta Effect: The secondary effect of column axial loads and lateral deflection on the moments in structural members.

Poisson's Ratio: Defined as the ratio of the unit lateral strain to the unit longitudinal strain. It is constant for a material within the elastic range. For structural steel, the value is usually taken as 0.3. It gradually increases beyond the proportional limit, approaching 0.5.

Rigid Frame or Structure: A structural framing system consisting of members joined together with moment or rigid connections, which maintain their original angular relationship under, load.

Seismic Load: Are assumed lateral forces acting in any horizontal direction that produce stresses or deformations in a structural member due to the dynamic action of an earthquake.

Sequence of Yielding: A breakdown of when elements are to be yielded in a structure with one following after the other.

Static Load: A load applied slowly and then remains nearly constant.

Stiffness: The resistance to deformation of a structural member, which can be measured by the ratio of the applied force to the corresponding displacement.

Story: That portion of a building which is between the upper surface of any floor and the upper surface of the floor next above.

Story Drift: The difference in horizontal deflection at the top and bottom of a story divided by height of story.

Strain Hardening: The condition when ductile steel exhibits the capacity to resist additional load than that which caused initial yielding after undergoing deformation at or just above the yield point.

Stress: An internal force that resists a load. It is the intensity of force per unit of area.

Structure: A mechanism designed and built or constructed of various parts jointed together in some definite manner to carry loads and resist forces.

Ultimate Load: The force necessary to cause rupture.

Ultimate Strength: The maximum stress attained by a structural member prior to rupture which is the ultimate load divided by the original cross-sectional area of the member.

Vibration: The oscillating, reciprocating, or other periodic motion of a rigid or elastic body or medium such as a floor when its position or state of equilibrium has been changed.

Wind Load: A force or lateral pressure in pounds per square foot that is applied to a member due to wind blowing in any direction.

Windward: The direction or side toward the wind. (Opposite of leeward)

Yield Point (Fy): Is that unit stress at which the stress-strain curve exhibits a definite increase in strain without an increase in stress, which is less than the maximum attainable stress.

CHAPTER 1

1.1 Introduction

Moment resisting frames (MRF) are the most commonly used framing system for reinforced concrete structures. According to the current Canadian practice, designers have two options for the seismic design of reinforced concrete frames (National Building Code of Canada, NBCC 1995). The first option is to design a ductile frame, which involves special design and detailing provisions to ensure ductile behavior. The second option is to design a nominally ductile frame. This option involves designing for twice the seismic lateral load as that for ductile frames, but without taking all the special provisions for good detailing in the design of the frame members. By allowing such a choice, the Code implies that either type of frames will provide equivalent seismic performance under the design level earthquake disturbance. The seismic design lateral loads and the level of seismic reinforcement detailing incorporated in a reinforced concrete moment resisting framed structure depend on its available ductility capacity. In "ductile" moment resisting frames, the design lateral loads reduce significantly, but high ductility capacity is ensured through strict detailing requirements to avoid premature modes of brittle failure. For frames with "nominal ductility," the design loads are higher, but very little seismic reinforcement detailing is required. According to the seismic design philosophy of the National Building Code of Canada (NBCC 1995), both approaches should offer the same level of seismic protection against the design earthquake at the construction site. Design procedures as prescribed by NBCC(1995) is discussed in Appendix A.

1.2 Objective

Reinforced concrete buildings designed according to early seismic provisions or, sometimes, without any seismic provision, have usually low strength and, in most cases, show limited ductility. Very often details are poor and, consequently, the critical zones do not behave in a ductile way, showing brittle mechanisms of failure. Because of these problems, the assessment of existing reinforced concrete (RC) structures requires a retrofitting procedure. A summary of models of the non-linear behavior of RC structures is discussed. A retrofitting is scheme accounts for the most important mechanical phenomena affecting the non-linear behavior of the RC frames. The influence of different

strength, ductility and deformation sources on the global behavior of existing buildings is studied and the needed capabilities of the retrofitting models are studied.

The objective of this investigation is to compare the levels of seismic behavior which ductile, nominally ductile and gravity load designed (GLD) frames, contribute to the evaluation of the levels of damage in RC structures. Finally, evaluate ways to retrofit non-ductile GLD frame buildings in order to improve their seismic resistance and performance by using FRP wrapping. Also, provide guidelines that can be used for the strengthening of reinforced concrete structures using externally fiber reinforced polymer (FRP) laminates or sheets. To achieve this aim, three five story concrete MRF are designed according to NBCC 1995, CAN3-A23.3 (1994) and ACI (prior 1971). Each of the frames is subjected to seismic lateral loads, wind and gravity loads. This investigation compares the behavior of these frames using a nonlinear "pushover" and time-history analysis. The seismic behavior of ductile, nominally ductile frames, GLD and retrofitted GLD and damage on each structure due the seismic loads is investigated.

1.3 Scope

The purpose of this study is to develop guidelines that can be used for strengthening of reinforced concrete structures using externally bonded fiber reinforced polymer (FRP) laminates or sheets. To achieve this goal, a series of inelastic pushover and time-history dynamic analyses carried out to evaluate inelastic behavior and seismic performance of the ductile, nominally ductile, gravity load designed (GLD) and retrofitted GLD frames. First, the needs for ductility and its proper use are discussed. Then emphasizing the importance of recognizing the differences of ductile and nominally ductile with GLD and retrofitted GLD RC moment resisting frames, deformability, ductility, and ductility ratio, as well as their interrelationship are studied in the literature review.

CHAPTER 2

Literature Review

2.1 Introduction to Earthquake Resistance Design

An earthquake (EQ) causes the ground under a structure to move rapidly back and forth imparting accelerations, "a", to the base of the structure. If the structure is completely rigid, forces of magnitude "F = ma" would be generated in it, where m is the mass of the structure. Since real structures are not rigid, the actual forces generated will differ from this value depending on the matching of the period of the building with the dominant periods of the earthquake. The determination of the force, F, is made more complicated because of any earthquake contains a wide and unpredictable range of frequencies and intensities of base acceleration. For buildings having short fundamental periods, the maximum acceleration may be several times the ground acceleration. Since severe earthquakes may have maximum ground accelerations range from 0.2g to 0.4g, this implies that the horizontal earthquake forces could be as large as or larger than the weight of the building, if the building remains elastic. The actual forces used in the design of buildings for earthquakes are smaller than indicated because inelastic action in structure tends to dissipate the earthquake forces. It is well recognized and accepted that in EQ-resistant design all structural members, their connections and supports should be designed (sized and detailed) with large ductility and stable hysteretic behavior so that the entire structure will also be ductile and display stable hysteretic behavior. There are two main reasons for this requirement. First, it allows the structure as a whole to develop maximum potential strength, which given by the summation of the maximum strength of each component. Secondly, large structural ductility allows the structure to move as a mechanism under its maximum potential strength, which results in dissipation of large amounts of energy. For clarity and convenience in discussing the reasons for this concern, a glossary of the terms that used in this study is given below.

Deformability is the capability of a material, structural component, or entire structure to deform before rupture (Bertero, V.V., 1988).

Ductility is the ability of a material, structural component, or entire structure to undergo deformation after its initial yield without any significant reduction in yield strength (Bertero, V.V., 1988).

The ductility ratio is the ratio of the maximum deformation that a structure or element can undergo without a significant loss of initial yielding resistance to the initial yield deformation (Bertero, V.V., 1988).

2.2 Elastic and Inelastic Behavior of Structures

The behavior of a structure under cyclic load is very similar to the behavior of a pendulum. Assume an un-damped elastic pendulum is deflecting to right. Its energy is stored in it in the form of strain energy. The stored energy is equal to the shaded area under the load- deflection diagram as shown in Figure 2.1(a). When the pendulum suddenly moves back to its original position, this energy re-enters to the system as kinetic energy and helps drive the pendulum to the left. This pendulum oscillates back and forth tracing a single linear path along the load-deflection diagram as shown in Figure 2.1(a). If the pendulum develops a plastic hinge at its base, the load-deflection diagram for the same lateral deflection would be as shown in Figure 2.1(b). When this pendulum suddenly moves back to its original position, only the energy indicated by the triangle *a-b-c* re-enters the system as kinetic energy, the rest being dissipated by plastic deformations, friction, heat, crack development. Studies of hypothetical elastic and elastic-plastic buildings subjected to a number of different earthquake records, suggest that the maximum lateral deflections of the elastic and elastic-plastic Structures are roughly the same. Figure 2.2 compares the load-deflection diagrams for an elastic structure and an elastic-plastic structure subjected to the same lateral deflection Δ_u. The ratio of the maximum deflection, Δ_u, to the deflection at yielding, Δ_y, is called the displacement ductility ratio, μ, $\mu = \Delta_u / \Delta_y$

From Figure 2.2 it can be seen that for a ductility ratio of four, the lateral load acting on the elastic-plastic structure would be 1/4 of that of the elastic structure, and the energy recovered in each cycle would be 1/16 great as than that of. Thus, if the structure is ductile, it can be designed for lower seismic forces.

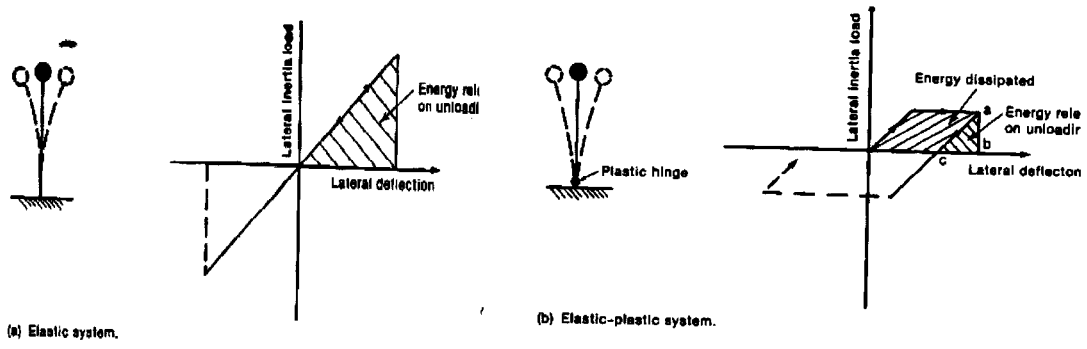

(a) (b)

Figure 2.1 Elastic and inelastic behaviors (MacGregor, J.G, 2000)

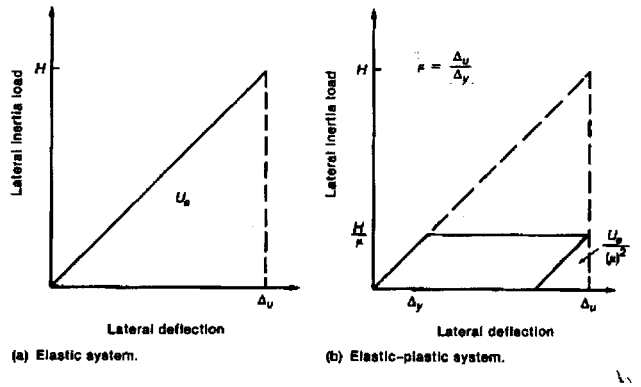

Figure 2.2 Load-deflection diagrams (MacGregor, J.G, 2000)

2.3 Design and Detail Provisions for Ductile and Nominally Ductile Frames

The different approaches used in the design of ductile and nominally ductile frames are briefly described here.

No special seismic design provisions are considered in design of nominally ductile frames. All the design actions are directly obtained from the results of the elastic static analysis. Detailing requirements are far less strict than those of the ductile frame. The main features in the design of nominally ductile frame are included as follows:

- Beams and columns must satisfy nominal detailing requirements (A23.3 Cls. 21.9.2.1 and 21.9.1.2)
- Beams and columns must have minimum shear strength (A23.3 Cl. 21.9.2.3)
- Joints must satisfy nominal detailing requirements and must be capable of transmitting shears from beam hinging (A23.3 Cl.1.9.1.2.4)

The main aim of designing ductile frame is to avoid brittle failure and story side-sway mechanisms (Hamdy K.A., 1991). The main features of the design methodology are included as follow:

- Strong columns-weak beams
- Design shear forces based on the probable strength of probable plastic hinges
- Good detailing
- Beams capable of significant flexural hinging (A23.3 21.3 and 21.7 Cls.)
- Columns properly confined and stronger than the beams (A23.3 21.4 and 21.7 Cls.)
- Joints properly confined and capable of transmitting shears from earn hinging (Cl. 21.6)

The factors affecting the ductility of RC are included as:

- The ductility of a beam increases as the ratio ρ/ρ_b goes down and as ρ/ρ' goes up where ρ_b is the reinforcement ratio for balance failure and ρ' is the ratio of compression reinforcement.
- The hoops provide confinement of core concrete, increasing beams ductility

The compressive strength of the concrete shall not exceed 55 MPa (A23.3 Cl. 21.2.3.1) because some high-strength low-density concretes display brittle crushing failures, the strength of low-density concrete shall not exceed 30 MPa unless good behavior is documented (A23.3 Cl. 21.2.3.2). Canadian Standard A23.3 Cl. 21.2.4.1, requires that the reinforcement resisting earthquake-induced force effects in frame members and walls in structures designed with force magnification factors R greater than 2.0, shall be weld able grade steel satisfying CSAG30.18 because weld able steel has better ductility than that of the regular grade steel and it has a controlled maximum yield strength

2.4 Capacity Design Provisions

Earthquake motions cause the structure to deform. In doing so, loads are induced in those members that resist the deformation. The most severely loaded members must be designed to dissipate energy through large plastic deformations without rupturing. Thus, the most severely loaded members act as fuses in the system, which prevent large load effects from occurring on members that would fail in a brittle manner, causing collapse. This design philosophy referred to as capacity design. Canadian Standard A23.3 Cl.

21.2.1.2 requires that structures in seismic regions be designed using capacity design. Because the detailing of the hinging regions is tedious to ensure adequate ductility, only few sections are designed to yield under the seismic loads, with the rest of the structure having enough strength to remain elastic. This means, the capacities of all the elements in the structure should exceed the capacity of the critical element that the designer wants to yield first.

If plastic hinges form in columns, the axial force causes a rapid degradation of the ability of the hinge to absorb energy while undergoing cyclic motions. As a result, the design of ductile moment-resisting frames attempts to force the structure to respond in what is referred to as strong column-weak beam action in which the plastic hinges induced by the seismic forces, will form at the ends of the beams, as shown in Figure 2.3. The hinging regions detail to allow the plastic hinges to undergo yielding in both positive and negative moment.

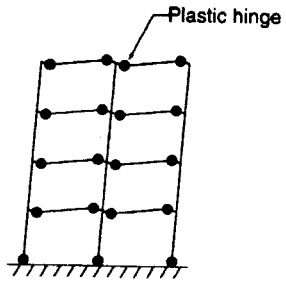

Figure 2.3 Plastic hinges

2.4.1 Flexural Members

Canadian Standard, A23.3 Cl. 21.3.1 defines a flexural member as the one proportioned to primary resist flexural loads with a factored axial compressive force of less than $(A_g f'_c/10)$.

Geometric limitations placed on the span-to-depth ratio ($l_n \geq 4d$) to avoid deep beam action. In addition, the width-to-depth ratio is limited ($b/d \geq 0.3$). Finally, the width of the member should not be either less than 250 mm, or more than the width of the supporting member plus 3/4d on either side. All of these limitations are intended to provide members that perform adequately in flexure.

Flexure reinforcement must satisfy the detailing requirement of the A23.3Cl21.3.2 such as:

- At least two bars must be provided continuously at the top and bottom.
- The areas of each of the top and bottom reinforcement at every section shall not be less than $1.4b_wd/f_y$. The reinforcement ratio, $\rho = A_s/bd$, shall not exceed 0.025 for either the top or bottom reinforcement. Normally, ρ would not exceed 0.015, and the upper limit of ρ is 0.025 for Grade 400 steel and most concrete strengths.
- The positive moment strength at the face of the beam-column joint shall not be less than half of the negative moment strength. This provides $\rho' \approx 0.5\rho$ and greatly improves the ductility of the ends of the beams
- At every section, the positive and negative moment capacity should not be less than one- fourth the maximum moment capacity provided at the face of joint.

Transverse reinforcement is required to confine the concrete and prevent buckling of the compression bars in the hinging areas (A23.3 Cl. 21.3.3), also to provide adequate shear strength. Hoops for confinement and to control buckling of the longitudinal reinforcement are required for the following cases:

- Over a length equal to 2d from the face of supports
- Over the length of regions where plastic hinges may occur, and for a distance of "d" on each side of these hinging locations
- At lap splices
- The spacing of the hoops is specified in A23.3 Cl. 21.3.3.3 in the rest of the beam either stirrups or hoops are required at a maximum spacing of d/2.
- Canadian Standard, A23.3 Cl. 21.1 defines a seismic hook as a hook on a stirrup, hoop, or cross-tie having a bend not less than 135° with a six bar-diameter (but not less than 100 mm) extension that engages the longitudinal reinforcement and projects into the concrete in the interior of the stirrup or hoop.
- A seismic cross-tie is defined as a continuous reinforcing bar having a seismic hook at one end and a hook not less than 90° with at least a six-diameter extension at the other end
- A hoop is a closed tie or a continuously wound tie. A closed tie can make up of several reinforcing elements each having seismic hooks at each end.

2.4.2 Columns

A23.3 Cl. 21.4 applies to columns in frames resisting earthquake forces and supporting a factored axial force exceeding $(A_g f'_c/10)$. Columns in frames in regions of high seismic

risk must satisfy two geometric requirements. The smallest dimension through the centroid of the column must be at least 300 mm and the ratio of shortest to longest cross-sectional dimensions shall not be less than 0.4. These limits ensure a minimum robustness and prevent lateral tensional buckling, which might occur with rectangular columns.

It is highly necessary that plastic hinges form in the beams rather than in the columns. Because the dead load must always transfer down through the columns and the damage to the columns should be minimized. Canadian Standard, A23.3 Cl. 21.4.2.1 strongly encourages the use of a strong column-weak beam design. Strong column-weak beam behavior is assured by ensuring $\sum M_{rc} \geq 1.1 \sum M_{nb}$

where $M_{rc,}$ is the factored moment resistance of the columns corresponding to the factored seismic load combination leading to the lowest axial load and to the lowest flexural strength. M_{rc} is computed using $\Phi_c = 0.6$ and $\Phi_s = 0.85$

M_{nb} is the nominal flexural resistance of the girder at the joint, calculated using $\Phi_c = 1.0$ and $\Phi_s = 1.0$. Columns that do not satisfy this equation must have transverse reinforcement satisfying A23.3 Cl 21.4.4 over their entire length. Since there is a possibility of the cover concrete spalling in the regions near the ends of the column, lap splices are permitted only in the center half of the column height (A23.3Cl. 21.4.3.2)

Transverse reinforcement in the form of spirals or hoops must be provided over a height of l_o from each end of the column to confine the concrete and restrain the longitudinal bars from buckling. The height l_o is the greater of (A23.3 Cl. 21.4.4.5)

- The depth of the column at the face of the joint, or at the section where flexural yielding may occur
- One-sixth of the clear span (height) of the column, or
- 450 mm

Within the length l_o, A23.3 Cl. 21.4.4.3 requires that the spacing of the transverse reinforcement shall not exceed:

- One-fourth of the minimum thickness of the column
- 100 mm
- 6 times the diameter of the smallest longitudinal bar

- 40 mm cover, for columns larger than 710 mm in diameter because the pressure on the insides of the hoops causes the sides of the hoops to deflect outward, hoops are less efficient than spirals at confining the core concrete

2.4.3 Joints

A23.3 Cl. 21.6.1.2 requires that joint forces be calculated by taking the stress in the flexural reinforcement in the beams as 1.25 f_y. This is analogous to using the probable strength in the calculations of shear in columns and beams in ductile frames. Canadian Standard, A23.3 Cl. 21.6.5 .6 limits the diameter of the longitudinal beam and column reinforcement that passes through a joint to $d_b \leq l_j/24$, where l_j is the width of the joint parallel to the beam or column bars. When hinges form in the beam, the beam reinforcement is stressed to the actual yield strength of the bar on one side of the joint and is stressed in compression on the other side. This results in very large bond stresses in the joint, possibly leading to slipping of the bar within the joint. The minimum bonded length of such bar in a joint is $24d_b$, which is considerably less than required by the development-length. Canadian Standard, A23.3 Cl. 21.6.2.1 requires hoop reinforcement around the column reinforcement, in all joints in ductile moment-resisting frames.

2.5 Performance Parameters and Criteria

Structural Engineers Association of California, (SEOAC), Vision 2000 Committee 1995 has proposed a performance-based approach to seismic design. Performance level is an expression of the maximum permissible extent of damage to a building when it is subjected to specific seismic design. Performance levels are defined as operational, life safe, near collapse and collapse (Brian Stonehouse B., 1998). Each has an associated damage state, ranging from negligible to complete. The maximum permissible transient inter-story drifts expresses as a percentage of story height. Three intermediate performances are as follow:

- Operational performance, 0.5% drift, light overall building damage, negligible damage to vertical load carrying elements, original strength and stiffness retained in lateral load carrying elements with minor cracking/yielding of structural elements.

- Life safe performance, 1.5% drift, moderate overall building damage, light to moderate damage of vertical load carrying elements with substantial capacity to carry gravity loads, some reduction of residual strength and stiffness in lateral load carrying element.
- Near collapse performance, 2.5% drift, severe overall damage, moderate to heavy damage of vertical load carrying elements, which continue to support gravity loads, negligible residual strength and stiffness in lateral load carrying element.

2.5.1 Performance Requirements of Buildings

A structure fails when its resistance reaches to failure point. A strong but brittle system and a weak but ductile system, shown in Figure 2.4, may equally survive an earthquake ground motion without collapse as long as the maximum response does not exceed the failure point.

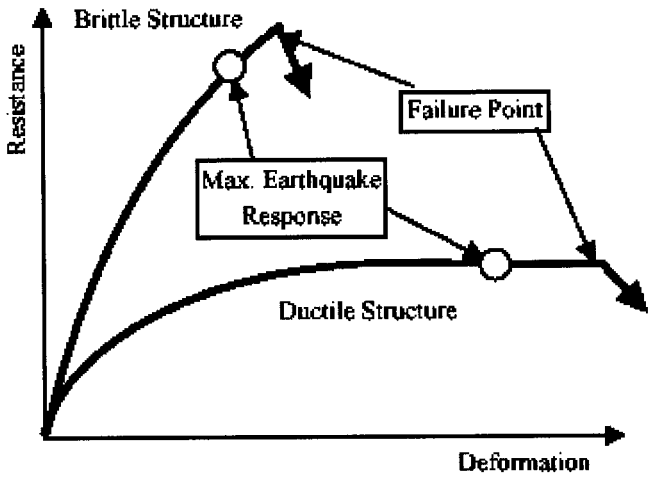

Figure 2.4 Earthquake resistance of structures (Otani, S., 2001)

Since the 1960s, it has believed that it is not feasible to design a building structure to remain elastic under intense ground motions. Therefore, seismic design has aimed that the structure should not suffer any structural damage (serviceability limit state) from frequent minor earthquakes. The structure, with the repair of damage, should be usable after an infrequent earthquake of major intensity, and the structure should not collapse (life safety limit state) for the safety of occupants during the largest possible earthquake at the construction site.

2.5.2 Minimum Strength and Ductility

Figure 2.5 shows schematically the expected performance of a building under frequent, infrequent, and very rare earthquake motions. A certain minimum resistance is necessary to limit the damage from frequent minor ground motions. Architectural elements, such as non-structural curtain walls, partitions and mechanical facilities, must be protected for continued use of a building after an earthquake.

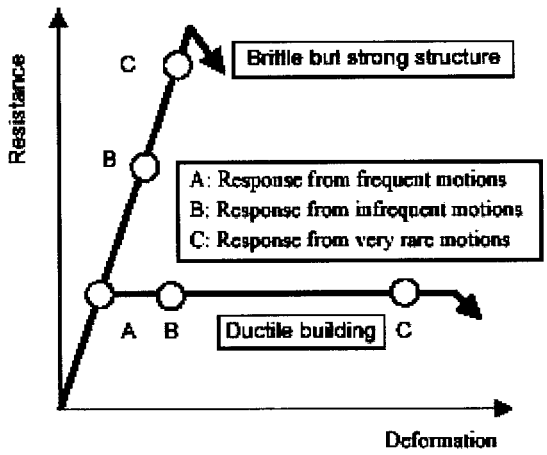

Figure 2.5 Performance objectives of building (Otani, S., 2001)

For the prevention of collapse, high resistance is necessary for a brittle structure and low resistance may allow for a ductile structure. The high lateral force resistance can be achieved by the use of structural walls. The deformation capacity of RC buildings has believed to be so small that sizeable lateral resistance must be provided in design to limit the plastic deformation. Therefore, it has normally believed that a reinforced concrete structure can satisfy serviceability requirements if the structure is designed to survive the maximum possible earthquake.

With understanding of reinforced concrete behavior, however, good reinforcement detailing has enforced in design and construction to enhance the deformation capacity. Therefore, a reinforced concrete building sometimes designs with low lateral resistance counting on ductility. It becomes essential that a structural engineer should examine the serviceability limit state from frequent but low-intensity earthquake motions and the level of structural damage from infrequent but major-intensity earthquake motions.

The lateral force resistance of a building is required in a building code, taking into account seismic risk, soil condition at construction site, building period, anticipated ductility and acceptable level of damage in a building, and structural irregularity. The level of minimum lateral resistance should be determined to control the serviceability of buildings from frequent earthquake motions and to protect the occupant's life by limiting the nonlinear deformation from the maximum possible earthquake motion. The design must satisfy, in addition to the minimum code requirements, the performance requirement set up by a building owner. The recent performance-based engineering emphasizes the protection of function in a certain kind of buildings for the continued operation and usage after major earthquake motions. This is important in design and construction of, for example, hospitals, computer and information centers, and disaster management facilities. The use of higher design earthquake forces may reduce the structural damage, but it is not sufficient to protect the function of the building. New technology such as base-isolation and energy dissipating devices and auto-adaptive media is available to achieve this purpose.

2.6 Fiber Reinforced Polymers (FRP)

2.6.1 Introduction to FRP

Fiber reinforced polymers (FRP) contain high-resistance fibers embedded in a polymer resin matrix and are produced as sheets, plates and laminates. They are rapidly becoming the materials of choice for the strengthening and rehabilitation of civil engineering structures. These lightweights, high-strength materials are attractive because of their resistance to corrosion, durability and easy installation (Matsuzaki, Y., 2000). Despite their relatively recent entry into civil engineering construction, FRP repair and strengthening methods are gaining wide acceptance as effective and economic infrastructure rehabilitation technologies. Indeed, the most remarkable development over the past few years in the field of FRP strengthening and repair has been the rapidly growing acceptance worldwide of these new technologies for an enormous range of practical applications. FRP rehabilitation projects have been extremely varied in nature and have included, for example, column and beam strengthening, seismic retrofitting, the FRP repair of corrosion-damaged beams and columns, as well as applications to numerous structural components. It is important to note, however, in this research

assumed the design procedures perform mainly on new concrete elements and not damaged ones. In some cases, the structural elements have been loaded or artificially aged to introduce damage before being strengthened. It should be noted that each FRP strengthening or repair project is unique due to the loading history, the conditions of the materials and the particular strengthening or repair requirements. The use of an FRP strengthening scheme should therefore take into account for the quality of the existing concrete and the site conditions for the installation of the FRP.

2.6.2 General Requirements

The following technical documents and drawings are required for the strengthening of reinforced concrete structures using FRP (Kenneth, N., 2001).

- Identification of the FRP to be used
- Required FRP mechanical properties
- Mechanical properties of the existing structural materials
- Location of the FRP strengthening with respect to the existing structure
- Dimensions and orientation of each layer of the FRP strengthening system
- Number of layers and sequence of installation
- Location and length of overlaps
- Summary of the considered design loads, allowable stresses, etc.
- Surface preparation requirements including the rounding of comers
- Installation procedure including surface temperature and moisture conditions and the minimum and/ or maximum delay between the installations of consecutive layers
- Required curing
- Surface finishing
- Transportation, storage, handling and pot life of resins
- Quality control, supervision and field-testing
- Load testing when required.

2.6.3 Evaluation of Existing Structures

In order to develop an appropriate FRP strengthening strategy first, an assessment of the existing structure or elements should be conducted to determine the condition of the existing concrete, to identify the causes of any deficiencies, to establish the load carrying capacity of the structure, and to evaluate the feasibility of using externally bonded FRP systems. The actual strength and properties of all the materials of the existing structure must be evaluated as well. The design of the FRP reinforcement should take into account any damage to the existing structure or materials. In the case of signs of possible steel corrosion, the design must take into account the possible reduction of the reinforcing bar section and a decrease of the bond between the concrete and the reinforcing bars.

2.6.4 Concrete Surface

The condition of the concrete surface is one of the most important aspects to be considered for strengthening a structure. Indeed, the concrete must be able to transfer the load from the structure to the FRP strengthening system. When the concrete is excessively cracked and/ or deteriorated, it must be replaced in the affected zones to obtain an adequate concrete tensile strength as required for the application of the FRP reinforcement. In some cases, the removal of an old concrete cover to the reinforcing bars and its replacement by a new one are essential preliminary steps to the strengthening of the structure. In applications involving confinement of concrete elements, the surface preparation should guarantee a continuous intimate contact between the concrete and the FRP confinement system.

In general, the preparation of the concrete surface prior to the installation of the FRP system may vary from one material to another. The following considerations must be approved before the installation process may proceed.

- The concrete surfaces must be free of particles and pieces that no longer adhere to the structure
- The surfaces must be cleaned from oil residuals or contaminants
- The concrete surfaces must be repaired or reshaped according to the original section with the material indicated in the plans
- Sections with sharp edges must be rounded to a minimum radius of 35 mm before installing the FRP system

- The crack widths of 0.3 mm and greater can affect the performance of the externally bonded FRP system through fiber crushing, especially when relatively high temperature gradients and vibrations are present
- Cracks wider than 0.3 mm should be pressured inject with epoxy. Smaller cracks submitted to aggressive environments (for example salts and chemical products) may also require injection in order to prevent corrosion of the steel reinforcement
- All laitance, dust dirt, oil, curing compound, existing coatings, and any other matter that could interfere with the bond of the FRP should remove
- An optimal surface roughness must be obtained. The surface should be blasted and cleaned prior to the FRP installation so that no additional materials, which could interfere with the bond, are re-deposited on the surface
- The concrete surface to which the FRP will apply should be generally smooth and small holes and voids should be filled with putty or a mortar polymer
- Rectangular cross-sections should have corners rounded or reshaped to a minimum radius of 35 mm to prevent stress concentrations in the FRP sheet and voids between the FRP and the concrete substrate. Roughened corners should smooth with an epoxy gel
- All surfaces to which the strengthening system will be applied should be dry before the resin system can be applied and concrete is considered dry 24 hours after the removal of the surface water

- Whenever there is a leakage of water through the concrete mass, special resins adapted to the actual leakage must be used
- The flatness, roughness and cleanliness prescribed for dry conditions must be assure.

2.6.5 Installation Procedures of FRP Systems

Appropriate installation procedures should be specified depending on FRP system and the specific structure involved. The temperature, humidity and moisture point at the time of installation can affect the performance of the FRP system. Resin and adhesive materials should not be applied to wet surfaces. The installation procedures of FRP systems are as following steps:

- Where is required, a primer should be applied to all areas on the concrete surface. The primer should be placed uniformly on the prepared surface at the specified rate of coverage. The Primer is composed of two parts, Part A that is a resin and Part B that is a hardener.
- Putty should be used in an appropriate thickness and sequence with the primer as recommended by FRP manufacture. Putty is used only to fill voids and smooth surface discontinuities prior to the application of other materials. Rough putty edged should be smoothed.
- The saturating resin should be applied uniformly to all prepared surfaces where reinforcing material is going to be placed. The sheets should become fully impregnate with resin prior to curing. The sheets can impregnate in a separate process before bonding to the concrete surfaces. In case of multiple layers of FRP, all layers must be fully impregnated within the resin system, so that the resin shear strength is sufficient to transfer the shear load between layers, and the adhesive strength is sufficient to FRP to concrete.
- Entrapped air between layers should be released or rolled out before resin sets.
- A minimum parallel overlapping of fibers must be assured when there is a discontinuity of the material for a given layer. The length of overlap specified by the designer should follow the recommendations of manufacture.
- For the confinement of columns, a minimum length of overlap parallel to the fibers must be assured between the beginning and the end of the same wrapped strip, regardless of the number of layers involved.
- For wrapping RC columns at their base in contact with the ground, the wrapping must be extended at least 500 mm below the surface level to protect the interior reinforcement of column from corrosion.
- FRP sheets are typically installed with an adhesive. The adhesive should be applied uniformly to the prepared surfaces where the sheets are going to be placed. The adhesive should be applied in rate recommended by the manufacture to ensure the full bonding of successive layers.

CHAPTER 3

Structural Configuration

3.1 Description of Building:

The three cases of study are considered in this investigation. As shown in Figures 3.1 and 3.6, each structure is assumed to be part of the lateral load resisting system of a building, with three bays in the E-W and the N-S directions. In the E-W direction, the bay widths are 7.0 m and 8.0 m and in the N-S direction are 6m. The building is five stories high. The story height is 4m for first floor and 3m for other stories resulting in a total building height of 16m. Plan dimensions are shown in Figure 3.1. The material properties are assumed to be constant throughout the height of the structure. The seismic loading assumes to be acting in the N-S direction. The typical interior N-S frame of building is designed as: I) ductile, II) nominally ductile and III) gravity load designed frame (GLD). This is resulted in three different frames. More details of the various assumptions and material properties of the structures are listed in Tables A.1 and A.2 of Appendix A.

3.2 Lateral Loads and Base Shear

The NBCC 1995 seismic base shear is given by:

$V = (V_e / R)\, U$

Where V_e is equivalent lateral seismic force representing elastic response, R is force modification factor (given R =2 for nominal ductile frame and R= 4.0 for ductile moment resisting frame structures), U= 0.6 is a calibration, V_e is the elastic lateral seismic force, which is given by:

$V_e = vSIFW$

Where v = 0.40 is zonal velocity ratio. Building is assumed to be located in the highest seismic zone. s is seismic response factor = $1.5 / \sqrt{T}$ for $T \geq 0.5$ seconds (given T = 0.1, N = 0.5 seconds, S = 2.121). T is the fundamental period of vibration, N is the total number of stories above the grade, I the is seismic importance factor assumed to be 1.0 as the building is intended for typical office occupancy, foundation factor is assumed to be F= 1.3, as the structure is assumed to be built on soft base soil. The dead load (W) of the building is calculated as 15482 kN. The calculated base shears are 5122.6 and 2561.3 kN for nominally ductile and ductile frame respectively. NBCC 1995 requires that the lateral loads to be distributed over the building height as follows:

$F = (V - F_t)\, h_x\, W_x / (\Sigma h_i\, W_i)$

Where, F_x is lateral force applied at level x, F_t = additional lateral force applied to the top of building (Ft = 0.0 if $T \leq 0.7$ seconds), W_i and W_x are portions of W at levels x and i respectively, h_i and h_x are the heights above the base to levels x and i respectively. The results of designed seismic lateral loads on frame-B for both cases of study are listed in Table A-4 of appendix A. NBCC 1995 requires that the effects of torsional moments be included in the design of the lateral force resisting system. Since there is no eccentricity in building, the accidental applied torsional moment is calculated using following formula at each level (x):

$T_x = (F_x)\ (\pm 0.1 D_{nx}) = 2.2\ F_x$

Where, D_{nx}=22m is Plan dimension of the building in the direction of the computed eccentricity. The calculated shear induced due to torsion is listed in Table A.3 of appendix A.

3.3 Initial Elastic Modeling

Initial elastic analysis of both structures is performed in order to determine the structural elements seismic design forces. The finite element based, structural analysis program SAP2000 (Version 8.0, 2002) used to determine initial element forces. Factored moments, including earthquake effects from an elastic frame analysis obtained using SAP 2000, are given in Tables A.4, A.6, A.7 and A.9 of Appendix A

3.4 Dimensions and Reinforcement Details of Beams and Columns

The general layout of reinforcement in beams and typical columns for both frames are shown in Figures 3.1 through 3.6.

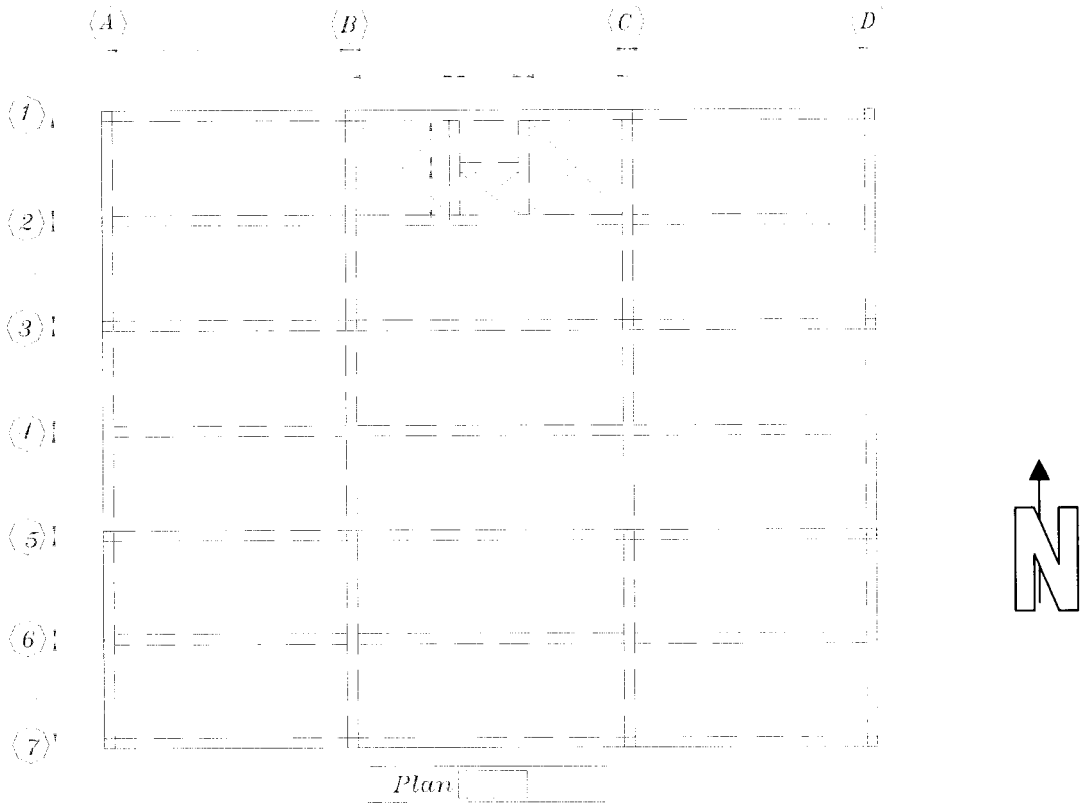

(a)

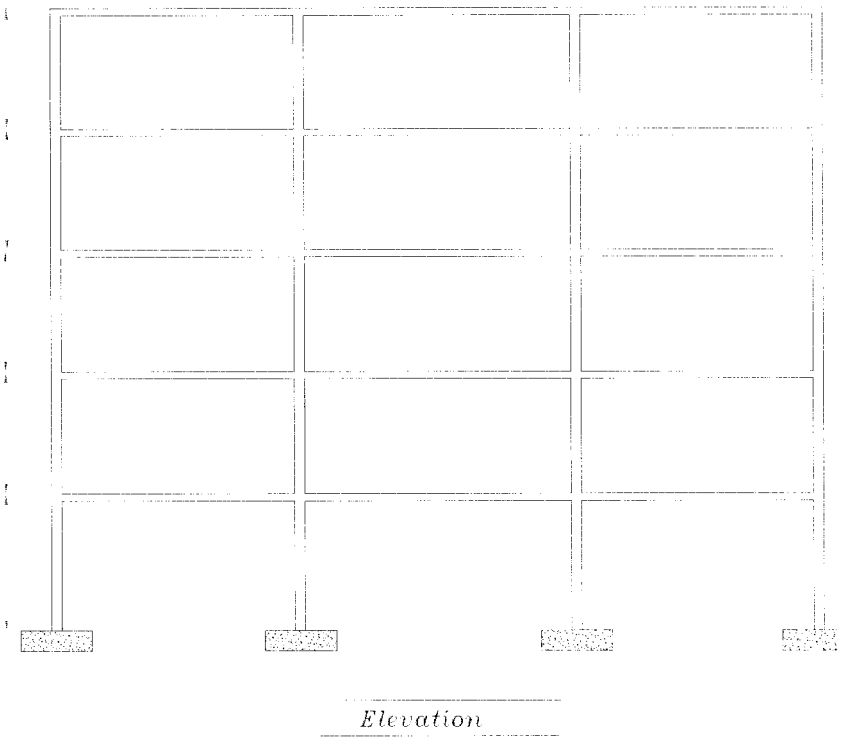

(b)

Figure 3.1 Plan view and elevation of the structures

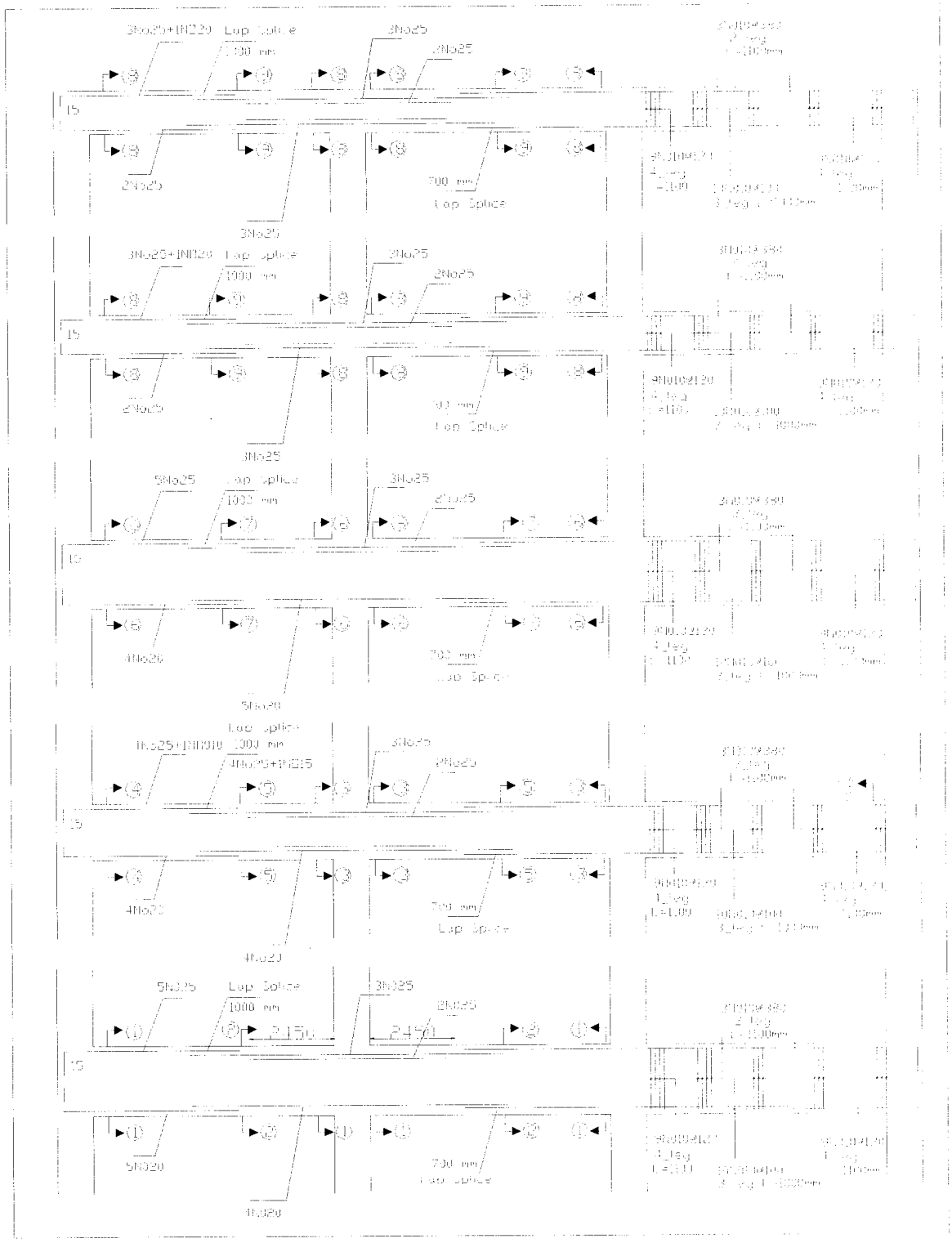

Figure 3.2 Detailing of flexural reinforcement in beams (ductile frame)

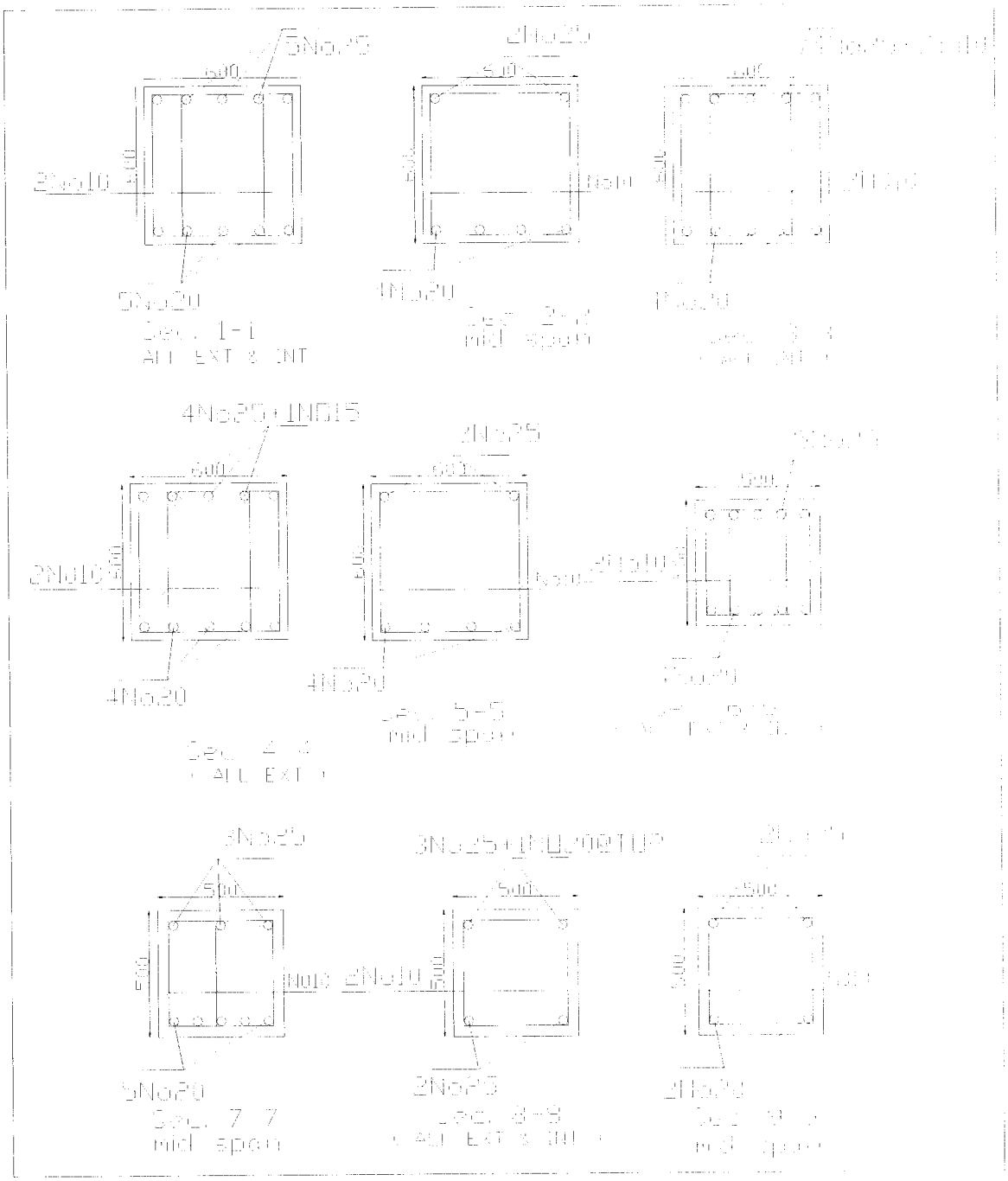

Figure 3.3 Detailing beams for seismic design (ductile frame)

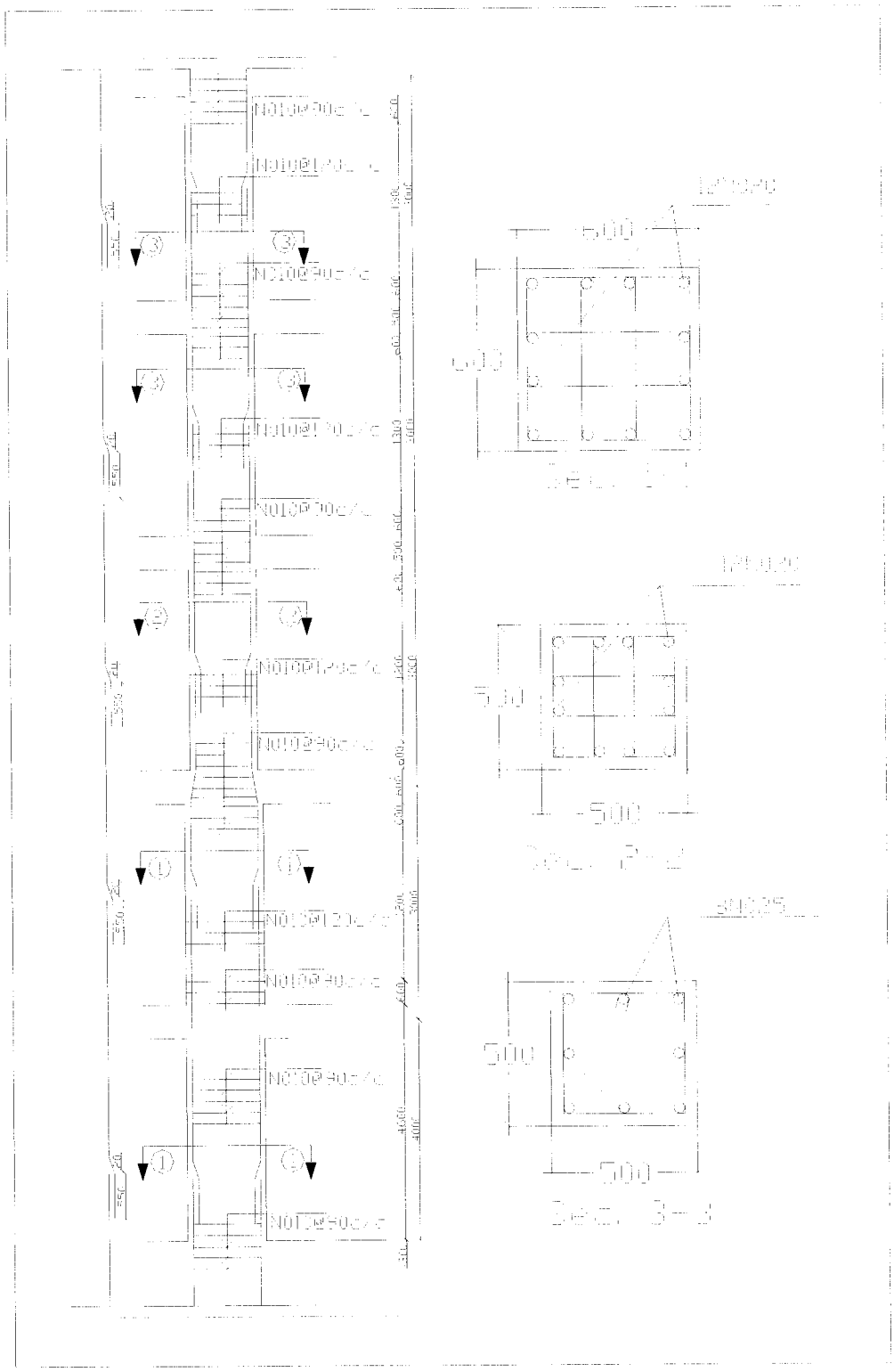

Figure 3.4 Column schedule (ductile frame)

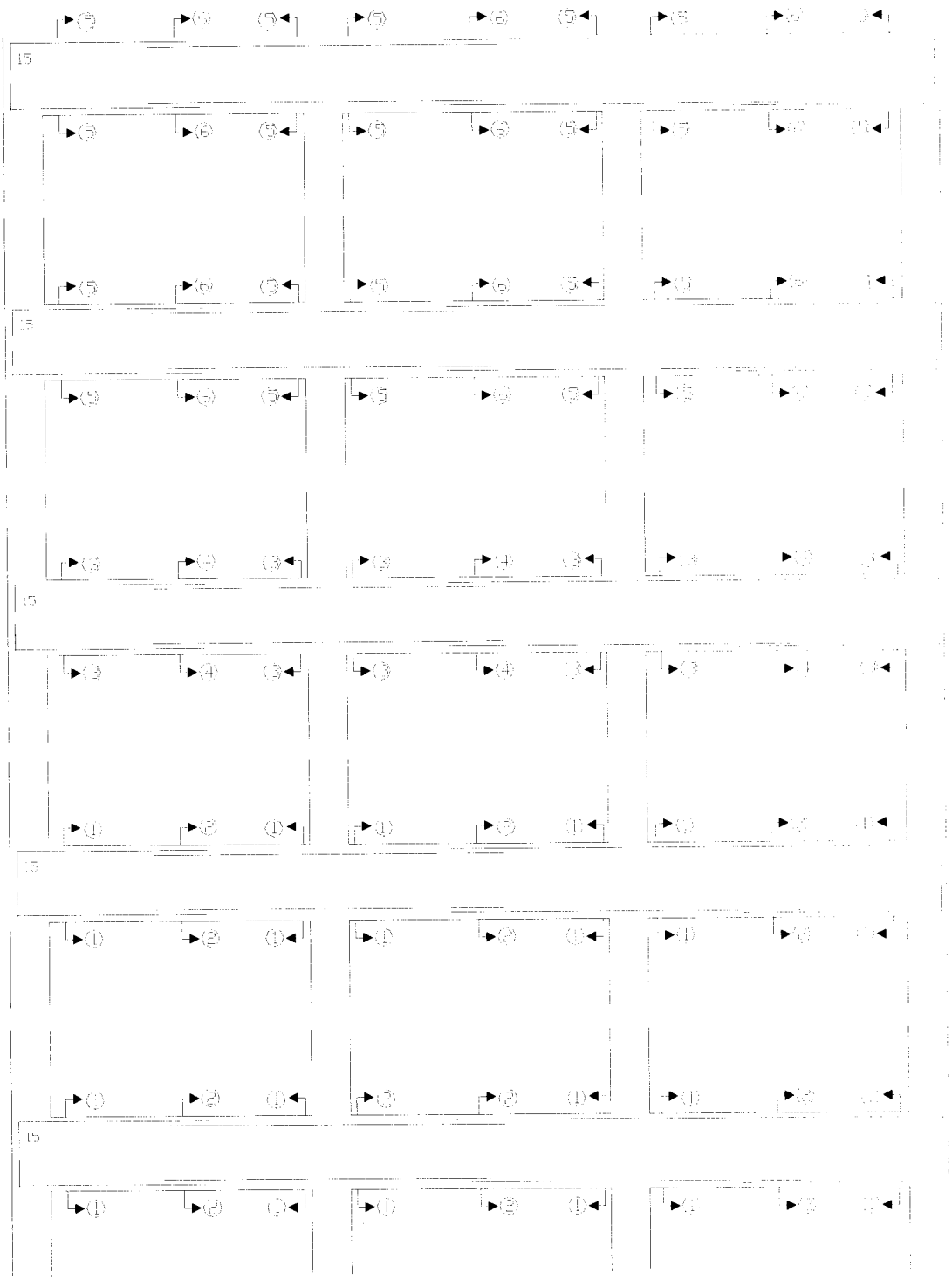

Figure 3.5 Detailing of flexural reinforcement in beams (nominally ductile frame)

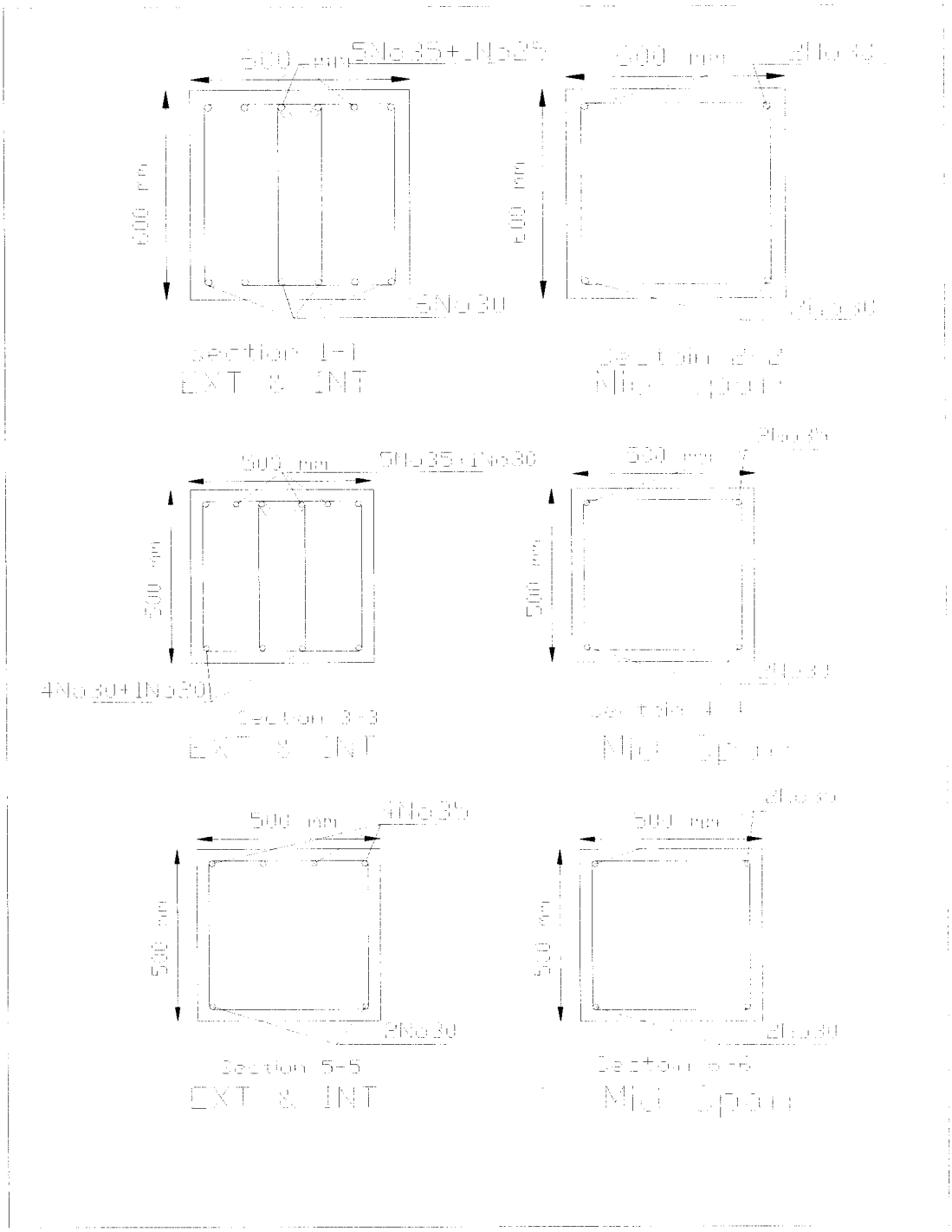

Figure 3.6 Detailing of beams for seismic design (nominally ductile frame)

CHAPTER 4
Pushover Analysis

4.1 Nonlinear Pushover Analysis

The inelastic nonlinear dynamic analysis program IRDAC is used to calculate the inelastic response of both structures (Ductile and Nominally Ductile frames) subjected to pushover loading. The pushover analysis, or collapse mode analysis is a simple and efficient technique to predict the seismic response of structures. A pushover analysis can obtain the resistance of the building against lateral loads, ductility capacity of structure and sequence of component yielding. The pushover analysis may be carried out using either force control or displacement control. In the investigation the structure, is subjected to an incremental distribution of lateral forces and the incremental displacement are obtained. With the increase in the magnitude of the loading, damages and failure modes of the structure are investigated. The pushover loading is inverted triangular with the effects of the cyclic behavior and load reversals being estimated by using a modified monotonic force-deformation criteria. A pushover analysis is performed on each structure to determine the base shear- lateral displacement envelope and the sequence of formation of plastic hinging. In such analysis, a monotonic load is applied to the nominally ductile structure until an ultimate load is approached. This corresponds to a value of $^{V}/_{W} = 0.278$ for ductile frame and a value of $^{V}/_{W} = 0.377$ for nominally ductile structure in terms of base shear coefficient. For each structure, the ultimate lateral loading is compared with seismic design lateral loading distribution of NBCC 1995. As results of the seismic analysis the design base shear coefficient for ductile frame is 0.165 and for nominally ductile frame is 0.33. The nonlinear dynamic computer program, IDARC includes several types of hysteretic response models. In this investigation, frames are modeled by commonly used bilinear model. Pushover analysis results are presented here in terms of both displacement and drift. Figure 4.1, shows the configuration of frames.

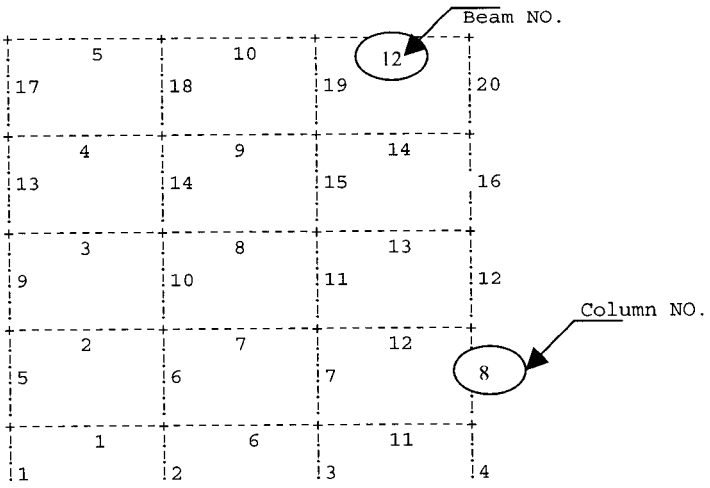

Figure 4.1 Frame elevation (IDARC)

4.2 Nonlinear Inelastic Structural Analysis Software (IDARC)

The inelastic dynamic analysis of reinforced concrete building structures program, IDARC, developed at NCEER (Kunnath et al. 1992), used to calculate both the static and dynamic inelastic responses of the structure to pushover loading and time history excitation respectively. This program contains the relevant modeling features and capabilities necessary for proper analysis. The need to evaluate structures which experience non-elastic behavior as designed by current seismic codes motivated the development of a specialized computer program which models such behavior in an efficient way. The primary modeling technique is employed in the computer program IDARC (Inelastic Damage Analysis of Reinforced Concrete Structures) is the representation of the overall behavior of components in terms of macro models. The computer program IDARC was introduced in 1987 to study the nonlinear response of multistory reinforced concrete buildings. The computer program IDARC was conceived as a platform for nonlinear structural analysis, in which various aspects of concrete behavior can be modeled, tested and improved upon. Program development and enhancements have been made primarily to link experimental research and analytical developments. The program includes the structural element types such as column elements, beam elements, shear wall elements, edge column elements and transverse beam elements. Column elements are modeled considering macro-models with inelastic flexural deformations, and elastic shear and axial deformations. Beam elements are modeled using a nonlinear flexural stiffness model with linear elastic shear deformations

considered. The nonlinear dynamic computer program, IDARC includes several types of hysteretic response models. A hysteretic model incorporates the effects of stiffness degradation, strength deterioration, and slip control (pinching). The effect of these features of reinforced concrete behavior under cyclic loading is included in the model through the selection of model hysteretic parameters. The program includes the damage model developed by Park and Ang (1984) to provide a measure of the accumulated damage sustained by the components of the structure, by each story level and the entire building. This damage index included the ratio of the maximum to ultimate deformations, as well as the ratio of the maximum hysteretic energy dissipated to the maximum monotonic energy, therefore capturing both components of damage. The program is consisted of static analysis to determine component properties and the ultimate failure mode of the building, dynamic response analysis, substructure and damage analysis, quasi-static or pseudo-dynamic analysis module for comparisons with experimental tests and pushover analysis. Pushover analysis is used to determine the force-deformation response characteristics of a structure. Using the results from this analysis, the actual nonlinear dynamic response of the structure can be estimated (Valles et al., 1996). A number of different options for the pushover analysis are available in this program such as displacement control, user defined force control distribution, a generalized power distribution, and a modal adaptive lateral force distribution. These options allow more realistic force distribution to be used in the pushover analysis. Nonlinear material behavior is specified by means of a generic hysteretic force-deformation model that incorporates stiffness degradation, strength deterioration and pinching or bond-slip effects. The final response quantities is expressed in terms of damage indices those provide engineers with a qualitative interpretation of the analysis.

The program was written in standard FORTRAN-77 and operates in a PC environment under MS-DOS or MS-Windows.

4.3 Modeling Assumptions

In developing analytical models of frame structures, assumptions used in this research are discussed first. Unites used to modeling structures are kN-mm. The moment curvature envelope describe the changes in force capacity with deformation during a nonlinear analysis. In models, IDARC can generate moment curvature envelopes for each element.

The material properties are assumed to be constant throughout the height of the structure. The material properties are specified as, reinforcement steel modulus E_s=200000 MPa; Yield strength f_y=400 MPa; concrete compressive strength f'_c=35 MPa. Default values of characteristics of steel stress-strain curve are specified as, ultimate strength (FSU=1.4*f_s), modulus of strain hardening (E_s/60) and strain at start of hardening (EPSH=3.0%). For concrete these default values are: initial Young's Modulus (EC= 57*$\sqrt{(f'_c*1000)}$), strain at maximum strength of concrete (EPSO=0.2%), stress at tension cracking (FT=0.12* f'_c), ultimate strain in compression (EPSU) and parameter defining slope of falling branch are derived by program and depending on section data. Note that in the formulation above, f'_c and E_s are considered in imperial units. Material properties used in the modeling of the structures are listed in Table A.1 of Appendix A.

According to the design considerations of nominally ductile frame modeling of columns minimal effectiveness of confinement, CEFF=0.5, is considered. As shown in Figure 4.2 in ductile frame because of well hoop arrangements well confinement, CEFF=1.0, is used. More detail of design and sectional properties are addressed in Appendix A

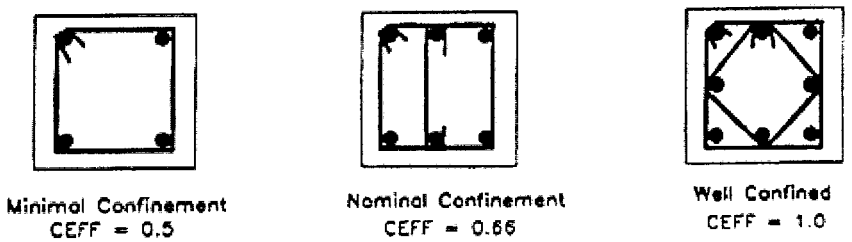

Figure 4.2 Effectiveness of confinement for some typical hoop arrangements

In RC frame buildings, beams are often cast monolithically with other structural elements, such as slabs. Therefore, section behavior can be affected by adjacent slabs due to slab acting together with the beam in flexure and it can significantly increase the negative bending strength of beams. According to earlier editions of ACI318, the slab effective flange width used in the design of T-Beams was computed as ¼ of the span length of beam, and its over hanging width on either side of web should not exceed 8 times of the thickness of slab nor half of the clear distance to next beam. According to this consideration the overhanging effective slab width for non-ductile GLD frame is taken as 8 times of the slab thickness, t_s=125mm, resulting a total effective slab width of 2000 mm plus width of beam it self. According current codes, the effective slab width

(excluding beam width) for interior beam is taken as 750mm plus width of beam. An increase in effective slab width causes a small increase in the ductility of the section (Wu, S, 1995).

4.4 Hysteretic Response Models

The nonlinear dynamic computer program, IDARC includes several types of hysteretic response models. A hysteretic model incorporates the effects of stiffness degradation, strength deterioration, and slip control (pinching). The effect of these features of reinforced concrete behavior under cyclic loading is included in the model through the selection of model hysteretic parameters. The new release of IDARC includes six types of hysteretic response curves as, Three parameter Park model, Tri-Linear Steel model, Bilinear hysteretic model, Kelvin model, Maxwell model and Smooth Hysteretic model. Currently, each of the programmed hysteretic models is used for different structural element. In this investigation, the behavior of the both structural elements is modeled by commonly used bilinear model (Sivaselvan, M.V., 1999). Figure 4.3 presents the branches of hysteretic model and typical hysteretic curves.

Stiffness degradation is experimental evidence that indicates the best expression for a function of attained ductility. The degradation is not obvious at small ductility. To model the reduced stiffness, all unloading branches are directed towards a common target point as shown in Figure 4.3. The modeling of strength decay is accomplished using two control parameters of ductility and dissipated hysteretic energy. Both parameters control the amount of strength loss per cycle until the previous maximum deformation is exceeded. Figure 4.3 also shows the modeling of strength decay. Pinched loops are typical in cyclic RC member behavior due to the presence of high shear forces, or from the opening and closing of cracks, or the result of rebar slippage at beam column interfaces. This behavior is modeled using a third primary control parameter which reduces the target force as the load path crosses the zero force axis as shown in Figure 4.3. The specification of hysteretic rules is rather empirical and should be based on available experimental data. Certain default data sets are established for typical connections, which represent average parameters. In a realistic design situation, a parametric study may be necessary to determine the limits of the response. Hysteretic behavior is specified at both ends off each member. Access to experimental results of the

cyclic force-deformation characteristics of components typical to the structure being analyzed provides the best means of specifying the hysteric degrading parameters. Table 4.1 and Figure 4.4 provide a number of qualitative insights into modeling of the hysteretic parameters. The loops shown in Figure 4.4 are only mean to show the relative effects of changing the parameters. The general meaning of the parameters can be characterized as follows:

An increase in HC retards the amount of stiffness degradation; an increase in HBD, HBE accelerates the strength deterioration; and an increase in HS reduces the amount of slip.

Table 4.1. Typical range of values for hysteretic parameters (Valles et al., 1996)

Parameter	Meaning	Value	Effect
HC	Stiffness degrading parameter	0 1 10 0 200 0	Severe degradation Nominal degradation Negligible degradation (default)
HBD	Strength degrading parameter (ductility-based)	0.0 0.1 0.4	No degradation (default) Nominal deterioration Severe deterioration
HBE	Strength degrading parameter (energy-controlled)	0.0 0.1 0.4	No deterioration Nominal deterioration (default) Severe deterioration
HS	Slip or crack-closing parameter	0.1 0.5 1.0	Extremely pinched loops Nominal pinching No pinching (default)

The values of the IDARC parameters used in the analysis of ductile frame are HC = 2.0, HBE = HBD = 0.001, and HS = 1.0 and for nominally ductile frame these values are HC = 0.1, HBE = HBD = 0.4, and HS = 0.1 for the control of stiffness deterioration, strength degradation, and pinching behavior respectively. In ductile frame, modeling a stable loop is used and for nominally ductile frame, modeling the deterioration is considered (Filiatrault A., 1998). Use of stable loops for ductile frame is the result of good detailing of the members.

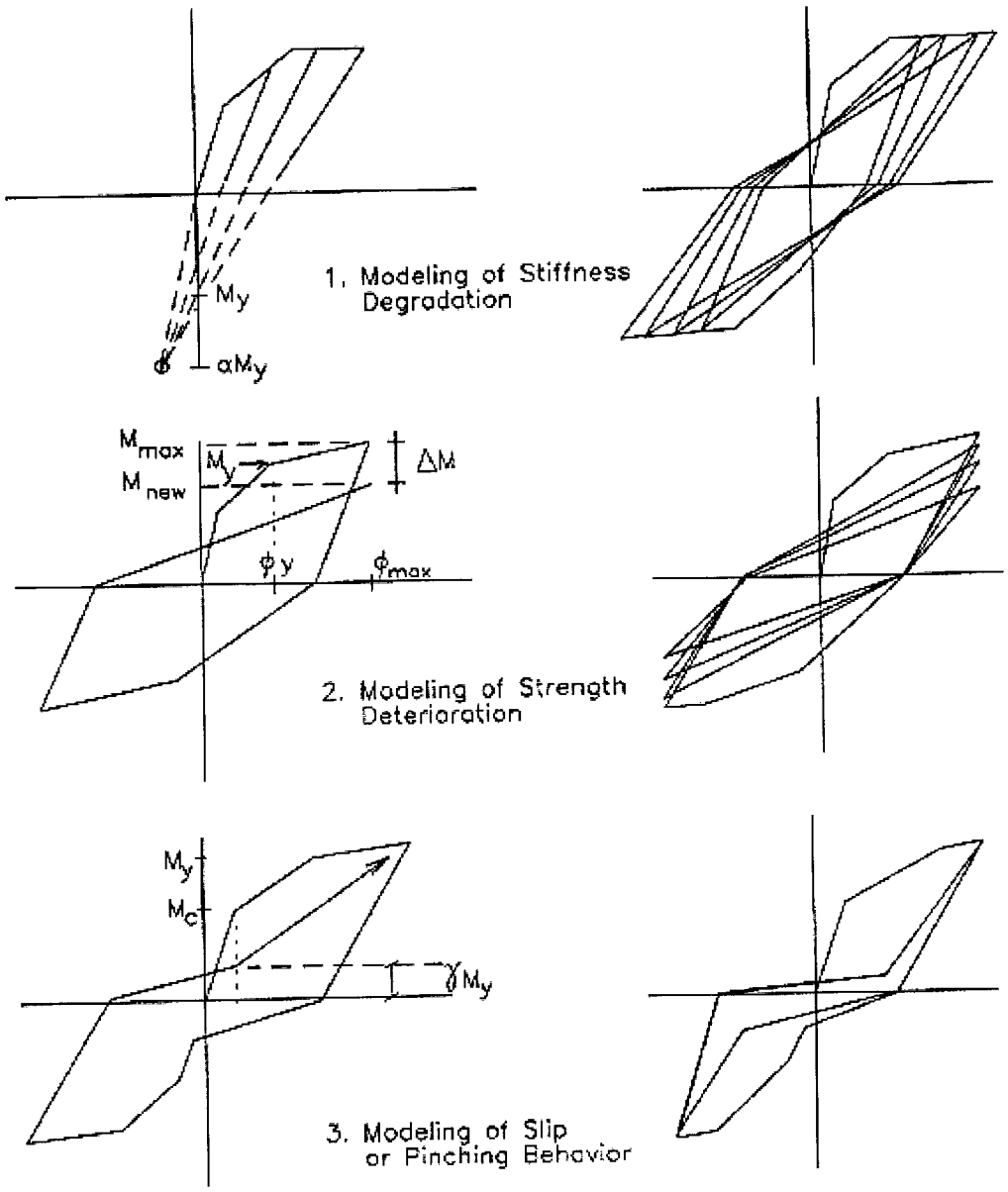

Figure 4.3 Three parameters of the hysteretic model (Valles et al., 1996)

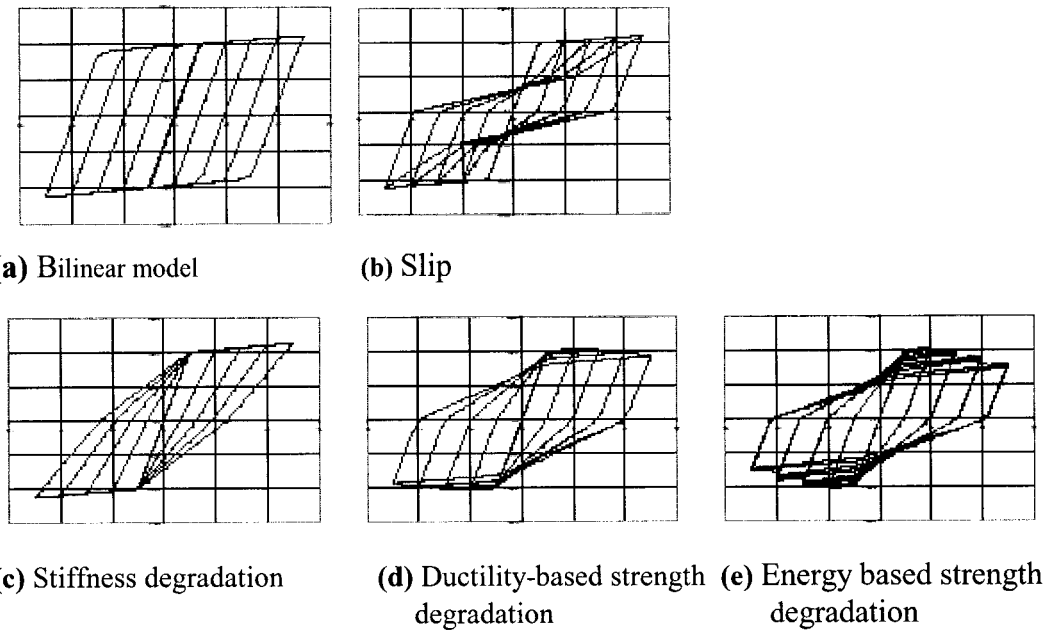

(a) Bilinear model **(b)** Slip

(c) Stiffness degradation **(d)** Ductility-based strength degradation **(e)** Energy based strength degradation

Figure 4.4 View of effects of degrading parameters on hysteretic behavior of bilinear model (Valles et al., 1996)

4.5 Results of Pushover Analysis

In order to investigate and compare the behavior of ductile and nominally ductile frames the designed frames are analyzed under monotonically increasing static lateral loading. The lateral loads are distributed over the height of the building. The displacement-base shears relationships of frames and comparison with NBCC design base shear obtained are shown in Figures 4.5, 4.6 and 4.7. These figures illustrate the base shear - lateral displacement envelope and the sequence of plastic hinging. The displacement-base shears relationships of frames determined during the pushover analysis gives an indication of the global response to lateral loading, including the over strength and deflections. The envelope for the structure with nominal ductility (R = 2) shows a descending behavior following the yield of structure. Note that the design base shear for nominally ductile frame is almost twice of ductile one. Therefore, the frames are designed on the base of assumed base shears. Figure 4.5 shown the ultimate load carrying capacity is v/w=0.377 and 0.278 for nominally ductile and ductile frame respectively.

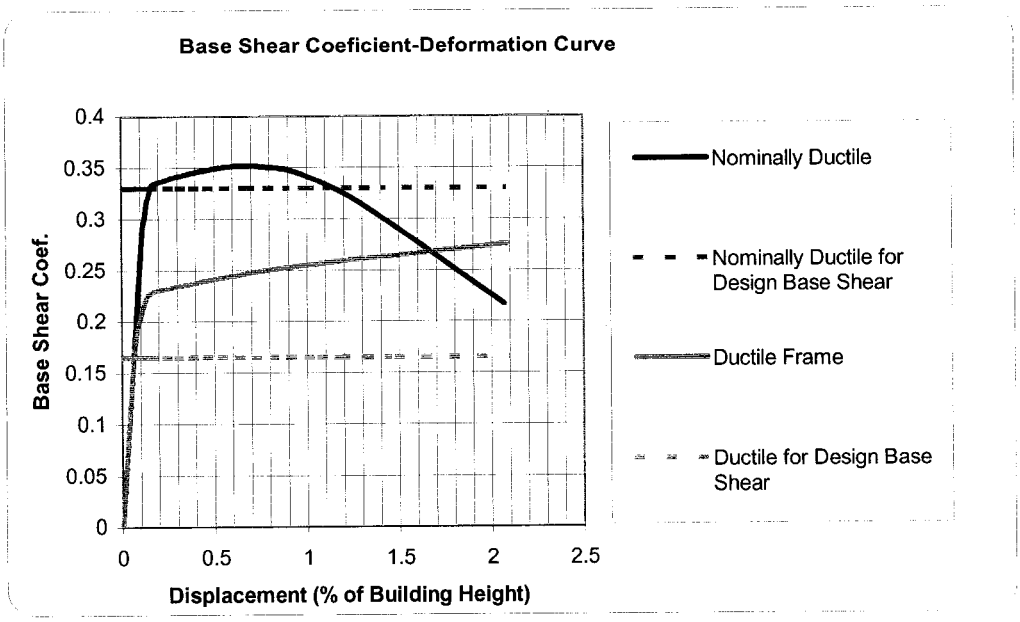

Figure 4.5 Base shear coefficient versus displacement percentage of height

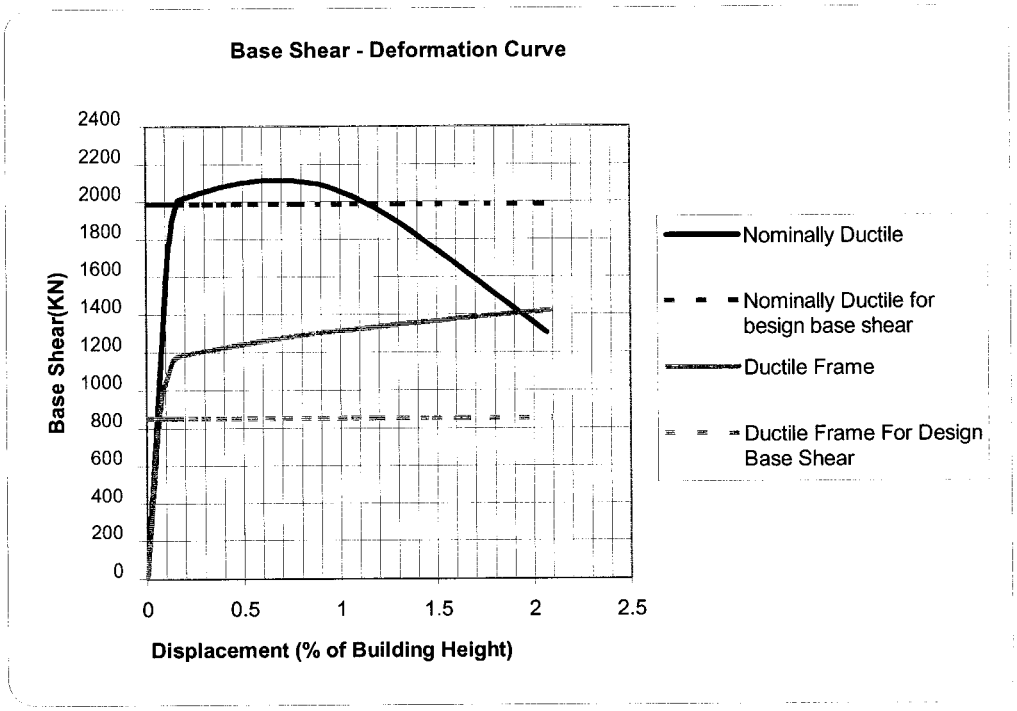

Figure 4.6 Base shear versus displacement percentage of height

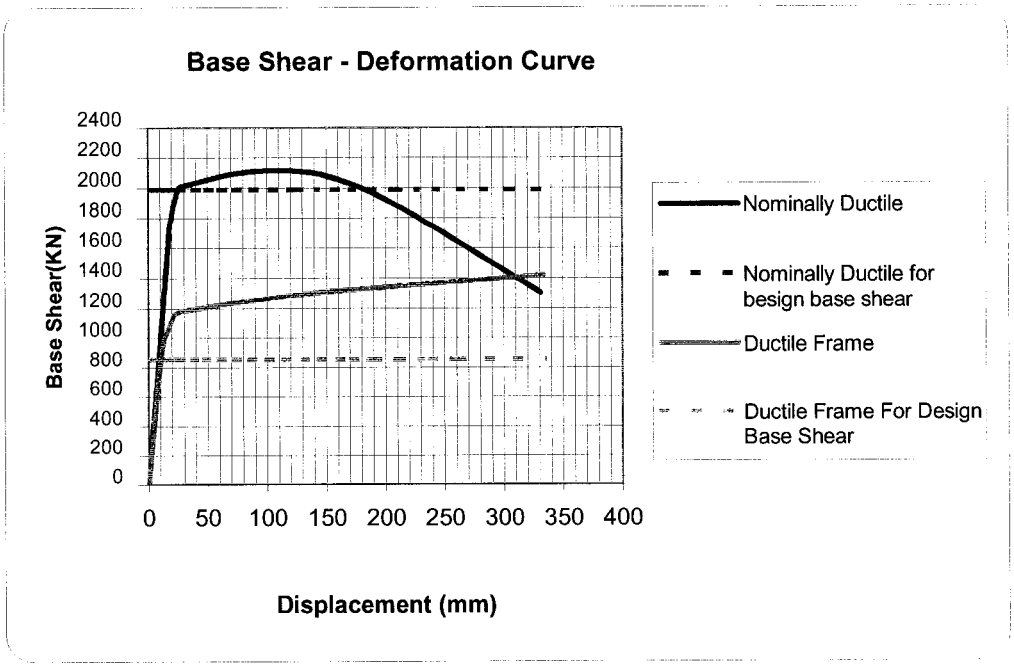

Figure 4.7 Base shear versus displacement (mm)

4.5.1 Over Strength Ratios Comparison

The over strength ratio is base shear divided by design base shear (Heldenbrecht, A.C, 1998). The results of ductile frame, indicate that first beams and columns yield at an over strength ratio of about 1.03 and 1.18 respectively. Similarly the over strength ratio of 0.99 and 0.925 are obtained at the first beam and column yield states for nominally ductile frame. The larger over strength ratio is observed in ductile frame than the nominally ductile structure. This significant over strength for the ductile structure, is mainly the result of the higher strength of the columns related to beams to ensure plastic hinges in the beams.

P-delta effect on structure caused by gravity loads acting on the deformed shape of the structures and it leads to an increase in lateral displacements and it has effect in increasing inter-story drifts and displacements. The P-delta effect may lead to a significant amplification of displacement and may lead to incremental collapse. P-delta effects are included in both cases.

The displacement ductility factor is defined as a measure of the ductility of the structure with regard to seismic loading. It is used in seismic design codes as the overall structural

ductility. Displacement ductility factor is expressed as the ratio of maximum displacement to the yield displacement and is given as, $\mu_{\Delta}=\Delta_{max.} / \Delta_y$

Where $\Delta_{max.}$ is the maximum displacement and Δ_y is the yield displacement.

The displacement ductility factor in both cases are calculated and compared. The results shown in Figure 4.8 illustrates that the ductile frame has larger ductility factor than nominally ductile frame. As expected improvement in ductility and better performance are obtained in ductile frame as compared to the nominally ductile frame. This is the result of the good detailing of the members in ductile frame even though the base shear of a nominally ductile is two times of ductile one.

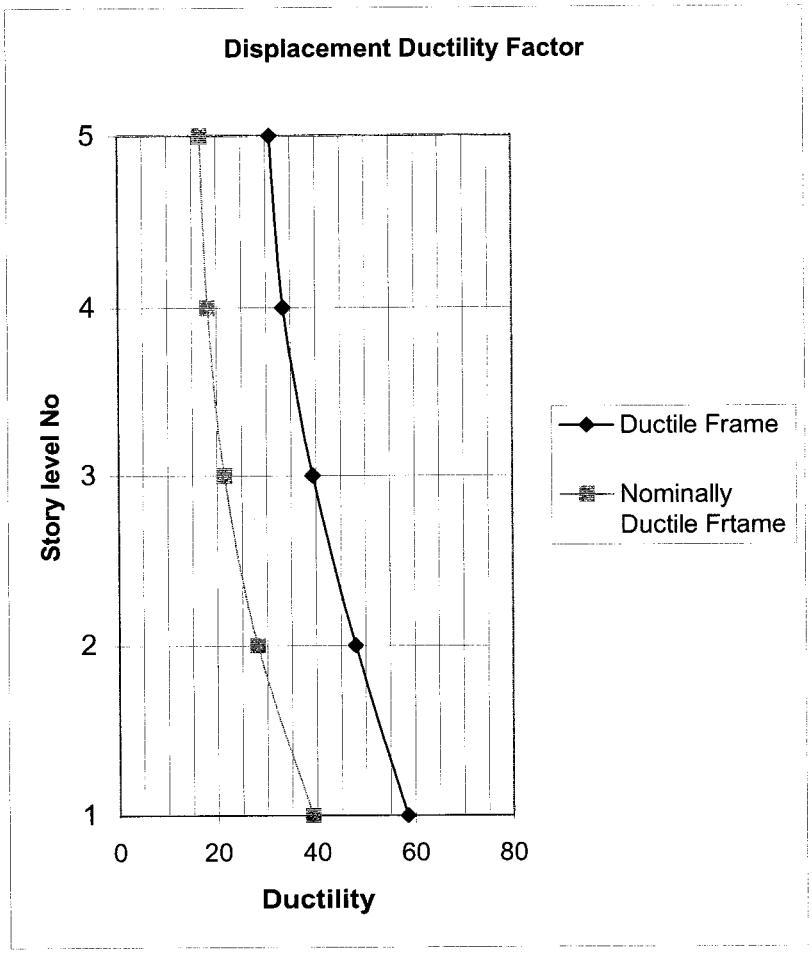

Figure 4.8 Displacement ductility factor

The story drift of a structure under lateral load effect is important factor in many different perspectives, such as performance-based design, structural stability and damage to non-structural components. Inter-story drifts are relative floor lateral displacements between

the two adjacent floors divided by the height of the story. Figure 4.9 shows that the maximum drift is equal to 6.7% in the 1st story and 1.67% in 2nd story for ductile frame while nominally ductile frame shows a drift of 7.8% in first story. The rest of the floors show less than 0.16% drift. The results obtained from pushover analysis illustrate differences between the drifts of ductile and nominally ductile frames.

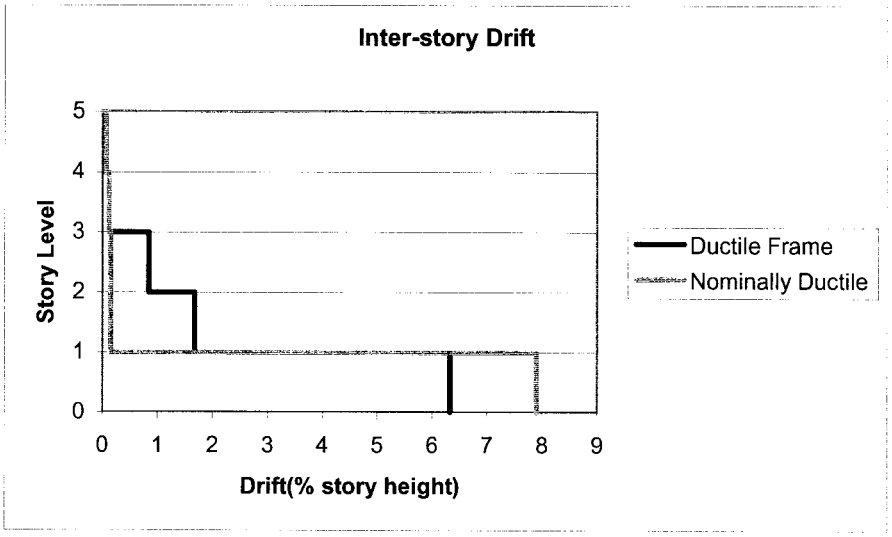

Figure 4.9 Inter-story drifts of frames (% of story height)

Figure 4.10 compares the maximum base shear-story displacement due to pushover loading for ductile and nominally ductile frames. The nominally ductile frame shows a displacement of 316 mm in the first story and rest of floors acts as rigid body. Ductile frame shows less deformations in the first floor (253 mm) as compared with the nominally ductile frame. The inelastic deformations in plastic hinges at the ends of beams in ductile frame cause relative movements in upper stories. The occurrence of plastic hinges and severe damages of columns in the first floor of nominally ductile frame cause this large deformation due to lack of strong column-weak beam mechanism.

4.6 Damage Analysis

Damage control in a building is a complex task. The response index is used to estimate the damage in RC ductile members is developed by Park & Ang (Park et al. 1984) and this model is used in IDARC. A global value of damage index can be used to characterize

damage in the ductile members of RC frames. In this case, the Park & Ang damage index, for a framed structure can be estimated using the following expression:

$DI_{P\&A} = \delta_m / \delta_u + \beta / \delta_u P_y \int d E_h$

Where δ_m is the maximum experienced deformation, δ_u is the ultimate deformation of the element, P_y is the yield strength of element, $\int d E_h$ is the hysteretic energy absorbed by the element during response history and β is a model constant parameter.(Teran, A., 1997)

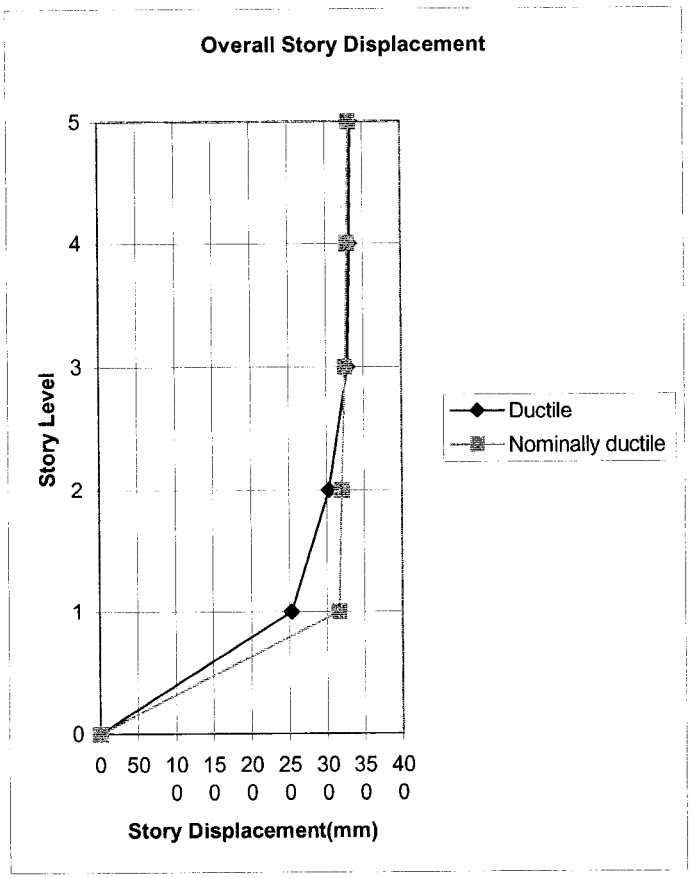

Figure 4.10 Base shear story displacement relationship

The overall structural damage obtained for ductile frame was 0.224 and for nominally ductile frame the overall damage index of 0.528 is observed. (obtained from pushover analysis). The overall damages of ductile frame is less than nominal ductile frame because of better performance of ductile frames due to stronger columns and better detailing. Interpretation of overall damage index is presented in Table 4.2.

Table 4.2 Interpretation of overall damage index (Park et al., 1986)

Degree of Damage	Physical Appearance	Damage Index	State of Building
Collapse	Partial or total collapse of building	> 1.0	Loss of building
Severe	Extensive crashing of concrete; disclosure of buckled reinforcement	0.4 - 1.0	Beyond repair
Moderate	Extensive large cracks; spalling of concrete in weaker elements	< 0.4	Repairable
Minor	Minor cracks; partial crushing of concrete in columns		
Slight	Sporadic occurrence of cracking		

4.6.1 Damage analysis in ductile frames

Table 4.3 and Figures 4.11 and 4.12 indicate the state of cracking/yielding and damage index statistics of ductile frame of ductile frame respectively in order to show the progression of damage as the load is increased. The sequence of yielding in Table 4.3 indicates that beams at 1st, 2nd and 3rd floors yielded resulting in plastic hinges occurring at the beams. The hinges form in the beams followed by four others at the base of the columns and then the columns in the first story yield. This behavior confirms the successful application of strong column-week beam theory in designing of ductile frame. The sequence of plastic hinging in the ductile structure conforms to the capacity design concept. Note that X and 0 express crack and yield states of frame and the numbers in parentheses indicate sequence of yielding.

4.6.2 Damage analysis in nominally ductile frames

Table 4.4 and Figures 4.13 and 4.14 indicate the state of cracking/yielding and damage index statistics of ductile frame of nominally ductile frame respectively in order to show the progression of damage as the load is increased. The sequence of yielding in Table 4.4 indicates that, first plastic hinges occur at the base of the columns. A severe yielding of

column at top of first story immediately follows. Finally, the plastic hinges are formed in the beams of first floor. This hinging pattern in the structure with nominal ductility is far from requirements of capacity design and energy dissipation criteria.

Table 4.3 Sequence of component yielding (Ductile frame)

NO.	STORY LEVEL	ELEMENT	BASE SHEAR	SEQUANCE OF YIELDING
1	1st	BEAM 1	0.1699	YIELDING DETECTED AT LEFT
2	1st	BEAM 6	0.1751	YIELDING DETECTED AT LEFT
3	1st	BEAM 11	0.1779	YIELDING DETECTED AT LEFT
4	1st	COLUMN 4	0.1945	YIELDING DETECTED AT BOT
5	1st	COLUMN 1	0.1973	YIELDING DETECTED AT BOT
6	1st	COLUMN 2,3	0.2000	YIELDING DETECTED AT BOT
7	2nd	BEAM 2,12	0.2055	YIELDING DETECTED AT LEFT
8	3rd	BEAM 3	0.2261	YIELDING DETECTED AT LEFT
9	1st	COL 1,2,3,4	0.2329	YIELDING DETECTED AT TOP
10	3rd	BEAM 13	0.2356	YIELDING DETECTED AT LEFT
11	3rd	BEAM 8	0.2384	YIELDING DETECTED AT LEFT
12	1st	BEAM 11	0.2411	YIELDING DETECTED AT RGHT
13	1st	BEAM 1,6	0.2439	YIELDING DETECTED AT RGHT
14	3rd	COL. 10,11	0.2466	YIELDING DETECTED AT TOP
15	2nd	COLUMN 6,7	0.2493	YIELDING DETECTED AT TOP
16	2nd	BEAM 2,7,12	0.2548	YIELDING DETECTED AT RGHT
17	2nd	COLUMN 5,8	0.2576	YIELDING DETECTED AT TOP
18	3rd	COLUMN 9,12	0.2658	YIELDING DETECTED AT TOP

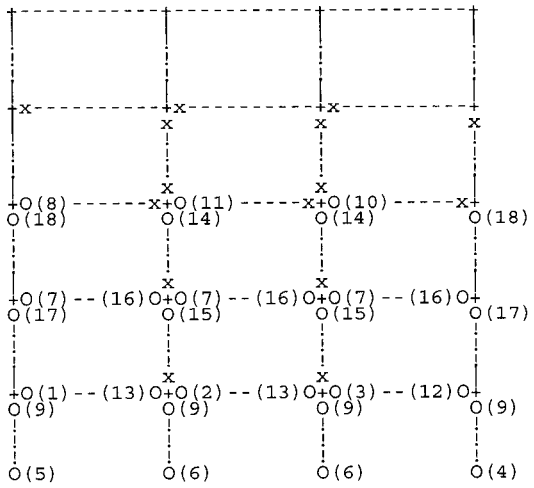

Figure 4.11 State of failure and sequence of yielding for ductile frame

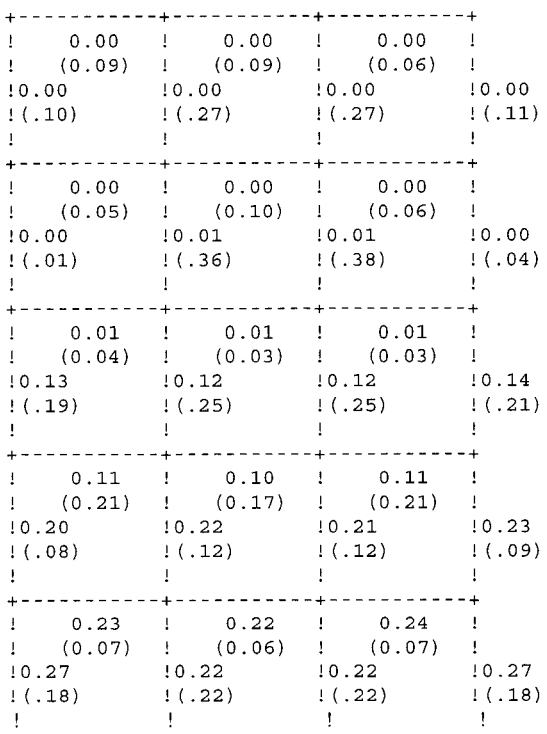

Figure 4.12 Damage index statistics of ductile frame

Table 4.4 Sequence of component yielding (Nominally Ductile)

NO.	STORY LEVEL	ELEMENT	BASE SHEAR	SEQUANCE OF YIELDING
1	1st	COLUMN 2	0.3015	YIELDING DETECTED AT BOT
2	1st	COLUMN 1,3	0.3053	YIELDING DETECTED AT BOT
3	1st	COLUMN 4	0.3091	YIELDING DETECTED AT BOT
4	1st	BEAM 11	0.3231	YIELDING DETECTED AT LEFT
5	1st	COLUMN 2,3	0.3376	YIELDING DETECTED AT TOP
6	1st	COLUMN 1,4	0.3411	YIELDING DETECTED AT TOP
7	1st	BEAM 1	0.3473	YIELDING DETECTED AT LEFT
8	2nd	BEAM 7	0.3503	YIELDING DETECTED AT LEFT

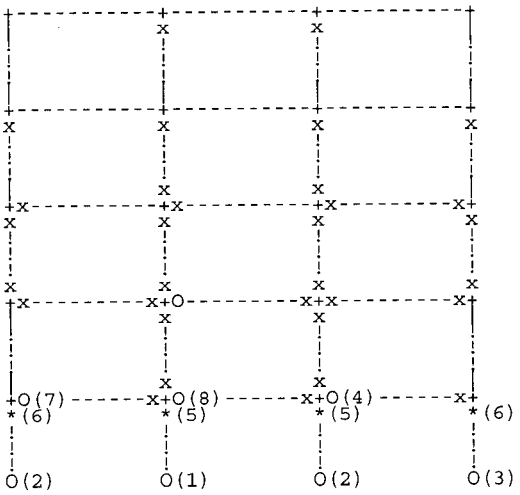

Figure 4.13 State of failure and sequence of yielding for nominally ductile frame

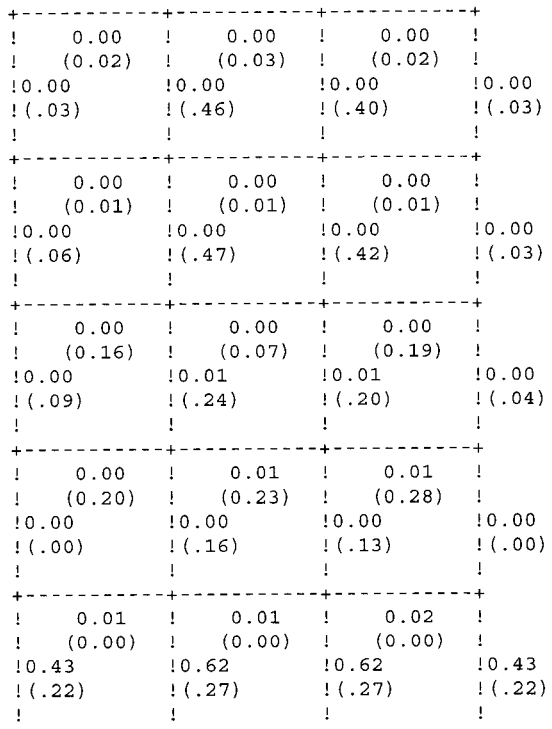

Figure 4.14 Damage index statistics of nominally ductile frame

4.6.3 Comparison of Sequence of Yielding

Figure 4.15 shows yielding of structural elements in nominally ductile frame where column yields at base shear coefficient of 0.3015. First beam yields at base shear coefficient of 0.3231. In ductile frame, first yielding occurs in beam at base shear of

0.1696 and first column yields at base shear of 0.1946. These results illustrate better response of ductile frame due to week beam- strong column considerations.

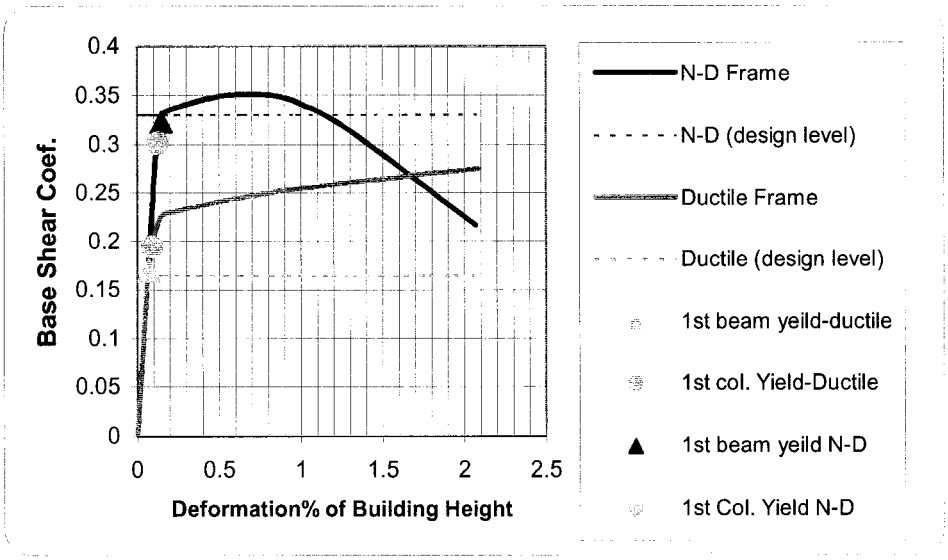

Figure 4.15 Sequence of first yielding of elements

4.7 Conclusion

The two cases of five story-four span reinforced concrete building under monotonic pushover are studied. The practical damage process is obtained from nonlinear pushover analysis. This investigation confirms that, this algorithm could apply to structural design process of buildings because of better behavior of ductile frames to undergo more deformation under seismic lateral loads and less shear stresses and better plastic energy dissipation. The capacity design process is implemented in the ductile structure. This caused the lateral strength of the ductile structure (R = 4) to be higher than the nominally ductile (R = 2) even though the nominally ductile frame is designed for twice as much lateral force as compared to the ductile frame. Because of plastic hinging pattern, the nominally ductile structure showed that it is far from an optimum design. In addition, because of better behavior of ductile frame, it can be carry to more lateral load and provide better seismic performance with the formation of plastic hinges at the end of the beams. Ductile frame has more capability of energy dissipation through the plastic hinges at the ends of the beams. Therefore, a ductile structure can be designed for lower seismic forces. The over strength ratios in both structures are presented in section 4.5.1. The larger over strength ratio in ductile frame as compared to the nominally ductile structure

is observed. It is mainly the result of higher ductility of the columns to ensure plastic hinges in the beams. The sequence of plastic hinging in the ductile structure conforms to the capacity design concept.

CHAPTER 5

Dynamic Analysis

5.1 Introduction

The inelastic dynamic analysis program IDARC is used to calculate the inelastic response of both structures (Ductile and Nominally Ductile frames) to time history analysis. The time history analysis predicts the seismic response of structures. In this investigation, the structure is subjected to Elysian Park (simulated) ground motion in Los Angeles site. Under this ground motion, damages and failure modes of the structures are studied. Dynamic analysis is performed on each structure to determine the lateral displacement envelope, story shear and story drifts, of frames and the sequence of plastic hinging. The nonlinear dynamic computer program, IDARC includes several types of hysteretic response models. In this investigation, frames are modeled by commonly used bilinear model as shown in Figure 4.3(a). The dynamic analysis results are presented in terms of story displacement, shear, and drift. The configurations of frames are shown in Figure 4.1.

5.2 Ground Motions

To form an earthquake data set as input ground excitation. A ground motion is selected from the earthquake database system at Joint Venture SAC (1997). Horizontal ground motion of Elysian Park for Los Angeles site with a probability of exceedence of 2% in 50 years is selected. A horizontal component is selected to give a peak ground acceleration of 1.29g, which provides excitation in proportion to the high seismic risk. The strong motion duration is about 30 seconds. Figure 5.1 presents the acceleration time-histories of this seismic event using a scale factor of 1.43. Table 5.1 provides detailed information on the records generated for Los Angeles site having probabilities of exceedence of 2% in 50 years. The time history for 2% in 50 years can be used to represent the maximum considered ground motions. This acceleration time history is derived from historical recordings or physical simulations also modified from different soil types.

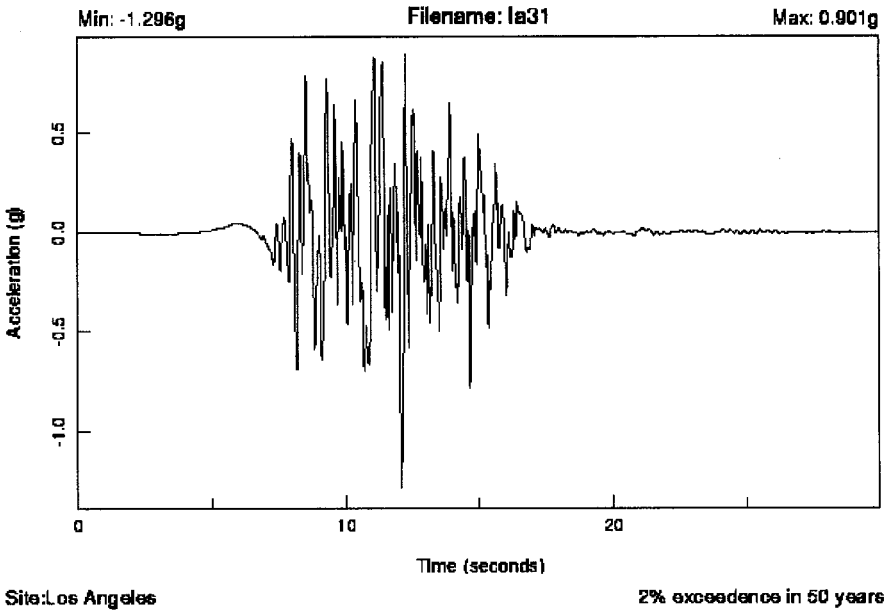

Figure 5.1 Elysian Park simulated record for Los Angeles site

Table 5.1 Details of Elysian Park simulated ground motions for Los Angeles site having a probability of exceedence of 2% in 50 years

SAC Name	Record	Earthquake Magnitude	Distance (km)	Scale Factor	Number of Points	DT (sec)	Duration (sec)	PGA (cm/sec^2)	PGA
LA 31	Elysian Park (simulated)	7.1	17.5	1.43	3000	0.01	29.99	1271.20	1.29g

In developing analytical models of frame structures for dynamic analysis, same assumptions are used as pushover analysis including, historic models, geometry, system of units and material properties. For the analysis carried out herein, to ensure accurate results, an integration time step of 0.005 seconds is used for nonlinear dynamic analysis. Approximately 5% of critical damping is assumed in this analysis.

5.3 Results of Time History Dynamic Analysis

In order to investigate and compare the behavior of ductile and nominally ductile frames, these frames are subjected to a seismic ground motion. The time-displacement relationships of frames for each story are shown in Figure 5.2. The time-displacement relationships of frames determined during the dynamic analysis gives an indication of the global response of these frames. The displacements are compared for both ductile and nominally ductile frames. As Figure 5.2 shows, the maximum response time histories

occur during the 16 seconds. In nominally ductile frame the maximum displacement at 1st floor is about 150 mm at representative base shear of about 2000 kN and in the rest of the stories a rigid body motion with almost same displacements is observed as shown in Figure 5.3. The nominally ductile frame showed poor response under the ground excitation. Inelastic deformations are concentrated mainly in the fist floor and rest of frame acts as a rigid body. Note that the nominally ductile frame is designed for twice-the lateral load compared to ductile frame.

The ductile frame is shown a improved performance as compared to nominally ductile frame. All floors displaced relative to each other and rigid body motion is less noticeable in this case. The maximum values of displacements are about 117, 171, 203, 207 and 208 mm for 1st through 5th floors respectively. The representative story shears are shown in Figure 5.4. These results indicate a better performance of ductile frame for an earthquake event as a result of strong column-weak beam consideration.

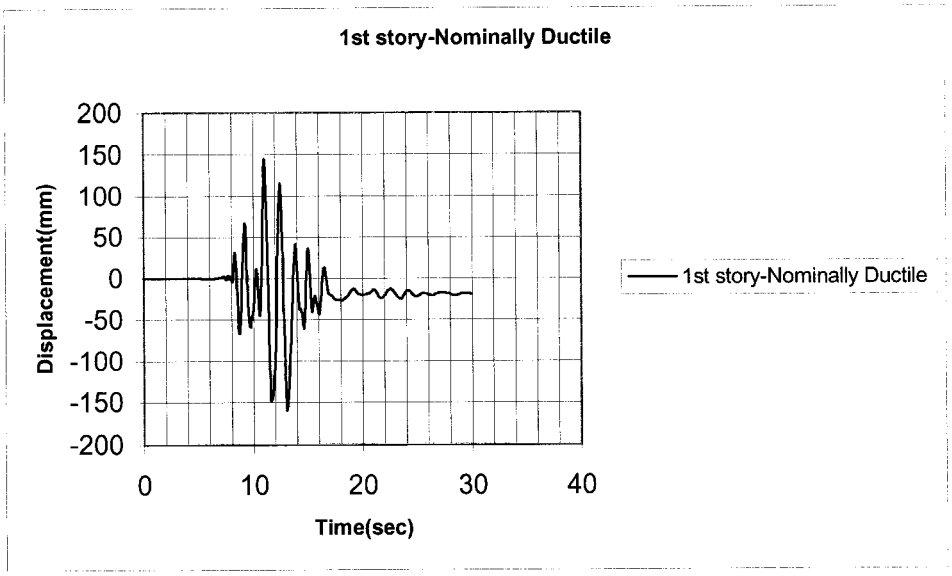

(a)

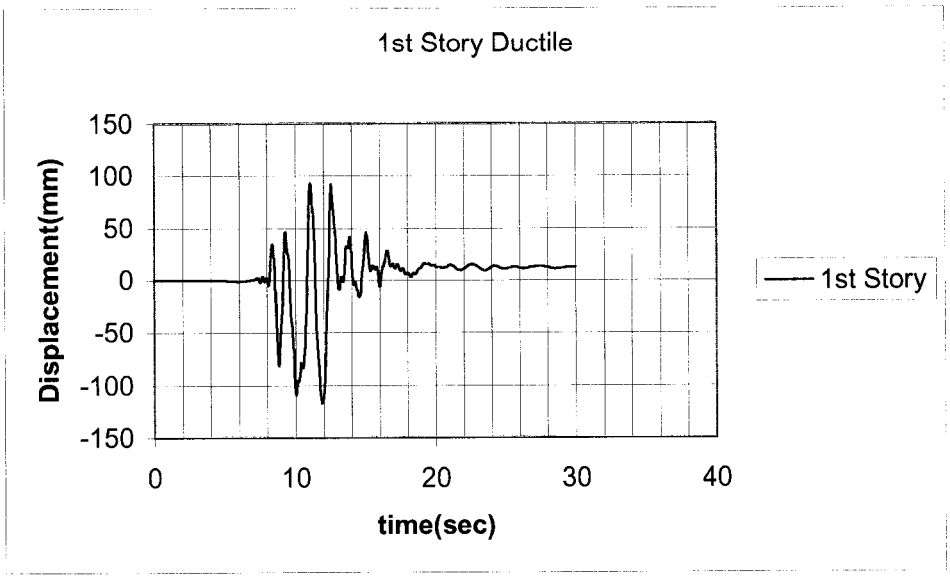
1st Story Ductile
Displacement(mm)
150
100
50
0
-50
-100
-150
0
10
20
30
40
time(sec)
1st Story

(b)

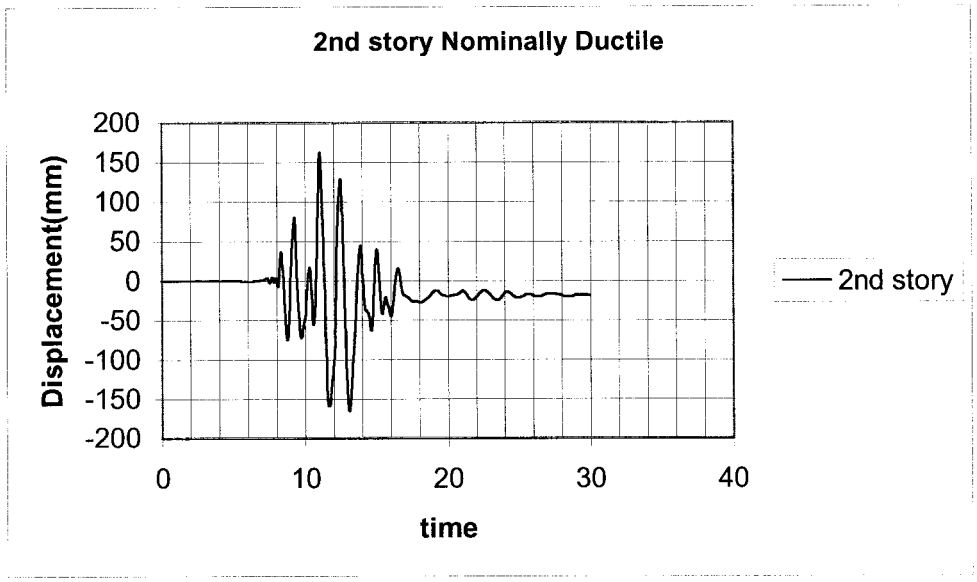
2nd story Nominally Ductile
Displacement(mm)
200
150
100
50
0
-50
-100
-150
-200
0
10
20
30
40
time
2nd story

(c)

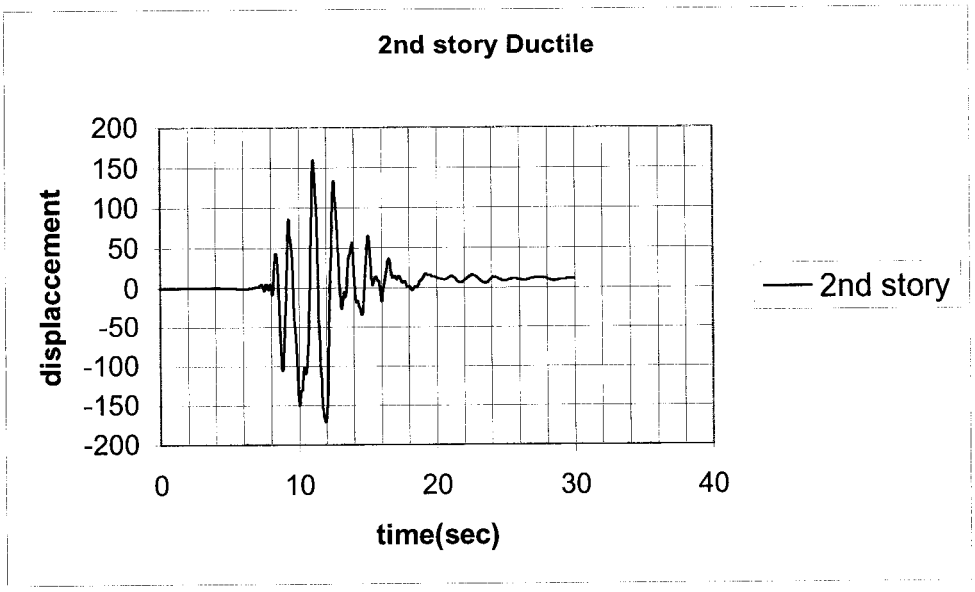
2nd story Ductile
displaccement
200
150
100
50
0
-50
-100
-150
-200
0
10
20
30
40
time(sec)
2nd story

(d)

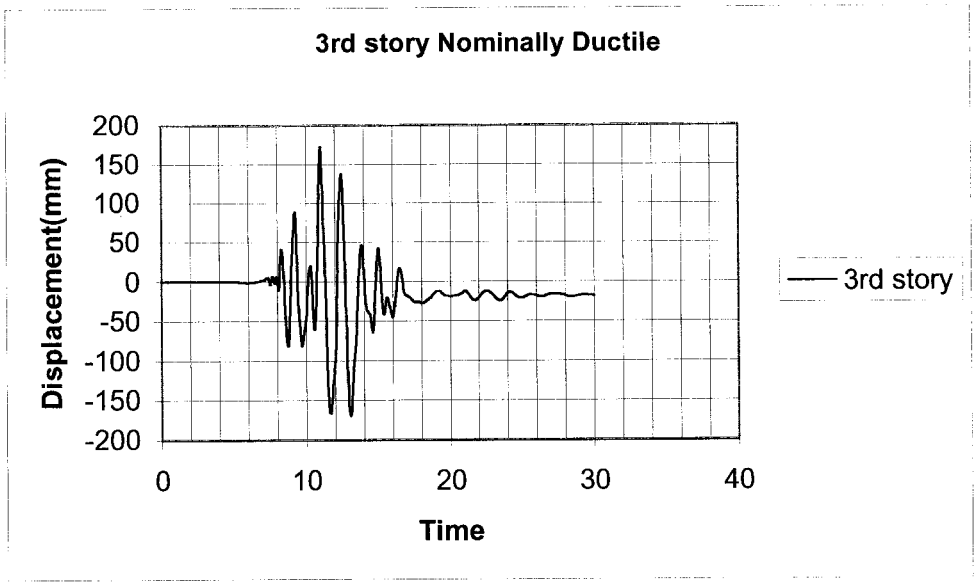
3rd story Nominally Ductile
Displacement(mm)
200
150
100
50
0
-50
-100
-150
-200
0
10
20
30
40
Time
3rd story

(e)

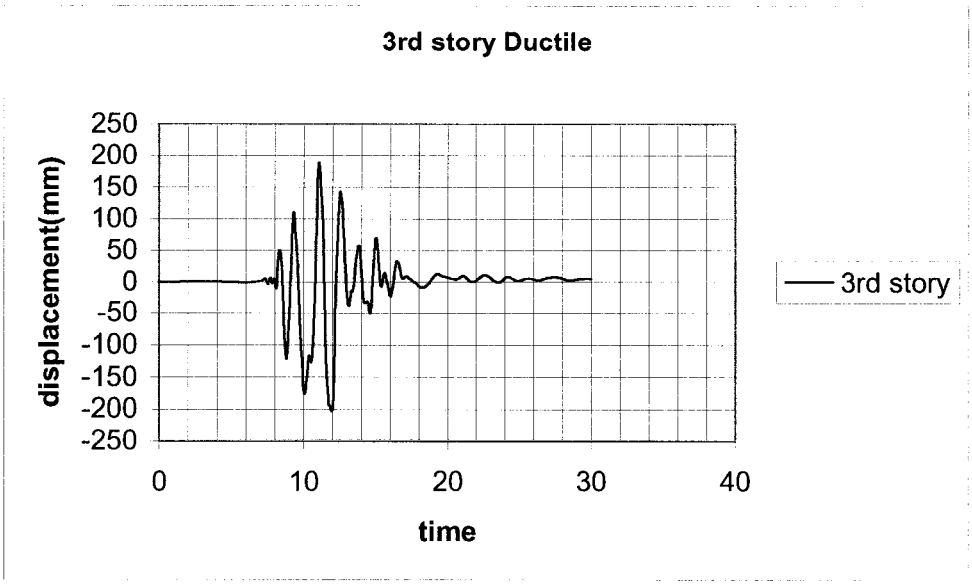
3rd story Ductile
displacement(mm)
250
200
150
100
50
0
-50
-100
-150
-200
-250
0
10
20
30
40
time
3rd story

(f)

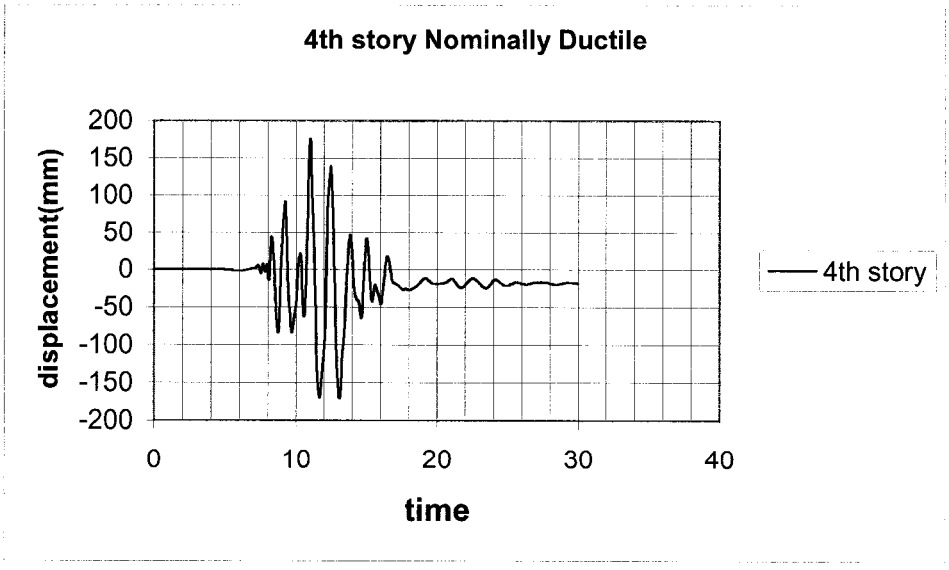
4th story Nominally Ductile
displacement(mm)
200
150
100
50
0
-50
-100
-150
-200
0
10
20
30
40
time
4th story

(g)

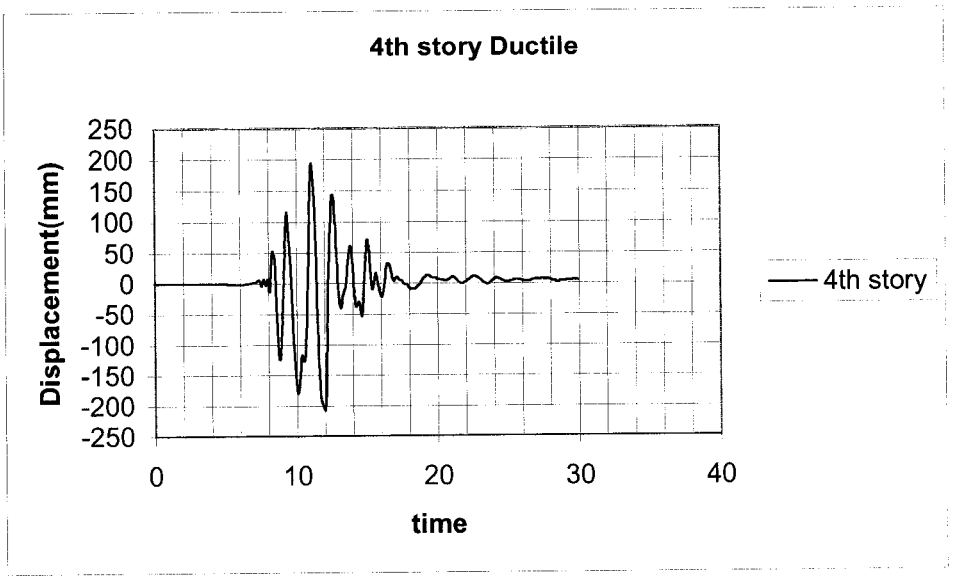

(h)

Figure 5.2 Time-displacement relationships

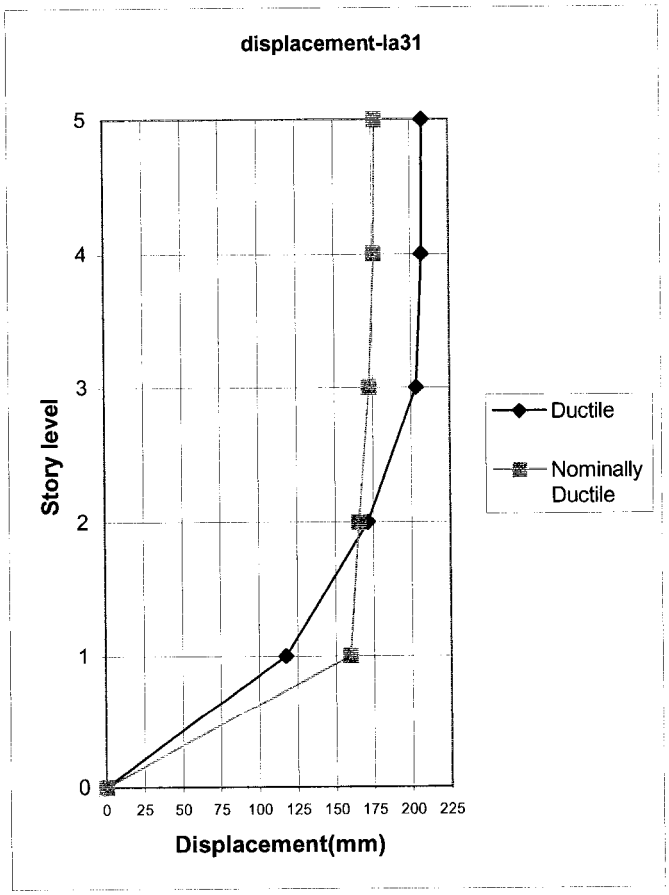

Figure 5.3 Maximum displacements

Figure 5.4 shows the time-story shear relationship for each story level for both structures. Due to a ground excitation the story shear, produced in nominally ductile frame is about 2000 KN while this is about 1000 KN for ductile frame. The nominally ductile frame designed for about twice of lateral load than that for ductile frame subjected to the same ground acceleration.

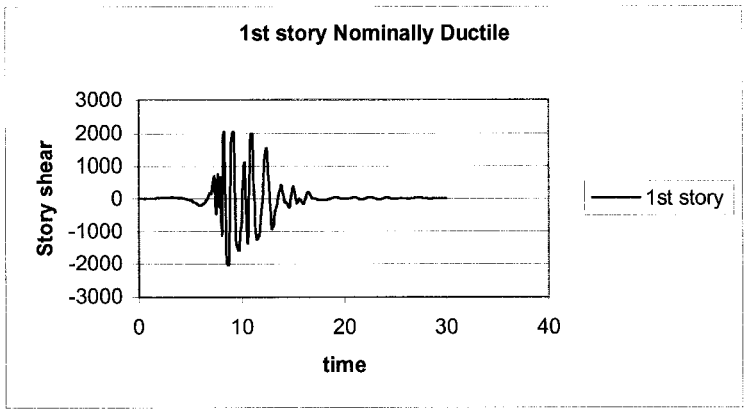

(a)

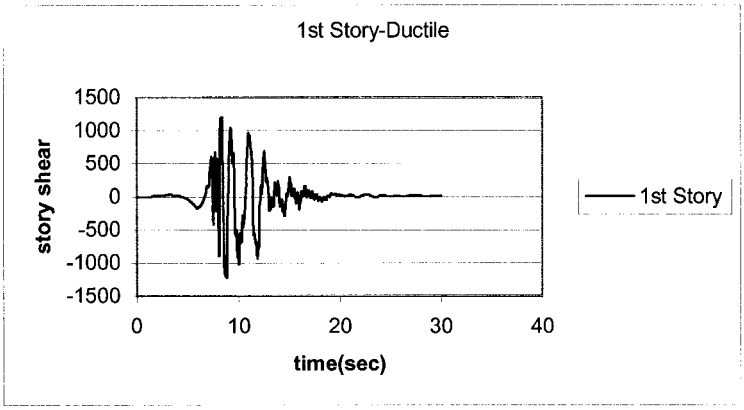

(b)

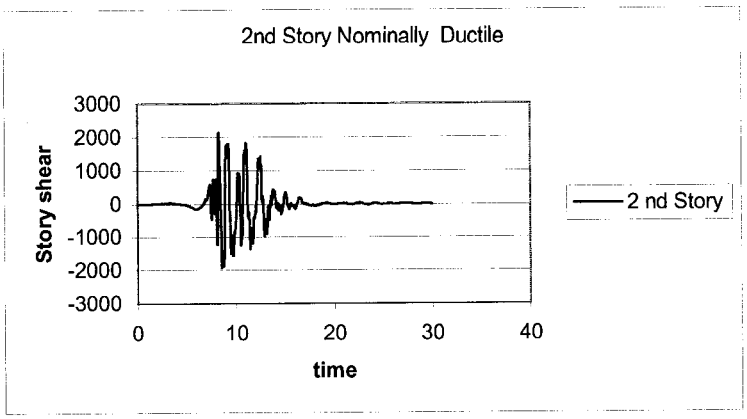
2nd Story Nominally Ductile
Story shear
3000
2000
1000
0
-1000
-2000
-3000
0
10
20
30
40
time
2 nd Story

(c)

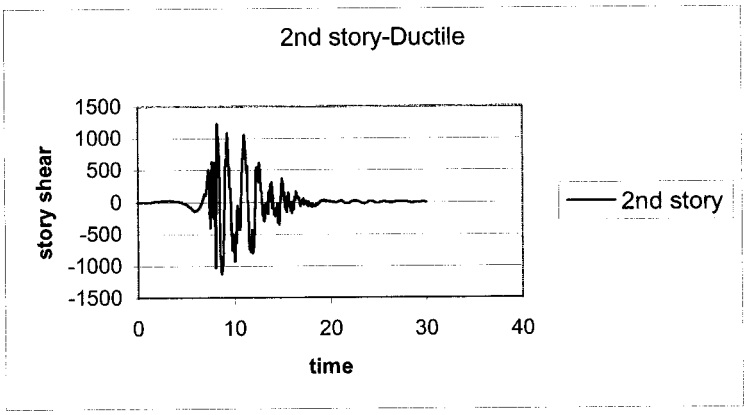
2nd story-Ductile
story shear
1500
1000
500
0
-500
-1000
-1500
0
10
20
30
40
time
2nd story

(d)

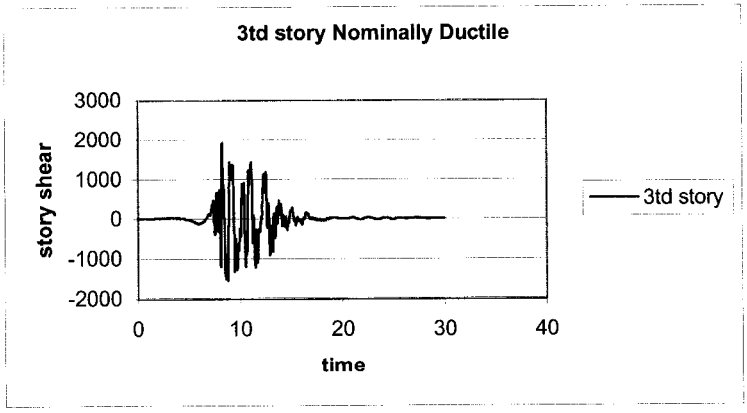
3td story Nominally Ductile
story shear
3000
2000
1000
0
-1000
-2000
0
10
20
30
40
time
3td story

(e)

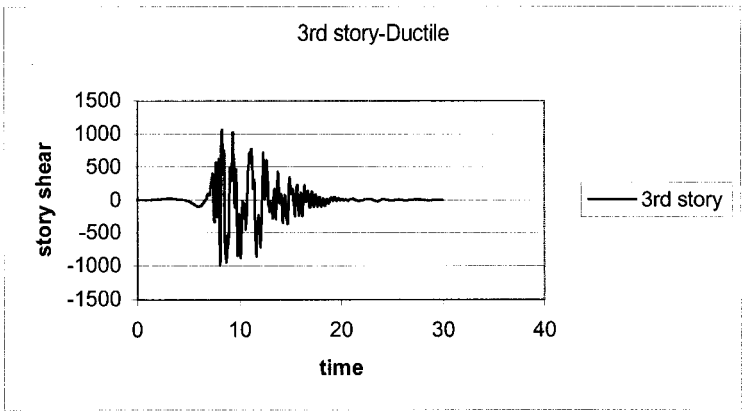

(f)

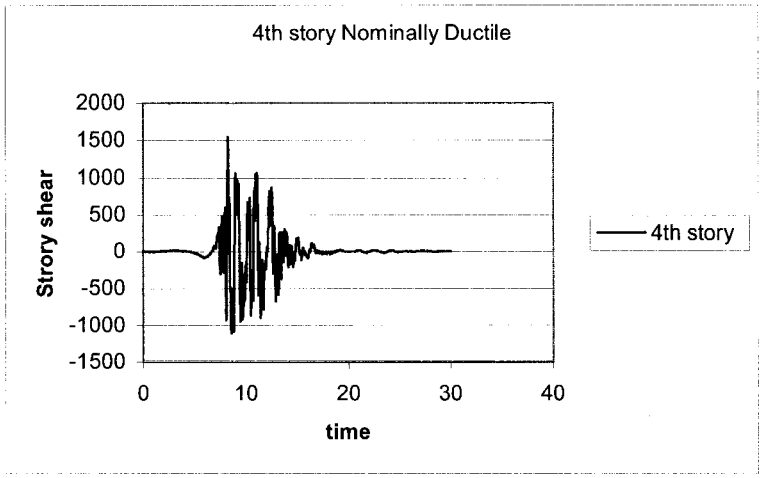

(g)

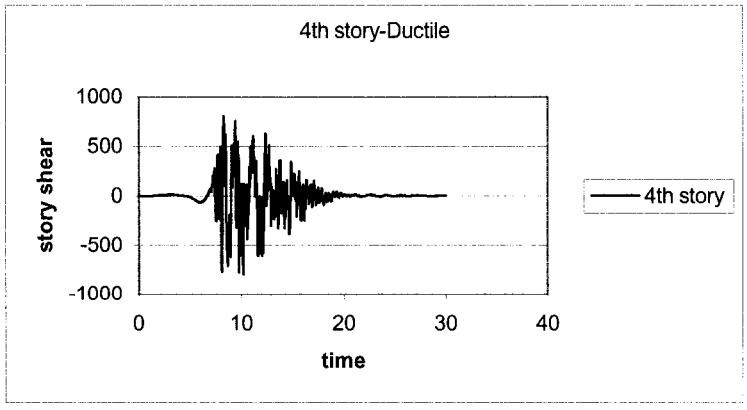

(h)

Figure 5.4 Time-story shear relationship

Figure 5.5 show the time acceleration relationships at 1st story level of nominally ductile and ductile frames. The time acceleration diagrams agree with the input wave data as shown in Figure 5.1.

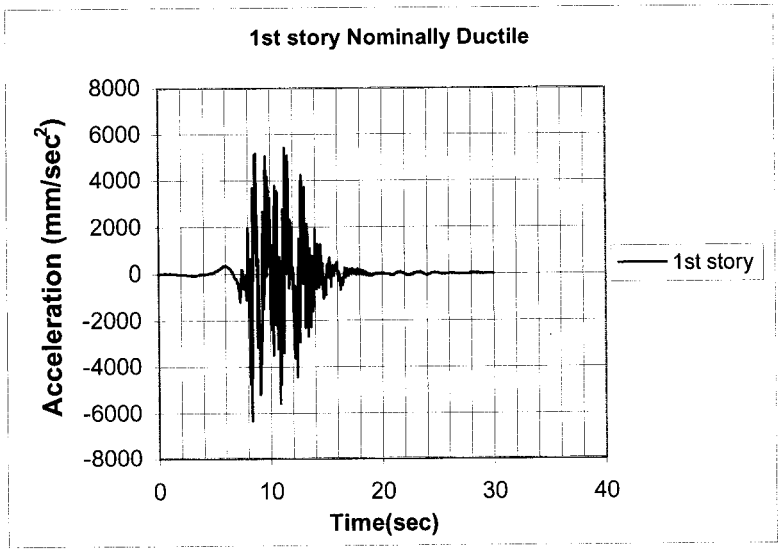

(a)

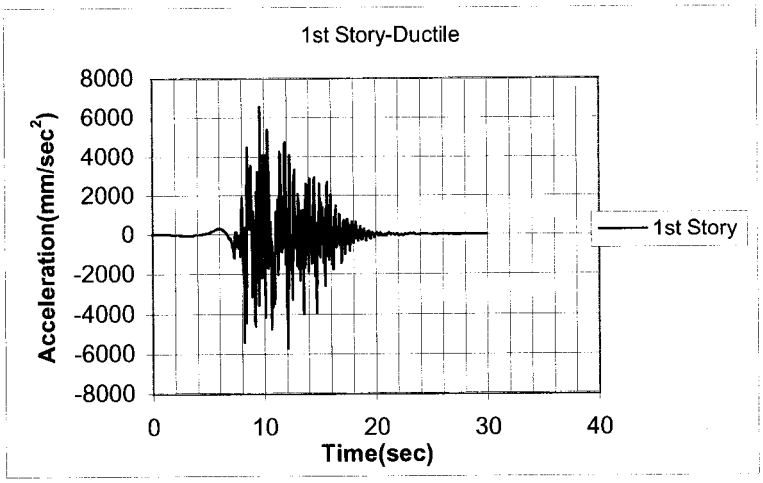

(b)

Figure 5.5 Time-acceleration relationships

Inter-story drifts are relative floor lateral displacement between the two adjacent floors divided by the height of the story. The results obtained from dynamic time history analysis illustrate the differences between the drifts of ductile and nominally ductile frames as shown in Figure 5.6. The maximum drifts of nominally ductile frame is about

4% as shown in Figure 5.7. The largest drifts reach to 2.9% in the fist floor and 2.2% in second floor of ductile frame. Lower drift in the first floor of nominal ductile frame displayed in comparison to rest of the floors; while in ductile frame floors displayed relative drifts to each other.

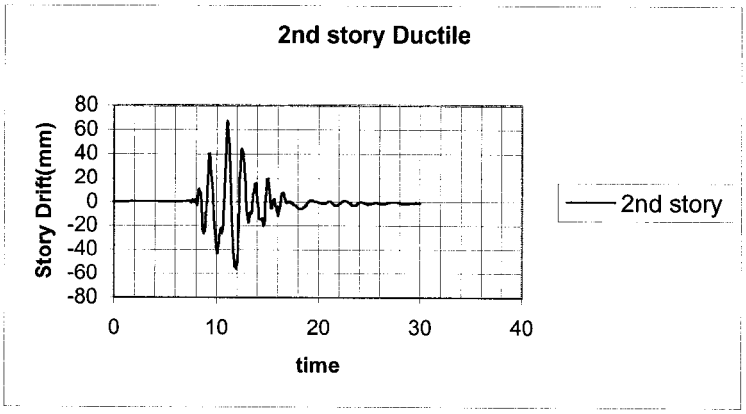

(a)

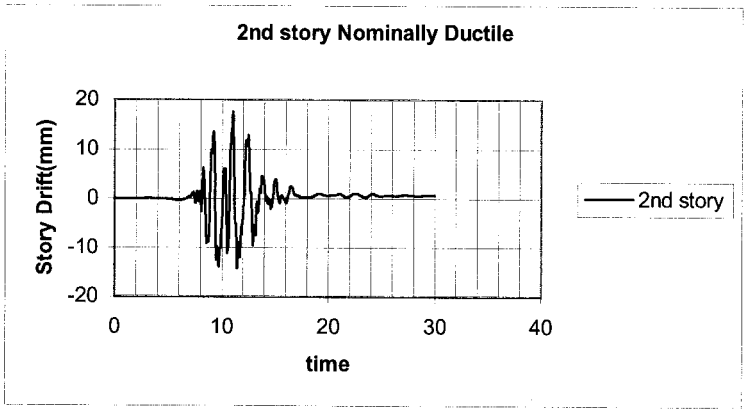

(b)

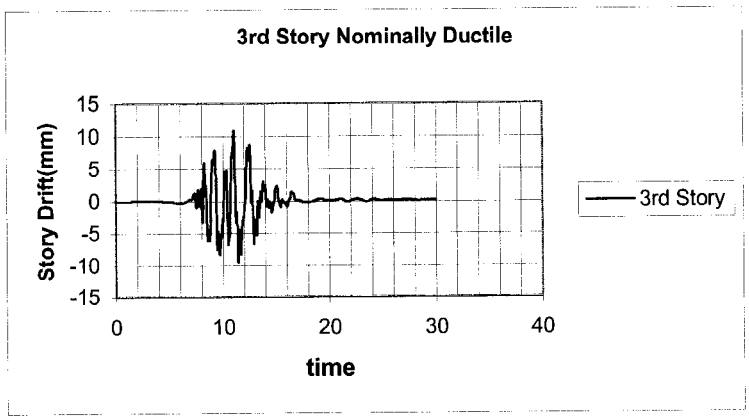
3rd Story Nominally Ductile
Story Drift(mm)
15
10
5
0
-5
-10
-15
0
10
20
30
40
time
3rd Story

(c)

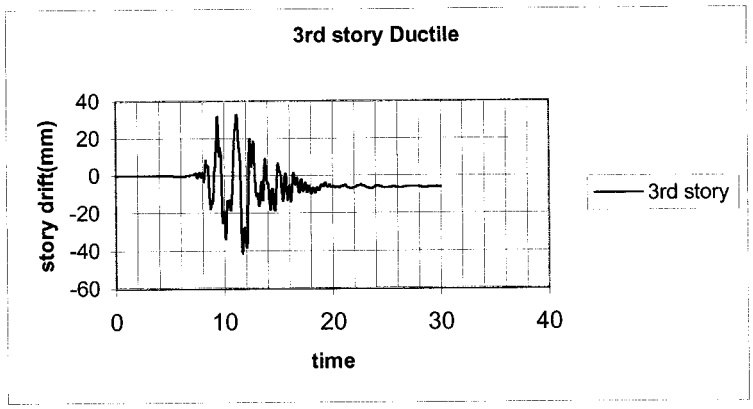
3rd story Ductile
story drift(mm)
40
20
0
-20
-40
-60
0
10
20
30
40
time
3rd story

(d)

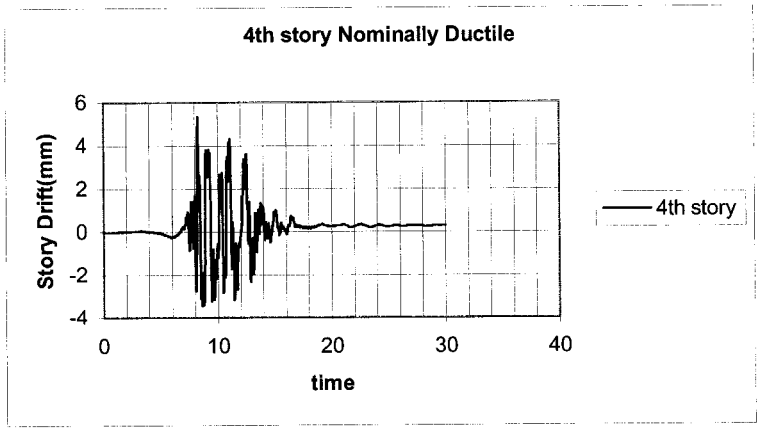
4th story Nominally Ductile
Story Drift(mm)
6
4
2
0
-2
-4
0
10
20
30
40
time
4th story

(e)

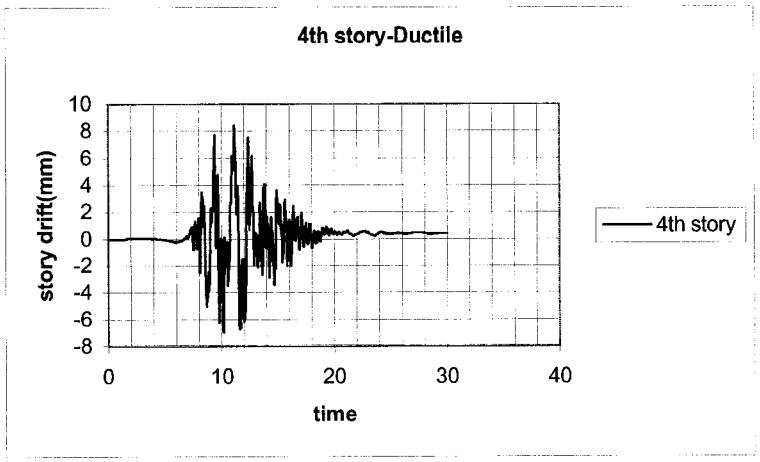

(f)

Figure 5.6 Time-drift relationships

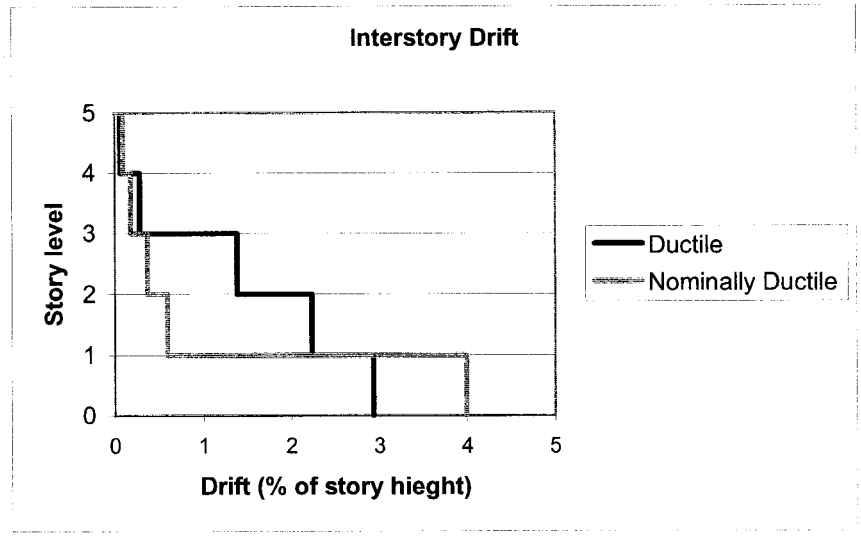

Figure 5.7 Inter-story drift comparisons

5.4 General Behavior and Cracking Patterns

The overall structural damage obtained for ductile frame is 0.128 and for nominally ductile frame is 0.433. These are similar to those of pushover analysis. Less overall damage occurred in the ductile frame as compare to the nominally ductile frame because of the better performance of ductile frames due to better confinement of columns and better detailing.

5.4.1 Damage analysis in ductile frames

Figure 5.8 illustrates the state of yielding/failure for ductile frame. This shows the progression of damage under dynamic analysis. Figure 5.9 shows the damage statistics index of ductile frame. The sequence of yielding in Figure 5.8 indicates that the beams at 1st and 2nd floors are yielded first as plastic hinges occurring at the beams end. Then the hinges are formed at the base of the columns after the beams yielded at 3rd floor. The columns then yielded in 2nd, 3rd and first floor respectively. Similar to pushover analysis, this behavior confirms the successful application of strong column-week beam theory in designing of ductile frame. The sequence of plastic hinging in the ductile structure conforms to the capacity design concept. Note that X, 0 and * express crack, yield and sever yield states of frame respectively and the numbers in parentheses indicate the sequence of yielding of beams, the columns and sequence of failure of structure (F).

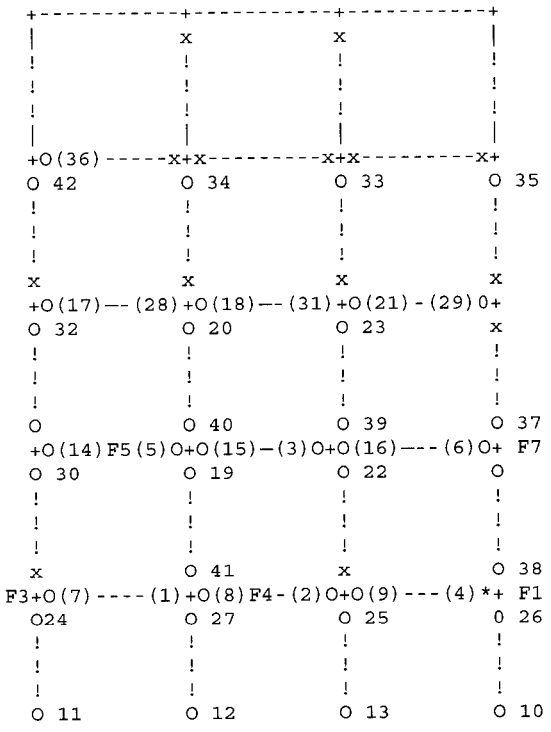

Figure 5.8 State of failure and sequence of yielding for ductile frame

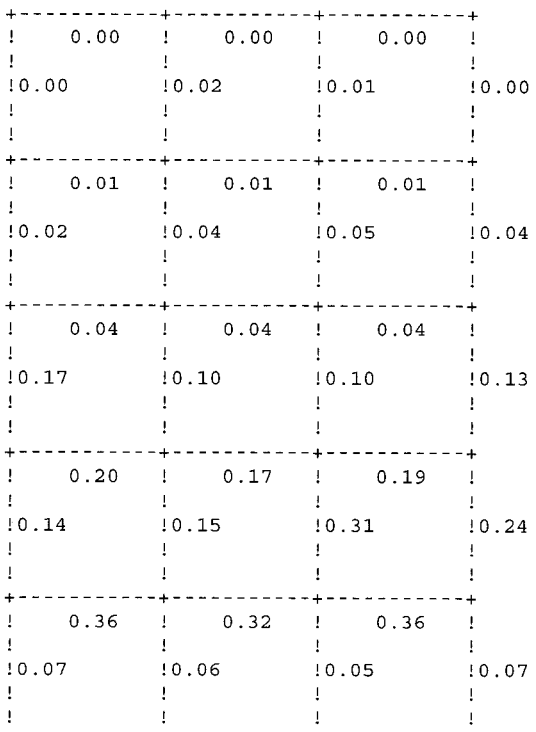

Figure 5.9 Damage index statistics of ductile frame

5.4.2 Damage Analysis in Nominally Ductile Frames

Figure 5.10 and 5.11 indicate the state of cracking/yielding and damage index statistics of nominally ductile frame in order to show the progression of damage under ground excitation. The sequence of yielding in Figure 5.10 illustrates that the first three plastic hinges are occurred at the exterior beam-column joints in the 1^{st}, 3^{rd} and 2^{nd} floors. Yielding of the base of the columns immediately follows. Then hinges are formed along the span of the first and 2^{nd} floors. Finally, the plastic hinges occur at the top of the interior and exterior columns. This hinging pattern in the structure for nominal ductility frame is far from an optimum design. Note that **x**, **0** and * express crack, yield and sever yield states of frames respectively.

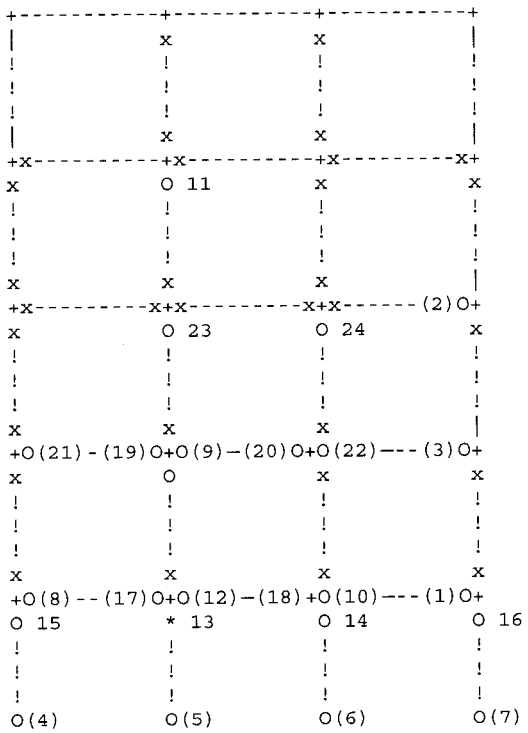

Figure 5.10 State of failure and sequence of yielding for nominally ductile frame

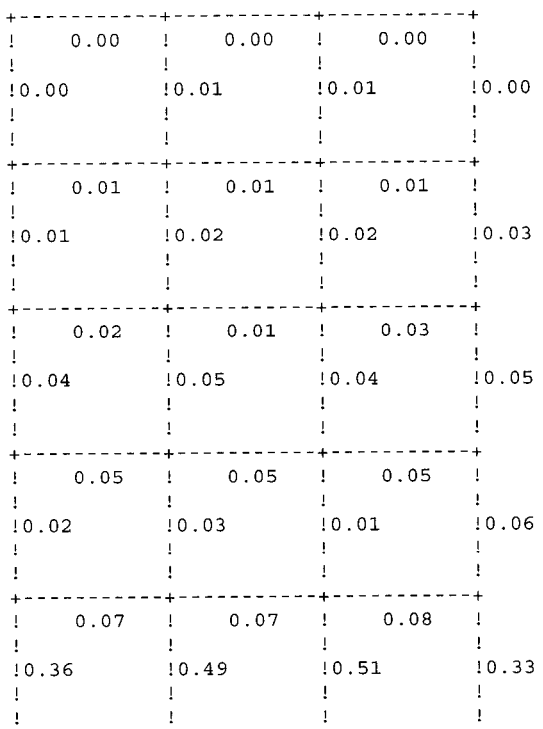

Figure 5.11 Damage index statistics of nominally ductile frame

5.4.3 Comparison of Damage Patterns of Structural Elements

The time-damage relationships of frames are investigated in order to determine the damage potential and response of each frame under ground excitation. Figure 5.12 show sever column damages in the 1st floor of nominally ductile frame with a damage index of about 0.45 while minor damages are obsorved in the beams. The damage index of 0.45 represents an un-repairable damage, extensive crashing of concrete and disclosure of buckled reinforcements. This behavior is confirmed the formation of an undesirable story-sway failure mechanism, lack of the strong column-weak beam considerations and forming of inelastic deformation in columns at first story level. In nominally ductile frame the 1st story is damaged severely while in the rest of stories, minor damage is observed. In conclusion, an undesirable dissipation of energy is indicated in the columns of 1st story level as a result of the formation of plastic hinges in these areas.

For ductile frame, more damages of beams (with index of about 0.1) rather than columns (DI=0.05) are observed. The minor damages are distributed throughout of the frame because of energy dissipation through all levels of the frame. This desirable behavior shows the strong column-weak beam consideration, which is representative of a better performance of ductile frame.

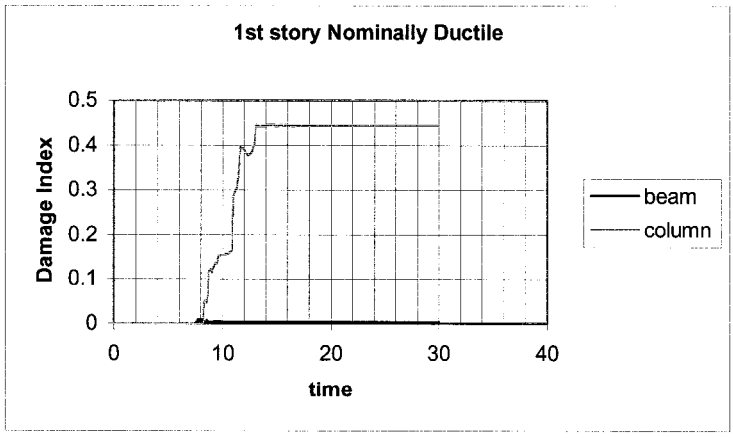

(a)

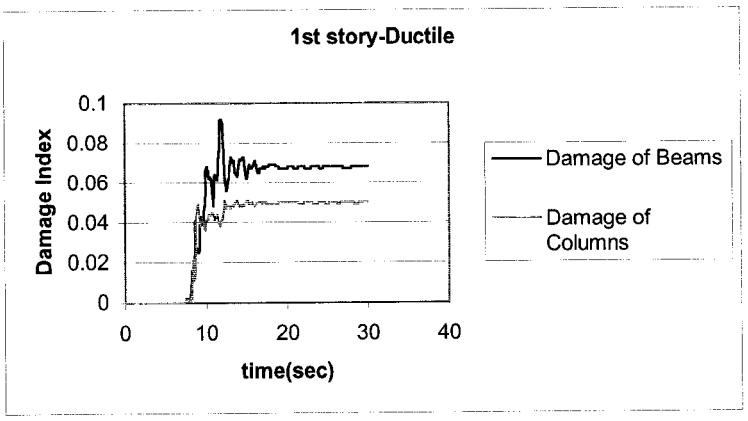
1st story-Ductile
Damage Index
0.1
0.08
0.06
0.04
0.02
0
0
10
20
30
40
time(sec)
Damage of Beams
Damage of Columns

(b)

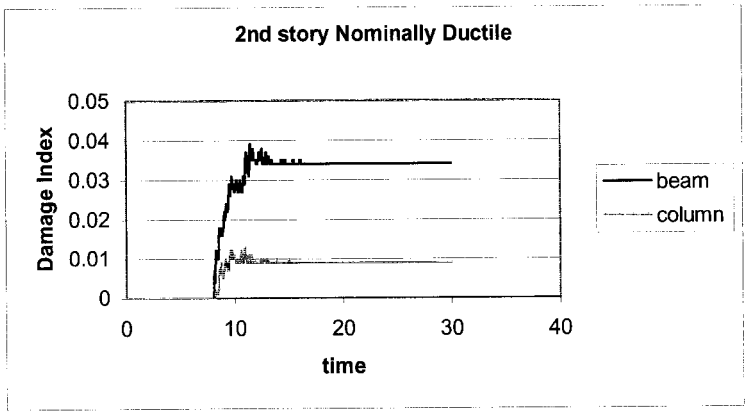
2nd story Nominally Ductile
Damage Index
0.05
0.04
0.03
0.02
0.01
0
0
10
20
30
40
time
beam
column

(c)

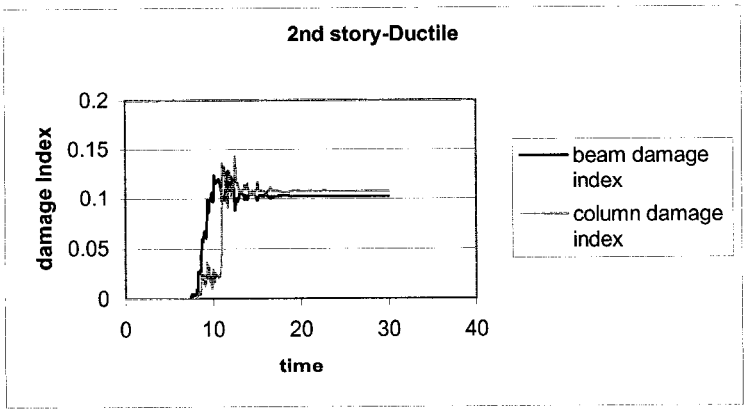
2nd story-Ductile
damage Index
0.2
0.15
0.1
0.05
0
0
10
20
30
40
time
beam damage index
column damage index

(d)

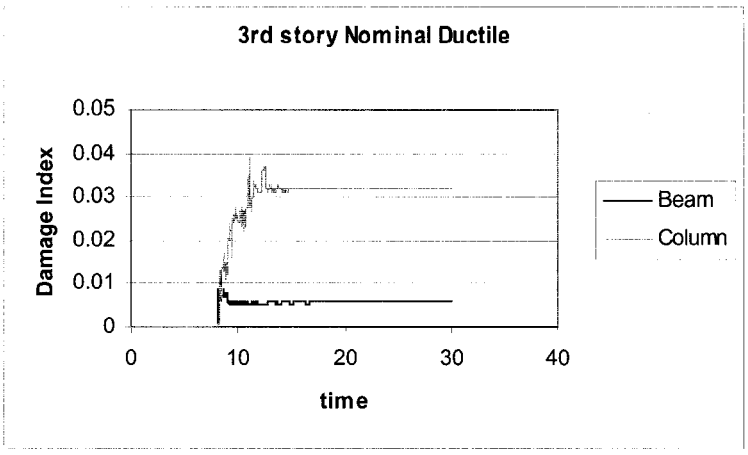
3rd story Nominal Ductile
Damage Index
0.05
0.04
0.03
0.02
0.01
0
0
10
20
30
40
time
Beam
Column

(e)

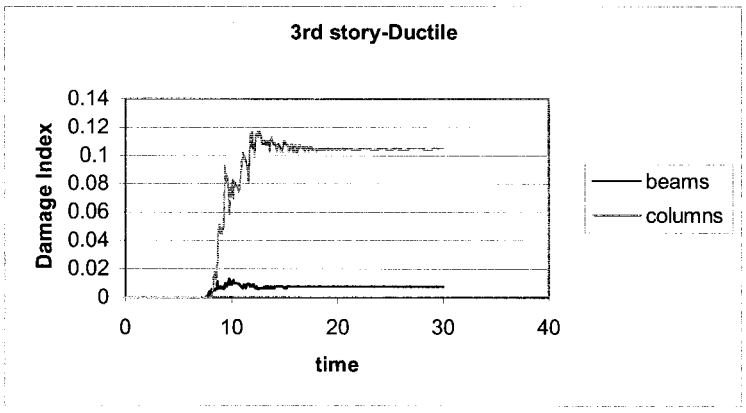
3rd story-Ductile
Damage Index
0.14
0.12
0.1
0.08
0.06
0.04
0.02
0
0
10
20
30
40
time
beams
columns

(f)

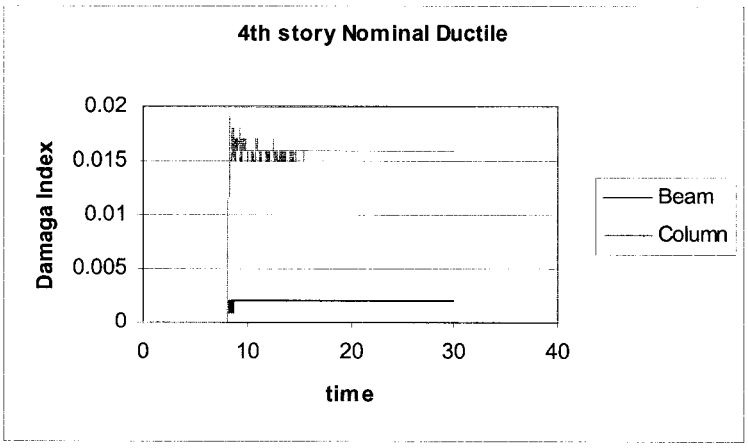
4th story Nominal Ductile
Damaga Index
0.02
0.015
0.01
0.005
0
0
10
20
30
40
time
Beam
Column

(g)

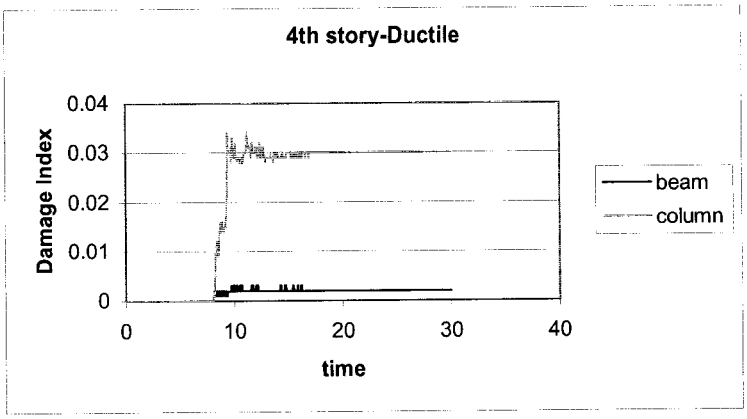

(h)

Figure 5.12 Time-damage relationships

CHAPTER 6

Gravity Load Designed (GLD) Frame Building

6.1 Introduction

In pervious chapters, the behavior of ductile and nominally ductile reinforced concrete (RC) building frames constructed in zones of high seismicity is discussed. In this chapter the seismic performance of an assumed existing five-story reinforced concrete building designed according to the provisions of ACI 318-63 is evaluated and compared to the performance of a similar ductile and nominally ductile frames designed according to current code provisions. Non-linear pushover analysis of the reinforced concrete frame is conducted. The building, which is assumed to be constructed prior to 1970's and is assumed to be located in Sandspit-BC. This Chapter presents structural engineering information on GLD building models. The structural system of GLD building is analyzed using nonlinear pushover and time history analysis. Structural members of this model are sized according to the requirements of the ACI 318-63. Since this Code did not include seismic requirements, framing systems are designed only for gravity and wind loads. The framing system developed for this project is designed for the same gravity loads considered for models of the ductile and nominally ductile frame.

6.2 The Global Behavior of GLD Existing Buildings

Some global behaviors of GLD existing buildings are as follows:

1. GLD frames have usually low strength and, in most cases, limited ductility.
2. Lack of capacity design consideration in the design process, proscribe non-ductile mode of failure such as soft-story sway mechanism.
3. Design to an allowable stress philosophy rather than a ultimate strength design philosophy, as was common before the late 1960's, contributes to the uncertainty of inelastic response of GLD buildings.
4. Usually details of GLD frames behave poorly
5. Consequently, the critical zones not only do not behave in a ductile manner, but also show a brittle mechanism of failure.

6. Columns generally are not designed to have strengths exceeding beam strengths, so column failure mechanisms often prevail.
7. Transverse reinforcement widely spaced and anchored with 90^{o} bends in potential plastic hinge regions of beams and columns. This may lead to a spalling of compressive concrete then lead to the buckling of longitudinal reinforcements and finally collapse of plastic hinge regions.

6.2.1 Features of Non-ductile GLD Frames

The following features of non-ductile GLD frames may influence seismic behavior and because of these problems, the assessment of existing RC structures requires a retrofitted procedure (Harries, K.A. and Bracci, J.M., 1995).

- The columns have light transverse reinforcement throughout the height
- Lapped splices are located just above the floor level in the maximum moment region.
- Discontinuous bottom longitudinal reinforcement, which is embedded in the beam column joint.
- Widely spaced beam stirrups.
- No transverse reinforcement in beam column joints.
- Relatively low strength of materials (steel and concrete) as compared with present material strength.
- Smaller tie diameter and larger tie spacing in columns.
- Lightly confined column lapped splices
- Lack of transverse ties for shear

6.3 Analyses and Design of GLD Buildings

6.3.1 Description of the GLD Building

The GLD building, as described in Appendix A, is a 5-story concrete frame building with plan dimensions equal to 22m in the east-west direction and 18m in the north-south direction. The height of the building, from grade level to the roof, is equal to 16 m. A plan view of the building is shown in Figure 3.1(a). The floor framing consists of 120mm thick concrete slabs. The gravity load resisting columns are fixed on foundations. The lateral force resisting system consists of moment-resisting frames in the both directions.

The geometry and material properties of structure are assumed same as other cases as discussed in chapter 4. More details of the various assumptions, material properties, geometry of the structures and parameters used in the design of the structures are listed in Tables A.1, A.8 and A.9 of Appendix A.

6.3.2 Determination of Lateral Loads

Lateral (wind) loads are calculated and applied on the GLD building frame. For wind load calculations, the frame is assumed to be located in a Sandspit-BC with high-risk seismic zone (v= 0.4). The structural GLD frame is designed for a lateral (horizontal) wind pressure equal to 0.63 KPa on the vertical surface of building. Table A.11 illustrates a summary of the manually calculated values for GLD frame (See Appendix A).

Components are selected and checked for the following load combinations as per the requirements of the ACI 318-63 Building Code

1.4DL+ 1.7LL

0.75 (1.4DL+ 1.7LL + 1.7WL)

1.05DL+1.275WL

Where

D, L, and W are dead, live, and wind loads, respectively.

Figure A.7 illustrates the resulting load combinations for dead, live and wind loads in an internal frame.

6.3.3 Design of GLD Building

The computer program SAP 2000 is used to model and analyze the GLD building. Rigid end offsets are not considered. Only one typical internal frame is modeled. Based on the same assumptions as two other previous cases of study namely ductile and nominally ductile frame, weights are calculated for each floor and each story of the building. The results of analysis are used to design the building. More details of the analysis and design of GLD Frames are presented in Appendix A.

In the preliminary design of the building, it is decided to use 450*250 mm beams and 300 mm in diameter circular columns as shown in Figures A.8 and A.9.

Initial elastic analysis of structure is performed to determine the structural elements internal design forces. Factored maximum axial force and moment, including wind and gravity load effects from an elastic frame analysis, are given in Tables A.12 and A.14 using the sign convention that positive moments cause compression in top fiber.

The building is designed by modifying the size of beams and columns in moment-resisting frames in such a way that they comply with the minimum requirements of the ACI 318-63. Beams and columns in moment-resisting frame are sized to resist wind and gravity-load effects only. For this proposes new sizes are established as shown in Figures A-8 and A-9. Summary of design and structural components details are presented in Appendix A.

6.4 Nonlinear Pushover Analysis of GLD Frame Building

Pushover analysis is performed on GLD structure to determine the base shear- lateral displacement envelope and the sequence of plastic hinging. In such an analysis, a monotonic load is applied to the GLD structure until an ultimate load is approached. This corresponds to a value of 0.0747 as the base shear coefficient. The nonlinear computer program, IDARC includes several types of hysteretic response models. In this investigation, frames are modeled by commonly used bilinear model similar to the other cases as described in chapter 4. Pushover analysis results are presented here in terms of both displacement and drift. Configuration of frames is same as shown in Figure 4.2. For frame modeling of columns the minimal effectiveness of confinement, CEFF=0.5, is considered as shown in Figure 6.1. This corresponds to the poor detailing of GLD frame. More detail of design and sectional properties is addressed in Appendix A. The hysteretic models of the structure are determined from experimental tests due to cyclic loading. The results of such experiments show unstable loops for GLD frames. Thus in GLD frame modeling, the strength and stiffness deterioration are considered (Kunnath, S.K., 1995). The values of the IDARC parameters used in the analysis of GLD frame are HC=0.1, HBE=HBD=0.4, and HS=0.1 for the control of stiffness deterioration, strength degradation, and pinching behavior respectively. In developing analytical models of GLD frame structure, other assumptions used are the same as ductile and nominally ductile

frames as discussed in chapter 4. The assumptions include, system of units and material properties.

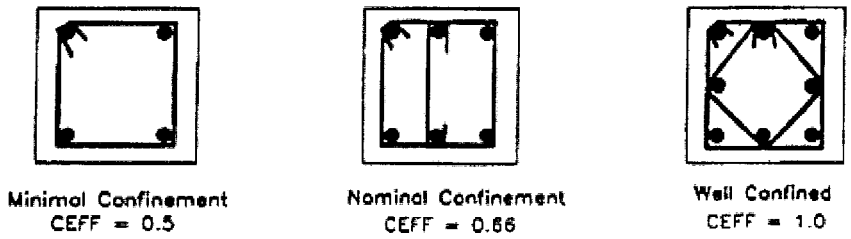

Figure 6.1 Effectiveness of confinement for some typical hoop arrangements

6.4.1 Results of Pushover Analysis

The GLD frame is analyzed under monotonically increasing static lateral loading. The lateral loads are distributed over the height of the building. The displacement-base shear relationships of frame are shown in Figures 6.2 and 6.3. The descending branch of load-deformation curve presents a non-ductile behavior of GLD frame. These Figures illustrate that the base shear can reach to peak value of 205 kN. The corresponding deformation at peak base shear of 0.0460 is 250 mm (1.56% of building height). As shown in Figure 6.2, the maximum deformation capacity of GLD frame is less than 1.6%. The descending slope of load-deflection curve represents a non-ductile behavior of GLD frame.

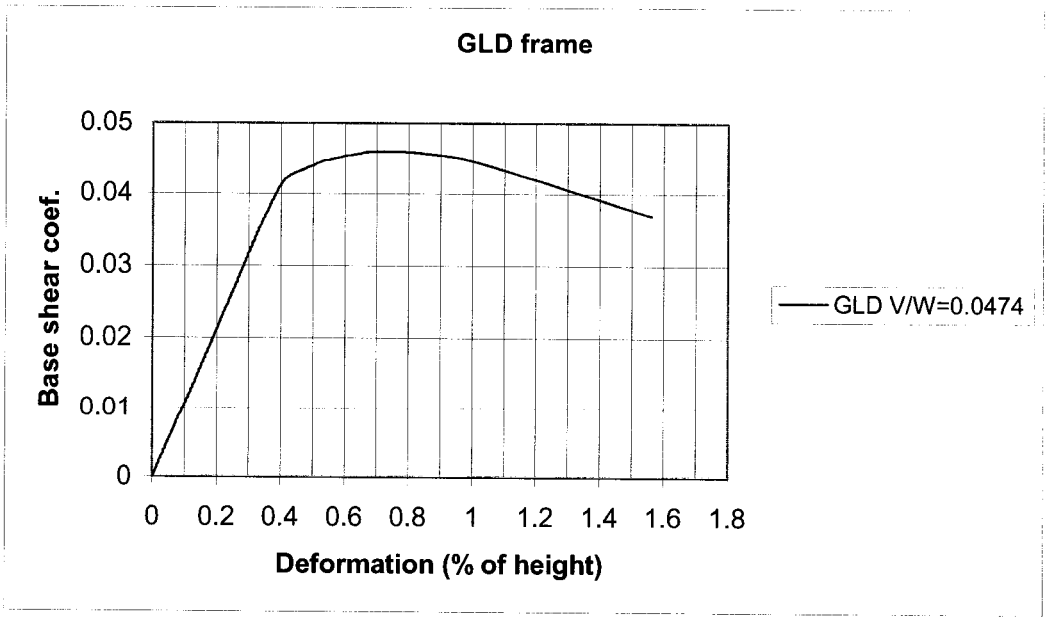

Figure 6.2 Base shear coefficient versus displacement percentage of height

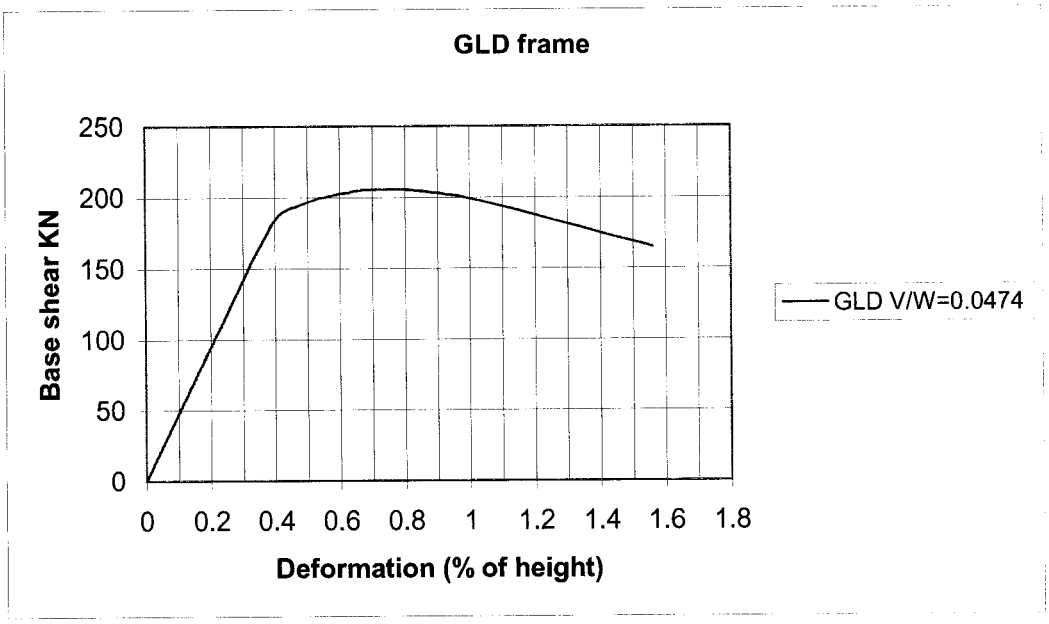

Figure 6.3 Base shear versus displacement relationships

The ratio of maximum displacement to the yield displacement is calculated in each story of GLD frame. This ratio represents the displacement ductility factor and is defined as a measure of the ductility of the structure with regard to seismic loading. The results shown in Figure 6.4 illustrate that the GLD frame has low ductility as expected, than ductile and nominally ductile frames. This may result in a non-ductile and brittle behavior of GLD structures.

The drifts are calculated for each story by dividing relative floor lateral displacement between the two adjacent floors to the height of the story. Figure 6.5 shows story drifts of GLD frame. Figure 6.5 shows that, the maximum drifts obtained in 1^{st} and 2^{nd} floor are equal to about 5% and 0.7% respectively.

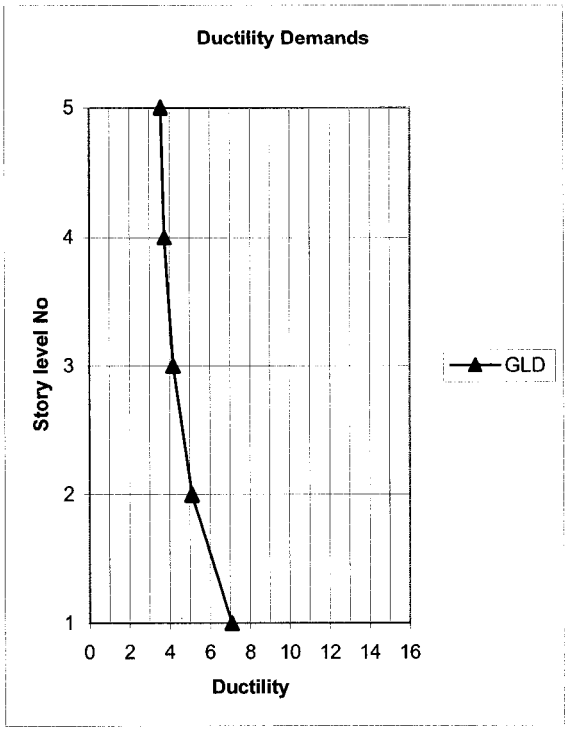

Figure 6.4 Displacement ductility (GLD Frame)

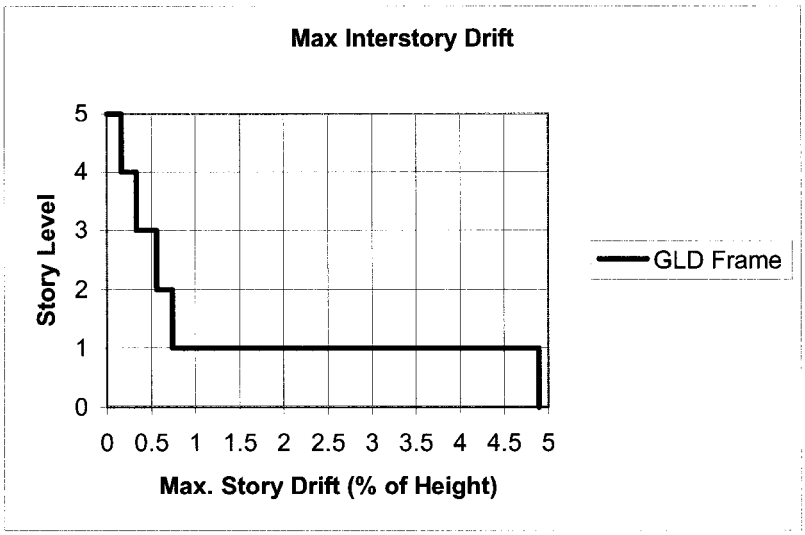

Figure 6.5 Inter-story Drift

Figure 6.6 shows maximum base shear-story displacement due to pushover loading in story levels for GLD frame. A large displacement of about 200mm takes place in the first story and rest of the floors act as a rigid body. The damage analysis illustrates, the

occurrence of plastic hinges and severe damages of columns in the fist floor which are the cause for this undesirable deformation due to lack of strong column-weak beam mechanism.

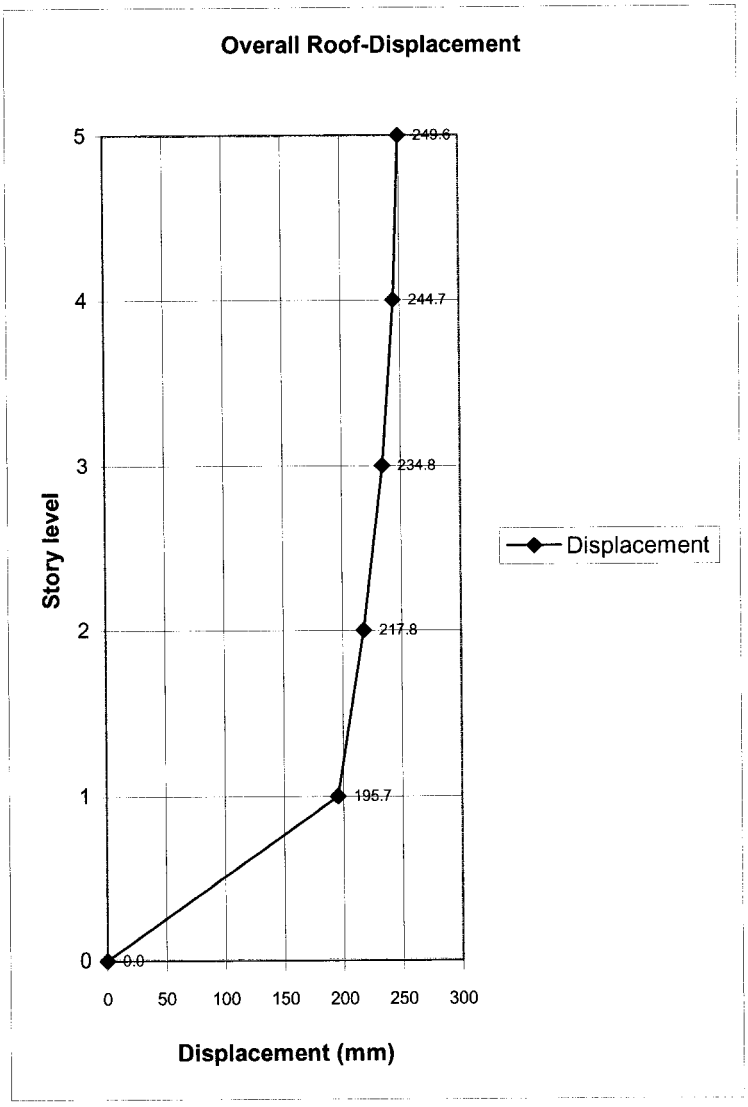

Figure 6.6 Base shear story displacement relationship

6.4.2 Damage Analysis in GLD Frames

Table 6.1, Figures 6.7 and 6.8 indicate the state of cracking/yielding and damage index statistics of GLD frame in order to show the progression of damage as the load is increased. The sequence of yielding in Table 6.1 indicates that an exterior beam at 1st floor has yielded first. Plastic hinges occur in the base of the columns at first floor and top of interior columns. Finally exterior columns yielded at 1st floor. Note that **x** and **0** express crack and yield states of frame and the numbers in parentheses indicate sequence of yielding.

Table 6.1 Sequence of component yielding (GLD)

NO.	STORY LEVEL	ELEMENT	BASE SHEAR	SEQUANCE OF YIELDING
1	1st	BEAM 1	0.0428	YIELDING DETECTED AT LEFT
2	1st	COLUMN 2,3	0.0448	YIELDING DETECTED AT BOT
2	1st	COLUMN 3	0.0448	YIELDING DETECTED AT TOP
3	1st	COLUMN 2	0.0451	YIELDING DETECTED AT TOP
4	1st	COLUMN 1	*	*
5	1st	COLUMN 4	*	*
6	1st	COLUMN 4	*	*

* These elements are yielded but there was no record of sequence of yielding in output data.

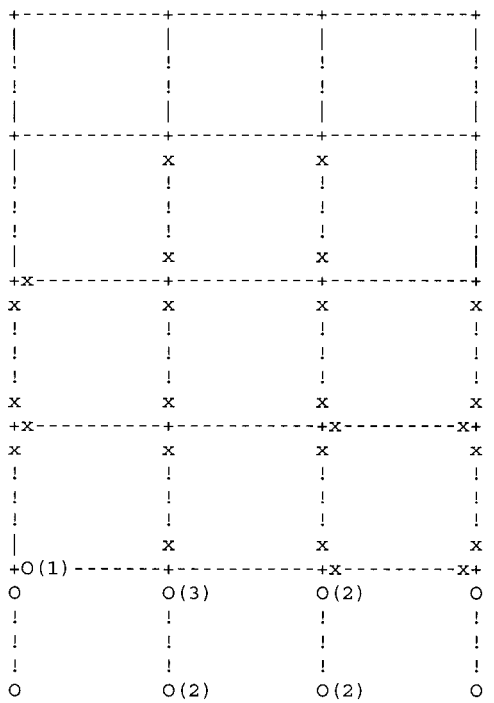

Figure 6.7 State of Failure and sequence of yielding for GLD frame

0.00 (0.04)	0.00 (0.04)	0.00 (0.04)	
0.00 (.13)	0.00 (.33)	0.00 (.30)	0.00 (.13)
0.00 (0.00)	0.00 (0.00)	0.00 (0.00)	
0.00 (.01)	0.00 (.50)	0.00 (.49)	0.00 (.00)
0.00 (0.08)	0.00 (0.00)	0.00 (0.00)	
0.01 (.10)	0.02 (.34)	0.02 (.36)	0.00 (.11)
0.01 (0.15)	0.00 (0.00)	0.01 (0.09)	
0.02 (.12)	0.03 (.20)	0.03 (.23)	0.01 (.21)
0.05 (0.03)	0.00 (0.00)	0.01 (0.01)	
0.20 (.28)	0.26 (.18)	0.26 (.19)	0.21 (.30)

Figure 6.8 Damage index statistics of GLD frame

The overall structural damage obtained for GLD frame is 0.203. Interpretation of overall damage index is presented in Table 4.1. Figure 6.9 shows that the first yielding of structural elements in GLD frame occurs in beam at base shear coefficient of 0.0428 and first column is yielded at base shear coefficient of 0.0448.

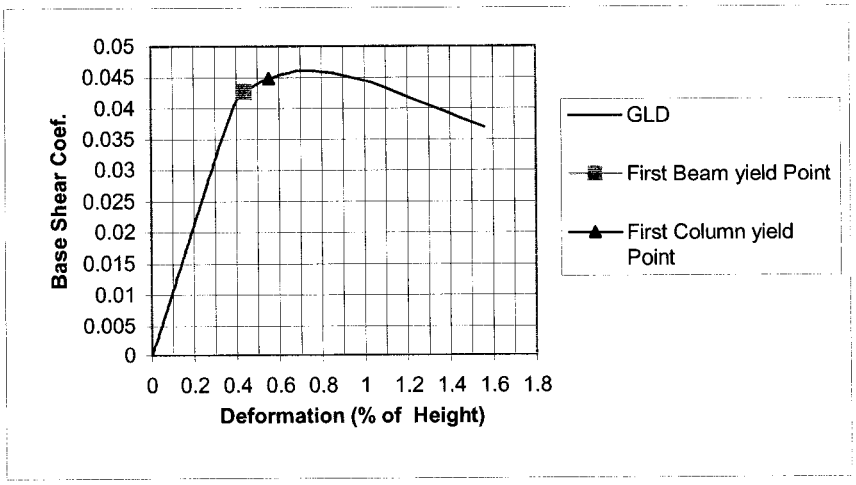

Figure 6.9 Sequence of yielding

6.5 Dynamic Analysis

6.5.1 Introduction

The inelastic nonlinear dynamic analysis program IRDAC is used to calculate the inelastic response of GLD structure described in section 6.3 to time history analysis. The time history analysis predicts the seismic response of structures. In this investigation the structure is subjected to Erzincan (1992) ground motion. Under this ground motion, damages and failure modes of the GLD structures are investigated. Dynamic analysis is performed to determine the lateral displacement envelope, story shear, story drifts, moment capacities of frame and the sequence of plastic hinging. The nonlinear dynamic computer program, IDARC includes several types of hysteretic response models. In this investigation frames are modeled by commonly used bilinear model as pervious cases. The dynamic analysis results are presented here in terms of both displacement and drift.

6.5.2 Ground Motions

To form an earthquake data set as input ground motions for the designed GLD frame, a ground motion was selected from the earthquake database system at Joint Venture SAC (Structural Engineers Association of California, Applied Technology Council and California Universities for Research in Earthquake Engineering) Horizontal ground motions for Los Angeles with a probability of exceedence of 2% in 50 years. A horizontal component is selected to give a peak ground acceleration of 0.643g (593.6 cm/sec^2) witch include a scale factor of 1.35. This provides an excitation in proportion to the moderate seismic risk. The ground motion duration is about 20 seconds. Figure 6.10 presents the acceleration time-histories of this seismic event.

Table 6.2 provides detailed information on the records generated for Seattle having probabilities of exceedence of 2% in 50 years.

Table 6.2 Details of Erzincan (1992) Ground Motions Having a Probability of Exceedence of 2% in 50 Years

SAC Name	Record	Earthquake Magnitude	Distance (km)	Scale Factor	Number of Points	DT (sec)	Duration (sec)	PGA (cm/sec^2)	PGA
SE23	1992 Erzincan	6.7	2	1.35	4156	0.005	20.775	593.6	0.643g

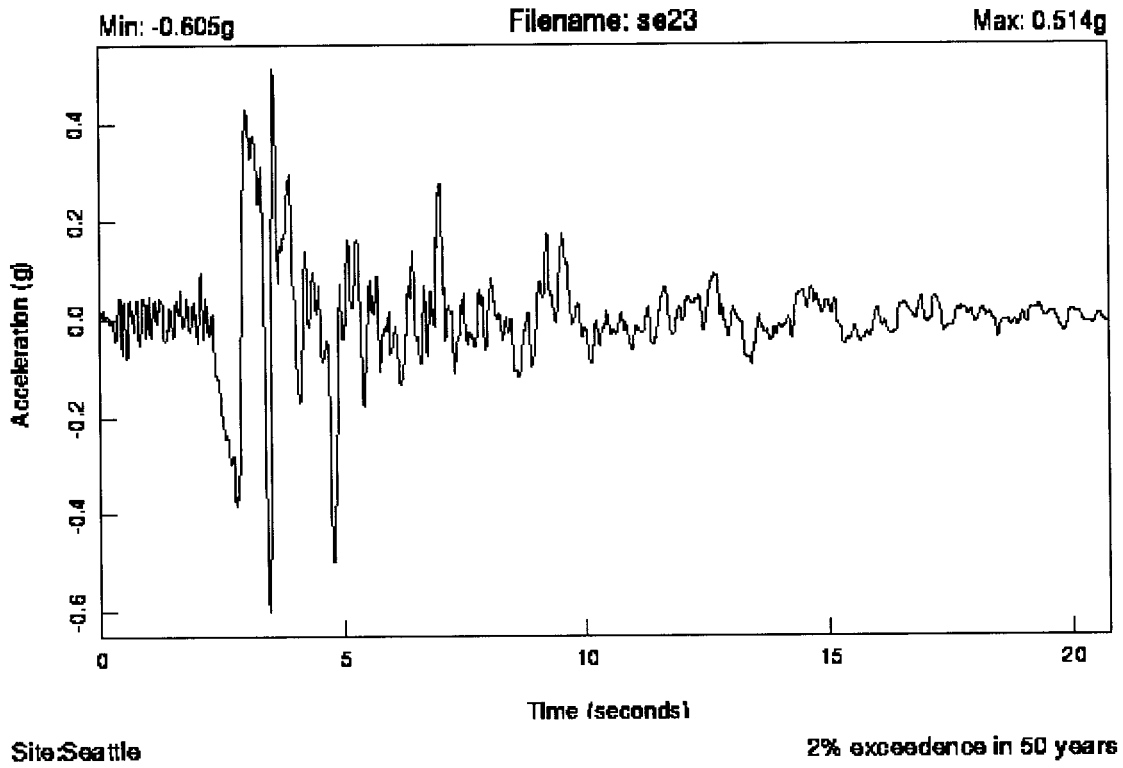

Figure 6.10 Erzancan (1992) Ground Motions

In developing analytical models of frame structure, assumptions used for dynamic analysis are same as pushover analysis in terms of hysteretic models, geometry, system of units and material properties. For the analysis carried out herein, to ensure accurate results, an integration time step of 0.005 seconds was used for nonlinear dynamic analysis. Approximately 5% of critical damping was assumed in this analysis

6.5.3 Results of Time History Dynamic Analysis

The GLD frame is dynamically analyzed due to the ground excitation. The time-displacement relationship for each story is shown in Figure 6.11. The maximum displacement at 1st floor is about 475 mm at representative base shears of about 200 kN and in the rest of stories a rigid body motion with almost same displacements is observed. The GLD frame showed a poor response to this ground excitation as inelastic deformations are concentrated mainly in first floor and rest of frame is acted as a rigid body.

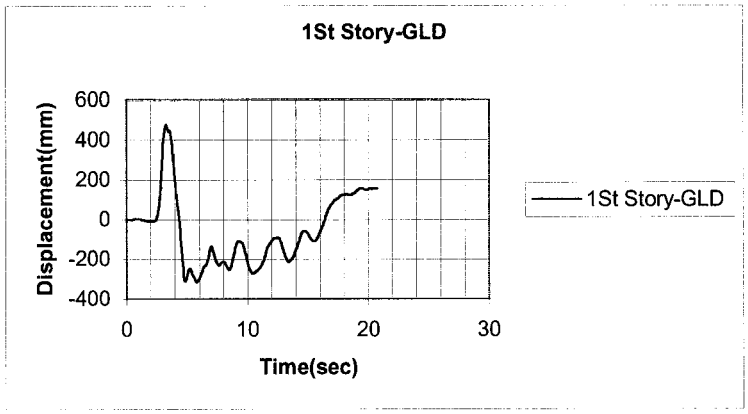
1St Story-GLD
Displacement(mm)
600
400
200
0
-200
-400
0
10
20
30
Time(sec)
1St Story-GLD

(a)

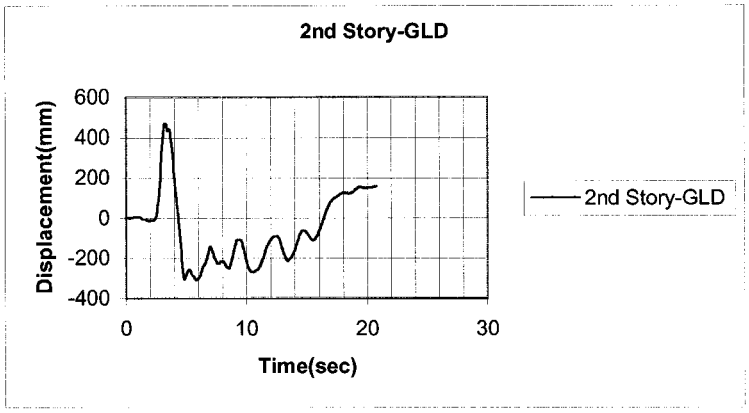
2nd Story-GLD
Displacement(mm)
600
400
200
0
-200
-400
0
10
20
30
Time(sec)
2nd Story-GLD

(b)

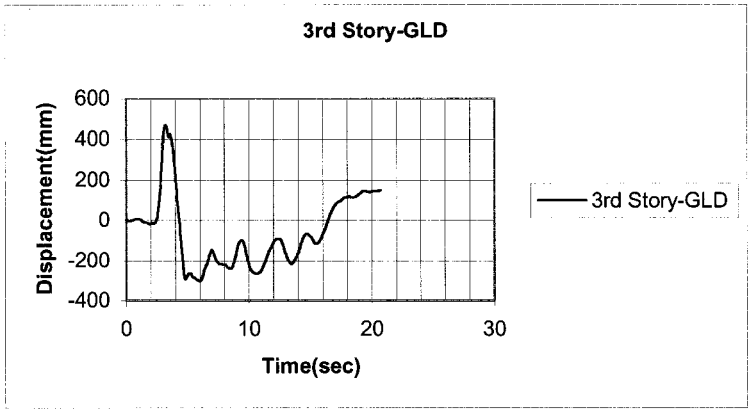
3rd Story-GLD
Displacement(mm)
600
400
200
0
-200
-400
0
10
20
30
Time(sec)
3rd Story-GLD

(c)

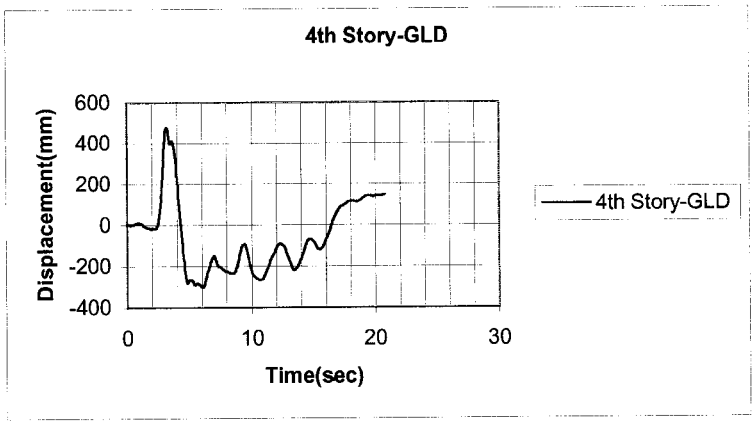

(d)

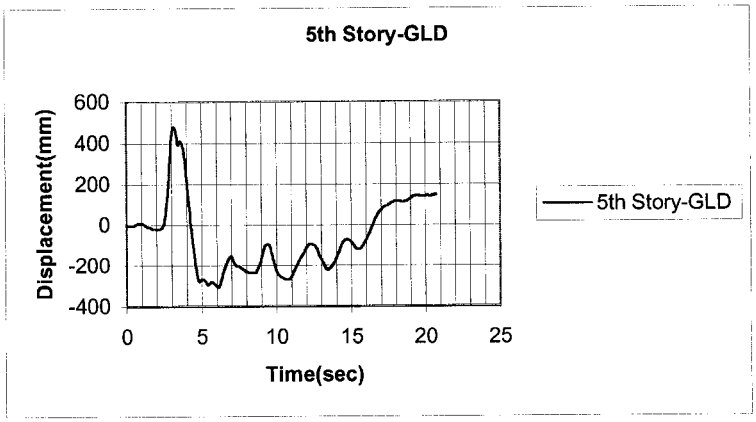

(e)

Figures 6.11 Time-displacement relationships

The maximum values of displacements from time-history analysis in each story are plotted in Figure 6.12. A large deformation of about 475mm in first story is observed. The rest of the floors act as a rigid body. As similar behavior is observed in pushover analysis, plastic hinges and severe damages of columns occurred in the fist floor and caused an undesirable deformation due to column-sway mechanism.

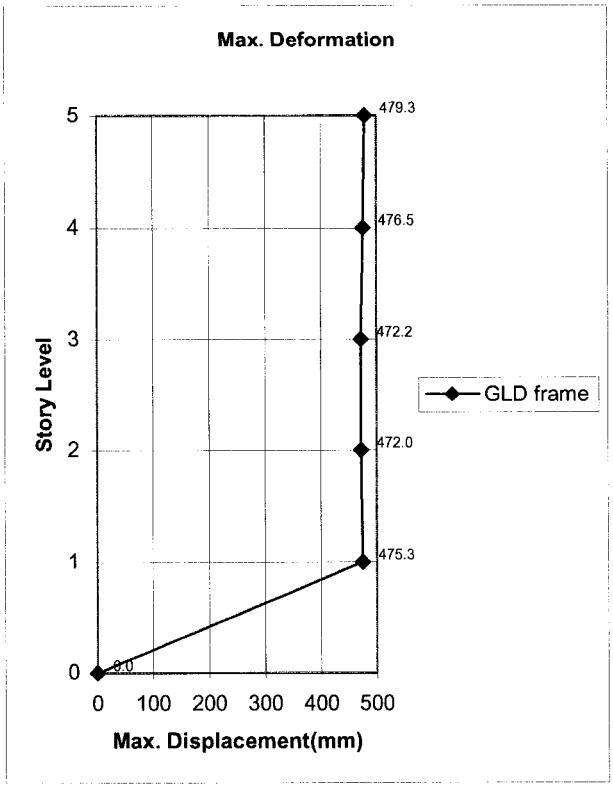

Figure 6.12 Maximum displacement (GLD)

Figure 6.13 illustrates the time-story shear relationship for each story level for GLD structure

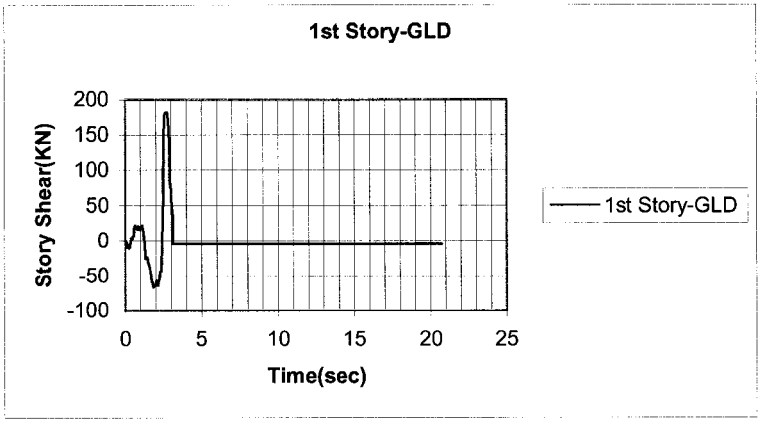

(a)

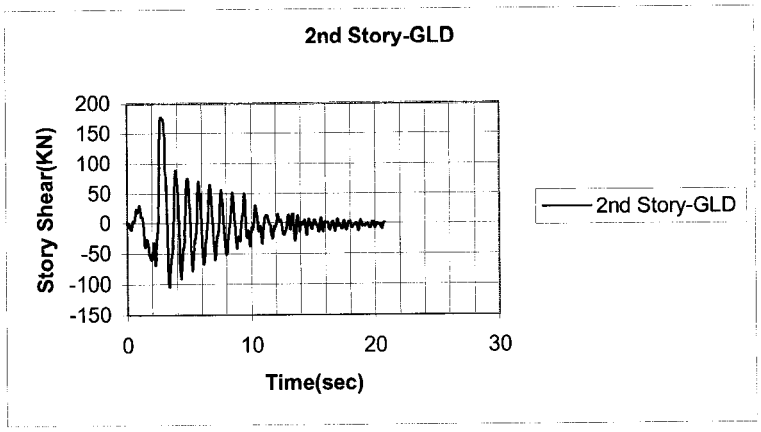
2nd Story-GLD
Story Shear(KN)
200
150
100
50
0
-50
-100
-150
0
10
20
30
Time(sec)
2nd Story-GLD

(b)

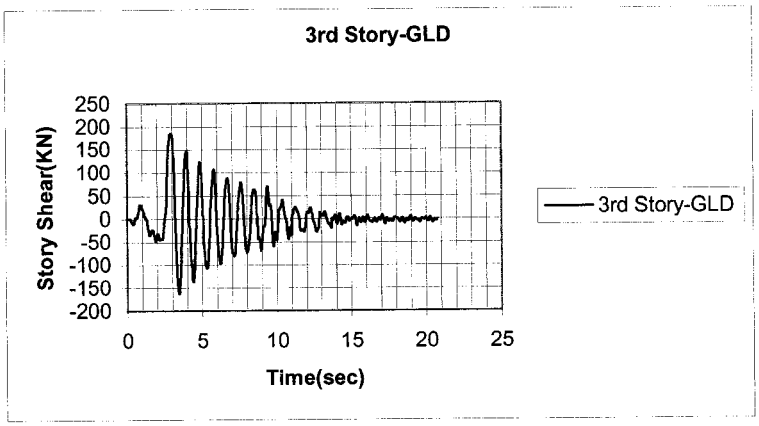
3rd Story-GLD
Story Shear(KN)
250
200
150
100
50
0
-50
-100
-150
-200
0
5
10
15
20
25
Time(sec)
3rd Story-GLD

(c)

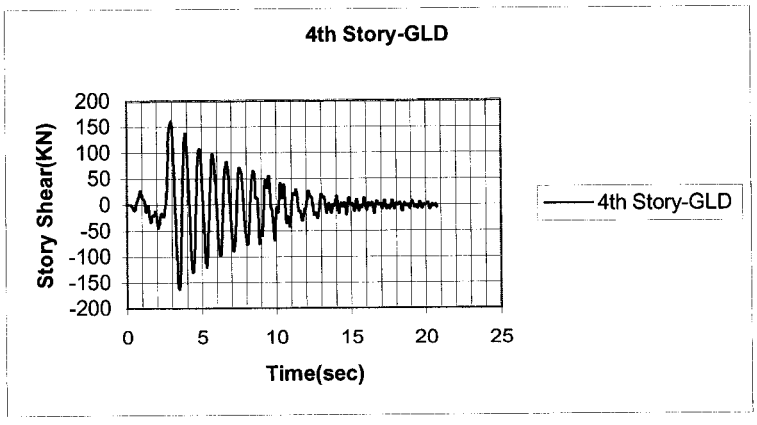
4th Story-GLD
Story Shear(KN)
200
150
100
50
0
-50
-100
-150
-200
0
5
10
15
20
25
Time(sec)
4th Story-GLD

(d)

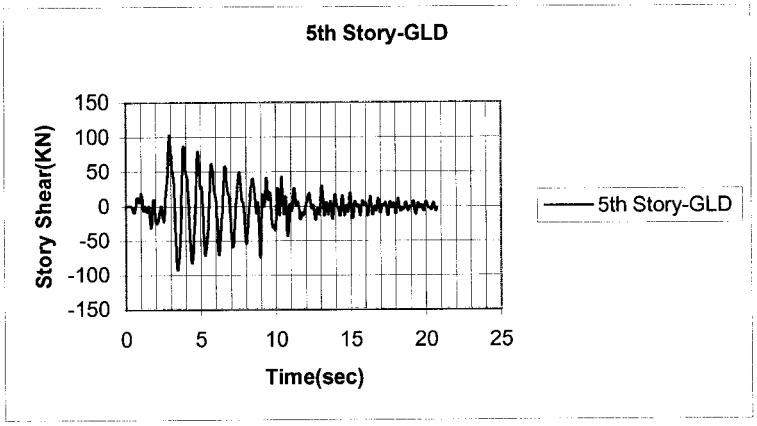

(e)

Figures 6.13 Time-story shear relationships

Figure 6.14 illustrate time-acceleration relationships of GLD frame for the fist floor. The time acceleration diagrams agree with the input wave data as shown in Figure 6.10.

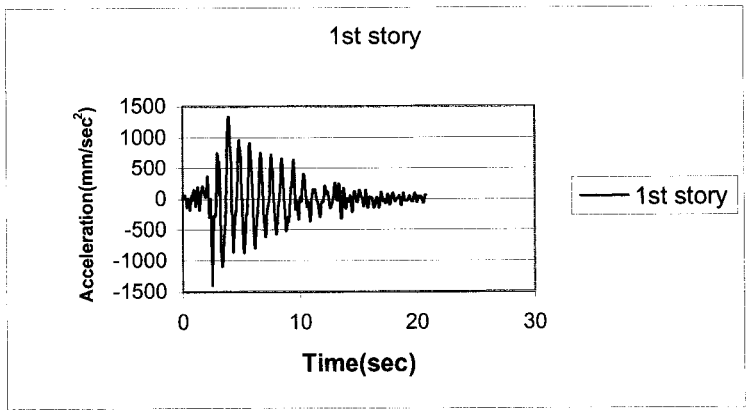

Figure 6.14 Time-acceleration relationships

The results obtained from dynamic time history analysis illustrate the maximum drifts of GLD frame reaches to 11.8% of story height, as shown in Figure 6.15.

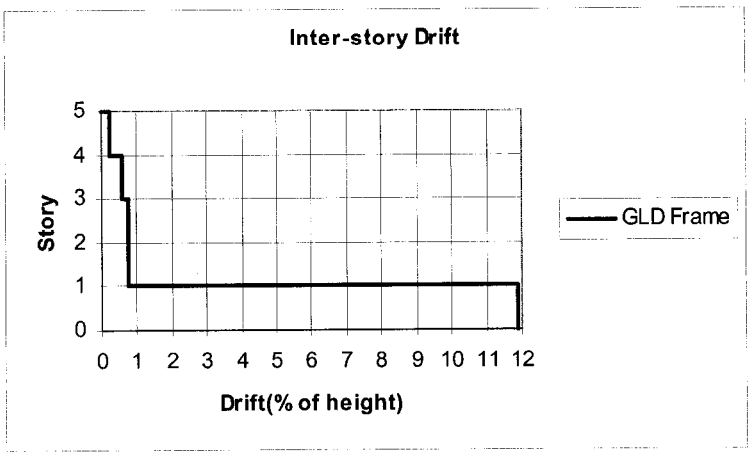

Figure 6.15 Inter-story Drift

6.5.4 General Behavior and Cracking Patterns

For GLD frame an overall sever damage index of 0.780 is observed. Figures 6.15 and 6.16 indicate the state of cracking/yielding and damage index statistics of GLD frame in order to show the progression of damage under Erzancan ground excitation. The sequence of yielding in this Figure illustrates that; first plastic hinges are occurred at the base of columns in 1st floor. Then a hinge is occurred along the exterior span of the first floor. Next, yielding of the exterior column is observed at top of 2nd floor. Finally, the plastic hinges are occurred at interior columns of the 3rd and 4th stories. This hinging pattern in GLD frame is far from energy dissipation mechanism in beams. Most damages occur in columns rather than in beams, which is the result of local story mechanism. In general, these results illustrate poor response of GLD frame structure.

6.5.5 Comparison of Damage Patterns of Structural Elements

Figure 6.18 shows damage patterns of GLD frame. Severe column damages occur in the first floor of GLD frame with a damage index of about 0.85 while minor damages are observed in the beams. The damage index of 0.85 represented an un-repairable damage, extensive crushing of concrete and disclosure of buckled reinforcements. This behavior is similar to nominally ductile frame and confirms the formation of an undesirable story-sway failure mechanism, lack of the strong column-weak beam considerations and forming of inelastic deformation in columns at first story level.

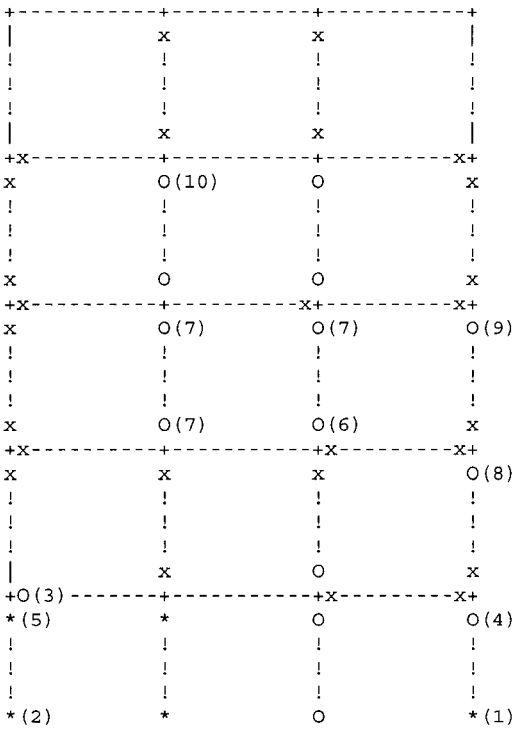

Figure 6.15 State of failure and sequence of yielding for GLD frame

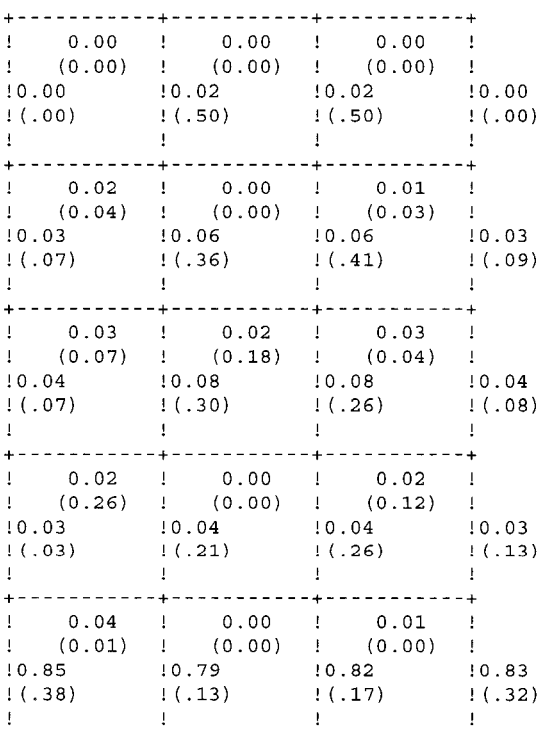

Figure 6.16 Damage index statistics of GLD frame

In general, the first story damaged severely and in the rest of stories minor damages are observed. In conclusion, an undesirable dissipation of energy is indicated in columns of 1st story as a result of the formation of plastic hinges in these areas.

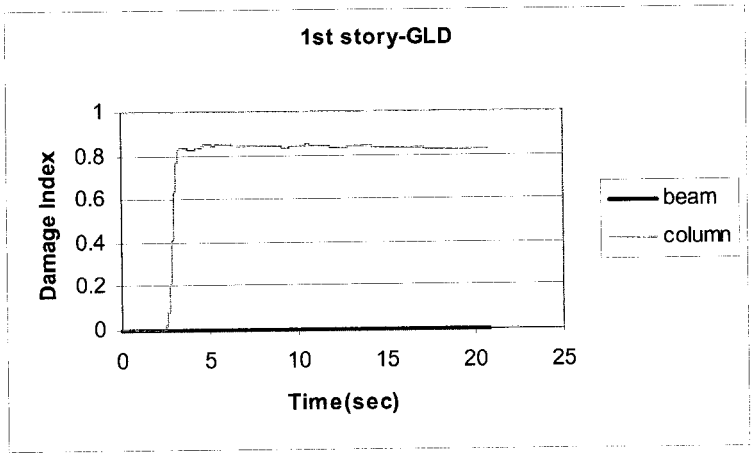

(a)

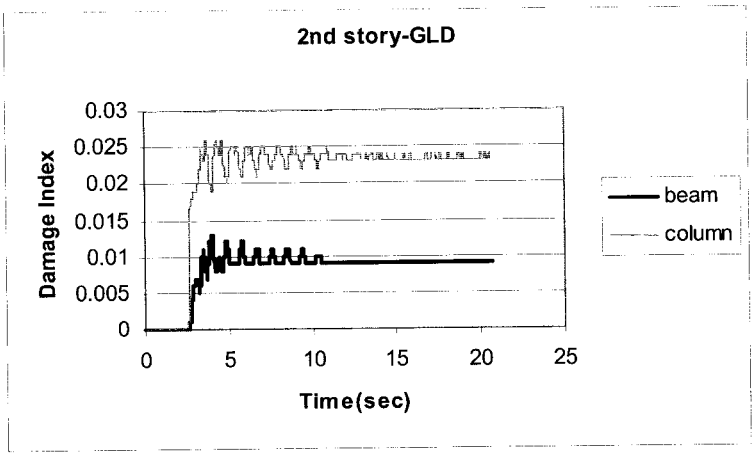

(b)

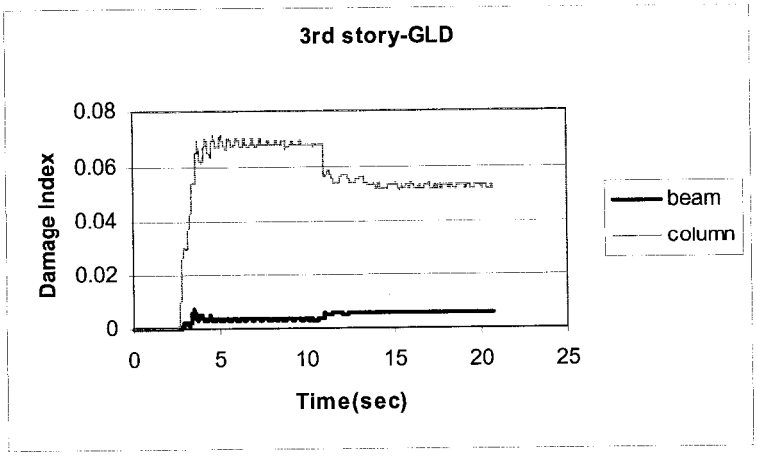

(c)

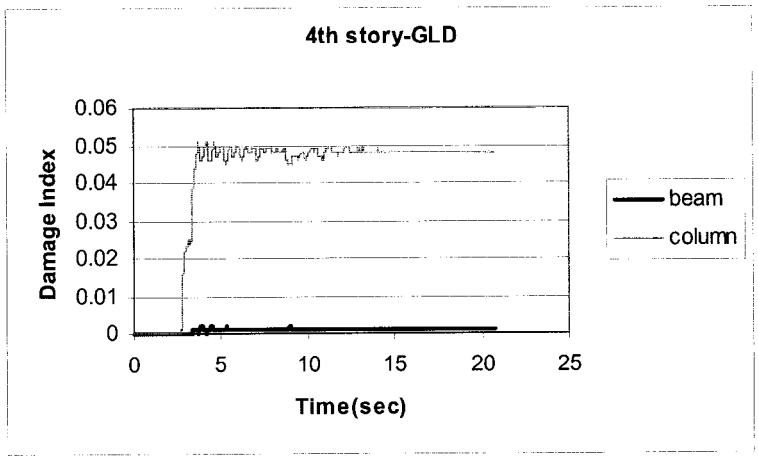

(d)

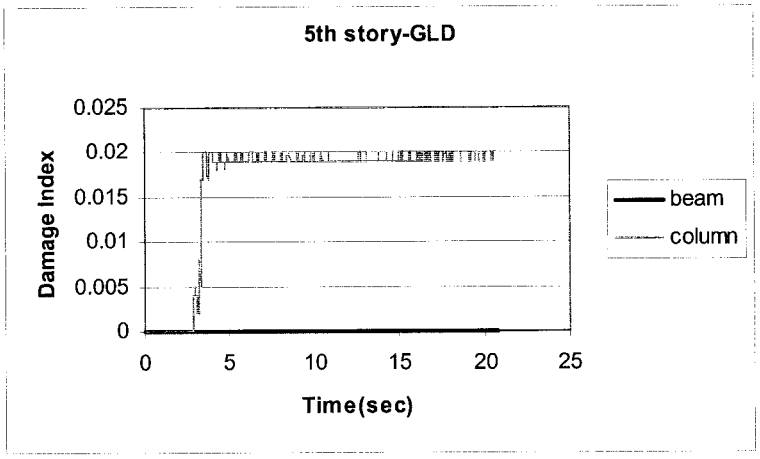

(e)

Figure 6.18 Time-damage relationships

6.6 Conclusion

Structures designed according to earlier Codes with inadequate seismic provisions have not performed satisfactorily during recent earthquakes. The seismic performance of an existing five-story reinforced concrete building designed according to the ACI 318-63 is evaluated. Non-linear pushover and time history dynamic analyses of the reinforced concrete frame are conducted. The results of the analyses indicate that damages are undesirable when the existing GLD frame is subjected to monotonic pushover and dynamic loads. This information is useful in the design of the required rehabilitation scheme and retrofitting of GLD Structures to provide an identified level of protection.

The GLD frame is compared to the performance of a similar frame designed according to current code provisions, which is described in Chapter 8.

CHAPTER 7

Seismic Retrofitting of GLD Buildings

7.1 Introduction

When the strength and ductility capacities of structure do not meet the seismic demands, retrofitting of the structure is required. The seismic behavior and performance of existing GLD buildings are discussed in Chapter 6. This Chapter investigates retrofitting of non-ductile GLD reinforced moment resisting frame buildings and also presents comparative analytical results of retrofitted 5 story GLD RC frame structure subjected to earthquake ground motion and pushover loading. This frame is analyzed under confined conditions produced by fiber composite wrapping. The retrofitting approach focuses in improvement of ductility capacity of columns to achieve adequate overall performance of structure and forming a more favorable failure mechanism in retrofitted GLD structure than mechanism that would form in non-retrofitted structure.

7.2 Introduction to Fiber Reinforced Polymers (FRP)

Fiber reinforced polymers (FRP) contain high-resistance fibers embedded in a polymer resin matrix and are produced as sheets, plates and laminates. They are rapidly becoming the materials of choice for the strengthening and rehabilitation of civil engineering structures. These lightweights, high-strength materials are attractive because of their resistance to corrosion, durability and ease of installation. Despite their relatively recent entry into civil engineering construction, FRP repair and strengthening methods are gaining wide acceptance as effective and economic infrastructure rehabilitation technologies. Indeed, the most remarkable development over the past few years in the field of FRP strengthening and repair has been the rapidly growing acceptance worldwide of these new technologies for an enormous range of practical applications. FRP rehabilitation projects have been extremely varied in nature and have included, for example, column and beam strengthening, seismic retrofitting, the FRP repair of corrosion-damaged beams and columns, as well as applications to numerous structural components. Fiber reinforced polymers (FRP) sheets are composed of continuous fibers embedded in resin matrix that allows the fiber work together as a single element. Carbon fiber reinforced polymers (CFRP) are used in this study for retrofitting proposes. The properties of this sheet as provided by the manufacturers and used for this study, are

presented in Table 7.1. The adhesive properties as provided by manufacture are shown in Table 7.2

Table 7.1 FRP sheet properties as provided by manufacturer (Elmorsi, M.S.E, 1998)

Fiber type	Ultimate tensile strength (MPa)	Ultimate strain (%)	Modulus of elasticity(GPa)	Design thickness (mm)
Mbrace CF 130 CFRP	3550	1.5	235	0.165

Table 7.2 Adhesive properties as provided by manufacturer (Elmorsi, M.S.E, 1998)

Adhesive type	Tensile strength (MPa)	Tensile modulus (GPa)	Ultimate elongation (%)	Flexural strength (MPa)	Flexural modulus (GPa)
Mbrace Primer	12	0.717	3.0	24	0.593

7.3 Seismic Retrofitting of RC Columns

Strengthening of RC columns in a moment resistant, frame building subjected to seismic loads is a challenge of a structural engineer. Lack of seismic design provisions is combined with poor performance of GLD buildings may result in failure of these structures due to seismic ground motions. There are several ways to improve the seismic behavior and seismic retrofitting of GLD frames. One of them is through increases of the confinement of concrete especially in columns. As the ultimate load is approached, the concrete in columns dilates and exerts pressure on the confined columns. This interaction leads to increases of the ultimate compressive strength of the concrete, confinement and ductility. Confinement of concrete also substantially increases the deformation capacity of RC columns. In general these improvements lead to the changing of the failure mode of the structure from column-swaying to beam-swaying failure mode and a better overall behavior of structure due to seismic ground motions.

7.4 Analytical Procedure of Retrofitting

This section presents the results of analyses of GLD frame building, retrofitted using FRP wrapping that cause increases the local ductility capacity. Ductility is an important factor to be considered in seismic design of RC structures. The structure should exhibit a ductile behavior to survive in an event of earthquake. Thus, this investigation is focused on

improvement of ductility capacity in selected regions to achieve adequate overall structural performance by sustaining inelastic deformations without significant strength degradation during an earthquake excitation.

A plastic hinge is defined as a region of a member where inelastic flexural curvatures (plastic deformations) occur. The length, over the plastic deformations is assumed to be constant, is known as equivalent length of plastic hinge. Accurate prediction of length of plastic hinges is very important to determine the length of column within which it should be wrapped to ensure the ductile performance to be achieved. In RC column, the equivalent length of plastic hinge is calculated based on curvature distribution and deflections measured in the experimental tests. Several researches have proposed expressions for the length of plastic hinges. Some of which are given in Table 7.3

Table 7.3 Length of plastic hinges

Models	Equation for of Length of Plastic Hinge
Priestly and Park	$L_p= 0.08L+ 6\ d_b$
Corley	$L_p= 0.2(L/d)d^{0.5}+ 0.5d$
Mattock	$L_p=0.05L+ 0.5d$

Where

L_p= Length of Plastic Hinge

L= distance of the critical section from the point of flexure (in)

d_b= longitudinal bar diameter (in)

d= effective depth of the member (in)

7.4.1 Theoretical Analysis of RC Columns Confined by Fiber Composites

For RC structures, the maximum slenderness ratio for a short circular column under an axial load is given by:

$L_u / D_g \leq 6.25/\sqrt{(p_f / f'_c A_g)}$

$0.77*4000/300=10.26 \leq 7.5/\sqrt{(1661000/(35*96211.3)}=10.67$

$\alpha_1=0.85-0.0015\ f'_c= 0.798$

$\beta_1=0.97-0.0025\ f'_c=0.882$

The ultimate confinement pressure due to FRP strengthening, f_{lfrp}, can be determined as:

$f_{lfrp},= N_b\ \Phi_{frp}\ f_{frpu}\ t_{frp} / D_g$

Where

N_b, Φ_{frp}, f_{frpu}, t_{frp}, D_g are the number of layers, resistance factor for FRP (Φ_{frp}=0.75), ultimate tensile strength of FRP (MPa), thickness of one layer and external diameter of circular column, respectively. By taking 2 layers of FRP, the ultimate confinement pressure for 1st story columns can be calculated as:

f_{lfrp},= 2*2*0.75*3550*0.165/ 350 = 5

The volumetric ratio of FRP strength is defined as:

ω_W= 2 f_{frp}/ Φ_c f'$_c$ = 2*5/(0.6*35) =0.476

Compressive strength of confined concrete, f'$_{cc}$ is given by,

f'$_{cc}$= f'$_c$ (1+ α_{pc} ω_W)= 35(1+ 0.476)=51.66 Mpa (Valles, R.E.)

The factored axial load resistance, P_{rmax}, for a confined column is given by:

P_{rmax}= K_e[α_1 Φ_c f'$_{cc}$ (A_g – A_{st}) + Φ_s f_y A_{st}] (Kenneth, N., 2001)

Where α_{pc} is the performance coefficient for a circular column and depends on the FRP stiffness and ultimate strain, the concrete strength, the quality of application and the fiber-resin-concrete bond. A coefficient α_{pc} of 1.0 is suggested.

P_{rmax}= 0.85[0.798*0.6*51.66 (96211.3 – 2500) + 0.85*400*2500= 2505 kN

The program IDARC uses Park and Paulay (1975) model to set up moment-curvature envelops for columns and is based on the confining stress relation of Richart et al. (1925) as:

f'$_{cc}$= f'$_c$ + 2.05 ρ_s f_y

51.66= 35+ 2.05 *400 ρ_s

ρ_s= 0.02

The volumetric ratio of confinement steel to concrete cover, ρ_s,

ρ_s= A_h Π d_c / (s A_{cc})

Where A_h, d_c, s and A_{cc} are the cross- sectional area of the hoop steel, diameter of hoop steel, the spacing of hoops and area of core concrete respectively.

By assuming No.10 hoop steel the spacing of hoops, s, assumed as 10mm. Thus the equivalent section of concrete is No.10@10mm for first story columns. By repeating same calculations the equivalent section after FRP wrapping calculated as N0.10@15mm

7.4.2 Ultimate Deformation Capacity Computation

The only factor considered to influence the ultimate deformation capacity of the section is the degree of confinement. Since confinement does not significantly affect the maximum compressive stress, the present formulation only considers the effect of confinement on the downward slope of the stress-strain curve as shown in Figure 7.1. The parameter ZF is a factor that defines the shape of the descending branch. The Park and Kent model (1971) is used in IDARC as given by the following equation below:

$ZF = 0.5/ (\varepsilon_{50u} + \varepsilon_{50h} - \varepsilon_0) = 155$

Where

$\varepsilon_{50u} = (3 + \varepsilon_0 f'_c)/ (f'_c - 1000) = (3 + 0.002 * 5076)/ (5076 - 1000) = 0.00322$

$\varepsilon_{50h} = 0.75\ \rho_s \sqrt{(b/ s_h)} = 0.75 * 0.0032 \sqrt{(9.535/ 13.78)}\ 0.002008$

$\varepsilon_0 = 0.002$

In which the concrete strength is prescribed in psi, ρ_s is the volumetric ratio of confinement steel to core concrete, b (in) is the width of confined core and S_h (in) is the spacing of hoops. The effect of introducing this parameter is to define additional ductility to well-confined columns. Improved formulations for stress-strain behavior of confined concrete can be found in a publication by Pauly and Priestly (1992). Note that by assigning a zero value for this parameter as default, data is generated at element input level by the program.

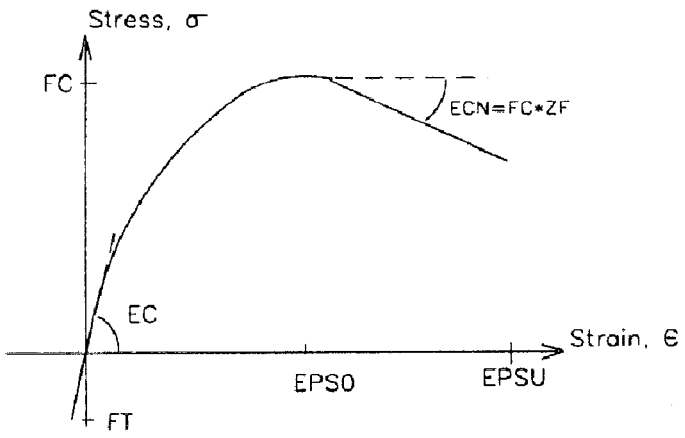

Figure 7.1 Stress-strain curve for unconfined concrete (Valles, 1996)

7.5 Nonlinear Pushover Analysis of Retrofitted GLD Frame Building

Pushover analysis is performed on retrofitted GLD structure to determine and compare the base shear- lateral displacement envelope, the sequence of plastic hinging and overall performance. A monotonic load applied to the retrofitted GLD structure is increased until

an ultimate load is approached. This corresponds to a value of $^{V}/_{W}$=0.11 in the base shear coefficient.

In developing analytical models of retrofitted frame structures, assumptions used in terms of material properties, geometry of structure, hysteretic rules, resistance factors and fundamental design assumptions of FRP are discussed first.

The specified concrete compressive strength f'_c is selected to be 35 MPa. Two types of concrete, confined and un-confined are used for retrofitted and non-retrofitted elements respectively as discussed earlier. The concrete properties are summarized in Table A.1(a). Grade 400 MPa steel bars are used for principal reinforcement as well as for transverse reinforcement. The yield and ultimate tensile strengths of reinforcement are summarized in Table A.1. The properties of CFRP materials may differ considerably from one manufacturer to another. These are defined as the mean value of the particular properties such as ultimate strength, ultimate strain, etc. The mechanical properties provided are based on either fabric thickness or FRP thickness. The resistance factor ϕ_{frp} is used for an FRP system depend on the type of material, conditions of use, and degree of exposure to aggressive agents. In this study Carbon Fiber Reinforcement Polymer (CFRP) types are used to retrofitting elements.

Two different types of hysteretic rules are used for modeling of retrofitted and non-retrofitted elements. Based on the results of previous experimental tests, retrofitting column develops more stable loops. For other elements of retrofitted frame the same factors as GLD frame are assumed. The values of the IDARC parameters are used in the analysis of retrofitted columns are HC = 0.5, HBE = HBD = 0.1, and HS = 1.0 for the control of stiffness deterioration, strength degradation, and pinching behavior of retrofitted columns respectively. Typical range of values for hysteretic parameters is presented in Table 4.1.

The equations used in this research are based on the following fundamental assumptions

1. Plane sections remain plane
2. Perfect bond exists between the concrete and steel, and between concrete and FRP

To compute the factored flexural strength of reinforced concrete beams strengthened with FRPs, resistance factors Φ_{frp} are required. Resistance factors for the concrete, Φ_c=0.6 and steel reinforcement, Φ_s=0.85, are prescribed in the C.S.A Standard. The resistance factor of the FRP will vary depending on parameters such as the intended use, type of FRP, and

exposure conditions. Various values of Φ_{frp} have been suggested for carbon FRPs. For example, Khalifa et al. (1998) proposed Φ_{frp} = 0.7. Triantafillou and Antonopoulos (1999) suggest Φ_{frp} = 0.78 for the case of FRP rupture, and Φ_{frp} = 0.75 for debonding or if the strain in the FRP is limited to a certain value that does not allow FRP rupture. For glass FRPs, the ACT 440 F draft document (2000) suggests values of Φ_{frp} ranging from 0.6 to 0.76. In this investigation the resistance factor of Φ_{frp} =0.75 is considered.

Pushover analysis results are presented here in terms of both displacement and drift. Configuration of frames is same as shown in Figure 4.1. For frame modeling of columns the well confined effectiveness of confinement, CEFF=1, is considered as shown in Figure 6.1. This corresponds to the improvements obtained in retrofitted GLD frame. All other assumptions of non-retrofitted members are same as GLD frame as discussed in Chapter 6.

7.5.1 Results of Pushover Analysis

To investigate and compare the behavior of retrofitted GLD frame, it is analyzed under monotonically increasing static lateral loading. The lateral loads are distributed over the height of the building. The displacement-base shear relationships of retrofitted frame obtained are shown in Figures 7.2 and 7.3. The lateral load carrying capacity of retrofitted structure is improved from 212 kN for the GLD frame to 491.3 kN for the retrofitted frame. A significant improvement in lateral load carrying capacity of retrofitted structure (more than twice of GLD frame) is observed. As shown in Figure 7.2, the maximum deformation capacity of retrofitted frame is increased up to 2.7% of building height as compared to 1.55% for the GLD frame. The shape of the load-deflection curve represents a ductile behavior of retrofitted frame.

The displacement ductility factor in retrofitted case shows a maximum value of 16. The result shown in Figure 7.4 illustrates a significant enhancement in ductility capacity of retrofitted frame over the GLD frame. This improvement is the result of the ductile behavior of retrofitted GLD structure.

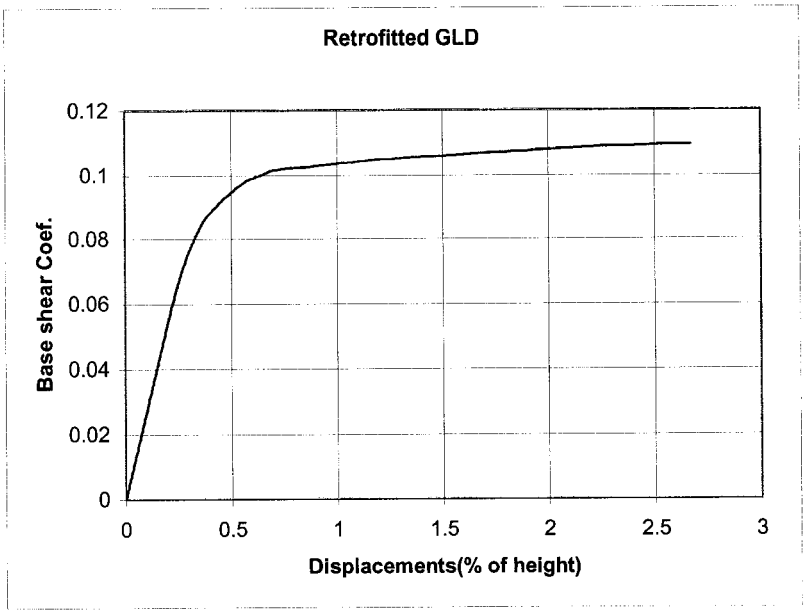

Figure 7.2 Base shear coefficient versus displacement percentage of height

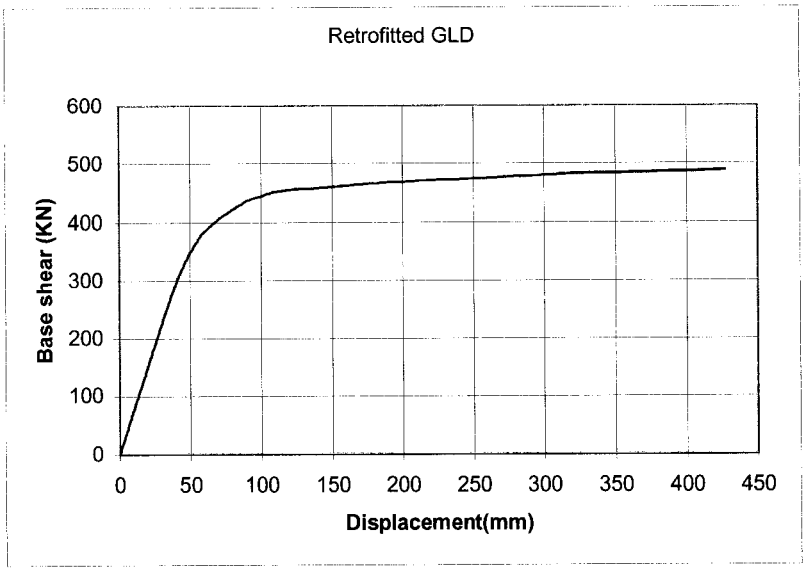

Figure 7.3 Base shear versus displacement (mm)

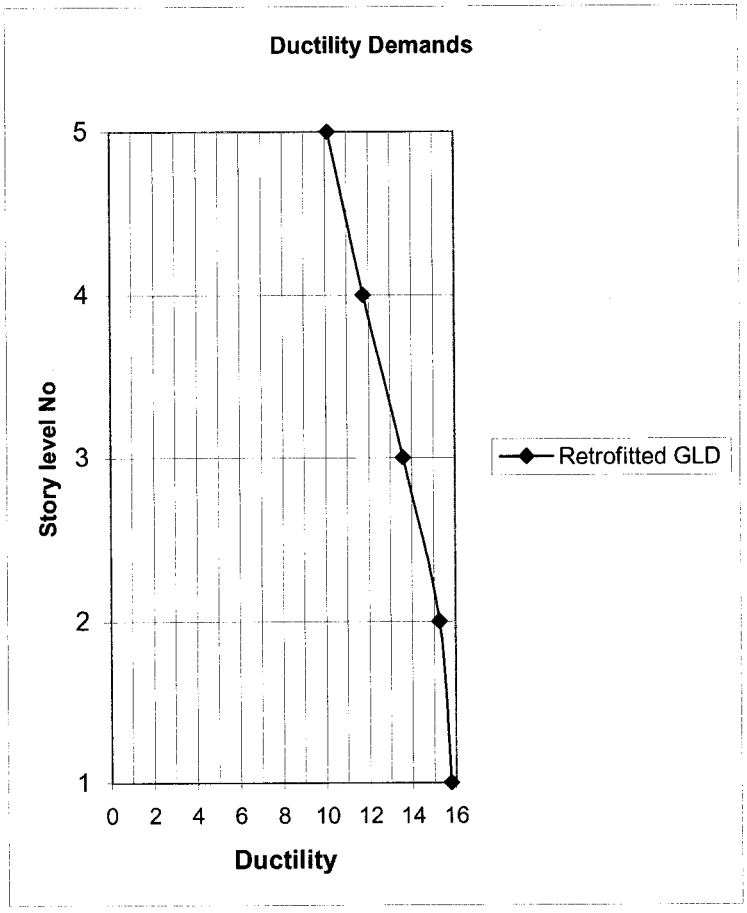

Figure 7.4 Displacement ductility (Retrofitted GLD Frame)

Figure 7.5 shows story drifts of retrofitted GLD frame. As Figure 7.5 presents the maximum drift obtained is equal to 4.8% at first floor and 4.5% at second floor.

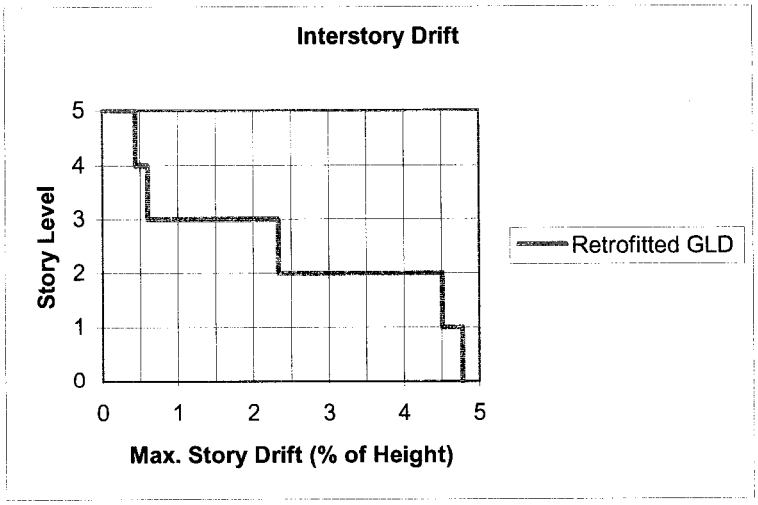

Figure 7.5 Inter-story drift (pushover analysis)

Figure 7.6 presents maximum base shear-story displacement due to pushover loading in story levels for retrofitted GLD frame. The story-displacement curve shows the expected parabolic shape. This type of behavior, which represents a beam-sway mechanism, occurs throughout the retrofitted frame. Upper stories are exhibited movements instead of a rigid body motion, which GLD frame is exhibited. As showed in Figure 7.6, this significant enhancement is the result of strong column-weak beam mechanism instead of local story mechanism in GLD frames. As the damage analysis illustrates in upgraded frame, the occurrence of plastic hinges is changed to beams instead of columns. This behavior is caused a desired deformation due to strong column-weak beam mechanism.

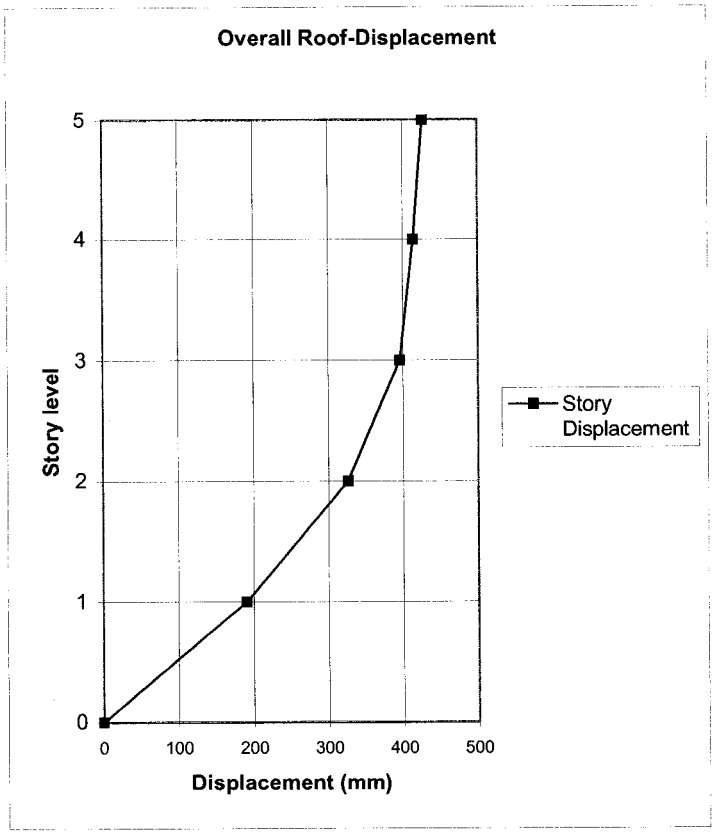

Figure 7.6 Base shear- story displacement relationship

7.5.2 Damage Analysis

Figures 7.7 and 7.8 as well as Table 7.4 indicate the state of cracking/yielding and damage index statistics of retrofitted GLD frame in order to show the progression of damage as the load is increased. The sequence of yielding in Table 7.4 indicates that the beams at 1st and 2nd floors have yielded as a result of plastic hinge formation at the beam ends. The hinges continue to occur at four other locations at the base of the 1st story columns. Then, interior columns in the 2nd and 3rd story have yielded. Plastic hinges continue to occur at upper story levels. This behavior confirms the successful changing of the failure mechanism from local story failure to strong column-weak beam mechanism in retrofitted GLD frame. The sequence of plastic hinging in the retrofitted GLD structure conforms to the capacity design concept. Note that **x** and **0** express crack and yield states of frame and the numbers in parentheses indicate sequence of yielding.

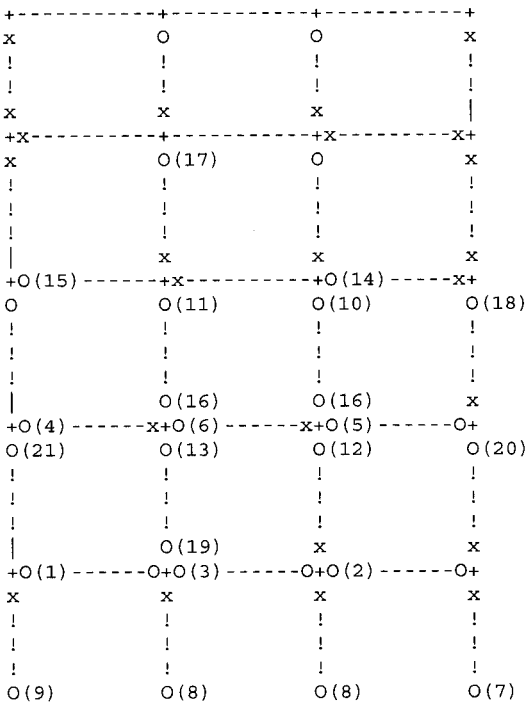

Figure 7.7 State of failure and sequence of yielding for retrofitted GLD frame

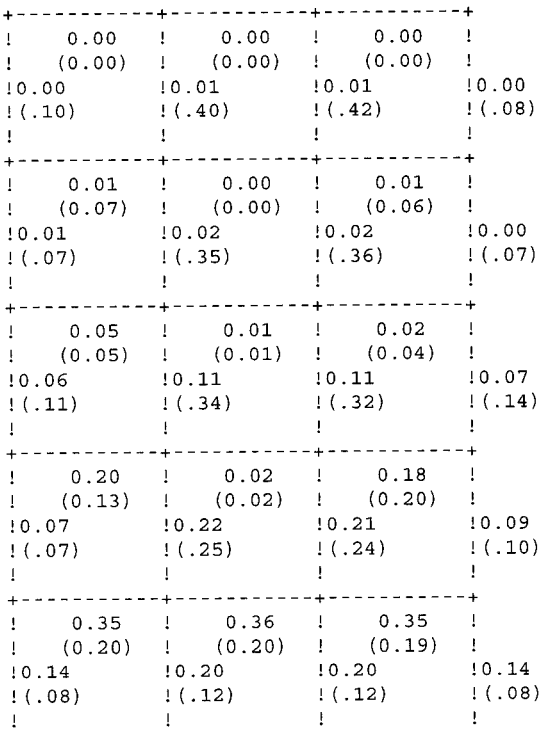

Figure 7.8 Damage index statistics of retrofitted GLD frame

Table 7.4 Sequence of component yielding of retrofitted GLD

NO.	STORY LEVEL	ELEMENT	BASE SHEAR	SEQUANCE OF YIELDING
1	1st	BEAM 1	0.0693	YIELDING DETECTED AT LEFT
2	1st	BEAM 11	0.0748	YIELDING DETECTED AT LEFT
3	1st	BEAM 6	0.0775	YIELDING DETECTED AT LEFT
4	2nd	BEAM 2	0.0808	YIELDING DETECTED AT LEFT
5	2nd	BEAM 12	0.0847	YIELDING DETECTED AT LEFT
6	2nd	BEAM 7	0.0880	YIELDING DETECTED AT LEFT
7	1st	COLUMN 4	0.0902	YIELDING DETECTED AT BOT
8	1st	COLUMN 2, 3	0.0924	YIELDING DETECTED AT BOT
9	1st	COLUMN 1	0.0940	YIELDING DETECTED AT BOT
10	3rd	COLUMN 11	0.0984	YIELDING DETECTED AT TOP
11	3rd	COLUMN 10	0.0990	YIELDING DETECTED AT TOP
12	2nd	COLUMN 7	0.1000	YIELDING DETECTED AT TOP
13	2nd	COLUMN 6	0.1006	YIELDING DETECTED AT TOP
14	3rd	BEAM 13	0.1012	YIELDING DETECTED AT LEFT
15	3rd	BEAM 3	0.1017	YIELDING DETECTED AT LEFT
16	3rd	COLUMN10,11	0.1023	YIELDING DETECTED AT BOT
17	4th	COLUMN14,15	0.1039	YIELDING DETECTED AT TOP
18	3rd	COLUMN 12	0.1061	YIELDING DETECTED AT TOP
19	2nd	COLUMN 6	0.1083	YIELDING DETECTED AT BOT
20	2nd	COLUMN 8	0.1088	YIELDING DETECTED AT TOP
21	2nd	COLUMN 5	0.1094	YIELDING DETECTED AT TOP

The overall structural damage obtained for retrofitted GLD frame is 0.234. Interpretation of overall damage index is presented in Table 4.1. Figure 7.9 shows, that the yielding of structural elements in retrofitted GLD frame occur in the first column at base shear coefficient of 0.0902 and then first beam is yielded at base shear coefficient of 0.0693. This type of behavior indicates that the plastic hinges are occurred in beams as a result of a desirable strong column-weak beam mechanism in retrofitted GLD frame.

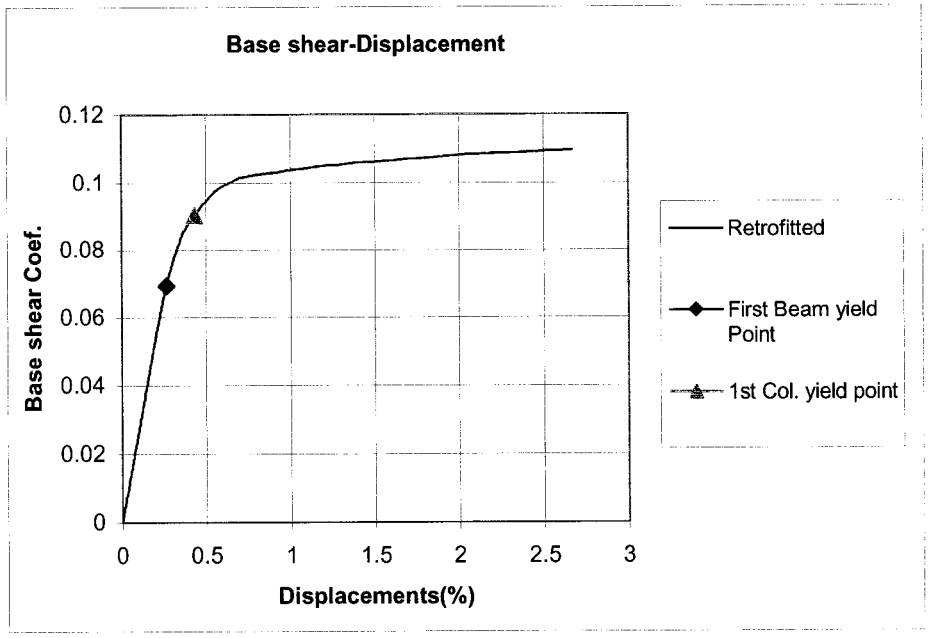

Figure 7.9 Sequence of yielding

7.6 Dynamic Analyses

7.6.1 Ground Motions

The same data set as input ground motions for the designed GLD frame is selected as discussed previously. A horizontal component is selected to give a peak ground acceleration of 0.7616g (630.78 cm/sec^2) with scale factor of 1.6, which provides excitation in proportion to a moderate seismic risk. The ground motion duration is about 20 seconds. Figure 7.10 presents the acceleration time-histories of this seismic event. Table 7.5 provides detailed information on the records generated for Seattle having probability of exceedence of 2% in 50 years.

Table 7.5 Details of Erzincan (1992) ground motion having a probability of exceedence of 2% in 50 years

SAC Name	Record	Earthquake Magnitude	Distance (km)	Scale Factor	Number of Points	DT (sec)	Duration (sec)	PGA	PGA (cm/sec^2)
SE23	1992 Erzincan	6.7	2	1.6	4156	0.005	20.775	0.7616g	630.78

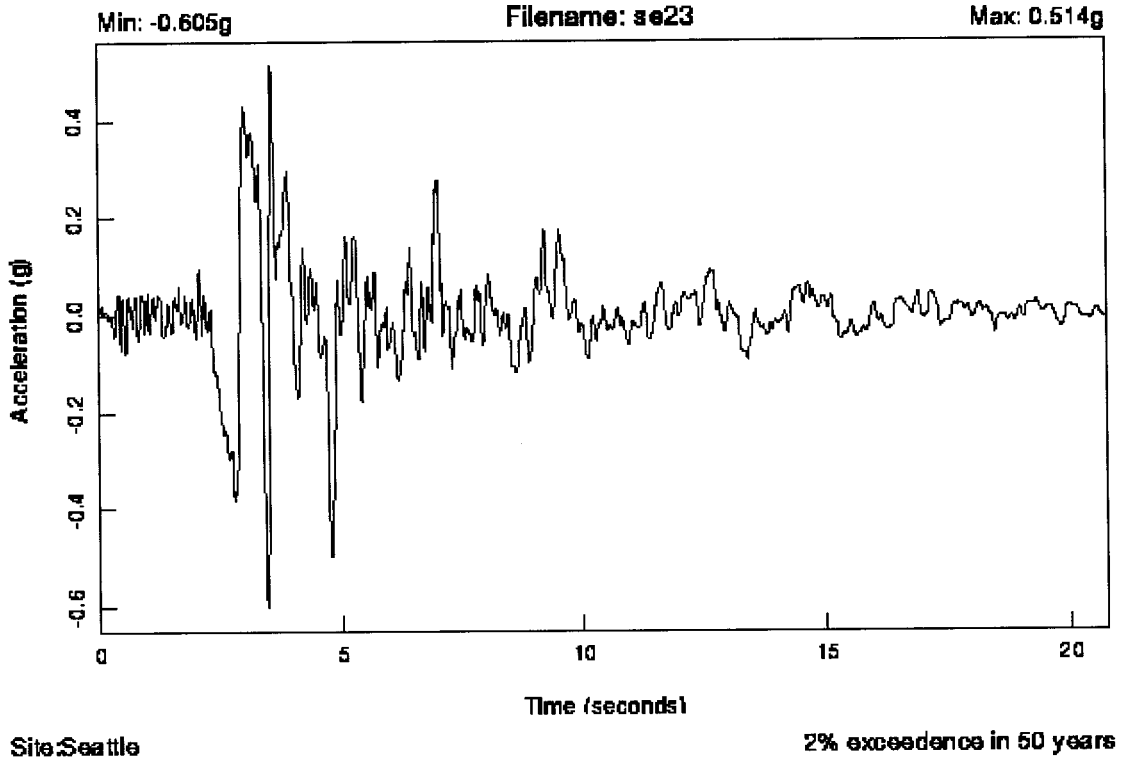

Figure 7.10 Erzancan (1992) ground motion

In developing analytical models of frame structure, assumptions used for dynamic analysis are same as pushover analysis in terms of hysteretic model, geometry, system of units and material properties. For the analysis carried out herein, to ensure accurate results integration time step of 0.005 seconds is used for nonlinear dynamic analysis. Approximately 5% of critical damping is assumed in the analysis

7.6.2 Results of Time History Dynamic Analysis

The time-displacement relationships of retrofitted GLD frame for each story is presented in Figure 7.11. The maximum values corresponding to peak displacements at each story are plotted in Figure 7.12.

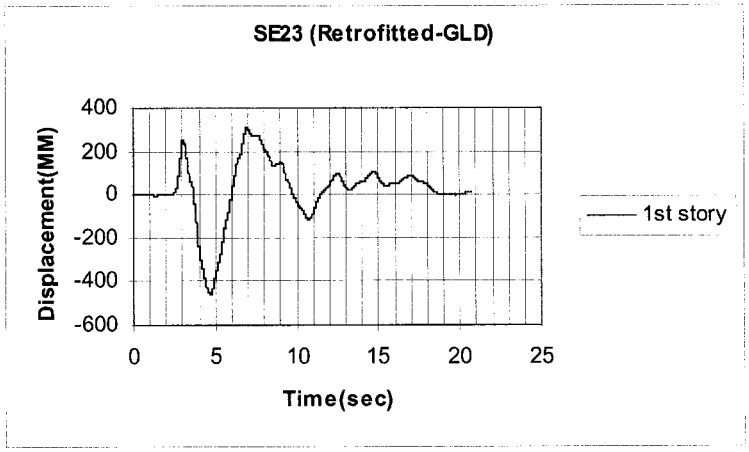
SE23 (Retrofitted-GLD)
Displacement(MM)
400
200
0
-200
-400
-600
0
5
10
15
20
25
Time(sec)
1st story

(a)

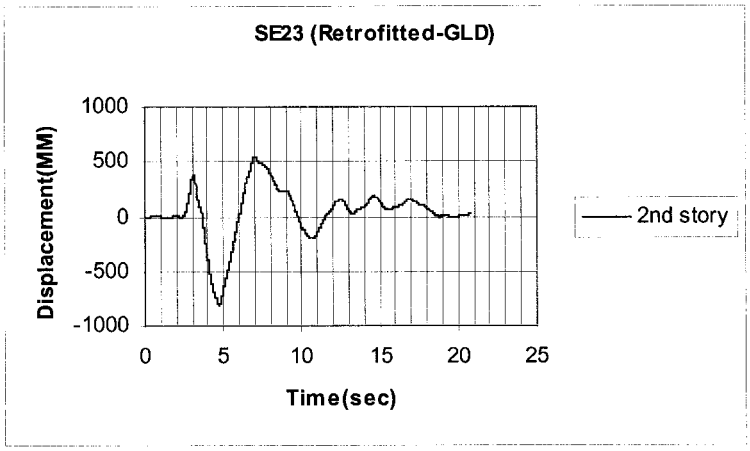
SE23 (Retrofitted-GLD)
Displacement(MM)
1000
500
0
-500
-1000
0
5
10
15
20
25
Time(sec)
2nd story

(b)

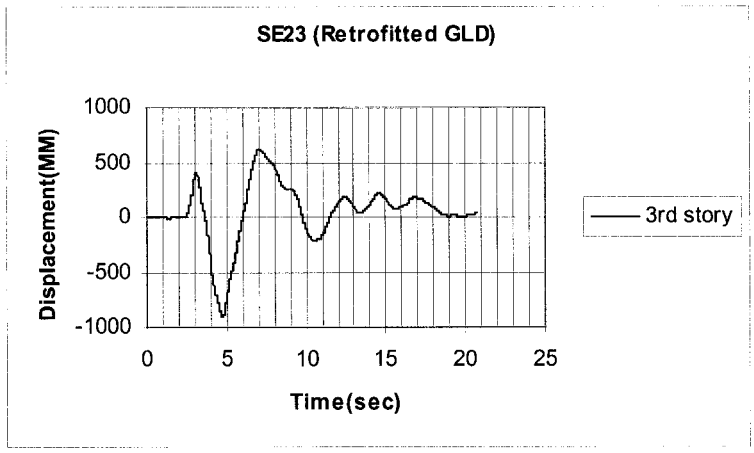
SE23 (Retrofitted GLD)
Displacement(MM)
1000
500
0
-500
-1000
0
5
10
15
20
25
Time(sec)
3rd story

(c)

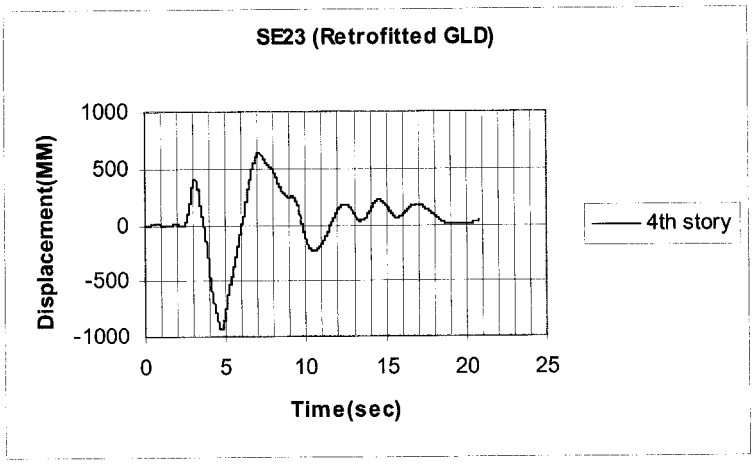

(d)

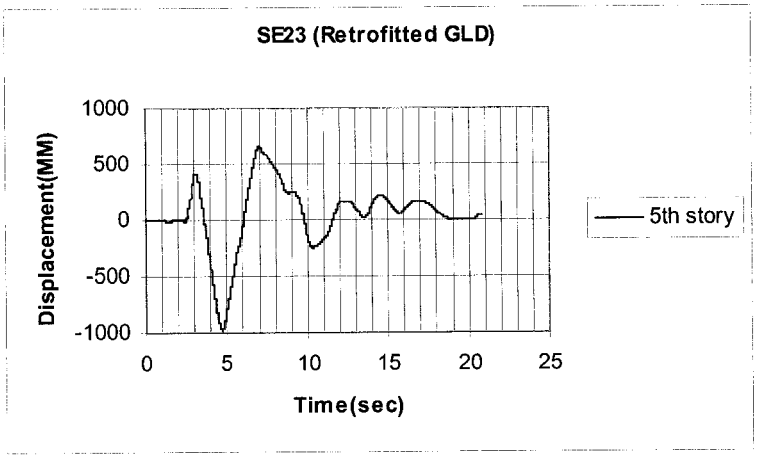

(e)

Figure 7.11 Time-displacements relationships.

Figure 7.12, indicates the displacement envelope is almost similar to that obtained using the pushover analysis. A significant change in deformation form of building throughout the story levels is observed as compared to the GLD frame. Inelastic deformations in plastic hinges at the end of beams are indicated movements in upper stories. This significant enhancement is the result of strong column-weak beam mechanism instead of story-sway mechanism observed in the GLD frame. Figure 7.13 shows story drifts of retrofitted GLD frame for dynamic analysis. Figure 7.13 presents the maximum drift obtained is equal to 11.5% for the first floor and 11.7% for second floor.

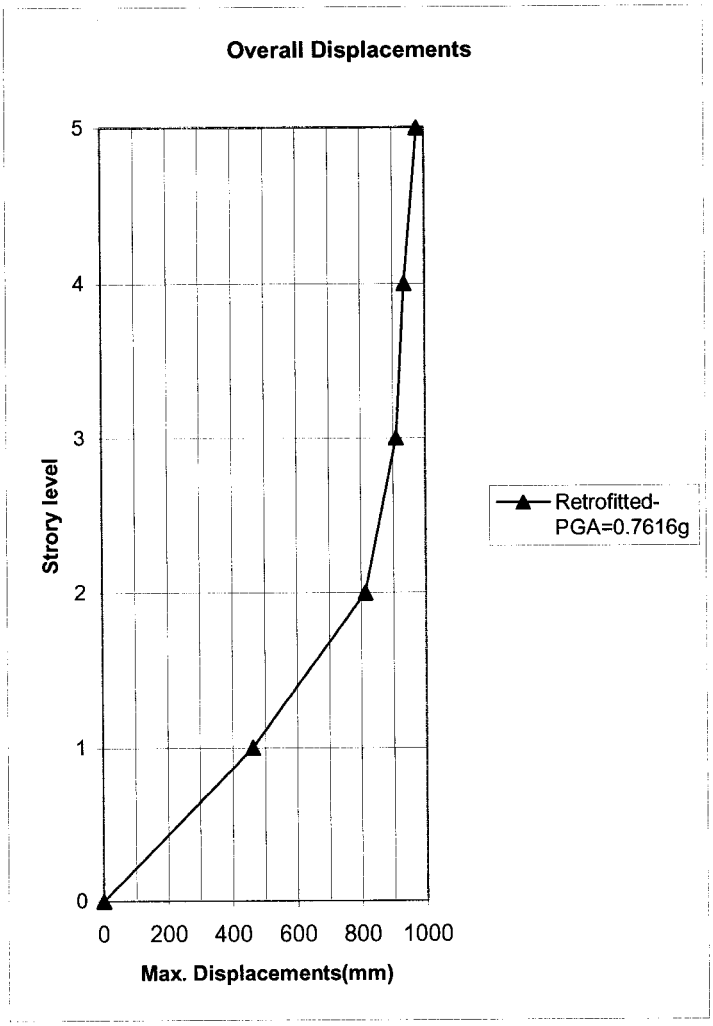

Figure 7.12 Maximum displacement (Retrofitted GLD)

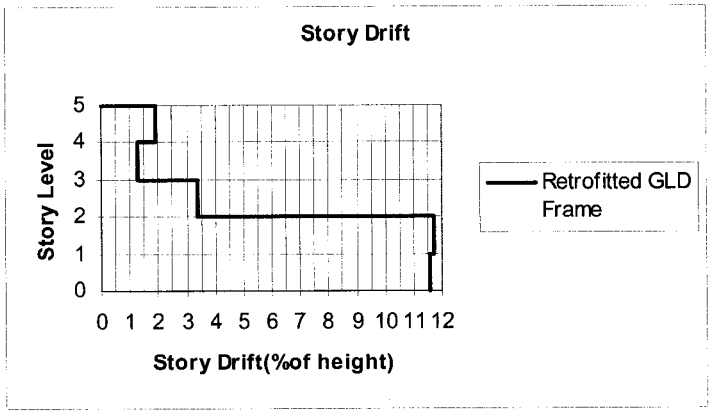

Figure 7.13 Inter-story Drift (Retrofitted GLD)

Figure 7.14 illustrates the time-story shear relationship for each story level for the retrofitted GLD structure. As a higher PGA (0.12g) in earthquake input wave as compared to that of GLD frame assumed the maximum story shear produced in retrofitted GLD frame is about 550 kN while this value is about 200 kN in GLD frame. These results in terms of story shear, produced from retrofitted GLD frame, are more than twice of GLD frame. This shows that the upgraded structure is capable of sustaining higher base shear.

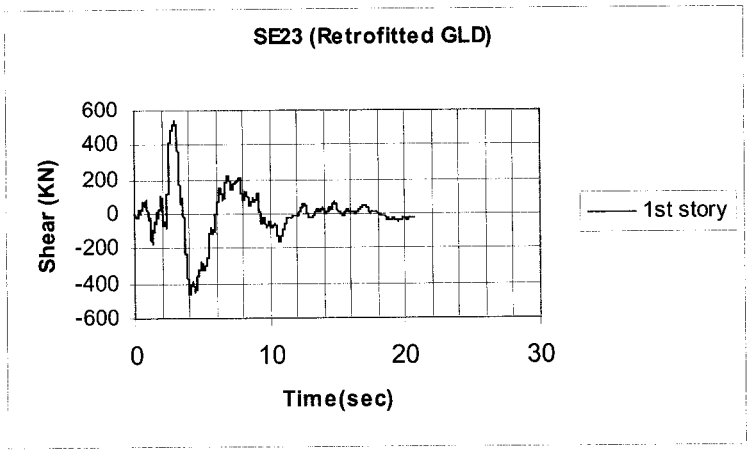

(a)

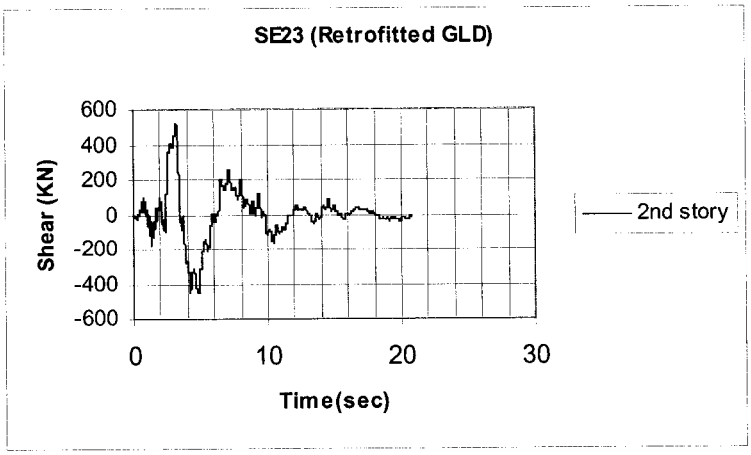

(b)

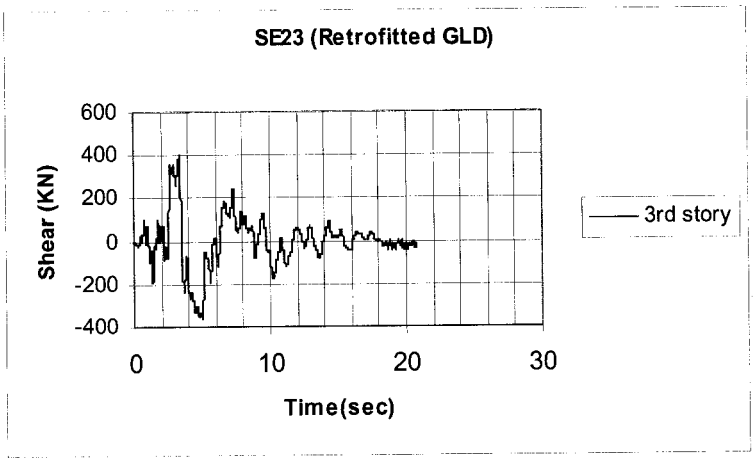

(c)

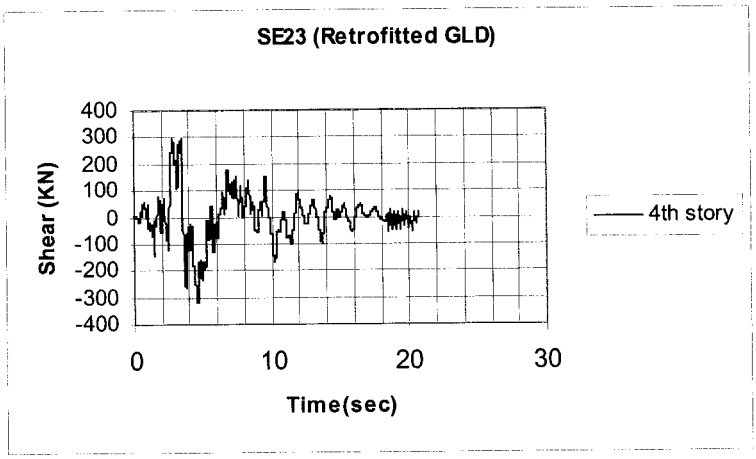

(d)

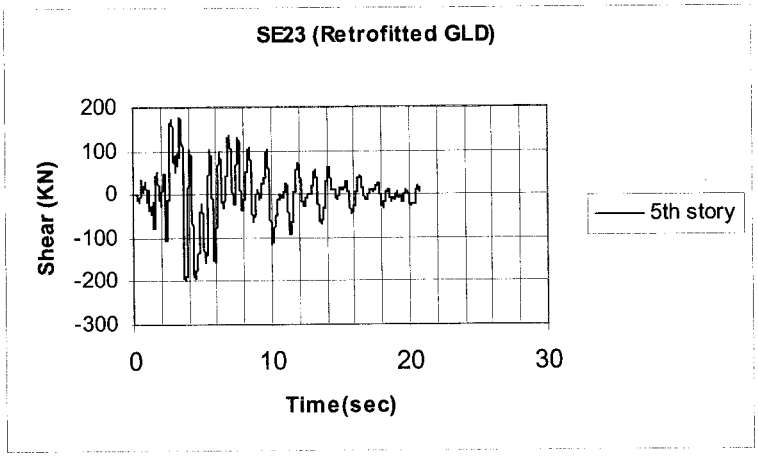

(e)

Figures 7.14 Time-story shear relationships

Figure 7.15 illustrates time-acceleration relationships of retrofitted GLD frame for first floor. The time acceleration diagrams agree with the input wave data as shown in Figure 7.10.

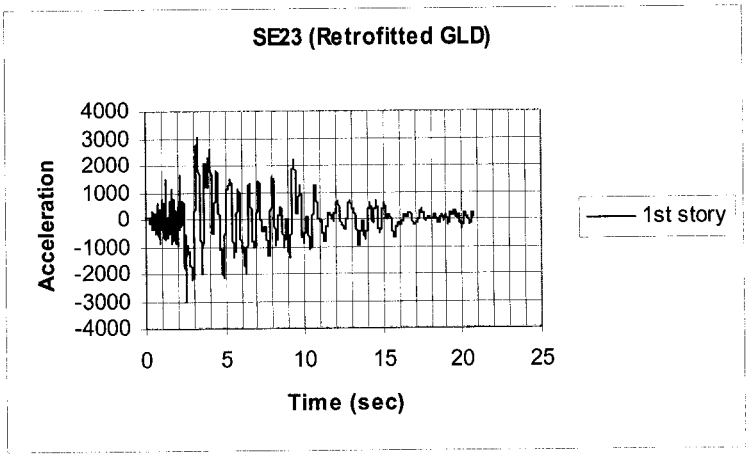

Figure 7.15 Time-acceleration relationship

7.6.3 General Behavior and Cracking Patterns

The overall structural damage obtained for GLD frame is 0.780. For retrofitted GLD frame the overall damage index observed is 0.562. The results obtained show a similar trend in response. This is due to the enhancement obtained in performance of retrofitted frame and resulting confined columns.

Figures 7.16 and 7.17 show the state of cracking/yielding and damage index statistics of retrofitted GLD frame in order to show the progression of damage under higher seismic ground excitation. The sequences of yielding in these Figures illustrate that; first plastic hinges are occurred at the beams of 1st and 2nd floors followed by yielding of columns at the base. Next, yielding of the interior columns occur at the top of 2nd, 3rd and 1st floors respectively. This sequence of yielding confirms that higher stories are involved in energy dissipation rather than only first story as observed in GLD frame. Then a hinge is formed along exterior beam of 3rd floor followed by yielding of interior columns at the top of 4th story. The exterior columns and interior columns at top of 1st and bottom of 3rd story are yielded respectively. Yielding of exterior columns at top of 2nd floor is followed. Plastic hinges are formed at top of exterior columns of 3rd floor. This is followed by yielding of interior columns of 4th story at bottom. Next, exterior columns of 5th floor at top and bottom are yielded. Finally, plastic hinges are formed in beams of 2nd, 3rd and an exterior beam of 4th floor respectively. This hinging pattern in the structure with retrofitted GLD frame is an indication energy dissipation mechanism in beams as a result of ductile behavior of upgraded structure. Most damages are occurred in the beams

rather than columns. In general, these results illustrate significant enhancement in overall response of retrofitted GLD frame.

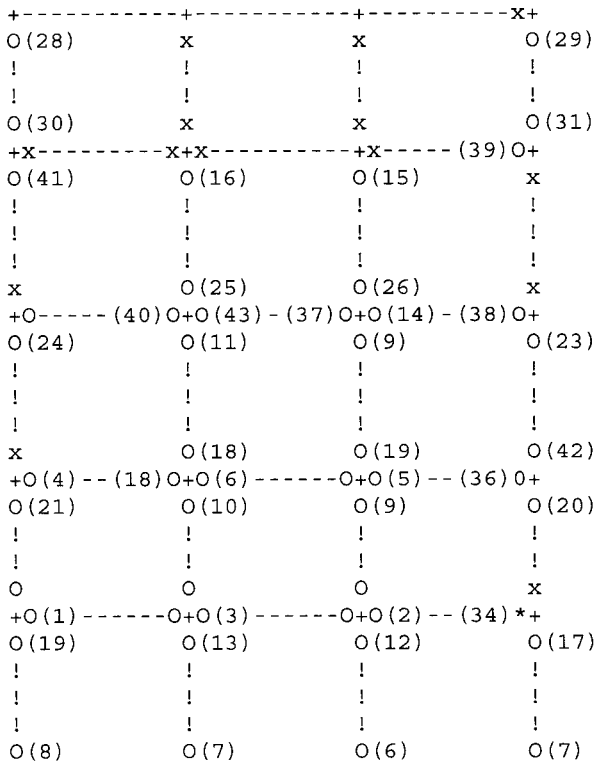

Figure 7.16 State of failure and sequence of yielding for retrofitted GLD frame

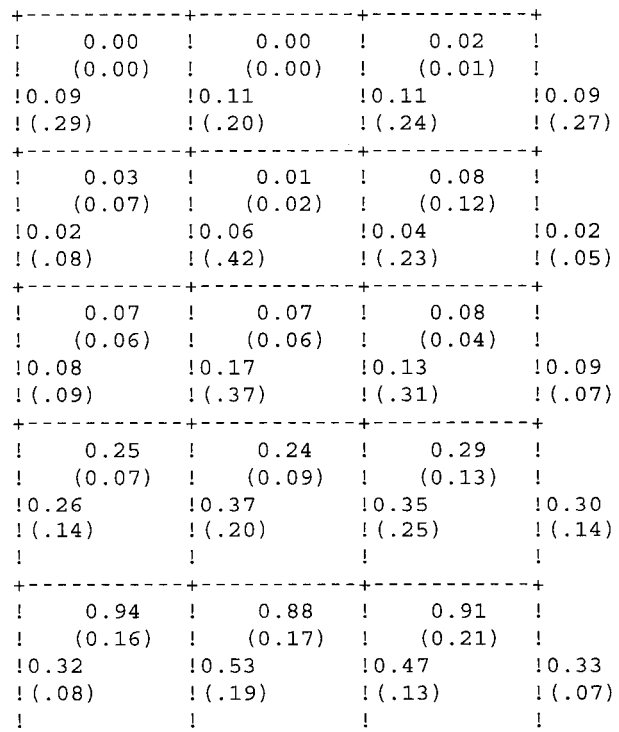

Figure 7.17 Damage index statistics of retrofitted GLD frame

7.6.4 Comparison of Damage Patterns of Structural Elements

Figure 7.18 illustrate damages obtained in each beam and column elements under ground acceleration. Results shows that less damage occurred (with index of 0.53) in columns of the first floor rather than in beams in comparison with the GLD frame. The damages are distributed throughout all levels of the frame as a result of energy dissipation. This desirable behavior conforms the strong column-weak beam consideration, which indicates a better performance of retrofitted GLD frame.

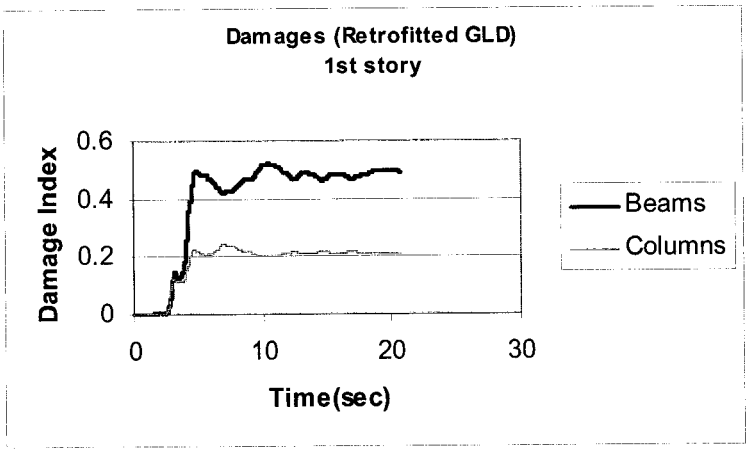

(a)

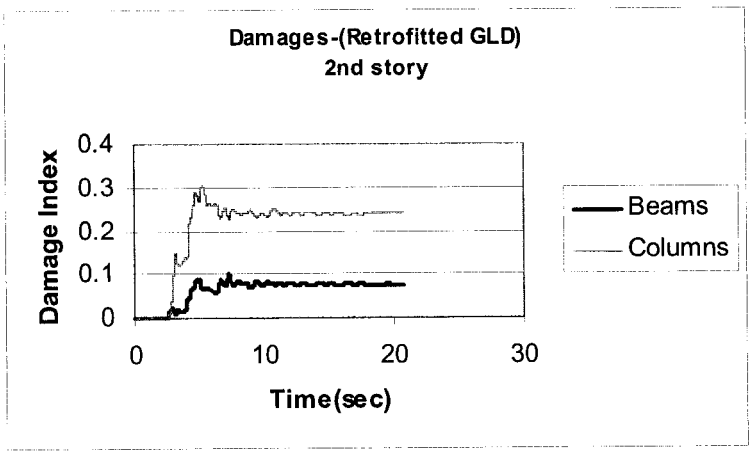

(b)

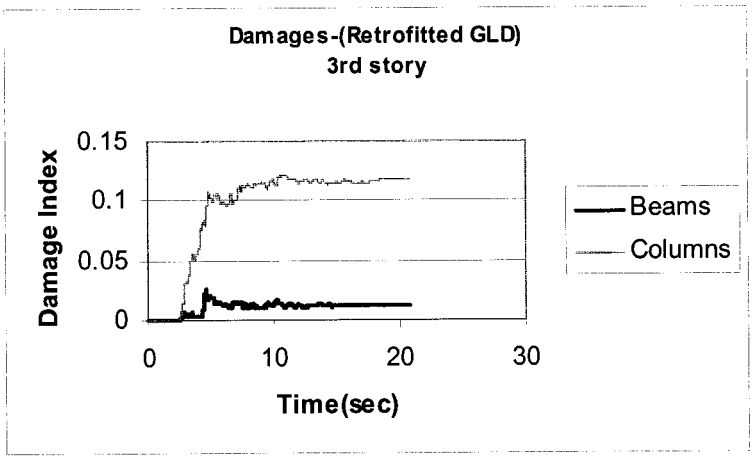

(c)

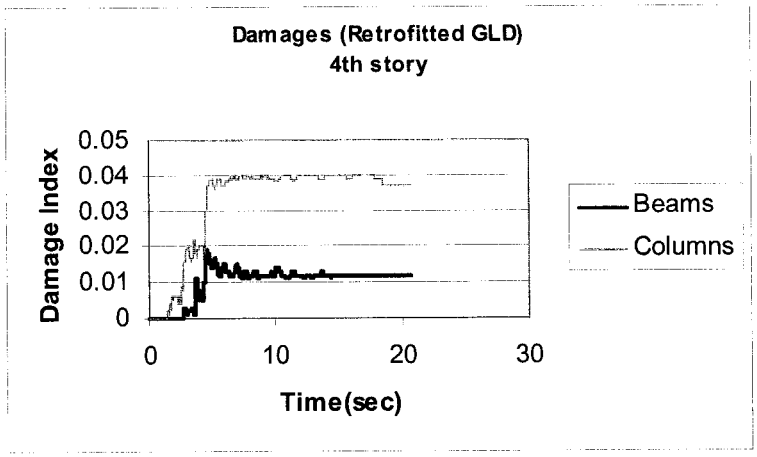

(d)

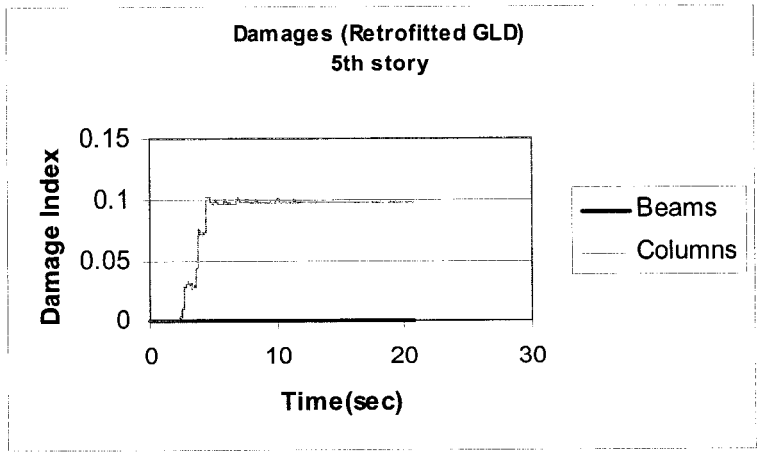

(e)

Figures 7.18 Time-damage relationships

7.6.5 Forming a Favorable Failure Mechanism

The relationship between strength of beams and columns framing into a joint are compared in order to determine whether beam-sway or column-sway mechanisms are likely to form in GLD and retrofitted frames. Figure 7.19(a) shows a beam-sway mechanism where, a desired weak beam-strong column performance develops. A column-sway mechanism involves the formation of plastic hinges at top and bottom of all columns at one level of a frame as shown in Figure 7.19(b). As discussed by Priestly [1996], the potential for developing a column-sway mechanism can be determined from the value of a sway potential index, S_p. This is defined by comparing the flexural capacities of beams and columns at all joints at a given level of frame. If $S_p > 1$, a high probability exists to forming a column sway mode (Priestely, M.J.N., 1996).

The GLD structure shown in Chapter 6 exhibited column-sway failure mechanism that placed large deformations in the first floor and plastic hinges are formed in lower story columns. GLD frame is far from energy dissipation mechanism in beams due to non-ductile behavior of this structure. Most damages are formed in the columns rather than the beams, which is the result of lack of weak beam-strong column considerations in previous design codes. The energy dissipation in beams plastic hinges is typically larger than that in column plastic hinges. In general, GLD frame performed poorly. After retrofitting, the results show that the retrofitted structure develops plastic hinges at beam-ends and at the base of first story columns under an intense earthquake and pushover loading. The result shows that in retrofitted frame, flexural yielding at beam-ends can dissipate input energy. Plastic deformations are uniformly distributed throughout the structure and also large deformation is reasonable in beam members where no axial force acts. Some strengthening should be provided at the lower level columns to delay the yield hinge formations because it is not desirable to form plastic hinges in the columns, to avoid large deformations. Finally, it is desirable to change the failure mechanism of GLD frame from column-sway (soft story) mechanism to beam-sway mechanism as indicated in Figure 7.19. In retrofitted structure the behavior of frame is improved to avoid undesirable soft story-sway mechanism. Providing extra ductility in the region where yielding is not desired but minor yielding of some columns in story is tolerated as long as the column should be able to support the gravity loads. In this investigation to provide a desirable mechanism, a FRP wrapping is used to increase ductility capacity and strength of columns.

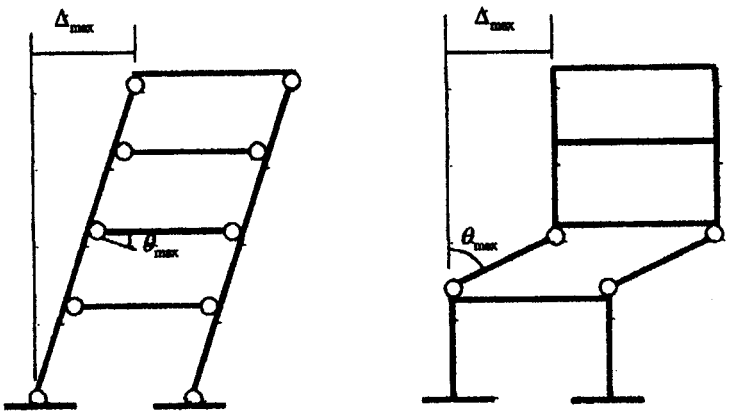

(a) Beam-sway mechanism **(b)** Column-sway mechanism (soft story)

Figure 7.19 Failure mechanisms

7.7 Conclusion

In this research, the FRP sheets are used to retrofit the GLD structure. An improvement in failure mechanism is observed. In retrofitted GLD frame, columns have less damages than beams therefore, plastic hinges are occurred at the beam elements instead of columns. Also the retrofitted GLD frame is studied under monotonic pushover and a ground excitation. The significant enhancements are achieved in overall behavior of retrofitted GLD frame. After retrofitting, energy dissipation mechanism is occurred in beams as a result of ductile behavior of the structure. In general, these results illustrate significant improvement on the response of retrofitted GLD frame.

CHAPTER 8

Comparison of Results of Analysis

8.1 Comparison of Ductile, Nominally Ductile and GLD Frames

The behavior of ductile, nominally ductile and GLD frames were analyzed under monotonically increasing static lateral loading. Figures 8.1 and 8.2 show the displacement-base shears relationships of frames obtained from results of pushover analyses. The base shear - lateral displacement envelope and the sequence of plastic hinging are presented in Figure 8.3. The envelope for the structure with nominal ductility (R = 2) and GLD frames shows a descending curve due to reduced ductility of these frames.

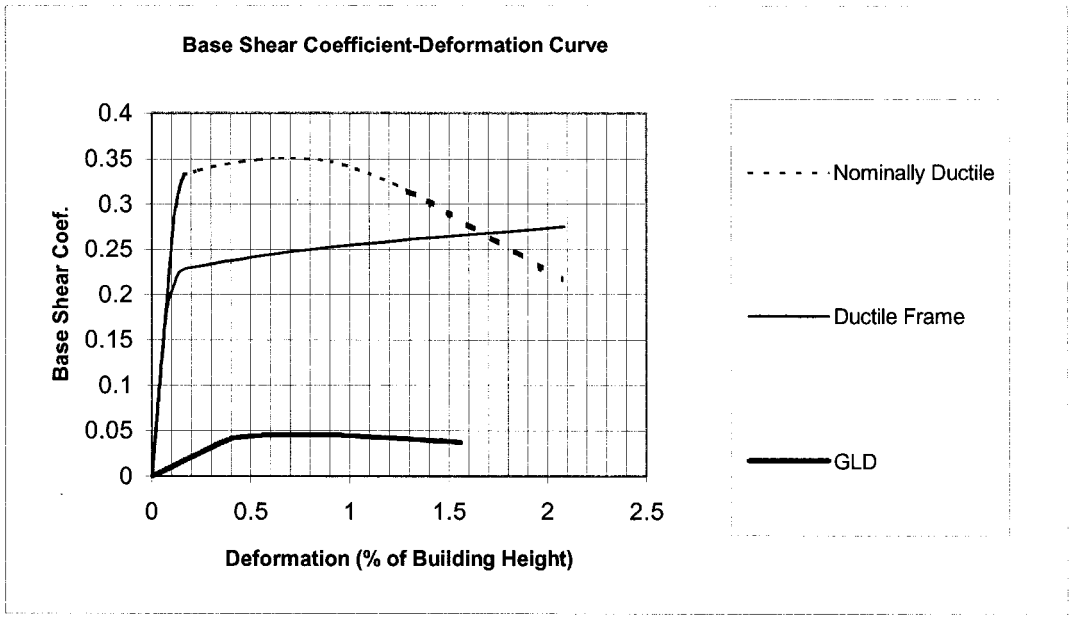

Figure 8.1 Comparison of base shear coefficient versus deformation (% of height)

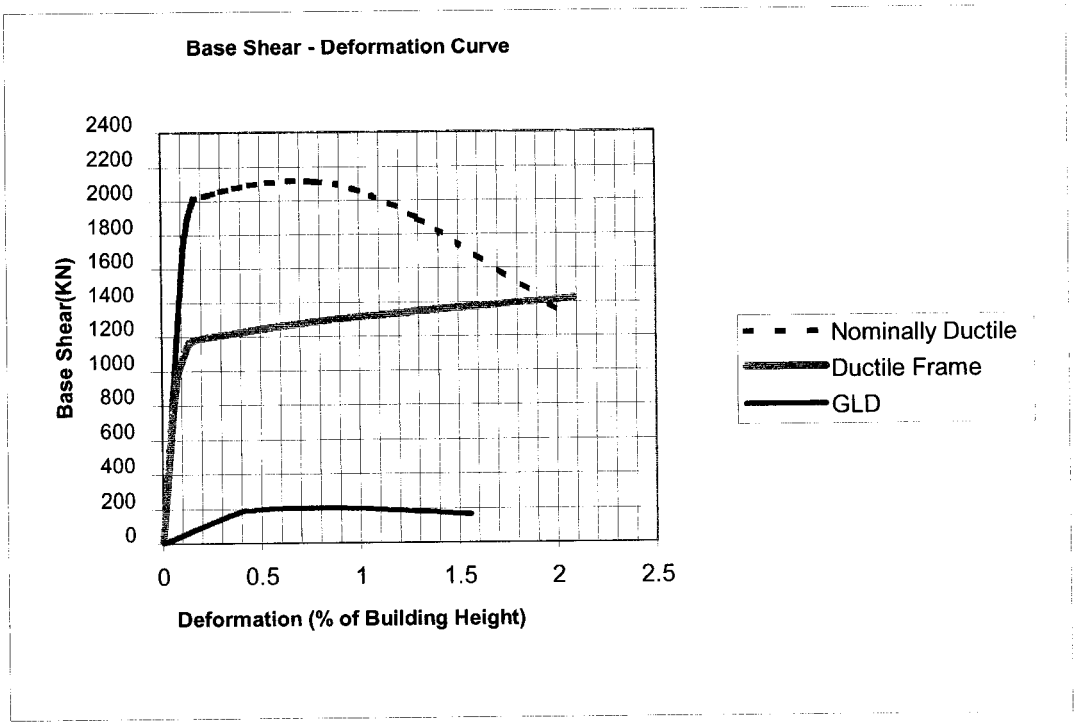

Figure 8.2 Comparison of base shear versus deformation (% of height)

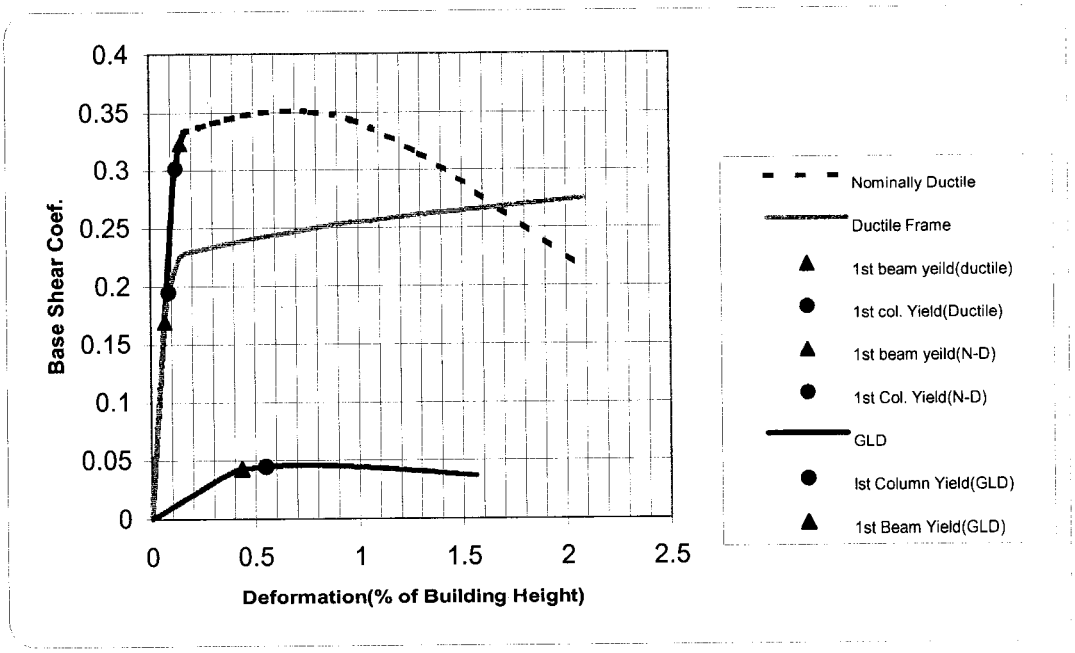

Figure 8.3 Sequence of plastic hinging

Figure 8.4 presents base shear story displacement due to pushover loading at each story levels.

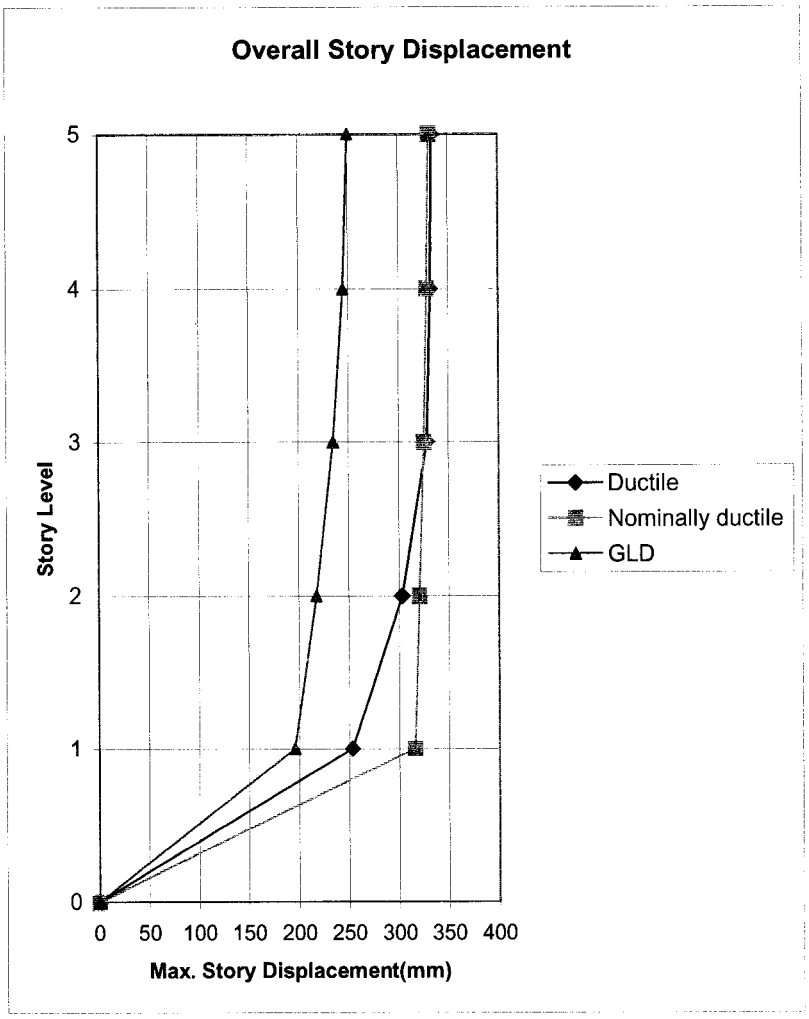

Figure 8.4 Base shear story displacement relationship

The displacement ductility factor for the three cases is compared and shown in Figure 8.5. The ductile frame has largest ductility demand followed by nominally ductile frame and finally the GLD frame. It can be seen that ductile frame shows better behavior than the nominally ductile frame and the GLD frame. This is the result of the good detailing of the members for the ductile frame.

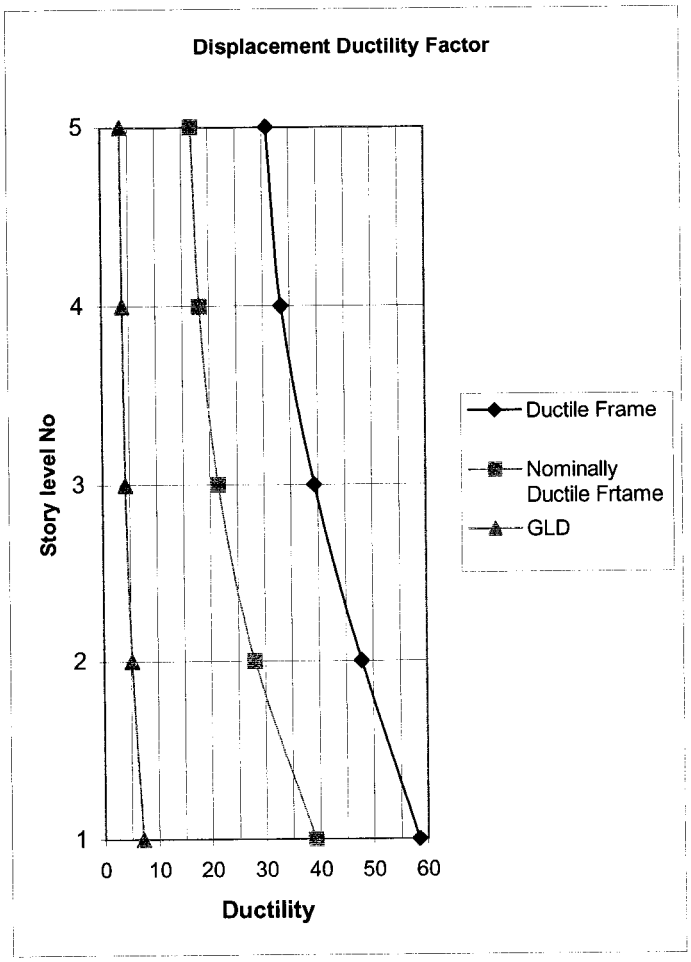

Figure 8.5 Comparison of Displacement ductility factor

8.2 Comparison of GLD Frame and Retrofitted GLD Frame

The displacement-base shears relationships of frames are compared between the GLD and the retrofitted GLD frame. Figures 8.6 and 8.7 present the comparison of the results obtained from pushover analyses. The base shear - lateral displacement envelope and the sequence of plastic hinging are presented. The envelope for the GLD structure shows the descending curves representing low ductility of GLD frame, compare with retrofitted GLD frame.

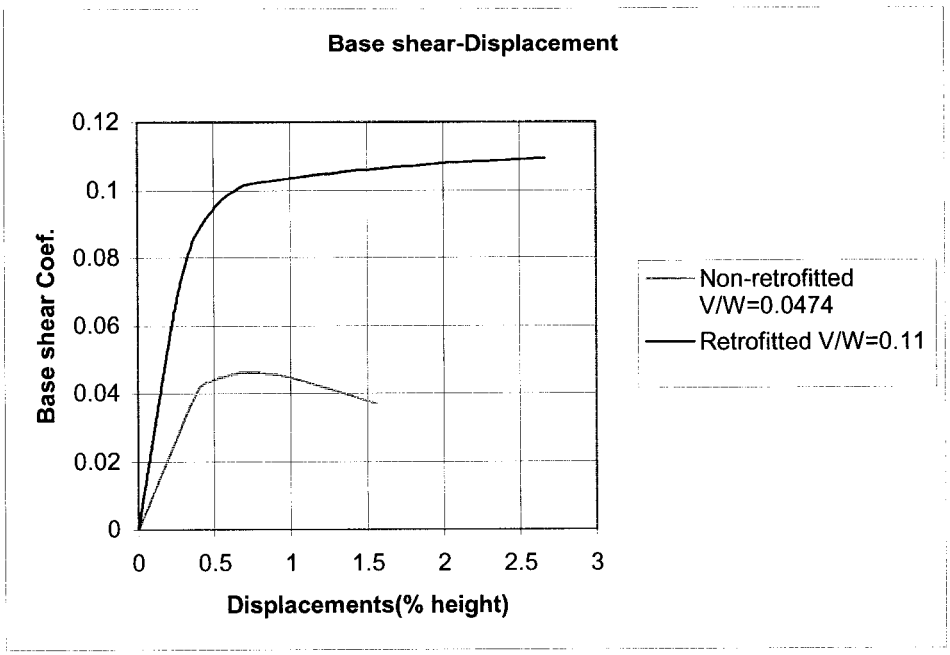

Figure 8.6 Comparison of base shear coefficient versus displacement (percentage of height)

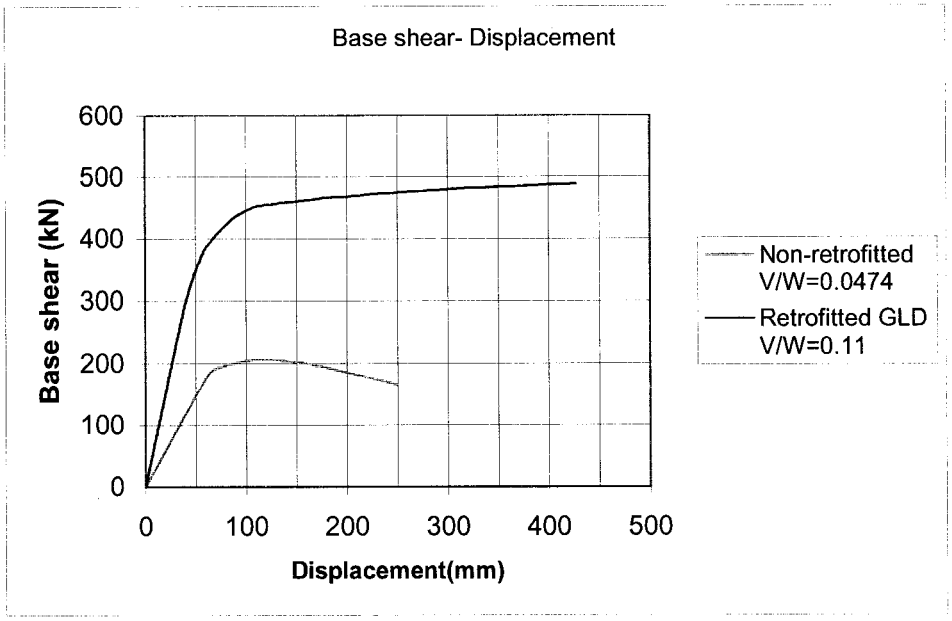

Figure 8.7 Comparison of base shear versus displacement

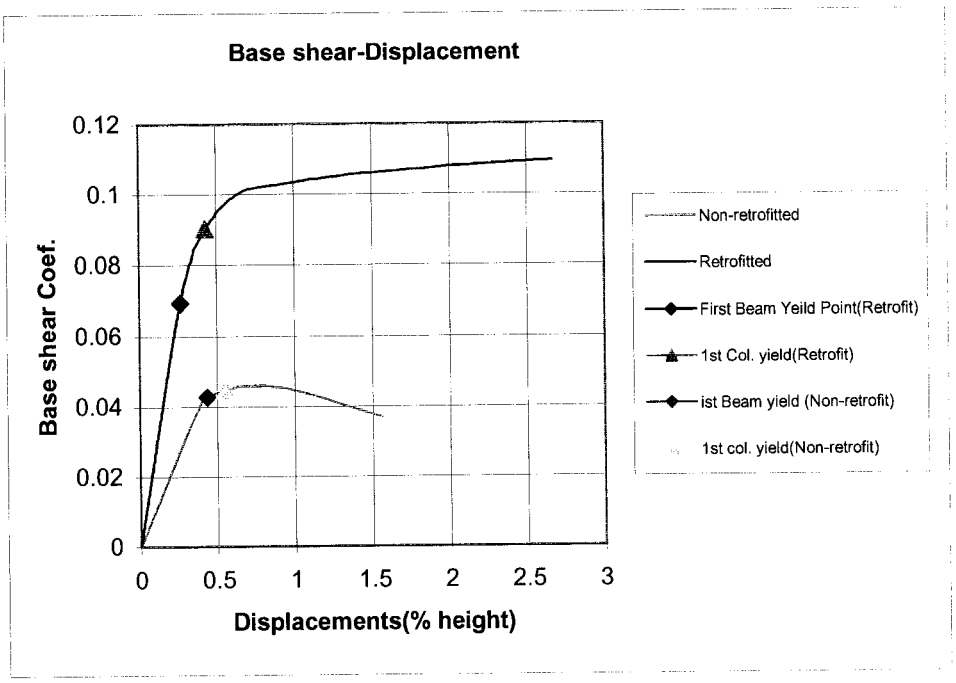

Figure 8.8 Sequence of plastic hinging

Figure 8.9 and 8.10 compares the displacements profiles of GLD and retrofitted GLD frames due to pushover loading and dynamic loading respectively. The hysteretic characteristics are used to represent inelastic behavior of RC frames. The results at peak response indicate that the plastic displacement profile is nonlinear, with larger displacements occurring in the lower floor. The profile of retrofitted GLD frame corresponds to developing of a beam-sway (soft story mechanism) in lowest floor. Profile of retrofitted frame shows the expected parabolic shape. This type of behavior, which represents a beam-sway mechanism, occurs throughout the retrofitted frame. The inter-story drifts are compared between the GLD and the retrofitted GLD in Figure 8.11. This is obtained from the results of pushover analysis.

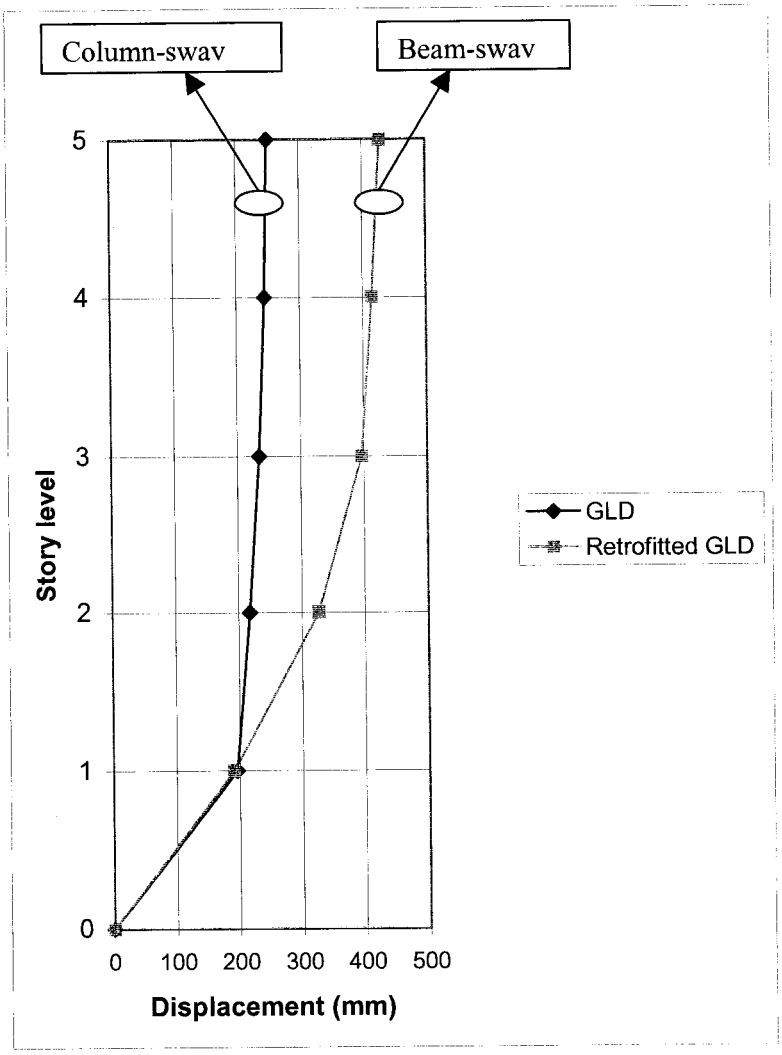

Figure 8.9 Plastic displacement profile (pushover analysis)

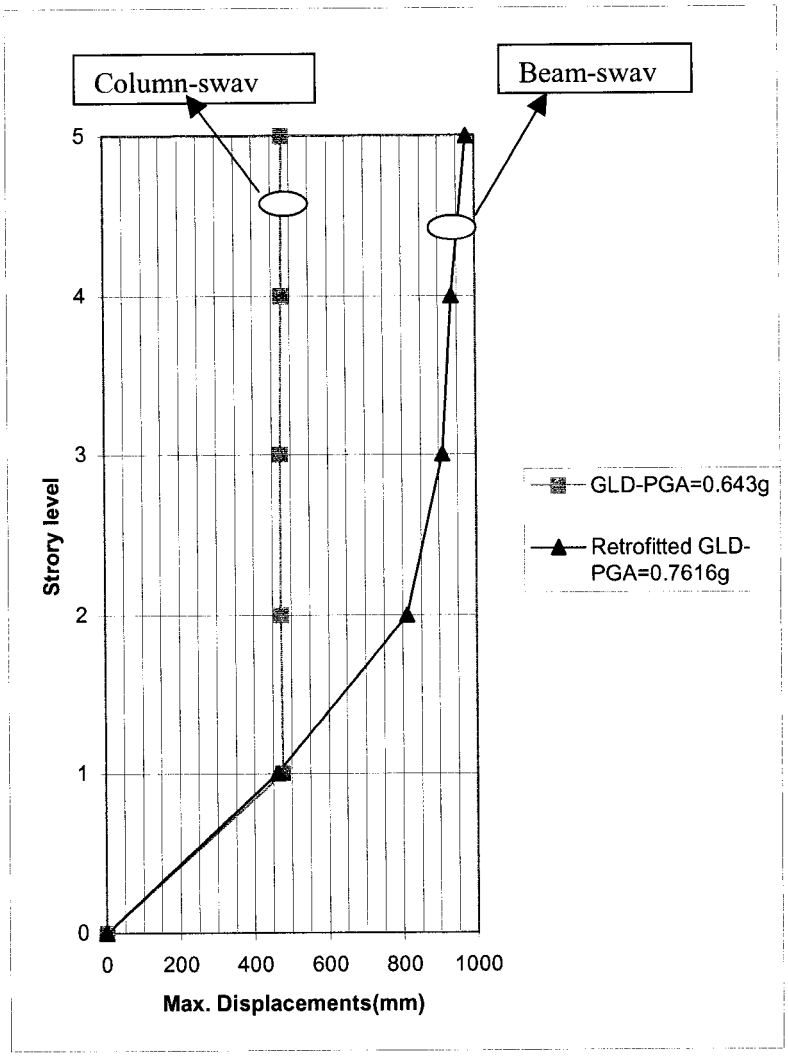

Figure 8.10 Plastic displacement profile (dynamic analysis)

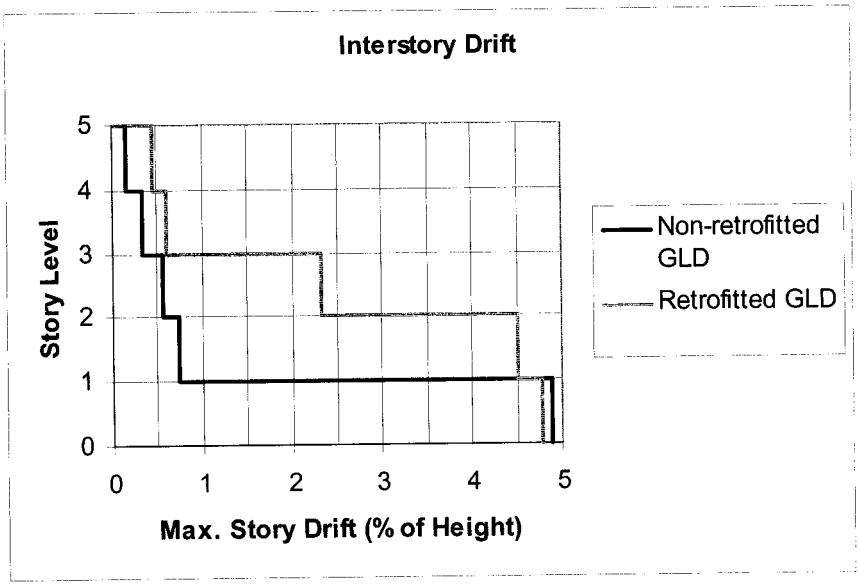

Figure 8.11 Inter-story Drift

The time-displacement relationships of GLD and retrofitted frames for each story are shown in Figures 8.12. The maximum displacement of GLD frame at 1st floor is about 475mm at a representative base shear of about 200 kN and in the rest of stories, a rigid body motion with almost the same displacements is observed. The relative movements are observed throughout of the retrofitted frame. The maximum values of displacements are changed to about 462, 812, 909, 935 and 976 mm for 1st through 5th floors respectively.

This result indicates that, the GLD frame is performed poorly. Inelastic deformations are concentrated mainly in the first floor and rest of frame is acted as a rigid body. The retrofitted frame exhibits a better performance for an earthquake event due to strong column-weak beam consideration.

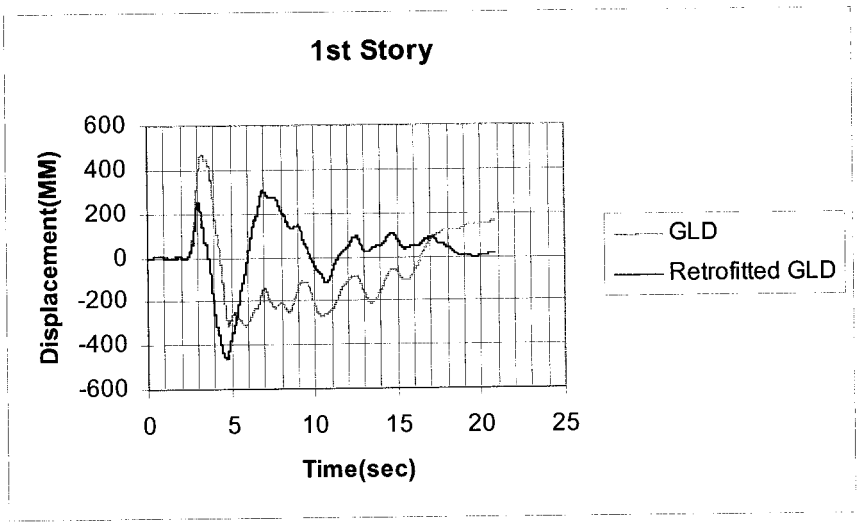
1st Story
Displacement(MM)
600
400
200
0
-200
-400
-600
0
5
10
15
20
25
Time(sec)
GLD
Retrofitted GLD

(a)

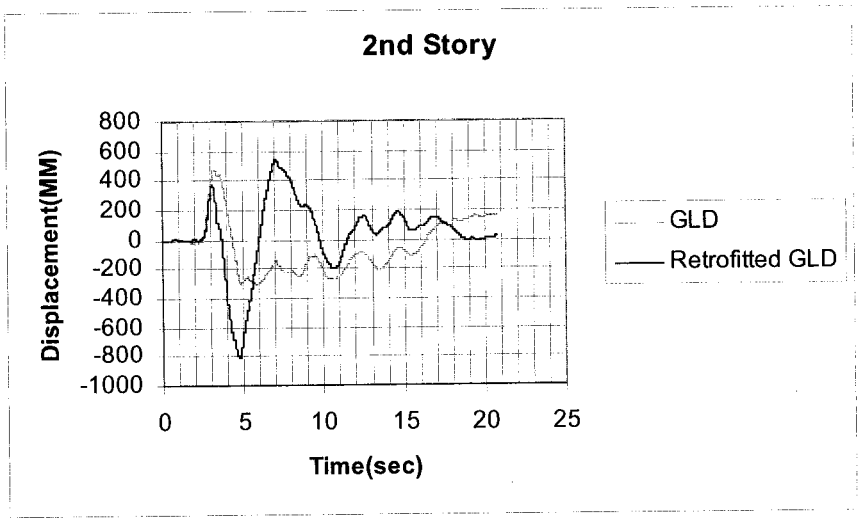
2nd Story
Displacement(MM)
800
600
400
200
0
-200
-400
-600
-800
-1000
0
5
10
15
20
25
Time(sec)
GLD
Retrofitted GLD

(b)

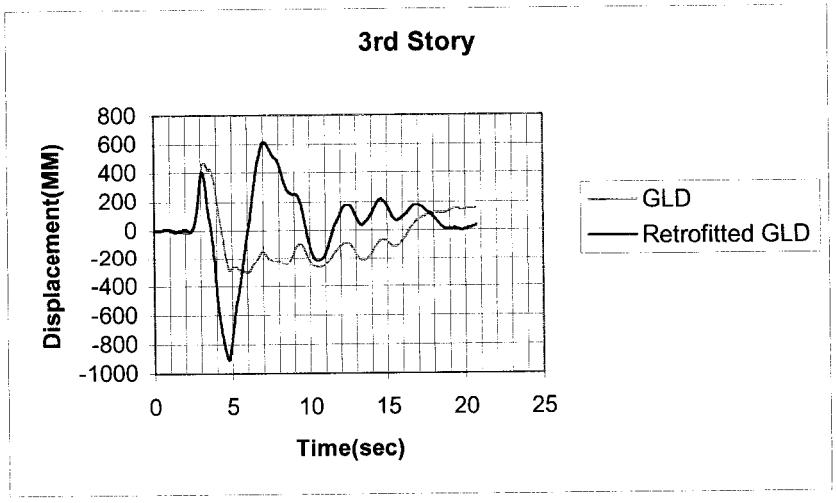
3rd Story
Displacement(MM)
800
600
400
200
0
-200
-400
-600
-800
-1000
0
5
10
15
20
25
Time(sec)
GLD
Retrofitted GLD

(c)

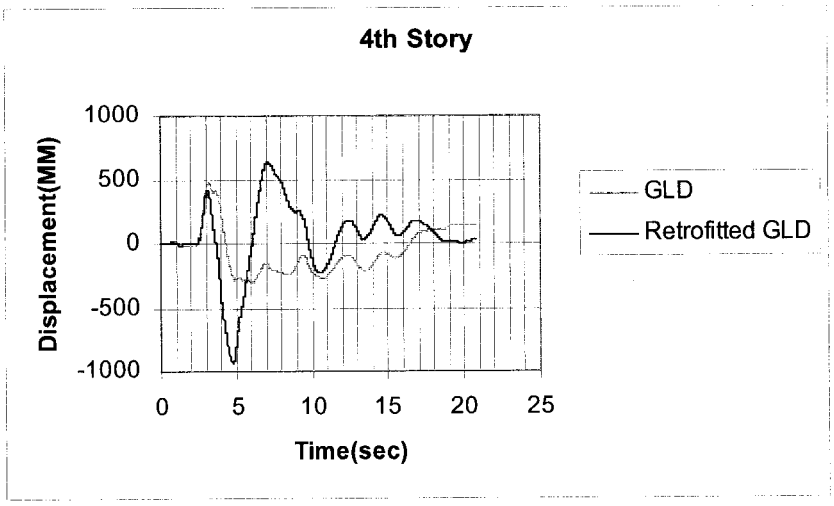

(d)

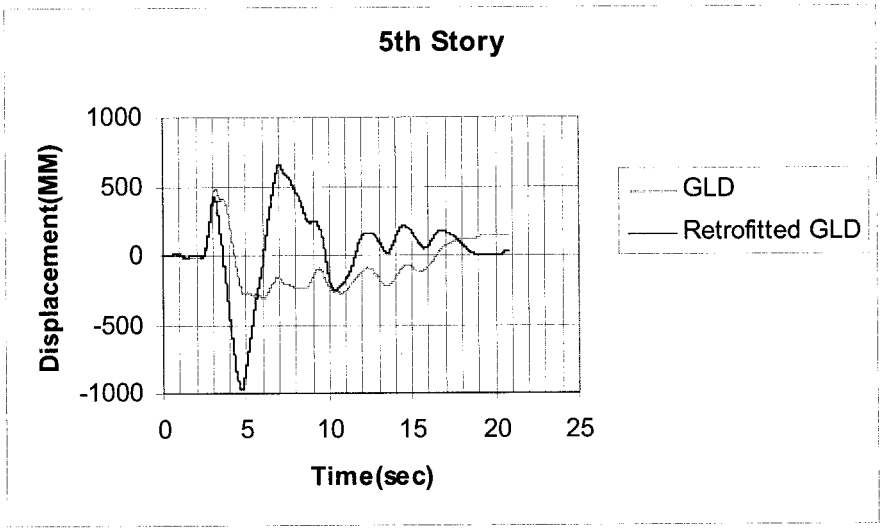

(e)

Figure 8.12 Comparison of time-displacements

Figure 8.13 compares the time-story shear relationship for each story level for GLD and retrofitted GLD structures. Due to seismic ground excitation the GLD frame undergoes an average story shear of about 200 kN while, the corresponding value for the retrofit case is about 550 kN. These results conform that the upgraded structure can sustain higher base shear.

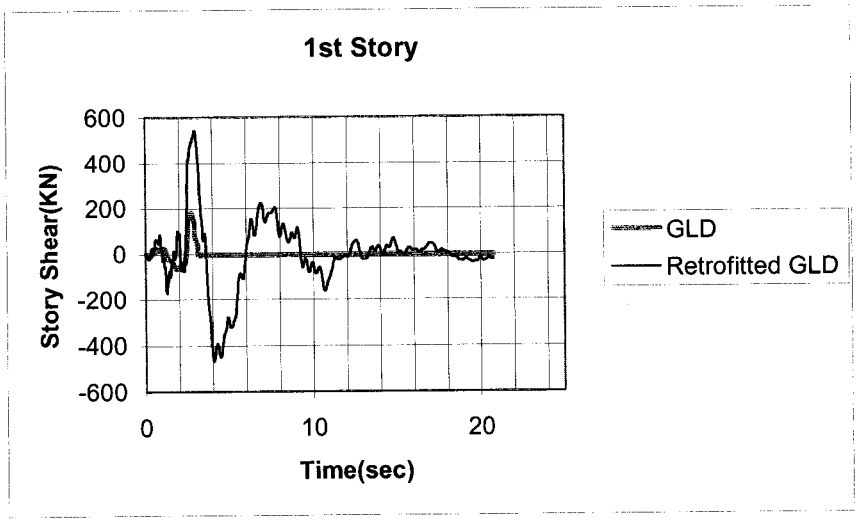

(a)

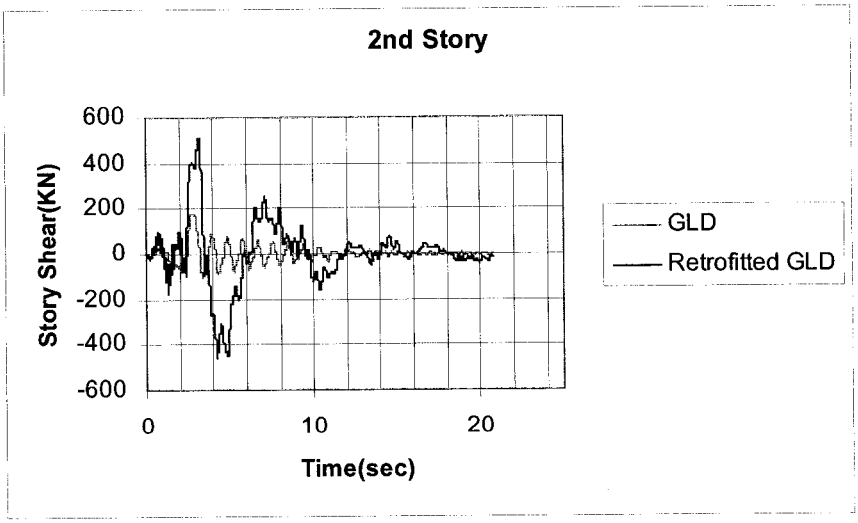

(b)

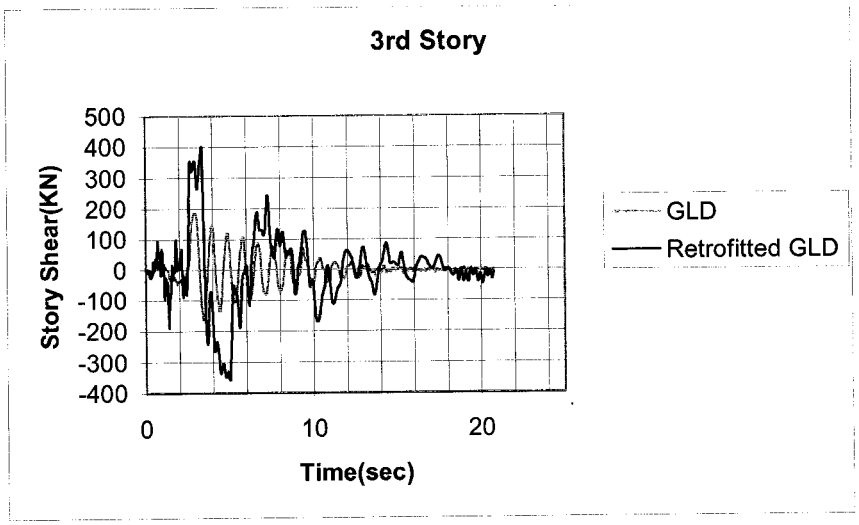
3rd Story
Story Shear(KN)
500
400
300
200
100
0
-100
-200
-300
-400
0
10
20
Time(sec)
GLD
Retrofitted GLD

(c)

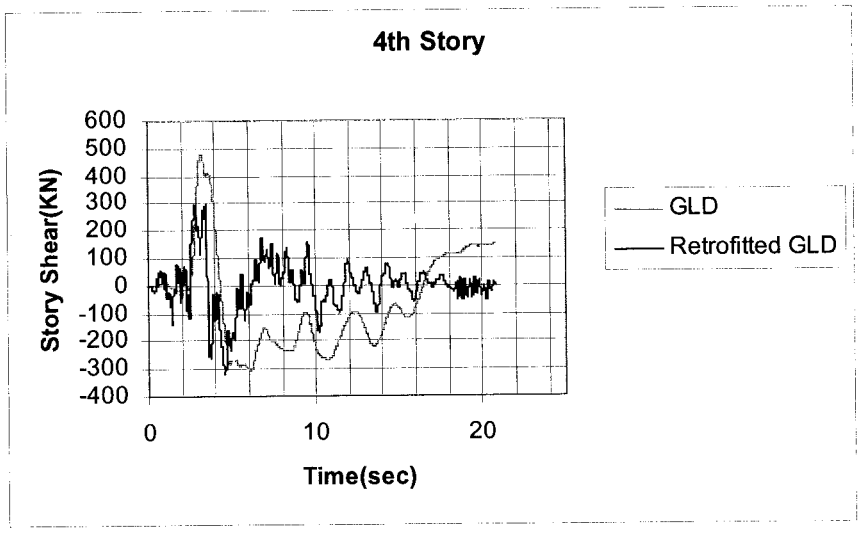
4th Story
Story Shear(KN)
600
500
400
300
200
100
0
-100
-200
-300
-400
0
10
20
Time(sec)
GLD
Retrofitted GLD

(d)

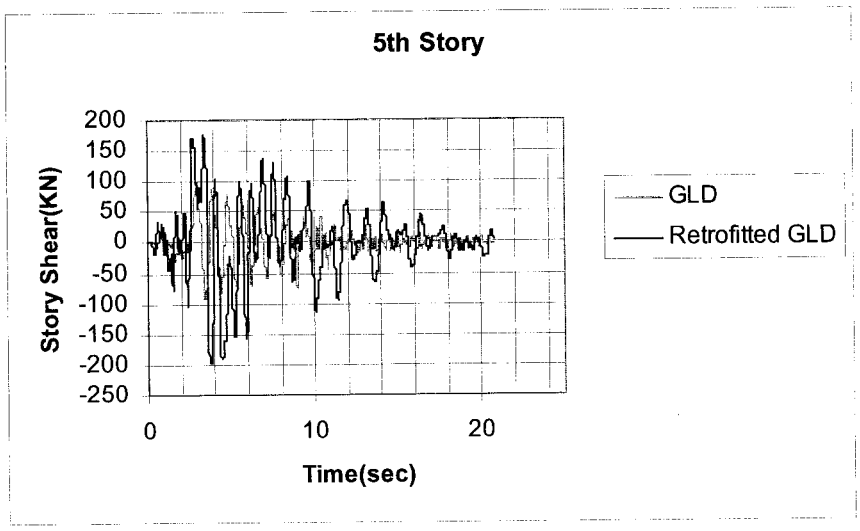

(e)

Figure 8.13 Comparison of time-story shear

Figure 8.14 compares damages obtained in GLD and retrofitted GLD frames. A sever column damages is obtained in 1st floor of GLD frame with a damage index of about 0.85 while minor damages are occurred (with a index of 0.23) in columns of retrofitted frame. Figure 8.14(a) shows, that the beams are not damaged in 1st story of GLD frame, while they experience damage with an index of 0.53 in the retrofitted frame. In GLD frame 1st story damages severely and in the rest of stories minor damages are observed. An undesirable dissipation of energy is indicated in columns of 1st story as a result of energy dissipation in columns of GLD frame. In retrofitted GLD frame, beams are damaged more than columns throughout the frame. The damages are distributed throughout the frame as a result of energy dissipation through all levels of frame. This desirable behavior shows the strong column-weak beam consideration for the retrofitted GLD frame. The results confirm the occurrence of an undesirable single story failure mechanism, lack of the strong column-weak beam considerations and forming of inelastic deformation in columns of GLD frame in the 1st story. This behavior is changed to the strong column-weak beam mechanism and a better performance in the retrofitted GLD frame.

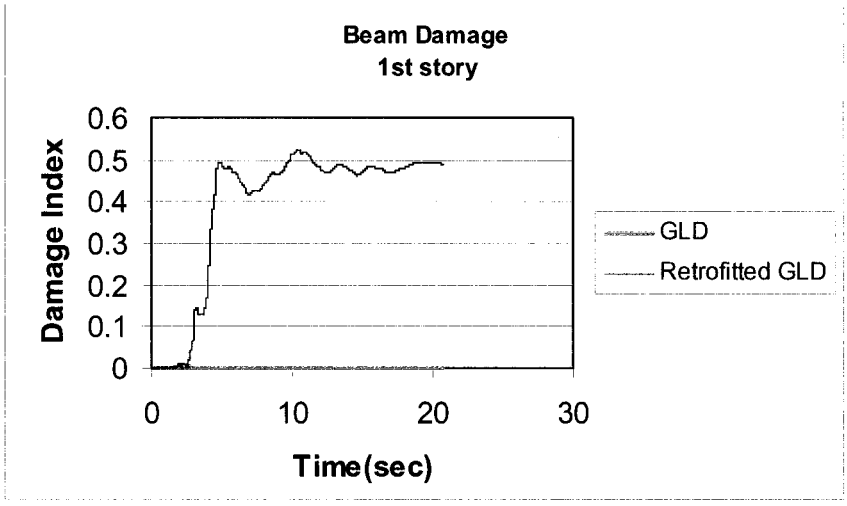
Beam Damage
1st story
Damage Index
0.6
0.5
0.4
0.3
0.2
0.1
0
0
10
20
30
Time(sec)
GLD
Retrofitted GLD

(a)

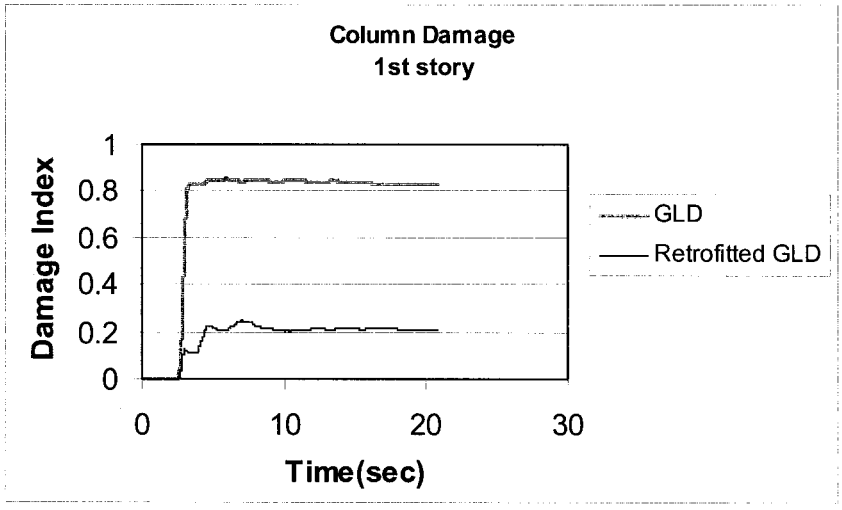
Column Damage
1st story
Damage Index
1
0.8
0.6
0.4
0.2
0
0
10
20
30
Time(sec)
GLD
Retrofitted GLD

(b)

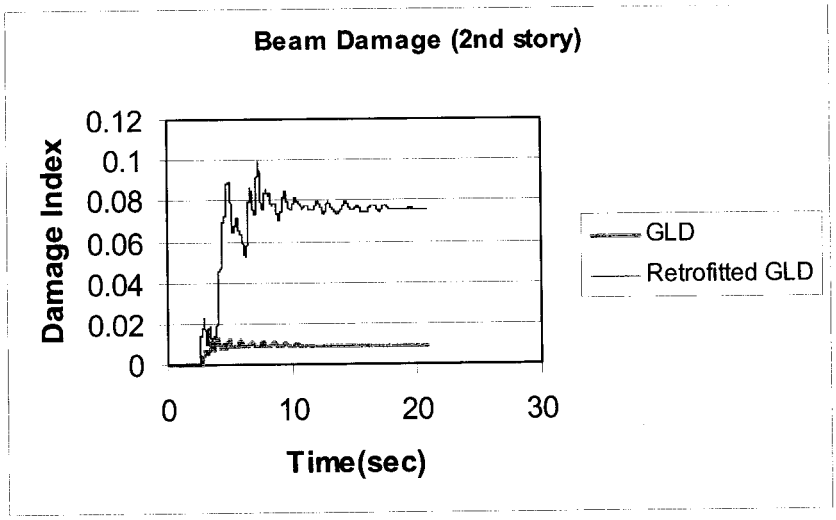
Beam Damage (2nd story)
Damage Index
0.12
0.1
0.08
0.06
0.04
0.02
0
0
10
20
30
Time(sec)
GLD
Retrofitted GLD

(c)

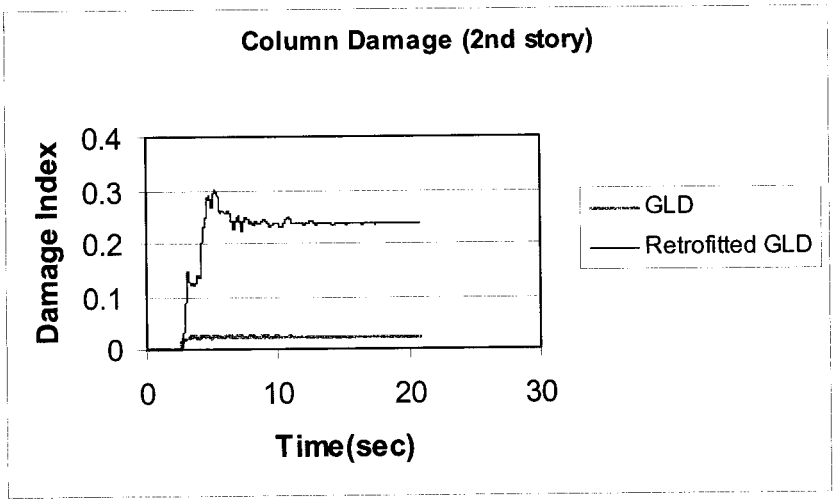
Column Damage (2nd story)
Damage Index
0.4
0.3
0.2
0.1
0
0
10
20
30
Time(sec)
GLD
Retrofitted GLD

(d)

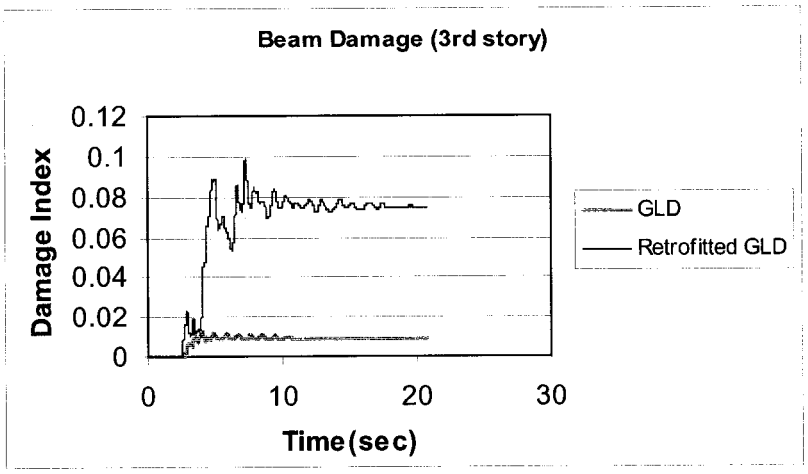
Beam Damage (3rd story)
Damage Index
0.12
0.1
0.08
0.06
0.04
0.02
0
0
10
20
30
Time(sec)
GLD
Retrofitted GLD

(e)

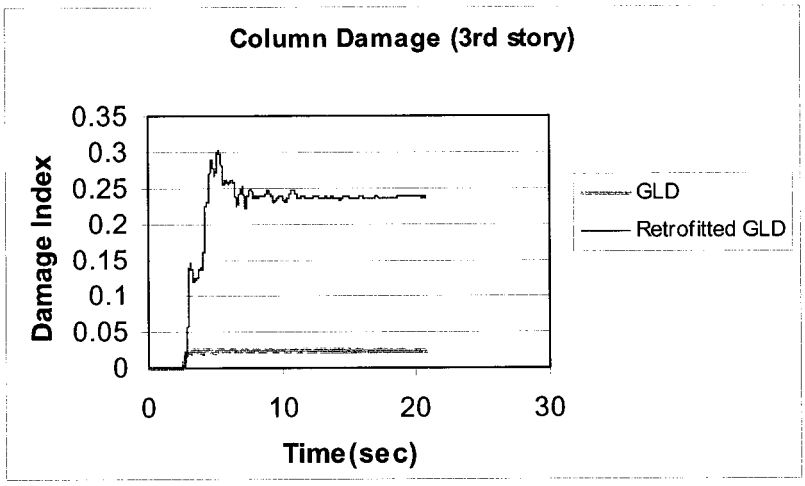
Column Damage (3rd story)
Damage Index
0.35
0.3
0.25
0.2
0.15
0.1
0.05
0
0
10
20
30
Time(sec)
GLD
Retrofitted GLD

(f)

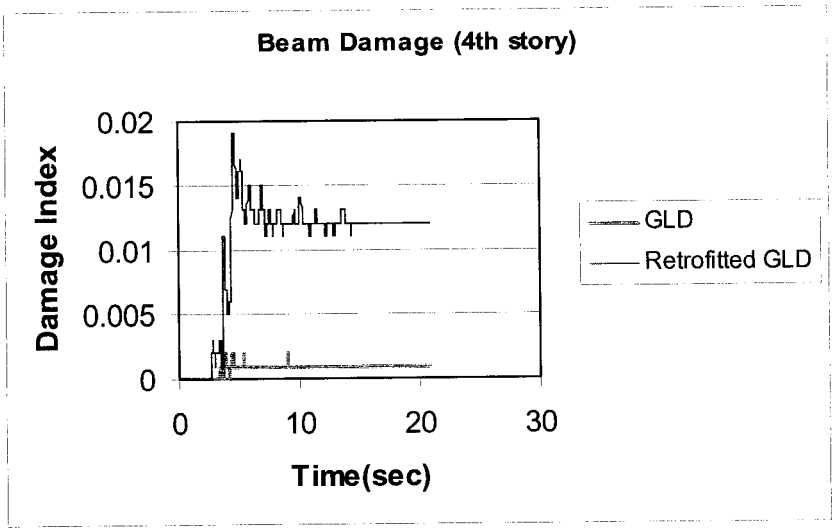
Beam Damage (4th story)
Damage Index
0.02
0.015
0.01
0.005
0
0
10
20
30
Time(sec)
GLD
Retrofitted GLD

(g)

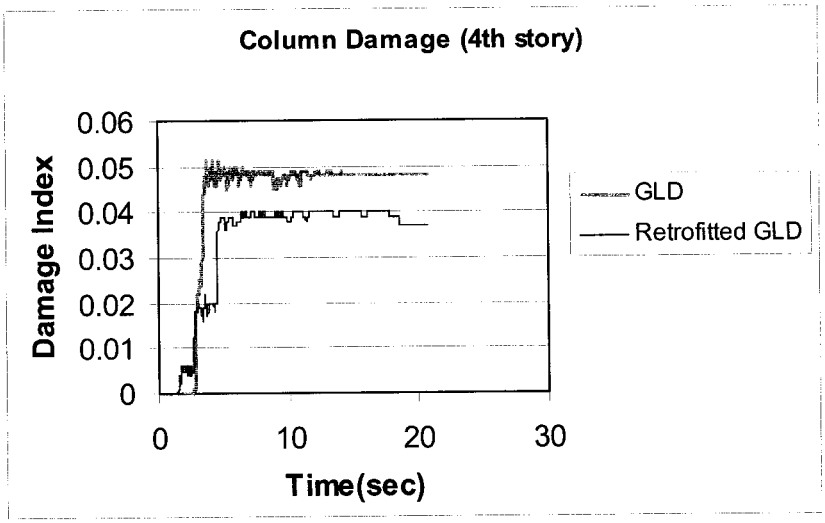
Column Damage (4th story)
Damage Index
0.06
0.05
0.04
0.03
0.02
0.01
0
0
10
20
30
Time(sec)
GLD
Retrofitted GLD

(h)

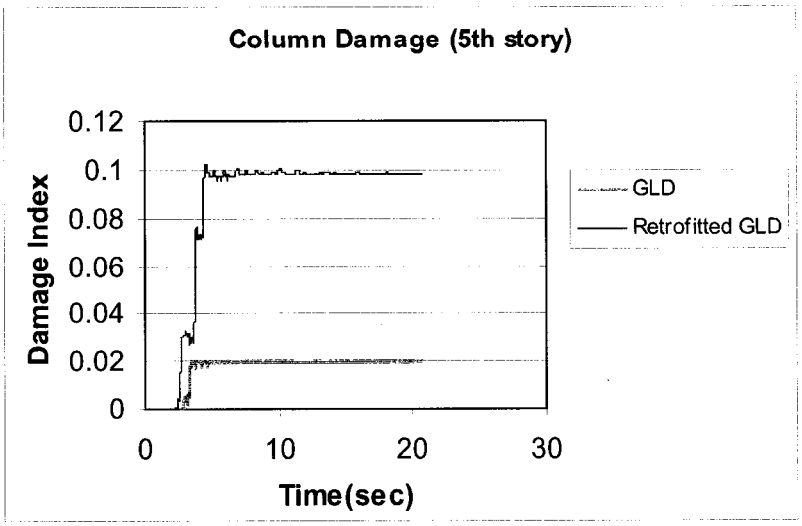

(i)

Figure 8.14 Comparison of element damages

CHAPTER 9

Conclusions and Recommendations

9.1 General

The analytical results described in this investigation, provided a better understanding of seismic behavior of ductile, nominally ductile, GLD and upgraded GLD frame structures. The goal of this research was to examine the improvements and enhancements that can actually be achieved using CFRP retrofitting technique and to investigate the effects of the FRP wrapping on the behavior of the GLD frame, its failure mechanisms, and its ductility to define design criteria. The results presented can be applied to design of the structural retrofitting by changing the failure mode and by providing improvements in terms of strength and/or ductility.

Reinforced concrete, exhibits an increase in compressive strength when subjected to confinement. This characteristic was advantageously used in the design of reinforced concrete columns, for instance, in which the load capacity was considerably increased when the column was properly confined with ties or spiral reinforcement. In this investigation, exterior reinforcement in the form of fiber composite wrapping was used to retrofit or repair concrete columns. Wrapping with fiber composites caused significant increase in the ductility, confinement and load carrying capacity of the columns. Also this research presented comparative analytical results of ductile, nominally ductile, GLD and retrofitted 5 story RC frame structure subjected to earthquake ground motion and pushover loading. Retrofitted GLD frame was analyzed under confined conditions produced by fiber composite wrapping. The results showed a considerable increase in the overall performance of the structure and increase in local ductility capacity. Ductility is a very important factor to be considered in seismic design of RC structures. The structure should exhibit a ductile behavior to survive in, an earthquake event. Thus, this investigation was focused on the improvement of ductility capacity in selected regions to achieve adequate overall structural performance by sustaining inelastic deformations without significant strength degradation during an earthquake vibration.

9.2 Improvements and Enhancements Achieved

Composite materials, known as fiber-reinforced polymers (FRP), have shown a great potential for the retrofitting and/or strengthening of reinforced concrete structures. The presented retrofitting technique using FRP has an advantage due to economically consideration, flexibility, non-welding, lightweight and easy handling in construction.

The most preferable retrofitting technique for existing GLD buildings is the jacketing of RC columns with fiber sheets because of the advantages mentioned above. This investigation has shown that externally bonded FRP composites could greatly enhance and improve the ductility level, load carrying capacity, energy dissipation capability and global performance of a building. The following enhancements were achieved as compared to existing GLD structures.

1. The peak lateral load carrying capacity was increased from V= 211.7kN to V=491kN.
2. The upgraded GLD frame showed a good displacement ductility capacity due to the formation of a multistory mechanism almost twice of that the non-ductile GLD which a local story mechanism formed.
3. Time-history dynamic analysis applied on GLD and retrofitted GLD frame showed 19 percent enhancement on seismic resistance of structure due to Erzancan (1992) ground acceleration.
4. A change in story-sway failure mechanism to multistory week beam-strong column failure was obtained due to forming of the plastic hinges in beams rather than columns.
5. An enhancement was obtained in overall damage of structure. The overall damage index obtained from pushover analysis on GLD frame for base shear coefficient of $^{V}/_{W}$=0.0474 was 0.203, while for the retrofitted frame, the damage index was 0.234 for $^{V}/_{W}$=0.11. Under dynamic analysis with PGA=0.643, the GLD frame damaged index was 0.780. For the same wave with PGA=0.7616, the overall damage index of 0.562, was observed for the retrofitted frame.
6. As a result of damage analysis obtained, an improvement observed in controlling damages. Column damaging controlled failure was observed in GLD frames but beam yielding failure showed first in retrofitted frame. As a result of load increment, the

first level of damage of retrofitted frame moved failure from columns to the beams, and then, further damages formed in columns.

7. The FRP composites with only two wraps increased the axial load carrying capacity of columns by about 44 percent.

9.3 Summary and Conclusions

The results of the analytical program confirmed that the confining action by FRP wrapping of columns could be a flexible retrofit technique for existing GLD buildings. In fact, it could modify the strength and/or ductility of the structure by using FRP wrapping. In this way the design of the retrofitting could be oriented to induce a favorable collapse mode of the upgraded frame.

The upgrade of the seismic performances of existing GLD reinforced concrete structures is an important issue that involves economic and social aspects in different areas of the world. In fact, the RC buildings, designed without seismic provisions, are often characterized by an unsatisfactory structural behavior due to the low available ductility and the lack of strength inducing an unfavorable global failure mechanisms. In these cases, some constructive details of the GLD frames can be pointed out as the potential critical causes of brittle failure mechanisms, which are sensitive to the cyclic damage. For example, in a column, the lack of appropriate size and spacing of ties, which does not guarantee the required level of confinement, can cause the collapse of the column end, resulting in crushing of the unconfined concrete, instability of the steel reinforcing bars in compression and pull out of those in tension.

The present research mostly focused on the problems related with the seismic upgrading of GLD frames and in particular, on column ductility. Some of the critical points are related to the columns and could be potential causes of failure in a non-seismically designed structure subjected to an earthquake are as follows:

1. Weak column-strong beam condition
2. Longitudinal reinforcement less than 2% of the concrete cross section
3. Poor confinement provided by the big spaced ties
4. Lapped splices of the longitudinal reinforcement above the construction joint

Finally, based on the analytical results, the following conclusions and recommendations are presented in order to improve the seismic performance of RC moment resistant frame buildings.

1. The ductile frame (R=4) performed very well during the severe ground acceleration and pushover loading. A better response was illustrated in ductile frame due to weak beam- strong column considerations. It showed the capacity design philosophy and ductility level as applied in current Canadian standards are effective.
2. The nominally ductile frame (R=2) was stronger than ductile frame due to enlarged member sections but the results showed lower ductility and lateral load carrying capacity. A brittle failure mechanism of this structure was observed in comparison with ductile frame. The nominally ductile frame performed as expected under the ground motions and pushover loads. Inelastic deformations were concentrated mainly in the first floor and the rest of the floors acted as a rigid body. The lack of the incorporation of the week beam-strong column concept, could question the level of seismic protection offered by this type of structures.
3. A comparison of pushover and dynamic analysis results indicated that, the pushover analyses are not being able to simulate the exact behavior of RC moment resisting frames subjected to strong seismic ground motions. The primary benefits of pushover analyses are to obtain a sense of the general capacity of the structure to sustain inelastic deformation.
4. Failure in lower level columns of GLD frame controlled the low ductility capacity and failure mode of the structure. But significant improvement was achieved by retrofitting schemes on overall behavior and failure mode of GLD structure.
5. The present study showed that the FRP wrapping of columns in existing GLD buildings could easily provide adequate seismic performance of non-ductile GLD RC frame buildings in seismic regions.
6. It was demonstrated that the inelastic behavior of non-ductile RC frame buildings is strongly affected by changing the ductility levels of columns by providing confinement in critical regions.
7. FRP wrapping of columns could significantly improve the ductility level and energy dissipation capability of structure throughout of story levels.

8. In designing of retrofitting of structures, attention must be paid to the mode of failure and strengthening of columns. To satisfy the weak beam-strong column mechanism, strengthening of the beams near the plastic hinging regions should be avoided to allow dissipation of energy in these regions.
9. The improvement obtained from the results presented illustrate that, this established retrofitting procedure of non-ductile GLD frames buildings, is suitable for use by practicing engineers engaged in the seismic retrofit of actual structures.

9.4 Practical Benefits

The damage analysis of GLD structures demonstrated the poor performance of older existing non-ductile GLD buildings. The retrofitting of deficient buildings is an urgent task of the owner; the owner is responsible for maintaining the performance of his building to the existing Code level. In this investigation, an attempt was made to provide an economically and efficient seismic retrofitting assessment procedure that can be employed on existing GLD building.

9.5 Recommendations for Further Study

Base on the results and conclusions obtained, the following recommendations appear to merit future investigations:

I. Only a moment resistant RC building was treated in this research. Future studies should consider other types of buildings in order to developing new retrofit techniques.
II. A limited number of factors have been carried out in present research to evaluate the seismic behavior of FRP retrofitted RC buildings. More considerations should be given to confirm the effect of different factors and variables.
III. Further experiments on the hysteretic models of IRDAC may better represent the actual hysteretic responses of FRP jacketed sections to adequately model the FRP retrofitted structures.
IV. Further work is needed to implement the FRP applications into structural analysis software to evaluate concrete elements strengthened using FRP sheets.
V. The trend between the rate of increment in ductility and the number of wraps need to be investigated.

VI. Further research is needed to specifically examine the long-term durability of both FRP materials and repaired members, the influence of on-site conditions on material properties and environmental effects of FRPs.

REFERENCES

1. ACI 318-63, 1968, " building Code Requirements for Reinforced Concrete", American Concrete Institute, Detroit, Michigan.

2. Brian Stonehouse B., Heldenbrecht A.C., and Kianoush M.R., 1998, "Evaluation of the Level of Seismic Protection Afforded to Reinforced Concrete Shear Wall Systems".

3. Bracci, J.M., Reinhorn, A.M., and Mander, J.B., 1995, "Seismic Resistance of Reinforced Concrete Frame Structures Designed for Gravity Loads", ACI Structural Journal, V.92, No.5.

4. Bertero, V.V., 1988, "Ductility Based Structural Design", Department of Civil Engineering, State University of California, United State of America.

5. CSA A23.3, 1994, "Design of Concrete Structures" Canadian Standards Association, Rexdale, Ontario, Canada.

6. Elmorsi, M.S.E, 1998, "Analytical Modeling of Reinforced Concrete Beam Column Connections for Seismic Loading", PhD Thesis, Department of Civil Engineering, McMaster University, Hamilton, Ontario, Canada.

7. Filiatrault A., Lachapelle E., and Lamontagne P., Apr. 1998, "Seismic Performance of Ductile and Nominally Ductile Reinforced Concrete Moment Resisting Frames", Experimental Study, Canadian Journal of Civil Engineering, Volume 25, Issue 2, Start Page 331, Ottawa, Canada.

8. Filiatrault A., Lachapelle E., and Lamontagne P., Apr. 1998, "Seismic Performance of Ductile and Nominally Ductile Reinforced Concrete Moment Resisting Frames", Analytical Study, Canadian Journal of Civil Engineering, Volume 25, Issue 2, Start Page 342, Ottawa, Canada.

9. Hamdy K.A., Tso W.K., and Ghobarah, 1991," Seismic Damage Potential to Ductile and Nominally Ductile Concrete Frames".

10. Harries, K.A., Richles, J.M., Sause, R., Pessiki, S., and Walkup, S.L., "Seismic Retrofit of Non-ductile Reinforced Concrete Buildings Columns Using FRP Jackets", 6th U.S National Conference on Earthquake Engineering.

11. Heldenbrecht, A.C, and Naumoski N., 1998, "Seismic Performance and Ductile Medium Height Reinforced Concrete Frame Buildings Designed in Accordance with the Provisions of the 1995 National Building Code of Canada ", Canadian Journal of Civil Engineering, 26:606-617, 1999.

12. Kunnath, S.K., Hoffmann, G., Reinhorn, A.M., and Mander, J.B., 1995, "Gravity Load- Designed Reinforced Concrete Buildings", ACI Structural Journal, V.92, No.4.

13. Kenneth, N., 2001, "Strenthening Reinforced Concrete Structures with Externally-Bonded Fiber Reinforced Polimers", Design Manual No.4, ISIS CANADA (The Canadian Network of Centres of Excellence on Intelligent for Innovative Structures) University of Sherbrooke, Canada.

14. MacGregor, J.G., Bartlett,M. F., (2000), "Reinforced Concrete Mechanics and Design", McCrown Hill.

15. Memon, M.S., 2002, "Seismic Behavior of Square Concrete Columns Retrofitted with Glass Fiber Reinforced Polymers (GFRPs)", M.A.Sc. Thesis, Graduate Department of Civil Engineering University of Toronto.

16. Matsuzaki, Y., Nakano, K., Fuji, Sh., and Fukoyama, H., 2000, "Seismic Retrofit Using Continuous Fiber Sheets", 12th World Conference of Earthquake Engineering (12WCEE 2000).

17. National Building Code of Canada, (NBCC), 1995, Associate Committee on the National Building Code, National Research Council of Canada, Ottawa, Ont.

18. Otani, S., 2001," Earthquake Resistant Design of Reinforced Concrete Buildings", University of Tokyo, Hongo, Bunkyo-Ku, Tokyo 113-8656 Japan (Presented at First International Conference on Concrete and Development, at Tehran, Islamic Repablic of Iran, April 30 to May 2, 2001).

19. Park, R., and Paulay, T., 1975, "Reinforced Concrete Structures" John Wiley & Sons, New York.

20. Priestely, M.J.N., 1996, "Displacent-Based Seismic Assessment of Reinforced Concrete Buildings" University of California, San Diego, La Jolla, California.

21. Sivaselvan, M.V., 1999, "Hysteretic Models For Cyclic Behavior of Deteriorating Inelastic Structures", M.Sc. Thesis, Department of Civil, Structural and Environmental Engineering, State University of New York at Buffalo.

22. SAC System Performance, "Development of Earthquake ground motions", http://nisee.berkeley.edu/data/strong_motion/sacsteel/ground_motions.html, Federal Services of Pasadena, California.

23. SAP2000 Version 8.0, June 2002, "Linear and Nonlinear Static and Dynamic Analysis and Design of Structures", Computers and Structures, Inc., Berkeley, California, USA.

24. Structural Engineers Association of California (SEAOC), Vision 2000, 1995, "Performance Based Seismic Engineering of Buildings", San Francisco, Calif.

25. Teran, A., 1997, "Energy Concepts and Damage Indices" Gilmore University of Autonoma Metropolitana Mexico City (Presented at the EERC-CUREe Symposium in Honor of Vitelmo V. Bertero, Berkeley, California.

26. Valles, R.E., Reinhorm, A.M., Kunnath, S.K., Li, C., and Madan, A., "IDARC a Computer Program for Inelastic Damage Analysis of Buildings", Civil Engineering Department, State University of New York at Buffalo.

27. Wu, S, 1995, "Seismic Analysis and Retrofit of Non-ductile Reinforced Concrete Frame Buildings", PhD Thesis, Lehigh University, Bethlehem, Pennsylvania.

Appendix A

A.1 Design Procedures:

The design base shear, **V**, specified by the NBCC for each structure is given by ($V= V_e U/ R$), Where $\mathbf{V_e}$ is the required base shear if the structure would remain elastic under the design earthquake, U is a calibration factor equal to 0.6, and R is a force reduction factor, which depends on the ductility capacity of the lateral load resisting system. The force modification factor, R, is chosen according to the ductility level for which the frames are designed. For ductile frames R = 4.0 and for nominally ductile frames R = 2.0. The use of R = 4 for the ductile structure was justified by implementing the strict seismic detailing requirements contained in the Canadian concrete standard (CSA 1994). The structure with nominal ductility (R = 2), on the other hand, incorporated only nominal detailing, according also to the Canadian concrete standard, since its design lateral loads were higher than the ductile structure and, according to the seismic design philosophy of the NBCC, the ductility demand by the design earthquake should be limited.

The material properties are presented in Table A.1

Table A.1 (the material properties)
(a) Steel and concrete

Material	**Properties**
Longitudinal Reinforcing Steel	Young Modulus E_S=200000 MPa Yield strength f_y=400 MPa Ultimate Strength f_{SU}=560Mpa Strain at Hardening EPSH= 3.0% Modulus at Hardening 1356
Transverse Reinforcing steel	Young Modulus E_S=200000 MPa Yield strength f_y=400 MPa Ultimate Strength f_{SU}=560Mpa Strain at Hardening EPSH= 3.0% Modulus at Hardening 1356
Concrete	Compressive Strength f'c=35 Mpa Initial Elastic Modulus E_C=28000 Strain at Max. Comp. Strength EPSO=2% Tensile Strength f_T=4.2

(b) FRP sheet properties as provided by manufacturer

Fiber type	Ultimate tensile strength (Mpa)	Ultimate strain (%)	Modulus of elasticity (Gpa)	Design thickness (mm)
Mbrace CF 130 CFRP	3550	1.5	235	0.165

(c) Adhesive properties as provided by manufacturer

Adhesive type	Tensile strength (Mpa)	Tensile modulus (Gpa)	Ultimate elongation (%)	Flexural strength (Mpa)	Flexural modulus (Gpa)
Mbrace Primer	12	0.717	3.0	24	0.593

A.2 Design Loadings:

The frames are designed for the critical combinations of gravity and seismic loads as per NBCC 1990. The following is a list of the gravity loads

Table A.2 Table of loading

(a) Roof

Roof	**Loads**
Snow Loads	1.5 kpa
Roof insulation	0.25 kpa
Mechanical services loading on all floors	0.5 kpa
Slab (125mm)	3 kpa
Total Dead Load	3.75 kpa
Total Live Loads	2.4 kpa
External walls	1.85 kpa

(b) Typical Floors

Typical Floor	**Loads**
Slab (125mm)	3 kpa
Mechanical services loading on all floors	0.5 kpa
Partitions	1 kpa
Total Dead Load	4.5 kpa
Total Live Loads	2.4 kpa

Figure A.1 illustrates the resulting load configurations for both dead and live loads upon the one internal frame.

A.3 Determination of Seismic Loading

For seismic base shear calculations, the frames are assumed to be located in a high-risk seismic zone (v= 0.4). The following is the currently recommended procedure used to determine seismic loading upon a structure. Table A.3 illustrates a summary of the calculations involved, comparing manually calculated values for nominal ductile frame (case study#1) with ductile frame (case study#2). The procedure is broken down into a series of steps as follow:

Determine of the minimum lateral seismic force, v:

$V = (V_e / R) U$

Where

V_e = equivalent lateral seismic force representing elastic response

R = force modification factor that reflects the capability of a structure to dissipate energy through inelastic behavior (given R = 2 for nominal ductile frame and R= 4.0 for ductile moment resisting frame structures)

U = factor representing level of protection based on experience (U = 0.6)

The equivalent lateral seismic force representing elastic response, V_e is: $V_e = vSIFW$

Where

V = zonal velocity ratio (given v = 0.40)

s = seismic response factor = $1.5 / \sqrt{T}$ for $T \geq 0.5$ seconds (given T = 0.1, N = 0.5 seconds, S = 2.121)

T = fundamental period of vibration

N = total number of stories above the grade

I = seismic importance factor equal to 1.5 for post-disaster buildings, 1.3 for schools and 1.0 for all other buildings (given I = 1.0 for office buildings)

F = foundation factor which varies from 1.0 for buildings founded on rock, to 2.0 for buildings founded on very soft and fine-grained soils with depths greater than 15 m (given F = 1.3)

W = 15482 KN (Total dead load of the structure including the 25% of the design snow load)

Therefore, the seismic base shear, V, is:

$V = (0.40)(1)(2.121)(1.3)(0.6)\ (15482)\ /2 = 5122.6$ KN (case study#1)

$V = (0.40)(1)(2.121)(1.3)(0.6)\ W/4 = 2561.3$ KN (case study#2)

Distribute the total lateral seismic force, V along the height of the building:

$F = (V - F_t)\ h_i\ W_i / (\Sigma h_i\ W_i)$

Where

F x = lateral force applied at level x

Ft = additional lateral force applied to the top of building (Ft = 0.0 if $T \leq 0.7$ seconds)

W_i and W_x are portions of W at levels x and i respectively

h_i and h_x are the heights above the base to levels x and i respectively

Determine the accidental applied torsional moment at each level (x):

$T_x = (F_x)\ (\pm 0.1 D_{nx}) = 2.2\ F_x$

Where

D_{nx} = Plan dimension of the building in the direction of the computed eccentricity

(D_{nx} =22)

Determine the shear induced due to torsion in "Frame-B"

$F_{xt} = T_x\ Y / I = 4\ T_x / 274$

Where

F_{xt} is distributed torsion with the force in frame-b due to T_x and I is moment of inertia

$I = \Sigma AY^2 = 2(1*11^2 + 4^2) = 274$

Note: Four frames in the North-South direction will absorb the applied torsion. These frames all possess the same stiffness; therefore the shear induced by torsion will be proportional to their distance from the center of stiffness.

Table A.3 illustrates the results of designed seismic lateral loads on frame-B for both cases of study.

Table A.3 Comparison of designed seismic lateral loads on frame-B for both cases of study

Floor	$h_{i(M)}$	$w_{i(MN)}$	$h_i w_i$	Ratio	$F_{X(KN)}$ C.S.#1	$F_{X(KN)}$ C.S.#2	T_X C.S.#1	T_X C.S.#2	F_{xt} C.S.#1	F_{xt} C.S.#2	Total C.S.#1	Total C.S.#2
Roof	16	2.75	44	0.286	1465	732.5	3223	1611.5	48.3	24.2	414.6	207.3
5	13	3.28	42.6	0.277	1419	709.5	3121.8	1560.9	46.8	23.4	401.6	200.8
4	10	3.28	32.8	0.213	1091	545.5	2400	1200	36	18	308.7	154.4
3	7	3.28	22.96	0.149	763.3	381.6	1679.3	839.5	25.2	12.6	216	108
2	4	2.89	11.56	0.075	384.7	192.35	846.3	423.2	12.7	6.35	108.9	54.5
1		Σ=15.48	153.9									

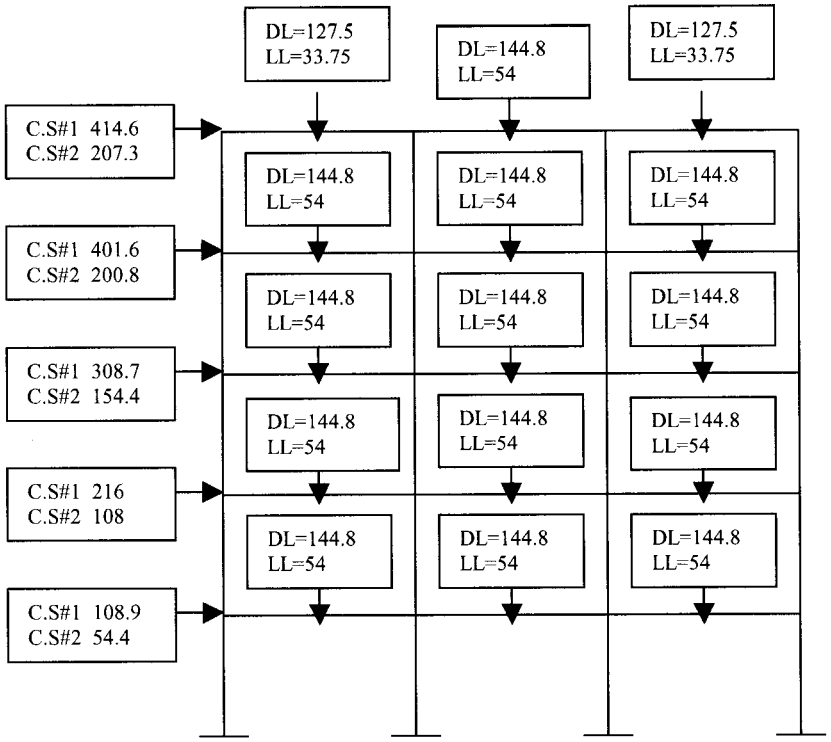

Figure A.1 load configurations of frame-B (ductile and nominally ductile frames)

A.4 Design of Frame-B as a Nominal Ductile Frame:

In the preliminary design of building, it has been decided to use 600*600 mm beams and columns in first and second floors and 500*500 through 5th floor as shown in figure A.2 and A.3.

Initial elastic analysis of structures is performed in order to determine the structural elements seismic design forces. The finite element based, structural analysis program SAP2000 is used to perform element forces. Factored moments, including earthquake effects from an elastic frame analysis by sap2000, are given in Tables A.4 using the sign convention that positive moments cause compression in top fiber.

According NBCC1995 Load combination including earthquake shall be as follow

- 1.25D + 1.5L
- 1.0D ± ϒ(1.0) E
- 1.0D + ϒ(1.5L ±1.0 E)

Table A.4 Moments From as Elastic Analysis of Nominal Ductile Frame

(a) First Floor

Moment	Sp1-3	Sp1-3	Sp1-3	Sp3-5	Sp3-5	Sp3-5	Sp5-7	Sp5-7	Sp5-7
L.C	Ext.M	Mid S	Int.M	Int.M	Mid S	Int.M	Int.M	Mid S.	Ext.M
L.C#1	-228.9	219.6	-228.9	-228.9	206.2	-224	-224	219.6	-228.9
L.C#2									
Sway R	+637.5		-800.7	+492.3		-743.8	+538.9		-847
Sway L	-852.7		+542.4	-744.4		+491.7	-797.1		+631.9
L.C#3									
Sway R	+620.3		-821.7	471.8		-764.1	+518		-864.3
Sway L	-869.9		+521.4	-764.9		+471.5	-818		+614.6

(b) Third Floor

Moment	Sp1-3	Sp1-3	Sp1-3	Sp3-5	Sp3-5	Sp3-5	Sp5-7	Sp5-7	Sp5-7
L.C	Ext.M	Mid S	Int.M	Int.M	Mid S	Int.M	Int.M	Mid S.	Ext.M
L.C#1	-208.5	216.5	-217.9	-217.9	207.6	-217.9	-217.9	216.8	-209
L.C#2									
Sway R	+386.5		-585.3	+332.1		-501.9	+343.6		-623.3
Sway L	-628.3		+346.7	-582.5		+331.5	-582.2		+381.5
L.C#3									
Sway R	+367.3		-604.9	311.6		-602	+324.3		-642.6
Sway L	-647.4		+327.1	-603		+311.5	-601.5		+362.2

(c) 4^{th} and 5^{th} Floors

Moment	Sp1-3	Sp1-3	Sp1-3	Sp3-5	Sp3-5	Sp3-5	Sp5-7	Sp5-7	Sp5-7
L.C	Ext.M	Mid S	Int.M	Int.M	Mid S	Int.M	Int.M	Mid S.	Ext.M
L.C#1	213.9	215.2	-218.1	-218.1	209.6	-218.1	-218.1	214	-216
L.C#2									
Sway R	+198.7		-415.6	+183.1		-431.5	+179.1		-445.4
Sway L	-447.9		+180.7	-431.8		+182.8	-414		+196.1
L.C#3									
Sway R	+179.3		-485.2	162.2		-450.4	+159.6		-465.4
Sway L	-467.3		+161.2	-452.7		+163.8	-433.6		+176

Calculate the Steel Required for Flexure at 1^{st} and 2^{nd} Floors (600*600):

Minimum reinforcement for flexural reinforcement $=1.4b_w d/ f_y = 1135$ mm^2

Interior and Exterior supports-negative moment:

Maximum negative moment = -869.9 KN-m

$A_S = M_f/(\varphi_s f_y j d) = 869.9 * 10^6/(0.85*400*0.85*540.8) = 5566$ mm^2

j=0.85

According A23.3 CI. 21.4.2.2 the slab bars parallel to the beam, lying within 3 times the slab thickness on each side of the web as part of the negative moment steel when calculating M_r .The slab steel parallel to the beam stem will be shrinkage and temperature steel. Typically this would be a No.10 bar at 300 mm on centers. If so, there would be 1No.10 bar within $3h_s$ on each side of the beam with total area= 2 *100 mm^2 .We require *5566 -200 = 5366* mm^2 additional steel. Try 5No.35 plus No.25 plus 2No.10 bars of slab. These fit into the width of the beam. Total As including the slab bars = 5700 mm^2. This exceeds As_{min} = 1135 mm^2-OK

$a = (\varphi_s A_s f_y)/\alpha_1 \varphi_c f'_c b = 0.85*5700*400/(0.805*0.6*35*600) = 191$ mm

$M_r = \varphi_s A_s f_y (d-a/2) = 0.85*5700*400(540.8-191/2) = 863$ KN-m

A23.3 Cl. 21.3.2.1 limits $\rho < 0.025$ in this section $\rho = 5700/(600*540.8) = 0.0175 < 0.025$

Check if the steel yields: a/d = 191/540.8 = 0.35 and according A23.3 Cl. 10.5.2, the steel will yield if $c/d \leq 700/(700+f_y)$ Substituting $c = a/\beta_1$ where $\beta_1 = 0.895$, the steel will yield if $a/d \leq 700\beta_1/(700+f_y)=0.57$

Since a / d is less than this, the steel yields at failure.

Try 5No.35 plus 1No.25 plus 2No.10 bars of slab at the interior support.

Interior and Exterior Supports-Positive moment:

From Table 4, the maximum Positive moment from a frame analysis was 637.5 KN-m, From A23.3 Cl 10.3.3; the effective width of the top flange is 1940 mm.

Try 6No.30 bars, A., = 4200 mm2, Mr = 676 > 637.5 KN-m

Mid span-Positive moment:

Maximum positive moment at mid span = 219.6 KN-m but not less than one quarter of the maximum moment resistance provided at either end of the beam = 0.25 *869.9=217.5 KN-m. A_s should not be less than the minimum = 1135 mm^2. Try 2No.30 bars,

A_s = 1400 mm^2, Mr = 246.3KN-m > M_f=219.6

Minimum Positive and Negative Moment Capacities

A23.3 Cl. 21.3.2.2 requires that the minimum positive and negative moment capacities at any section along the beam not be less than 0.25 times the maximum negative moment capacity provided at either joint. 2 No.30 bars are adequate as minimum steel.

Calculate the Steel Required for Flexure at 3rd Floor (500*500):

Exterior and Interior Supports-negative moment:

Maximum negative moment = -647.4 KN-m

Try 5 No.35, plus 1 No.30, plus 2 No.10 slab bars, A_s=5900 mm^2, M_r=646.2 KN-m, O.K

Exterior and Interior support-Positive moment:

From Table A.4.2, the maximum Positive moment from a frame analysis was 386.5 KN-m, but A23.3 CL. 21.3.2.2 requires that the positive moment capacity at the face of the joint not be less than 0.5 times negative moment capacity = ½*647.4 =323.7 KN-m. Therefore, design moment is 386.5 KN-m. Try 4No.30, plus 1No.20, A_s=3100, M_r=402 O.K

Mid span:

Maximum positive moment at mid span = 216.8 KN-m but not less than one quarter of the maximum moment resistance provided at either end of the beam = 0.25*646.2=161.6 KN-m. A_s should not be less than the minimum = 771.4 mm^2. Try 2No.30 bars,

A_s = 1400 mm^2, Mr = 246.3KN-m > M_f=216.8

Calculate the Steel Required for Flexure at 4^{th} and 5^{th} Floor (500*500 mm):

Exterior and Interior support-negative moment:

Maximum negative moment = -485.15 KN-m

Try 4No.35, plus 2 No.10 slab bars, A_s = 4200 mm^2, M_r = 508.8 KN-m Satisfactory

Exterior and Interior support-Positive moment:

From Table 5-3, the maximum Positive moment from a frame analysis was 198.7KN-m,

Minimum reinforcement for flexural reinforcement =$1.4b_wd/ f_y$ =771.4 mm^2

Try 2No.30, A_s=1400, M_r=197.8, Satisfactory

Mid span:

Maximum Positive moment= 215.2 Try 2No.30 bars, A_s = 1400 mm^2, Mr = 246.3KN-m > M_f=215.2

Table A.5 Summery of designed sections and reinforcement of beams (nominally ductile)

Story	Beams	Sec.	Reinforcements	A_s	$\rho*10^{-3}$	M_r	M_f
1st	Int & Ext Supports(-ve)	600*600	5No35+1NO25@top	5700	17.5	863	869.9
	Int & Ext Supports(+ve)	600*600	6No30@bot	4200	12.87	676	637.5
	Mid Span	600*600	2No30@bot	1400	4.3	246.3	219.6
2nd	Int & Ext Supports(-ve)	600*600	5No35+1NO25@top	5700	17.5	863	782.4
	Int & Ext Supports(+ve)	600*600	6No30@bot	4200	12.87	676	527.7
	Mid Span	600*600	2No30@bot	1400	4.3	246.3	216
3rd	Int & Ext Supports(-ve)	500*500	5No35+1NO30@top	5900	26.68	646.2	647.4
	Int & Ext Supports(+ve)	500*500	4No30+1NO20@bot	3100	14	402	386.5
	Mid Span	500*500	2No30@bot	1400	6.31	246.3	216.8
4rh 5th	Int & Ext Supports(-ve)	500*500	4No35@TOP	4200	18.93	508.8	485.2
	Int & Ext Supports(+ve)	500*500	2No30@bot	1400	6.31	197.8	198.7
	Mid Span	500*500	2No30@bot	1400	6.31	246.3	215.2

A.5 Columns Design:

The floor-to-floor height is 4000mm at first floor with 600 mm deep beams in each floor. Giving a clear column height of 3200 mm. The column size and the floor-to-floor heights are 3000 mm in the other stories. The factored moments and axial loads from an elastic analysis for earthquake loads are given in Tables A.5 the column has 40 mm cover to the ties.

Tables A.6 Summery of moments and axial loads (nominally ductile)

(a) First floor

1st Story	Axial Load	Bottom Moment	Top Moment
L.C#1	1621.3	37	73.1
L.C#2			
Sway to Left	1029.2	962.4	-645.8
Sway to Right	1024.2	-962.5	644.4
L.C#3			
Sway to Left	1155	962.4	-645.9
Sway to Right	1159	-962.5	644.3

(b) Second floor

2nd Story	Axial Load	Bottom Moment	Top Moment
L.C#1	1295.1	112.9	110.9
L.C#2			
Sway to Left	794.2	647.1	-674.3
Sway to Right	790.7	-644.7	673.7
L.C#3			
Sway to Left	892.3	647.5	-674.4
Sway to Right	897.9	-644.3	502.2

(c) Third Floor

3rd Story	Axial Load	Bottom Moment	Top Moment
L.C#1	955.5	104.9	-102.2
L.C#2			
Sway to Left	582.6	500.1	-581.55
Sway to Right	580.5	-501.8	583.4
L.C#3			
Sway to Left	662.2	500.3	-581.6
Sway to Right	660.7	-502.2	583.7

(d) Forth & fifth floors

4th & 5th Stories	Axial Load	Bottom Moment	Top Moment
L.C#1	630.5	104.9	-102.2
L.C#2			
Sway to Left	377.3	344	-448.2
Sway to Right	376.6	-345.9	450.5
L.C#3			
Sway to Left	430	344.7	-450
Sway to Right	429.8	-346.4	451.3

As a first trial we select a 600 mm by 600 mm column with 8No.35 bars, A_{st}=8000mm^2, ρ= 0.022 A23.3 Cl. 21.4.3.1 limits A_s, to not less than 0.01*600*600=3600 mm^2 or more than 0.03*600*600=10800 mm^2. No.35 bars were

chosen. A23.3Cl. 21.6.3.2 limits the center-to-center spacing of column bars to the larger of 200 mm or one-third of the core dimension in that direction. Eight bars, three in each face, are satisfied this clause.

First and second floors: section 600*600 mm, 12No.30, A_{st} = 8400 mm^2, ρ= 8400/(600*600)=0.023

γ=h-2d_c / h= 600-2*56.25/600=0.81 $\Rightarrow$ γ=0.8

L.C#2 at 1st floor (600*600)

P_r/ A_g= 1029.2*10^3/(600*600)=2.8 $\Rightarrow$ M_{rc}=3.87*600^3=836 KN-m

L.C#3 at 1st floor

Same results as L.C#2

Spacing of ties: The minimum ties spacing is the smallest of :

- 16*35.7=571
- 48*11=528
- 600

Take s=500mm thus the final design is 8NO.35 with No.10@500

Third floor (500*500)

L.C#2 at 3rd floor

Try 8No.35, A_{st}=8000, γ=0.76, ρ=0.032

P_r/ A_g= 582.6*10^3/(500*500)=2.33 $\Rightarrow$ M_{rc}=4.5*500^3=562.5 KN-m

L.C#3 at 3rd floor

Try 8No.35, A_{st}=8000, γ=0.76, ρ=0.032

P_r/ A_g= 662.2*10^3/(500*500)=2.65 $\Rightarrow$ M_{rc}=4.5*500^3=562.5 KN-m

Forth and fifth floors (500*500)

L.C#3 at 4th & 5th floors

Try 8No.30, As_t=5600, γ=0.78, ρ=0.022

P_r/ A_g= 430*10^3/(500*500)=1.72$\Rightarrow$ M_{rc}=3.34*500^3=417.5 KN-m

Summery of column design:

- 1st and 2nd floors use section 600*600 with 12 No 30
- 3rd floor use section 500*500 with 8 No 35
- 4th and 5th floors use section 500*500 with 8 No 30

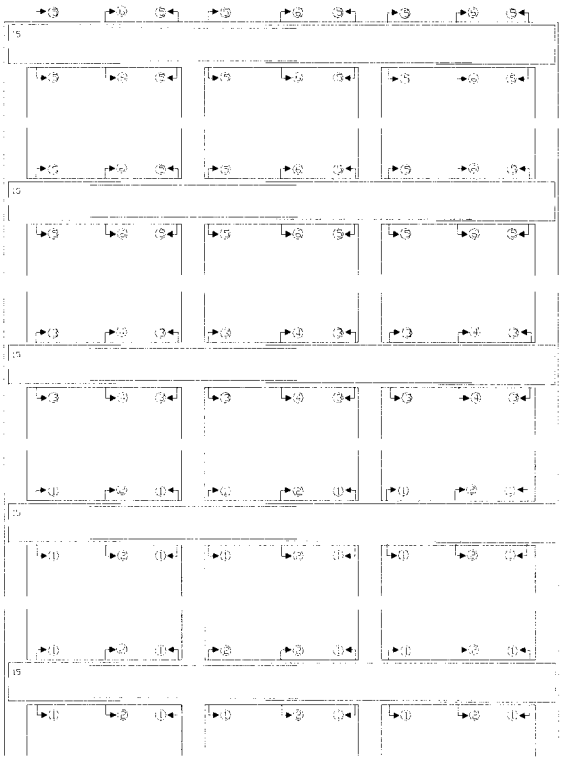

Figure A.2-Elevation of beam, longitudinal reinforcement (nominal ductile frame)

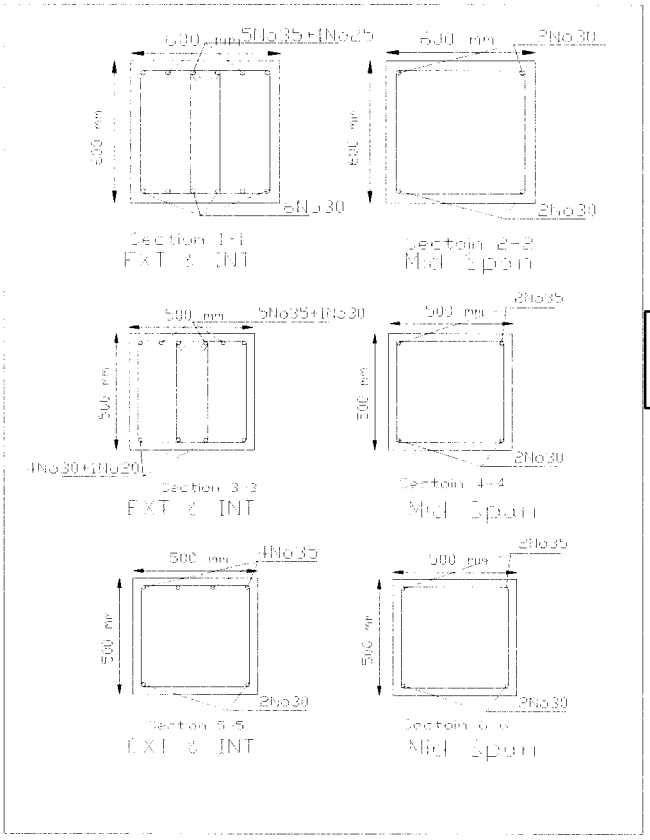

Figure A.3 Cross section of beams (nominal ductile frame)

A.6. Design of Frame-B as a Ductile Frame:

In the preliminary design of building, it has been decided to use 600*600 mm columns in first floor and 550*550 in third through 5th floor as shown in figure A.4 .The beam were chosen to have the same width as the columns not only to simplify the forming but also to improve the confinement of the beam-column joints.

Factored moments, including earthquake effects from an elastic frame analysis by sap2000, are given in table A.6 using the sign convention that positive moments cause compression in top fiber.

According NBCC1995 Load combination including earthquake shall be as follow

- 1.25D + 1.5L
- 1.0D ± ϒ(1.0) E
- 1.0D + ϒ(1.5L ±1.0 E)

Table A.7 Moments From as Elastic Analysis of Ductile Frame

(a) First floor

Moment	Sp1-3	Sp1-3	Sp1-3	Sp3-5	Sp3-5	Sp3-5	Sp5-7	Sp5-7	Sp5-7
L.C	Ext.M	Mid S	Int.M	Int.M	Mid S	Int.M	Int.M	Mid S.	Ext.M
L.C#1	-110.9	195.8	-197.7	-195	184.8	-197.3	-197.3	195.8	-111.2
L.C#2									
Sway R	+257.2		-437.9	+189.0		-412.4	+209.2		-449.3
Sway L	-452.8		+211.5	-412.7		+188.7	-435.6		+253.7
L.C#3									
Sway R	+241.4		-456.6	170.6		-430.5	+190.6		-465.2
Sway L	-468.6		+192.7	-431.1		+170.5	-454.2		+237.8

(b) Second floor

Moment	Sp1-3	Sp1-3	Sp1-3	Sp3-5	Sp3-5	Sp3-5	Sp5-7	Sp5-7	Sp5-7
L.C	Ext.M	Mid S	Int.M	Int.M	Mid S	Int.M	Int.M	Mid S.	Ext.M
L.C#1	-192.9	191	-193.4	-193.4	186.9	-193.4	-197.3	191	-193.6
L.C#2									
Sway R	+176.2		-378	+160.6		-381.5	+165.8		-395.8
Sway L	-399.1		+168.1	-381.9		+160.2	-375.8		+172.9
L.C#3									
Sway R	+158.3		-395.6	142.2		-399.3	+148.5		-413.9
Sway L	-417		+150.5	-400.2		+142.3	-393.1		+154.8

(c) Third floor

Moment	Sp1-3	Sp1-3	Sp1-3	Sp3-5	Sp3-5	Sp3-5	Sp5-7	Sp5-7	Sp5-7
L.C	Ext.M	Mid S	Int.M	Int.M	Mid S	Int.M	Int.M	Mid S.	Ext.M
L.C#1	-198.6	192.2	-194.4	-194.4	185.7	-194.4	-194.4	192.5	-199.1
L.C#2									
Sway R	+117.7		-310.6	+108		-322.6	+165.8		-336.3
Sway L	-339.4		+111	-323		+107.6	-375.8		+115.9
L.C#3									
Sway R	+134.4		-327.5	123		-340.7	+148.5		-354.7
Sway L	-357.7		+120.4	-341.5		+122.9	-393.1		+134.4

(d) 4th and 5th floors

Moment	Sp1-3	Sp1-3	Sp1-3	Sp3-5	Sp3-5	Sp3-5	Sp5-7	Sp5-7	Sp5-7
L.C	Ext.M	Mid S	Int.M	Int.M	Mid S	Int.M	Int.M	Mid S.	Ext.M
L.C#1	-205.1	192.2	-194.5	-194.5	188.6	-194.5	-194.5	205.7	-208.2
L.C#2									
Sway R	+111.2		-231.7	+106.2		-252.9	+103.6		-259.4
Sway L	-261		+1103.3	-253.1		+106	-230.7		+110.86
L.C#3									
Sway R	+129.8		-248.6	124.8		-269.5	+121.8		-279
Sway L	-279.6		+122	-272.1		+124.6	-247.6		+129.1

Checking of satisfactory of the definition of a ductile flexural member

- According A23.3 CI. 21.3.1 factored compression force should be less than $0.1A_g f'_c$ there is no axial loads thus it is satisfactory.
- Clear span not less than 4 times the effective depth. $L_n/d = 6000/545 = 11$ thus it is satisfactory.
- Width not less than 250 mm and no more than the width of the column plus 3/4d on each side of column thus it is satisfactory.

Thus, the beam satisfies the requirements of a beam. If it did not, it would be necessary to change the dimensions of the beam or design it in accordance with A23.3 Cl. 21.8 to resist greater earthquake load effects.

Calculate the Steel Required for Flexure at First Floor (600*600):

Minimum reinforcement for flexural reinforcement $=1.4b_w d/ f_y = 1145$ mm^2

Interior support-negative moment:

Maximum negative moment = -456.6 KN-m

$A_S = M_f /(\varphi_s f_y j d) = 456.6*10^6/(0.85*400*0.85*545) = 2899$ mm^2

J=0.85

Limits of the diameter of bars passing through a Joint (A23.3 CI. 21.6.5.6)

$d_b \leq \lambda(l_j / 24)$

Where $\mathbf{l_j}$ is the width of the joint parallel to the beam or column bars = 600 mm. Thus

$d_b \leq 1.0*600 / 24 = 25$mm (The largest bars we can use are No.25)

According A23.3 CI. 21.4.2.2 the slab bars parallel to the beam, lying within 3 times the slab thickness on each side of the web as part of the negative moment steel when calculating M_r .The slab steel parallel to the beam stem will be shrinkage and temperature steel. Typically this would be a No.10 bar at 300 mm on centers. If so, there would be 1No.10 bar within $3h_s$ on each side of the beam with total area= 2 *100 mm^2 .We require *2899 -200 = 2699* mm^2 additional steel. Try 5 No.25 plus 2No.10 bars of slab. These fit into the width of the beam. Total A_s including the slab bars = 2900 mm^2. This exceeds $As_{min} = 1145$ mm^2-oK

$a= (\varphi_s A_s f_y)/\alpha_1\varphi_c f'_c b= 0.85*2700*400/(0.805*0.6*35*600)=90.5$ mm

$M_{r=}\varphi_s A_s f_y(d-a/2)= 0.85*2700*400(545-94.5/2)=458.6$ KN-m> M_f=456.6 O.K

It is important not to over design these sections

A23.3 CI. 21.3.2.1 limits $\rho< 0.025$ in this section $\rho= 2700/(600*545)=0.0083 < 0.025$

Check if the steel yields: a/d = 90.5/545 = 0.17 and according A23.3 CI. 10.5.2, the steel will yield if $c/d\leq 700/(700+f_y)$ Substituting $c = a/\beta_1$ where $\beta_1= 0.895$, the steel will yield if $a/d\leq 700\beta_1/(700+f_y)=0.57$

Since a / d is less than this, the steel yields at failure.

- Use 5No.25 plus 2 No.10 top slab bars at the interior support.

Interior support-Positive moment:

From Table A.7, the maximum Positive moment from a frame analysis was 257.2 KN-m, but A23.3 CI. 21.3.2.2 requires that the positive moment capacity at the face of the joint not be less than 0.5 times negative moment capacity = ½*452.8=226.4 KN-m. Therefore, design moment is 257.2 KN-m

From A23.3 Cl 10.3.3, the effective width of the top flange is 1940 mm.

Try 5 No.20 bars, A., = 1500 mm2, Mr = 273 > 257.2 KN-m

Exterior Support-Negative Moment:

Maximum negative moment = -468.6 KN-m Following from the amount of steel required at the interior negative moment, we will need about 2500 mm^2. Assume that the temperature reinforcement in the slab accounts for 200 mm^2. Try 5 No.25, as including the slab steel = 2700 mm^2. Mr = -459 KN-m, assume OK. As satisfies the minimums.

Exterior support-Positive moment:

Maximum positive moment = +257.2 KN-m but not less than 0.5 times Mr for the negative moment steel chosen = 0.5 *459= 229.5 KN-m.

Use 5 No.20 bars, A_S = 1500 mm^2, Mr = 273 KN-m OK.

Mid span-Positive moment:

Maximum positive moment at mid span = 195.8 KN-m but not less than one quarter of the maximum moment resistance provided at either end of the beam =

0.25 *459=114.7kN.m.

A_s should not be less than the minimum = 1145 mm2. Try 4 No.20 bars, A_s = 1200 mm^2, Mr = 219 KN-m > M_f=195.8

Minimum Positive and Negative Moment Capacities

A23.3 Cl. 21.3.2.2 requires that the minimum positive and negative moment capacities at any section along the beam not be less than 0.25 times the maximum negative moment capacity provided at either joint. Four No.20 bars are adequate as minimum steel.

Calculate the Steel Required for Flexure at Second Floor (600*600):

Interior support-negative moment:

- Maximum negative moment = -400.2 KN-m

Try 4 No.25, plus1No.10, plus 2 No.10 slab bars, A_s=2300 mm^2, M_r=397 KN-m, O.K

Exterior and Interior support-Positive moment:

From Table 7.b, the maximum Positive moment from a frame analysis was 168.1 KN-m, but A23.3 CI. 21.3.2.2 requires that the positive moment capacity at the face of the joint not be less than 0.5 times negative moment capacity = ½*397 =198.5 KN-m. Therefore, design moment is 198.5 KN-m. Try 4No.20, A_s=1200, M_r=214.5, O.K

Exterior support-negative moment:

Maximum negative moment = -417 KN-m

Try 4 No.25+1No.15, A_s=2400 mm^2, M_r=412.7 KN-m, Satisfactory

Mid span:

Maximum positive moment at mid span = 191 KN-m but not less than one quarter of the maximum moment resistance provided at either end of the beam = 0.25*417=101 kN.m.

A_s should not be less than the minimum = 1145 mm2. Try 4 No.20 bars, A_s = 1200 mm^2, Mr = 219 KN-m > M_f=191

Calculate the Steel Required for Flexure at Third Floor (500*500 mm):

Exterior and Interior support-negative moment:

Maximum negative moment = -340.7 KN-m

Try 4 No.25, plus 2 No.10 slab bars, A_s = 2200 mm^2, M_r = 343.2 KN-m OK.

Exterior and Interior support-Positive moment:

From Table 8-3, the maximum Positive moment from a frame analysis was 134.4 KN-m, but A23.3 CI. 21.3.2.2 requires that the positive moment capacity at the face of the joint not be less than 0.5 times negative moment capacity = ½*340.7 =170.3 KN-m. Therefore, design moment is 170.3 KN-m.

Minimum reinforcement for flexural reinforcement =1.4b_wd/ f_y =960.6 mm^2

Try 2No.25, A_s=1000, M_r=163.5, Satisfactory

Mid span -Positive moment:

Try 2 No.25 plus 1 No.20 bars, A_s = 1300 mm^2, Mr = 210 KN-m > M_f=192.5

Calculate the Steel Required for Flexure at 4^{th} and 5^{th} Floor (500*500 mm):

Exterior and Interior support-negative moment:

- Maximum negative moment = -279.6 KN-m

Try 3 No.25, plus 2 No.10 slab bars, A_s = 1700 mm^2, M_r = 270.4 KN-m Satisfactory

Exterior and Interior support-Positive moment:

From Table 8-4, the maximum Positive moment from a frame analysis was 129.8 KN-m, but A23.3 CI. 21.3.2.2 requires that the positive moment capacity at the face of the joint not be less than 0.5 times negative moment capacity = ½*270.4 =135.2 KN-m. Therefore, design moment is 135.2 KN-m.

Minimum reinforcement for flexural reinforcement =$1.4b_wd/ f_y$ =960.6 mm^2

Try 2No.25, A_s=1000, M_r=163.5, Satisfactory

Mid span:

Maximum Positive moment= 205.7

Try 2 No.25 plus 1 No.20 bars, A_s = 1300 mm^2, Mr = 210KN-m > M_f=205.7

Compute the probable moment capacities, M p

In shear design of the shear assume that in the plastic hinges form at each end of the beam with the reinforcement stressed to 1.25fy and $\varphi_s = \varphi_c = 1.0$ thus:

At interior and exterior negative moment, A_s=2700 mm^2, M_r=459 KN-m we can compute probable moment as follow:

a_p=1*2700*1.25*400/(0.805*1*35*600)=79.8

M_p=1.0*2700*1.2*400*(545-79.8/2)=681.9KN-m

Same calculations repeated for other sections and results are shown in Table A.8

Table A.8 Summery of designed sections and reinforcement of beams (ductile frame)

Story	Beams	Sec.	Reinforcements	A_s	$\rho*10^{-3}$	M_r	M_f	M_p
1st	Int & Ext Supports(-ve)	600*600	5No25@top	2700	8.2	459	468.6	681.9
	Int & Ext Supports(+ve)	600*600	5No20@bot	1500	4.6	273	257.2	392.1
	Mid Span	600*600	4No20@bot	1200	3.7	219	195.8	
2nd	Int Supports(-ve)	600*600	4No25+1NO10@TOP	2300	7	397	400.2	587.6
	ExtSupports(-ve)	600*600	4No25+1NO15@TOP	2400	7.3	412.7	417	611.4
	Int & Ext Supports(+ve)	600*600	4No20@bot	1200	3.7	214.5	198.5	316.3
	Mid Span	600*600	4No20@bot	1200	3.7	219		
3rd	Int & Ext Supports(-ve)	500*500	5No25@top	2700	1.2	359.7	340.7	537.5
	Int & Ext Supports(+ve)	500*500	4No20@bot	1200	5.4	172.1	170.3	254.9
	Mid Span	500*500	5No20@bot	1500	6.7	212.1	1500	
4rh 5th	Int & Ext Supports(-ve)	500*500	3No25+1NO20@TOP	2000	8.9	276	279	410.6
	Int & Ext Supports(+ve)	500*500	2No25@bot	1000	4.5	144.8	135.2	214.2
	Mid Span	500*500	3No25@bot	1500	6.7	212	210	

A.7 Designs of Beams for Shear

Stirrups for shear in hinging region:

Cl. 21.7.3.1 require that V_c shall be taken equal to zero within a distance of equal to 2d = 1090 mm from the face of the columns. Outside this region V_c is given by

$V_c = 0.2\lambda\varphi_c\sqrt{f'_c}b_w d$. Because a major portion of the beam shear results from plastic hinges in the beam, we take the critical section for shear at the face of the column rather than d from the face of column.

Maximum shear (Exterior end)= 229.3 KN. Since $V_c = 0$, Vs = 229.3 KN

$V_{smax} = 0.8\lambda\varphi_c\sqrt{f'_c}b_w d = 0.8*1*0.6*\sqrt{35}*600*545*10^{-3}=928.6>229.3$ OK

$Vs=(\varphi_s A_v f_y d)/s \Rightarrow A_v/s=229.3*10^3/(0.85*400*545)=1.237\ mm^2/mm$

Try No.10 four leg stirrups $\Rightarrow$ Av = 400 mm^2 and s = 323 mm use No.10 four leg stirrups@300mm

Stirrups for shear in regions out of the hinges

$Vc = 0.2\lambda\varphi_c\sqrt{f'_c}b_w d = 0.2*1*0.6*\sqrt{35}*600*545*10^{-3}=232.1$ KN

Maximum shear at 2d away from external end < V_c and $V_f < 0.1\lambda\varphi_c\sqrt{f'_c}b_w d=686.7$ thus stirrups are only required to satisfy maximum spacing requirements and minimum stirrups (Cl. 11.2.8.4)

Maximum stirrup spacing is less of 600mm or 0.7d=381mm. The final spacing will be chosen to satisfy both shear and confinement. Use No10@380mm

Hoops for confinement

Cl.21.3.3.2 states hoops over a distance of 2d = 1090 mm from face of columns.

Every corner and alternate longitudinal bars must be at the corner of a stirrup in according Cl. 7.6.5.5.

Cl. 21.3.3.3 requires the first hoop at not more than 50 mm from the face of the column and a maximum spacing of hoops:

- d/4 = 545/4 = 136 mm
- 8 * smallest longitudinal bar diameter = 8 * 15 mm = 120 mm
- 24 * diameter of hoop bars = 24 * 10 = 240 mm for No.10 hoops
- 300 mm

Summery

Place first No.10, 4-leg hoop at 50 mm from face of columns at each end, plus 9 at 120, till L= 1100mm

A.8 Cutoff Points for Flexural Reinforcement

The bar cutoffs are calculated assuming the ends of the beam are hinging at $\pm M_p$ and the moment at the cutoff point is M_r for the bars remaining after the cutoff point.

Negative moment steel-interior support

There are 5 No.25 top bars for negative moment at the interior support. We will cut off 2 No.25 bars, and lap splice the remaining 3 No.25 bars. For the remaining 3No+ 2 No.10

slab bars at the first cutoff, M_r = 265.1 KN-m therefore the bars will be cutoff when the moment is 265.1 KN-m

$\Sigma M_o = 0 = 216.4*x-681.9+265.1=0$ this equation gives x=1.9m

Cl. 12.10.3 requires that the bars extend the larger of d = 545 mm or $12d_b$ =300 mm past this point. Therefore, we could cut off 2 No.25 at 1900 =545=2445 mm from the face of the interior column. The cutoff bars must extend id from the face of the column where, for No.25 top bars

$L_d=(0.45k_1k_2k_3k_4\ fy)/\sqrt{f'_c}= 0.45 * 1.3 * 1.0 * 1.0 * 1.0 * 400/\sqrt{35} *25=989$ mm

Since 2450mm exceeds 989 mm--0K.

Cut off 2 No.25 top bars at 2450 mm from the face of the interior column.

Extra stirrups requirements at the cutoff point unless the shear at the cutoff point is less than or equal to 2/3 of the shear capacity at the cutoff. (Cl. 12.10.5)

At the cutoff the stirrups are No.10 @300 mm

$V_f< 2/3\ V_r = 2/3(V_s+V_c)= 148kN \Rightarrow 2/3Vr = 2/3(V_c + V_s) = 2/3(215 + 148) = 2/3(247+232.1)=319.4 >$ shear at the cutoff point Therefore, extra stirrups are not required.

A.9 Design the lap splices for the continuous top and bottom steel

Cl. 21.3.2.1 requires two "continuous" bars both on the top and the bottom the lap splices required will be at mid span for both the top and bottom steel.

Top steel:

Two No.25 bars plus 2 slab bars are lap spliced. The negative moment is low here and hence the steel stress is low therefore A23.3 Cl. 12.15.2 allows a Class A lap splice with the length of $\mathbf{l_d}$, where $\mathbf{l_d}$ for the No.25 top bars is 989 mm.

Provide a 1000mm lap splice enclosed by hoops at the smaller of

- d/4 = 545 /4 = 136mm, or 100 mm

Lap splice 2 No.25 plus 2 No.10 slab bars 1000 mm at mid-span. Provide No.10 three-leg closed hoops at 100 mm $^c/_c$ along the length of the lap splice.

Bottom steel:

Four No.20 bars are lap spliced near the point of maximum positive moment under gravity loads only.

A Class B lap splice with the length of $1.3l_d$ is required, where $1.3l_d = 1.3 * 486$ mm = 633 mm, take 700mm lap splice at or near mid-span also the hoops already are provided by the top bar splices.

A.10 Columns Design:

The floor-to-floor height is 4000mm at first floor with 600 mm deep beams in each floor. Giving a clear column height of 3200 mm. The column size and the floor-to-floor heights are 3000 mm in the other stories. The factored moments and axial loads from an elastic analysis for earthquake loads are given in Tables A-10-1 to A-10-4. The column has 40 mm cover to the ties.

Tables A.9 Summery of moments and axial loads (ductile frame)

(a) First floor

1st Story	Axial Load	Bottom Moment	Top Moment	Shear
L.C#1	1605	39	68.2	30
L.C#2				
Sway to Left	980.1	439.6	-303.8	200.9
Sway to Right	-976.6	-440.7	303.9	201.2
L.C#3				
Sway to Left	1104.7	439.5	-303.8	200.9
Sway to Right	1109.8	-440.8	303.9	201.3

(b) Second floor

2nd Story	Axial Load	Bottom Moment	Top Moment	Shear
L.C#1	1265.3	110.9	94.4	85.6
L.C#2				
Sway to Left	759.6	266.1	-284.1	229
Sway to Right	757.2	-264.6	285.2	228
L.C#3				
Sway to Left	865.2	266.5	-284	229.4
Sway to Right	863	-265.1	285.2	228.2

(c) Third floor

3rd Story	Axial Load	Bottom Moment	Top Moment	Shear
L.C#1	941.9	95.2	-98.9	80.9
L.C#2				
Sway to Left	567.4	201.4	-241.6	184.6
Sway to Right	566	-202.4	242.7	185.4
L.C#3				
Sway to Left	646.4	201.9	-241.6	184.8
Sway to Right	639.3	-203.1	243.1	139.7

(d) Forth & fifth floors

4^{th} & 5^{th} Stories	Axial Load	Bottom Moment	Top Moment	Shear
L.C#1	621	107.1	-169.5	115.3
L.C#2				
Sway to Left	375.6	140.5	-190.9	138.1
Sway to Right	375.2	-141.6	192.3	139.1
L.C#3				
Sway to Left	428.1	-141.6	192.3	185.9
Sway to Right	418.6	141.6	-193.6	140

Initial Selection of Steel Area

As a first trial we select a 600 mm by 600 mm column with 12 No.20 bars,

A_{st}=3600mm^2, ρ= 0.01 A23.3 Cl. 21.4.3.1 limits A_s, to not less than 0.01*600*600=3600 mm^2 or more than 0.03*600*600=10800 mm^2. No.20 bars were chosen to avoid excessive splice lengths. A23.3Cl. 21.6.3.2 limits the center-to-center spacing of column bars to the larger of 200 mm or one-third of the core dimension in that direction. Twelve bars, four in each face, are satisfied this clause.

A.10.1 Strong Column-Weak Beam:

1^{st} floor:

According Cl21.4.2.2 the flexural capacity of columns must exceed the flexural capacity of beams to satisfy $\sum M_{rc} \geq 1.1 \sum M_{nb}$

Where M_{rc} is the sum of the factored resistances, M_r, for the two columns meeting at a floor joint corresponding to the factored axial loads in the columns, and M_{nb} is the sum of the nominal resistances, M_n, of the beams framing into the joint in the direction parallel to the earthquake forces. For the frame swaying to the right and left, the moments M_{nb} at the ends of the beams meeting at the top of the column

At the interior column, the top steel in the beams at 1st floor is 5No.25 bars plus 2 No.10 shrinkage and temperature bars in the slab, $A_s = 2700\ mm^2$ and $M_n = 459$ KN-m

The bottom steel in the beams is 5No.20 bars, $A_s = 1500\ mm^2$ and $M_n = 273$ KN-m

$1.1\sum M_{nb} = 1.1*(459+273) = 805.2$ KN-m

Now the lowest value of M_{rc} should be 805.2 KN-m and to determine $\sum M_{rc}$ we need to calculate the factored moment resistance of column above and below the beam-column joint. The lowest flexure resistance will occur at the highest or lowest axial load, thus the load combination 2 and 3 need to be checked. (Load combination 1 does not involved lateral load)

2nd floor:

The top steel in the beams is 4No.25 plus 1No.10 bars plus 2 No.10 shrinkage and temperature bars in the slab, $A_s = 2300\ mm^2$ and $M_n = 397$ KN-m

The bottom steel in the beams is 4No.20 bars, $A_s = 1200\ mm^2$ and $M_n = 214.5$ KN-m

$1.1\sum M_{nb} = 1.1*(397+214.5) = 672.6$ KN-m

3rd floor:

The top steel in the beams is 5No.25 plus 2 No.10 shrinkage and temperature bars in the slab, $A_s = 2700\ mm^2$ and $M_n = 359.7$ KN-m

The bottom steel in the beams is 4No.20 bars, $A_s = 1200\ mm^2$ and $M_n = 172.1$ KN-m

$1.1M_{nb} = 1.1*(359.7+172.1) = 585$ KN-m

4th & 5th floors:

The top steel in the beams is 3No.25 plus 1 No.20 plus 2 No.10 shrinkage and temperature bars in the slab, $A_s = 2000\ mm^2$ and $M_n = 276$ KN-m

The bottom steel in the beams is 2No.25 bars, $A_s = 1000\ mm^2$ and $M_n = 144.8$ KN-m

$1.1M_{nb} = 1.1*(276+144.8) = 462.9$ KN-m

Design of reinforcement in the column:

Check the satisfy of the definition of a ductile frame member subjected to axial load

A23.3 Cl. 21.4.1 lists requirements for a column, which is to be designed as a ductile frame member subjected to axial load under A23.3 Cl. 21.4:

- Column is part of the lateral force resisting system-QK
- Factored axial force exceeds $A_g f'_c/10 = 600 * 600 * 35/10 * 10^{-3} = 126$ KN O.K
- Shortest cross-sectional dimension not less than 300 mm OK

- Ratio of cross-sectional dimensions not less than O.4 OK
- Therefore, design the column according to A23.3 Cl. 21.4 satisfactory

First floor:

Section 600*600 mm, 12 No.20, A_{st} = 3600 mm^2, ρ= 3600/(600*600)=0.1

γ=h-2d_c / h= 600-2*61.05/600=0.8 $\Rightarrow$ γ=0.8

L.C#2 at 1st floor

P_r/ A_g= 980.1*10^3/(600*600)=2.72 $\Rightarrow$ M_{rc}=2.3*600^3=496.8 KN-m

Corresponding is M_{rc}=496.8 for both axial loads

L.C#3 at 1st floor

P_r/ A_g= 1109.8*10^3/(600*600)=3.1 $\Rightarrow$ M_{rc}=2.4*600^3=518.4 KN-m

Corresponding is M_{rc}=518.4 for both axial loads

Second floor:

L.C#2 at 2nd floor

P_r/ A_g= 759.6*10^3/(600*600)=2.15 $\Rightarrow$ M_{rc}=2.15*600^3=496.8 KN-m

Corresponding is M_{rc}=496.8 for both axial loads

L.C#3 at 2nd floor

P_r/ A_g= 865.2*10^3/(600*600)=2.4 $\Rightarrow$ M_{rc}=2.4*600^3=518.4 KN-m

Corresponding is M_{rc}=518.4 for both axial loads

L.C#2 at 2nd floor

P_r/ A_g= 759.6*10^3/(600*600)=2.1 $\Rightarrow$ M_{rc}=2.1*600^3=464.4 KN-m

Corresponding is M_{rc}=464.4 for both axial loads

Tables A.10 Summery of strong column-weak beam checking

Story	L.C.	$\sum M_{rc}$	$1.1\sum M_{nb}$	Check $\sum M_{rc} \geq 1.1\sum M_{nb}$
First	L.C#2 L.C#3	961.2 1015.2	805.2	O.K
Second	L.C#2 L.C#3	464.4+281.2=745.6 496.8+288=784.8	672.6	O.K
Third	L.C#2 L.C#3	281.2+281.2=562.4 288+288=576	585	Not Satisfactory
Forth & Fifth	L.C#2 L.C#3	281.2+281.2=562.4 288+288=576	462.9	O.K

The design of column at third floor is not satisfy code requirements thus the section changed as follow:

Try section 500*500 mm, 12 No.20, A_{st} = 3600 mm^2, ρ= 3600/(500*500)=0.015

Third floor

L.C#2 at 3rd floor

P_r / A_g= 567.4*10^3/(500*500)=2.3 $\Rightarrow$ M_{rc}=2.8*500^3=350 KN-m

L.C#3 at 3rd floor

P_r / A_g= 2.6 $\Rightarrow$ M_{rc}=2.875*500^3=359.4 KN-m

Column-Weak Beam check at third level:

$\sum M_{rc}$=281.2+350=631.2 $\geq$ 1.1$\sum M_{nb}$ =585 O.K.

$\sum M_{rc}$=288+359.4=647.4 $\geq$ 1.1$\sum M_{nb}$ =585

Summery of column design:

- 1st and 2nd floors use section 600*600 with 12 No 20
- 3rd floor use section 500*500 with 12 No 20
- 4th and 5th floors use section 500*500 with 8 No 20

A.11 Confinement Reinforcement Design

A23.3 Cl. 21.4.4.2(b) requires that the total cross-sectional area of hoop reinforcement not be less than the larger of:

$A_{sh}=0.3(s\ h_c\ f'_c/f_{yh})(A_g/A_{ch}-1)$

$A_{sh}=0.09(s\ h_c\ f'_c/\ f_{yh})$

Where h_c is the cross-sectional dimension of the core, measured from out-to-out of hoops, as hc = 600 -2 * 40 = 520mm (based on 50 mm cover to the vertical bars for a 3-hour fire resistance) and A_{ch} is the cross-sectional area of the core of the column, measured out-to-out of the transverse reinforcement as $A_{ch} = 520^2 = 270000mm^2$.

- A_{sh}/s =0.3(520*35/400)[600*600/(520*520)-1]=4.5 mm^2/mm
- A_{sh}/s =(0.09*520*35)/400=4.1 mm^2/mm

Thus, $A_{sh}/s = 4.5\ mm^2/mm$

Maximum hoop spacing

A23.3 CI. 21.4.4.3 sets the maximum hoop spacing as

(a) 0.25 times the minimum cross-sectional dimension = 0.25 * 600 = 150 mm

(b) 100 mm

(c) 6 times the diameter of the smallest longitudinal bar = 6 * 20 = 120 mm

S = 100 mm governs and No.10 hoops with 41egs in each direction as shown in

Fig.8 giving Ash = 400 mm^2 in each direction & $A_{sh}/s = 4.5 \Rightarrow S=90\ mm<100\ mm$

This layout satisfies A23.3 Cl. 21.4.4.4.

A23.3 Cl. 21.4.4.5 requires hoop reinforcement over a length L_o adjacent to each end of the column, where L_o is the larger:

(a) The depth of the member at the joint face = 600 mm,

(b) One sixth of the clear height of the column = 3200 /6 = 533 mm

(c) 450 mm

Thus, L_o = 600 mm governs. Throughout the rest of the height of the column, A23.3 Cl. 21.4.4.6 requires hoops at the smaller of

(a) 6 times the diameter of the longitudinal bars = 6 * 20 = 120 mm, or

(b) 150 mm

Use s = 120 mm for hoops located more than 600 mm from the ends of the column

Note: use same confinement reinforcement layout for columns in other floors

A.12 Shear Reinforcement Design of Columns:

A232.3Cl21.7.2.2 requires that column have a factored shear resistance that exceed the larger of

- Shear corresponding to probable moment resistance of beams, V_e, at each end of column
- Shear forces due to factored loads, V_f

$V_e = [\sum M_{pb,top} * k_c / \sum k_{c,top} + \sum M_{pb,bot} * k_c / \sum k_{c,bot}] / l_u$

Where k_c is the stiffness of the column equal to 4EI/l. The probable moment capacities of beams framing into the joint at top and bottom of the column are given in table 8. Since all the columns have the same stiffness then $k_c / \sum k_c = 0.5$

- $V_e = [(681.9+392.1)*0.5+(681.9+392.1)*0.5]/3.2 = 335.6$ KN
- $V_f = 201.3$

Therefore the design shear is $V_f = V_e = 335.6$ KN and according Cl.21.7.3.1 (b) V_c can be taken as 0.5 of the value of $V_c = 0.2 \lambda \varphi_c \sqrt{f'_c} b_w d = 1/2*0.2*1*0.6*\sqrt{0.35}*600*545*10^{-3} = 116.1$ KN therefore $V_s = V_f - V_c = 335.6 - 116.1 = 219.5$ KN

$A_v/s = V_s/(\varphi_s f_y d) = 219.5*10^3/(0.85*400*545) = 1.18$ mm^2/mm

Within the length l_o, hoops are placed at a spacing of 90mm in other hand requirement for shear is $A_v/s = 1.18$ mm^2/mm $\Rightarrow A_v/90 = 1.18$ mm^2/mm

$\Rightarrow A_{v)req.} = 106.2$ mm^2 but the hoops for confinement have $A_{v)conf.} = 400$ mm^2 and this is greater than $A_{v)shear.} = 106.2$ mm^2 therefore confinement hoops are satisfy shear reinforcement.

Outside of the lengths l_o, V_c is computed as $V_c = 0.2*1*0.6*\sqrt{35}*600*545 = 236$ KN and s=120 (specified for hooks at this region)

$A_v/s = V_s/(\varphi_s f_y d) \Rightarrow A_v/120 = (335.6-236)*10^3/(0.9*400*545) = 0.508 \Rightarrow A_v = 60.92$ mm^2

Since the hoops are provided more than this therefore the section is adequate for shear at this region

Final results: Provide 4 legs of No.10 hoops as shown in fig.8 at 45mm from end of column, and provide 4 legs of No.10 hoops at 120mm $^c/_c$ over rest of height of column. For the first floor the spacing would be s=100mm according Cl.21.4.4.7 over its full height also hoops shall extend at least 300mm into the footing.

A.13 Design Lap Splices For The Column Bars:

Cl.21.4.3.2 requires that splices be in the middle of column and should be design as tension splices. For No.20 bars we have:

$L_d=0.45*k_1\ k_2\ k_3\ k_4\ f_y/\sqrt{f'_c}\ d_b=0.45*1*1*1*1*0.8*400/\sqrt{35}*20=487$ mm

Since all the bars are spliced at the same location according Cl.12.15.2 splice has a length of 1.3 l_d =1.3*487=633 and the effective area of ties throughout the splice length is greater than 0.0015 h*s=0.0015*600*120=108 mm^2, the lap length can reduce by 83% (Cl12.17.3.4). Therefore the lap length=0.83*633=525mm. Take as 550mm

Final Results: Lap splice all vertical bars with a 550mm lap splice at mid height of column.

A.14 Design of an Interior Beam-Column Joint

Beams are 600 mm by 600 mm in section, frame into the 600 mm by 600 mm column on all four sides.

Define size of joint:

The joint has width, depth and vertical height of 600 mm. The area of a horizontal section through the joint, A_j, according A23.3 Cl. 21.0 is A_j = 600 x 600 =360000 mm^2.

Cl. 21.6.5.6 requires the diameter of bars passing through the joint to satisfy

$d_b \leq l_j$ / 24= 1*600/24=25mm, The largest bars in the column and beams are No.20 and No.25 -OK.

Transverse reinforcement for confinement:

A23.3 Cl. 21.6.2.1 requires confinement steel within the joint. Because the joint has beams on all four sides A23.3 Cl. 21.6.2.2 sets the amount of confinement steel as half of the confinement steel required in the ends of the columns

Confinement steel in the ends of the columns, A_{sh}/S = 4.6 thus confinement steel within the height of the joint, we require A_{sh}/S = 0.5 *4.6 = 2.3 mm^2/mm

The vertical spacing of the hoops (A23.3 Cl. 21.4.4.3) is the smaller of

- 0.25* the least dimension of Aj = 0.25 * 600 = 150mm
- 150 mm
- 6 * the diameter of the smallest column bar = 6 * 20 = 120 mm

The spacing of the hoops may not exceed 120 mm. The clear distance between the top and bottom beam steel is 480 mm. Provide 4 sets of hoops, the first at 75 mm below the

top steel and the rest spaced at 110mm. The required A_{sh} = 110 * 2.3 = 253mm^2. UseNo.10three-legged hoops (having A_{sh} = 300 mm2) crossties are provided in both directions because the earthquake can occur in either direction.

Compute shears on joint and check the shear strength :

The maximum probable moment capacities of beams are 681.9 KN-m and 392.1 KN-m At the joint the stiff nesses of the columns above and below the joint are the same, giving distribution factors of D F = 0.5 for each column. Thus the moment in the column over the joint is M_e = 0.5(381.9+392.1) = 537 KN-m

The shear in the column over the joint is V_e=(537+537)/3.2=336

The force in the steel in the beam on the left of the joint is

$T_1 = 1.25As/f_y = 1.25 * 2700 * 400 = 1350$ KN

The compression force in the beam to the left is $C_1 = T_1 = 1350$ KN

Similarly T_2 and C_2 in the beam = 1.25 1500*400*10^{-3} *400 = 750 KN

By summing horizontal forces we get the shear in the joint as $V_j = V_e - T_1 - C_2$ = 336-1350-750=-1764(to left)= 1764(to right)

The nominal shear strength of a joint confined on all four sides is (Cl. 21.6.4.1)

$V_r = 2.4\lambda\varphi_c\sqrt{f'_c} = 2.4* 1*0.6*\sqrt{35}*360000*10^{-3}$=3067 KN (Therefore the joint has adequate shear strength)

Summary

Provide 4 sets of No.10 three leg hoops at 110 mm $^c/_c$ in the joint

A.16 Conclusion:

A step-by-step description of design procedures for structural systems in which, fixed base ductile and nominal ductile frame is presented. The columns longitudinal reinforcement, however, are very different for both structures. The flexural strength of the columns for the ductile frame (R = 4) is based on the flexural capacity of the associated framing beams according to the weak beams - strong columns design philosophy adopted by the Canadian Concrete Standard (CSA 1994). The columns of the frame with nominal ductility (R = 2) were designed only to resist the factored loads. The transverse reinforcement is also quite different for each structure. The ductile structure incorporates full seismic details, composed of rectangular hoops, with 135 hooks, smaller spaces in critical locations of the beams, columns, and joints. The spacing of the hoops in

the structure with nominal ductility is larger in the columns and the beams, except in the beams near the column faces where the spacing is reduced, according to the provisions of the (CSA 1994). One important aspect of the design of beam-column joints is the development length of the longitudinal reinforcement required to ensure plastic hinges in the beams at the column faces. This aspect is particularly important for interior beam column joints where plastic hinges can develop in opposite directions on each side of the columns. The longitudinal reinforcement is therefore required to develop simultaneously its probable tensile strength on one side of the joint and its probable compressive strength on the other side of the joint.

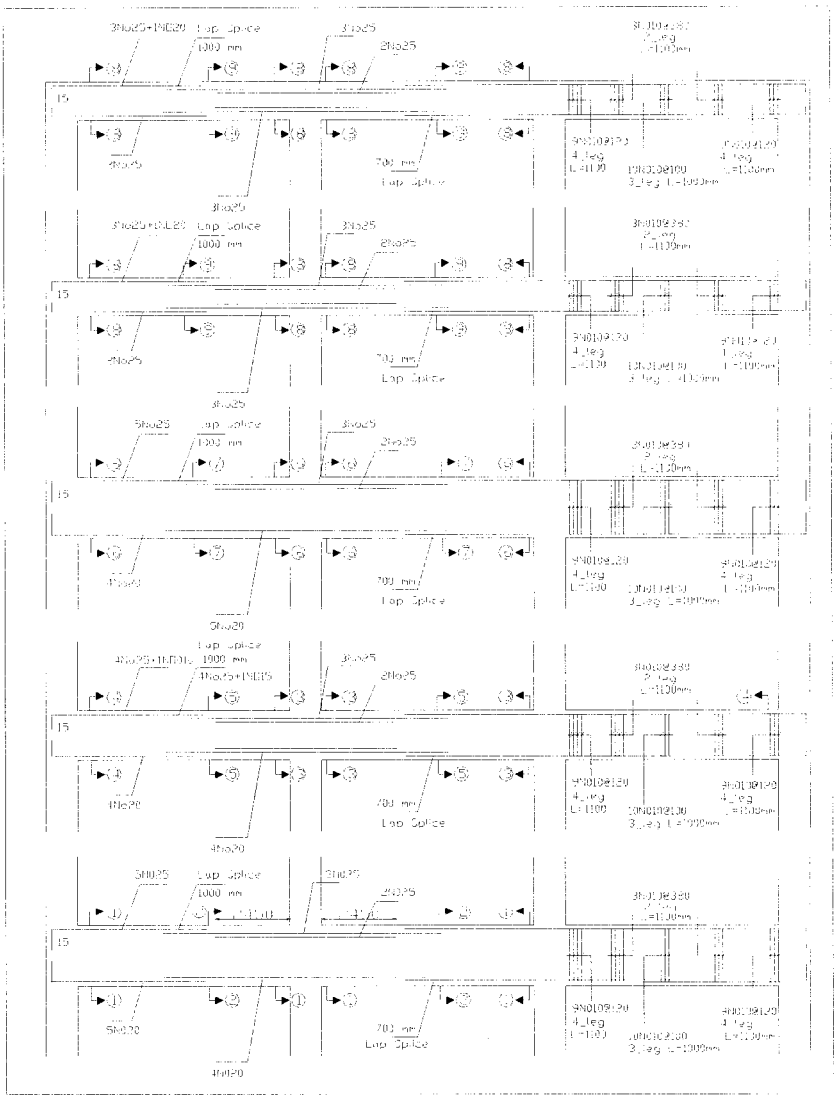

Fig A.4 Elevation of beam, longitudinal reinforcement (ductile frame)

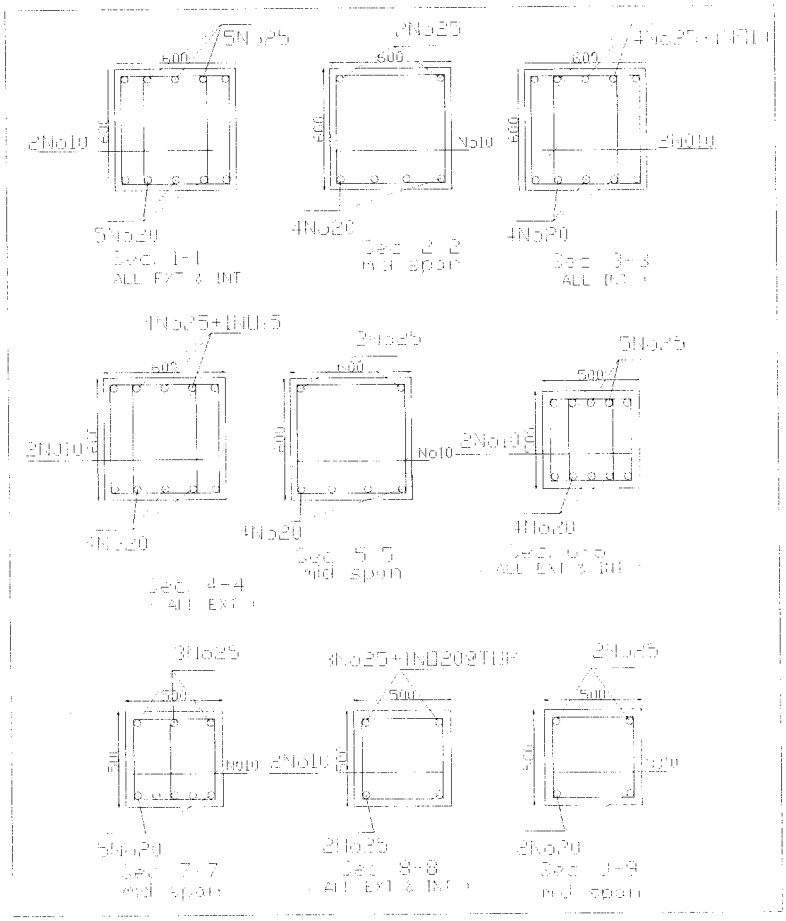

Figure A.5 Cross section of beams (ductile frame)

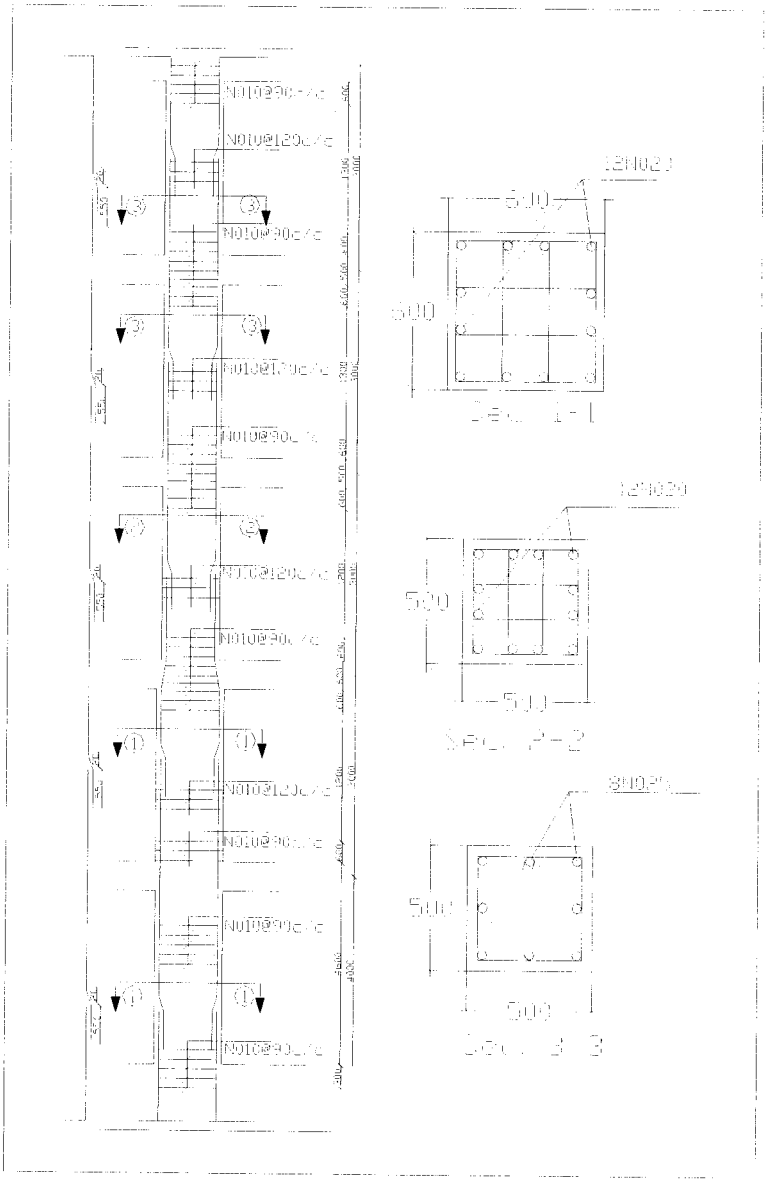

Fig A.6 Elevation and longitudinal reinforcement of typical column (ductile frame)

A.17 Design of GLD Frame

The GLD building is a 5-story concrete frame building that plan dimensions are equal to 22m in the east-west direction and 18m in the north-south direction. The height of the building, from grade level to the roof, is equal to 16 m. A plan view of the building showed in figure 3.3.1. The floor framing consists of 120mm thick concrete slabs. The gravity load resisting columns are fixed on foundations. The geometry of structure is assumed same as other cases of study.

A.17.1 Determination of lateral wind Loads

Lateral (wind) loads were calculated and applied on the GLD building frame. For wind load calculations, the frame is assumed to be located in a Sandspit-BC with high-risk seismic zone (v= 0.4). The structural GLD frame was designed for a lateral (horizontal) wind pressure equal to 0.63 Kpa on the vertical surface of project.

According to NBCC the specified external pressure or suction due to wind on part or all of a surface of a building shall be calculated from

$$\mathbf{P = q\ C_e\ C_g\ Cp}$$

Where

P = the specified external pressure acting statically and in a direction normal to the surface either as a pressure directed towards the surface or as a suction directed away from the surface,

q = the reference velocity pressure as provided in NBCC

Maximum wind pressure for Sandspit-BC with V=0.4 is equal to q=0.63 Kpa for (1/30 strength)

C_e = the exposure factor

C_g = the gust effect

C_p = the external pressure coefficient averaged over the area of the surface considered.

The net wind load for the building as a whole shall be the algebraic difference of the loads on the windward and the leeward surfaces, and in some cases may be calculated as the products of the external pressures or suctions and the areas of the surfaces over

$C_e=(H/2/10)^{0.2}=(16/2/10)^{0.2}=0.956$ (down Stream)

$C_e=(h/10)^{0.2}\geq 0.9$ (Exposure)

According Figure 7 of NBCC, C_p (Leeward)=0.75, C_p (Windward)=-0.55 and C_g=2.00 has been chosen.

Table A.11 illustrates a summary of the manually calculated values for GLD frame

Table A.11 Manually calculated values of designed wind lateral loads on frame-B for GLD Frame

Floor	$h_{i(M)}$	Z, m	mid point	C_{ew}	P(z)	Total Force(kn)	Force(kn)
			16	1.098	1.7		
Roof		16				55.77	13.9
	3		14.5	1.077	1.68		
5		13				109.36	27.3
	3		11.5	1.028	1.634		
4		10				105.96	26.5
	3		8.5	0.968	1.577		
3		7				101.97	25.5
	3		5.5	0.9	1.513		
2		4				116.5	29.1
	4		2	0.9	1.513		
Grade		0					

Components were selected and checked for the following load combinations per the requirements of the ACI 318-63 Building Code:

1.4DL+ 1.7LL

0.75 (1.4DL+ 1.7LL + 1.7WL)

1.05DL+1.275WL

Where

D, L, and W are dead, live, and wind loads, respectively.

Figure A.7 illustrates the resulting load combinations for both dead, live and wind loads upon the one internal frame.

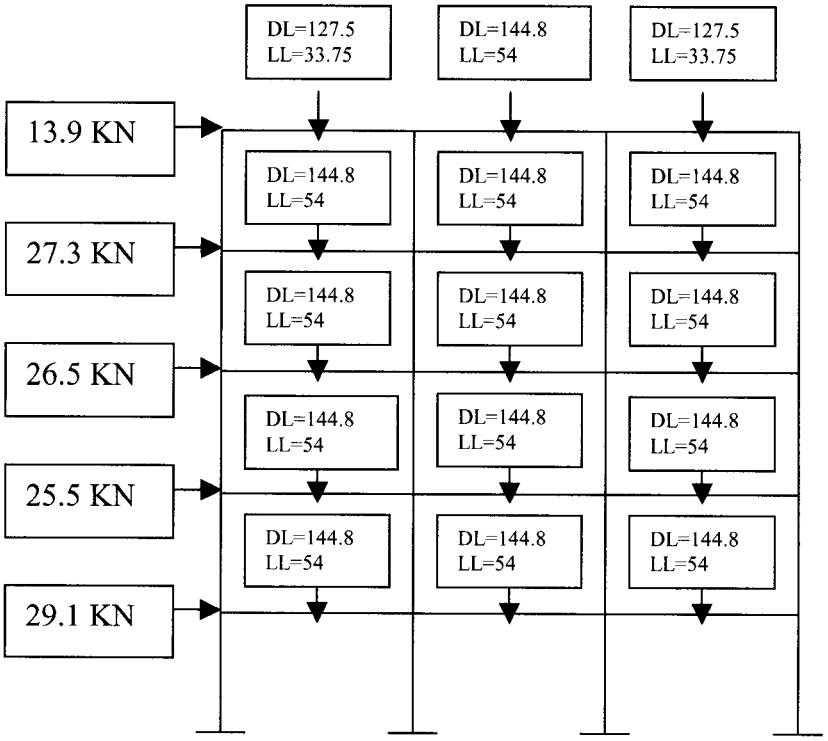

Figure A.7 load configurations of frame-B for GLD Frame

The building was established by modifying the size of beams and columns in moment-resisting frames in such a way that they comply with the minimum requirements of the 1963 Uniform Building Code. Beams and columns in moment-resisting frame were sized to resist wind and gravity-load effects only. For this proposes new sizes were established as shown in figures A.8 and A.9

Initial elastic analysis of structures is performed in order to determine the structural elements design forces. The finite element based, structural analysis program SAP2000 is used to perform element forces. Factored moments, including wind effects from an elastic frame analysis by sap2000, are given in Tables A.12

Table A.12 Maximum moments of beams from elastic analysis of GLD frame

Moment	Sp1-3	Sp1-3	Sp1-3	Sp3-5	Sp3-5	Sp3-5	Sp5-7	Sp5-7	Sp5-7
L.C	Ext.M	Mid S	Int.M	Int.M	Mid S	Int.M	Int.M	Mid S.	Ext.M
1st floor	-221.3	253	-263.8	-263.8	238	-263.3	-263.3	253	-221.3
2nd floor	-229.6	252.3	-256.1	-256.1	239.6	-256.1	-256.1	252.3	-229.6
3rd floor	-223.5	244.1	-246.1	-246.1	233	-246.1	-246.1	244.1	-223.5
4th floor	-231.8	243	240.4	-240.4	233.2	-240.4	-240.4	242.8	231.8
5thfloor	-152.6	203.7	-239.6	-239.6	239.3	-239.6	-239.6	203.7	-152.6

Calculate the steel required for flexure (interior Beams)

Minimum reinforcement for flexural reinforcement =1.4bwd/ fy =1135 mm2

Maximum negative moment = -249 KN-m

Maximum positive moment = 249.8 KN-m

Negative moment

F'_c=35 Mpa $\Rightarrow \beta_1$=0.8 and γ=0.85

Try section 250*450 with 4 No 25

Assumed the temperature reinforcement in slab as 200 mm^2 thus A_s=2200 mm^2

d=450-56.25=393.75 mm

$a=A_s f_y/(0.85 f'_c b)$=118.3 $\Rightarrow$ $M_u=\varphi A_s f_y(d-a/2)$= 0.9*2200*400(393.75-118.3/2)

M_u=265 KN-m > 249 KN-m o.k. Use section 250*450 with 4 No 25 top

Positive moment

Try section 250*4500 with 4 NO. 25 flexural bars (A_s=2000 mm^2) $\Rightarrow$ $M_u=\varphi A_s f_y(d-a/2)$

M_u=245 KN-m o.k. Try section 250*450 with 4 No 25 bot

$a=A_s f_y/(0.85 f'_c b)$= (2000*400)/(0.85*35*250)=107.6

Interior beams

Maximum negative moment (Ext.) = -187.2 KN-m

Try section 250*450 with 3 No 25 top (A_s=1800 mm^2)

$a=A_s f_y/(0.85 f'_c b)= (1800*400)/(0.85*35*250)=80.67 \Rightarrow M_{u=}=190.8$ KN-m > 249 KN-m

Use section 250*450 with 3 No 25 top

After cutoff point calculation the final flexural design is presented in figures A.8 and A.9

Table A.13 Summery of designed sections and reinforcement of beams (GLD)

Story	Beams	Sec.	Reinforcements	A_s	$\rho*10^{-3}$	M_r	M_f
All floors	Interior Supports(-ve)	250*450	4No25@top	2000	22	265	249
	Exterior Supports(-ve)	250*450	3No25@top	1500	18	190.8	187.2
	Mid Span	250*450	4No25@bot	2000	22	245	249

A.23 Columns Design:

The floor-to-floor height is 4000mm at first floor with 500 mm deep beams in each floor. Giving a clear column height of 3500 mm. The floor-to-floor heights are 3000 mm in the other stories. The factored moments and axial loads from an elastic analysis for gravity and wind loads are given in Tables A.13 The column has 40 mm cover to the ties.

Tables A.14 Summery of moments and axial loads in typical interior columns (GLD)

Interior Columns				Exterior Columns			
	L.C	Axial Force	Moment@bot	Moment@top	Axial Force	Moment@bot	Moment@top
1st floor	1	1661	1.97	-4.6	754.1	32.6	64.4
	2	1256.3	97	-78.4	501.7	109.87	-103.6
	3	910.8	96.5	-77.4	356.6	102.6	-89.3
2nd floor	1	1316.6	9.77	-7.9	591	-115.8	113.9
	2	993.4	63.8	-68.7	404.4	111.15	-120.4
	3	719.3	61.6	-66.9	291.2	85.4	-95
3rd floor	1	978.1.	3.7	-5.3	430.1	-73.3	82.3
	2	736.9	39.6	-45	302.1	78.6	-89.7
	3	538.8	38.8	-44	221.2	62.3	-71.5
4th floor	1	693.9	6.21	-5.24	275.6	-88	86
	2	480.6	27.4	-30	198.6	78.2	-82.2
	3	349.1	25.8	-28	149.3	58.3	-62.2
5th floor	1	303.1	3.86	-2.46	119.1	-92.2	103.3
	2	227.4	10.42	-12	87.5	71.8	-83.9
	3	167.3	11.5	-16.8	70.2	53	-66.1

Design of interior columns for first floor:

As a first trial we select a D_g= 350 mm circular column with 5No.25 bars,

A_{st}=2500mm^2, A_g= 96211.1 ρ= 2500/96211.3= 0.026

γ=h-2d_c / h= 350-2*53.9/350=0.7 $\Rightarrow\gamma$=0.7

Pr/ A_g= 1256*10^3/(350^2)=10.2 $\Rightarrow$ $M_{rc}/A_g h$=2.25 M_{rc}=2.25* 350^3=97 KN-m $\approx$97 KN-m

Use D_g= 350 mm circular column with 5No.25 bars

Spacing of ties:

The minimum ties spacing is the smallest of

- 16*29.9=478.4
- 48*6.35=304
- 350

Take s=300mm thus the final design is 5No.25 with #2 @300

Design of exterior columns for 1st and 2nd floors:

As a first trial we select a D_g= 350 mm circular column with 6No.20 bars,

A_{st}=1800mm^2, A_g= 96211.1 ρ= 1800/96211.3= 0.019

γ=h-2d_c / h= 350-2*53.9/350=0.7 $\Rightarrow\gamma$=0.7

For L.C.#2 Pr/ h^2= 591*10^3/(350^2)=4.8 $\Rightarrow$ M_{rc}/h^3=2.4 M_{rc}=2.4* 350^3=102.9≈115

For L.C.#3 Pr/ h^2= 404*10^3/(350^2)=3.3 $\Rightarrow$ M_{rc}/h^3=2.3 M_{rc}=2.4* 350^3=98.6≈111 ok

Use D_g= 350 mm circular column with 6No.20 bars

Design of interior columns at 2nd floor:

As a first trial we select a D_g= 300 mm circular column with 5No.25 bars,

A_{st}=2500mm^2, A_g= 70685.8 ρ= 1800/70685.8 = 0.035

γ=h-2d_c / h= 300-2*53.9/300=0.7 $\Rightarrow\gamma$=0.65

For L.C.#2 (γ=0.6) Pr/ h^2= 993.4*10^3/(300^2)=11 $\Rightarrow$ M_{rc}/h^3=2.4

(γ=0.7) Pr/ h^2= 993.4*10^3/(300^2)=11 $\Rightarrow$ M_{rc}/h^3=2.6 $\Rightarrow$ M_{rc}/h^3=2.5 (γ=0.75)

M_{rc}=2.5* 300^3=667.5≈68.7

For L.C.#3 Pr/ h^2= 719.3*10^3/(300^2)=8 $\Rightarrow$ M_{rc}/h^3=2.65 M_{rc}=2.4* 300^3=71.5>66.9 ok

Use D_g= 300 mm circular column with 5No.25 bars

Design of interior columns for 3rd floor:

As a first trial we select a D_g= 300 mm circular column with 5No.20 bars,

A_{st}=1500mm^2, A_g= 70685.8 ρ= 1500/70685.8 = 0.02

γ=h-2d_c / h= 300-2*53.9/300=0.65 $\Rightarrow\gamma$=0.65

For L.C.#2 (γ=0.6) Pr/ h^2= 736.9*10^3/(300^2)=8.2 $\Rightarrow$ M_{rc}/h^3=2.05

(γ=0.7) Pr/ h^2= 736.9*10^3/(300^2)=8..2 $\Rightarrow$ M_{rc}/h^3=2.3 $\Rightarrow$ M_{rc}/h^3=2.175

M_{rc}=2.175* 300^3=58.7>39.6 ok

For L.C.#3 ok

Use D_g= 300 mm circular column with 5No.25 bars

Design of exterior columns for 3rd floor:

As a first trial we select a D_g= 300 mm circular column with 5No.25 bars,

A_{st}=2500mm^2, A_g= 70685.8 ρ= 1800/70685.8 = 0.035

γ=h-2d_c / h= 300-2*53.9/300=0.65 $\Rightarrow\gamma$=0.65

For L.C.#2 (γ=0.6) $Pr/h^2 = 430.1*10^3/(300^2)=2.75$ ⎤ $\Rightarrow M_{rc}/h^3=2.95$

(γ=0.7) $Pr/h^2 = 430.1*10^3/(300^2)=3.15$ ⎦ (γ=0.65)

$M_{rc}=2.95*\ 300^3=79.6>73.3$

For L.C.#3 ok

Use D_g= 300 mm circular column with 5No.25 bars

Design of interior columns for 4th and 5th floors:

As a first trial we select a D_g= 300 mm circular column with 5No.15 bars,

$A_{st}=1000mm^2$, A_g= 70685.8 ρ= 1000/70685.8 = 0.015

$\gamma=h-2d_c / h=0.6 \Rightarrow \gamma=0.60$

For L.C.#2 (γ=0.6) $Pr/h^2 = 480.6*10^3/(300^2)=5.3$ $\Rightarrow M_{rc}/h^3=2.00$

$M_{rc}=2.0*\ 300^3=54>27.4$ o.k.

Design of exterior columns for 4th and 5th floors:

As a first trial we select a D_g= 300 mm circular column with 5No.25 bars,

$A_{st}=1000mm^2$, A_g= 70685.8 ρ= 1800/70685.8 = 0.035

$\gamma=h-2d_c / h= 300-2*53.9/300=0.65 \Rightarrow \gamma=0.65$

For L.C.#2 (γ=0.6) $Pr/h^2 = 275.1*10^3/(300^2)=2.75$ ⎤ $\Rightarrow M_{rc}/h^3=2.925$

(γ=0.7) $Pr/h^2 = 275.1*10^3/(300^2)=3.1$ ⎦ (γ=0.65)

$M_{rc}=2.925*\ 300^3=79.0>78.2$ o.k.

Summery of internal column design:

1st floor: Use D_g= 350 mm circular column with 5No.25 bars

2nd floor: Use D_g= 300 mm circular column with 5No.25 bars

3rd floor: Use D_g= 300 mm circular column with 5No.20 bars

4th & 5th floors: Use D_g= 300 mm circular column with 5No.15 bars

Summery of external column design:

1st & 2nd floors: Use D_g= 350 mm circular column with 6No.20 bars

3rd floor: Use D_g= 300 mm circular column with 5No.25 bars

4th & 5th floors: Use D_g= 300 mm circular column with 5No.25 bars

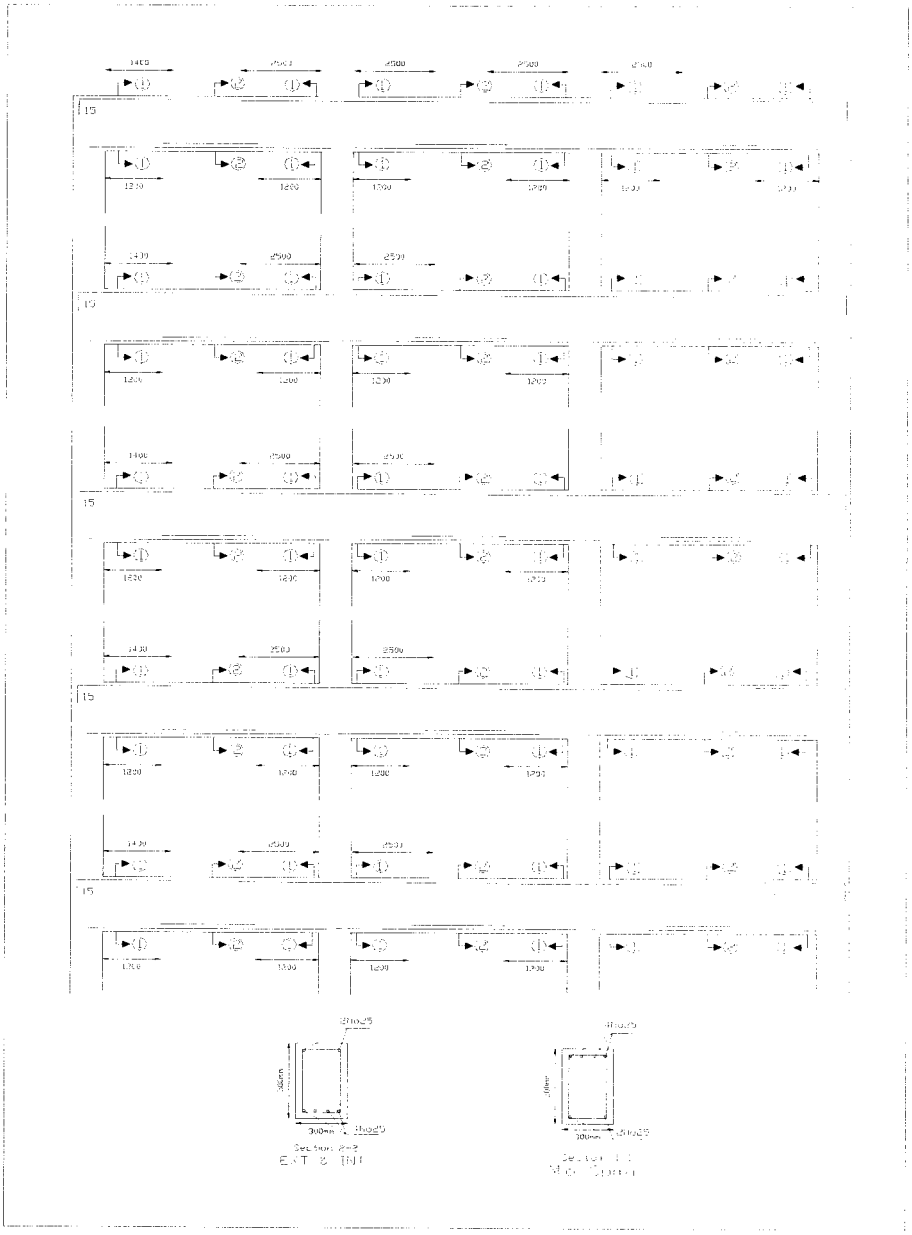

Figure A.8 Elevation of beam and longitudinal reinforcement (GLD Frame)

Figure A.9 Elevation of columns (GLD Frame)